



UNIVERSITY OF THE WITWATERSRAND

DEPARTMENT OF CIVIL ENGINEERING

hydrological research unit

REPORT No. 1/69

DESIGN STORM DETERMINATION
IN SOUTH AFRICA

J. F. A. Wiederhold



July, 1969

S Y N O P S I S

For the first time in South Africa an attempt has been made to analyse, on a country-wide basis, extremes of precipitation and to provide information in a form suitable for hydro-meteorological determination of the full range of design flood discharges in the Republic. The subject is divided into small-area and large-area storm precipitation.

Although the main emphasis is placed on large-area long-duration storms, for the sake of completeness, previous work on small-area short-duration storms is revised, brought up to date and incorporated in this dissertation. A single diagram depicts for the whole country (subdivided into summer-, winter- and year-round-rainfall) depth-duration-frequency relationships for point rainfall of duration ranging from 1/4 hour to 24 hours. Additional diagrams suggest means for estimating time distributions and depth-area-duration relationships for small-area storms.

In regard to large-area storms techniques are developed for the fitting of high-degree polynomial functions by computer to isopercental representations of storm rainfall to facilitate depth-area analyses. From scrutiny of the results of depth-area analyses of 170 well-distributed major large-area storms experienced since 1932 in South Africa the country is subdivided into 29 meteorologically homogeneous sub-regions. Within each sub-region available storm data are subjected to extreme value analysis to yield depth-area-duration-frequency relationships and regional diagrams are presented.

Estimates of precipitable moisture content of the atmosphere during each recorded storm and maximization according to ratio of maximum to ruling dew points provide an approach to probable maximum precipitation (PMP) in the form of an upper envelope curve.

The composite diagram for each sub-region shows the isohyetal map of the most severe storm recorded (as a guide to shape and orientation of a design storm), the depth-area-duration-frequency relationship and the PMP-area-duration graph.

Practical compilation of design storms for a variety of applications is illustrated by worked examples.

In appendices to the dissertation are details of the development of the surface-fitting procedures, and of explanation and streamlining of the computer programs.

A C K N O W L E D G E M E N T S

This report is based on work carried out by Mr. J.F.A. Wiederhold towards the degree of Master of Science in Engineering at the University. The author worked in the Hydrological Research Unit from March 1965 to March 1968 and at present is Operations Supervisor at the University Computing Centre.

By arrangement with the Secretary for Transport, meteorological data for this research were abstracted by members of the Hydrological Research Unit from records at the Weather Bureau, Pretoria.

The Storm Studies, results of which are embodied in this report, form part of the Unit's Floods Research programme which has been undertaken at the instigation of the South African Institution of Civil Engineers.

The major contribution to the Floods Research Fund administered by the Institution was that made by the South African Government Department of Water Affairs but many other State, semi-State and private organisations, firms and individuals have supported the research project. Contributors to the Fund are listed separately. A particularly valuable contribution is that made by the University in providing computer time, office accommodation and other facilities. In addition, for many years an annual grant has been made to me by the Council for Scientific and Industrial Research towards the salary of research assistants employed on this project.

On behalf of members of the Unit I express sincere appreciation to all who contributed financially or in other ways supported our endeavours.

We acknowledge with thanks the assistance and constant encouragement given by the Vice-Chancellor, Dr. G.R. Bozzoli, and by the Head of the Department of Civil Engineering, Professor J.E.B. Jennings.



D.C. Midgley
Professor of Hydraulic Engineering

Date ... 1/7/69

Contributors to the SAICE Floods Research Fund

State Departments

Bantu Administration and Development
Public Works
Transport
Water Affairs

South African Railway Administration

Provincial Administrations

Cape
Natal
Orange Free State
Transvaal

Chief Roads Engineer, S.W.A.

Municipalities

Durban
Johannesburg
Pietermaritzburg
Port Elizabeth
Randfontein
Springs
Vereeniging

Contractors

Basil Read (Pty) Ltd.
Christiani and Nielsen (S.A.) (Pty) Ltd.
Dorman Long (Africa) Ltd.
Reef Structures (Pty) Ltd.
The Roberts Construction Co. Ltd.
P.J. Yelland & Co. (Pty) Ltd.

Consulting Engineers

Baikoff, Theron en Vennote
B.S. Bergman & Partners
C.J. Littlewort
D.E. Alexander
Hawkins, Hawkins & Osborn
Kantey, Templer & Partners
Michal S. Zakrzewski & Partners
Ninham Shand & Partners
Ove Arup & Partners
Stewart, Sviridov & Oliver
Van Niekerk, Kleyn & Edwards
Watermeyer, Legge, Piesold & Uhlmann
W.J.S. van Heerden en Vennote

Others:

J.A. de Wet
University of Natal (Umgani Foundation)
Vaal River Catchment Association

T A B L E O F C O N T E N T S

	Page
Synopsis	i
Acknowledgements	iii
List of tables	ix
List of diagrams	x
CHAPTER 1 : Storm Studies in South Africa	1.1
1.1 Motivation	1.1
1.2 Storm Studies in other countries	1.3
1.3 Subdivision of Storm Study	1.4
1.4 Author's contribution	1.5
1.5 Scope of dissertation	1.6
CHAPTER 11 : Depth-Area-Duration Analysis	2.1
2.1 Selection of storms for analysis	2.1
2.2 Preparation of data	2.4
2.3 Isopercental patterns	2.5
2.4 Analytical procedures	2.6
2.5 Fitting the isopercental surface	2.10
2.6 Pilot Study	2.15
2.7 Visual comparisons	2.16
2.8 Alternative representations of depth-area distribution	2.21
2.9 Depth-area graphs	2.24

	Page
2.10 Time distribution of storm precipitation	2.26
2.11 Routines streamlined	2.29
2.12 Large-area storms library	2.31
2.13 Summary	2.33
 CHAPTER III : Depth-Area-Duration Frequency Analysis	 3.1
3.1 Stationarity	3.1
3.2 Homogeneity	3.2
3.3 Storm transposition	3.3
3.4 Regional subdivision	3.5
3.5 Regional analysis	3.7
3.6 Extreme value analysis	3.10
3.7 Extreme value analysis applied to depth-area- duration data	 3.15
3.8 Coaxial diagram	3.18
3.9 Average depth of precipitation	3.24
3.10 Accuracy of coaxial plot	3.25
3.11 Summary	3.25
 CHAPTER IV : Probable Maximum Precipitation (PMP)	 4.1
4.1 Evaluation of moisture content	4.2
4.2 Accuracy of moisture content estimates	4.5
4.3 Maximization of depth-area-duration curves ...	4.6
4.4 Statistical analysis of moisture content differences at two stations	 4.11

	Page
4.5 Error in maximized depth-area curve	4.12
CHAPTER V: Extension of small-area high-intensity	
storm analyses	5.1
5.1 Depth-duration-frequency analysis	5.4
5.2 Time distribution for intermediate durations	5.9
5.3 Areal distribution of small-area storms	5.13
CHAPTER VI: Design applications	
6.1 Probable maximum precipitation over Upper	
Orange River catchment	6.1
6.2 Discussion	6.6
6.3 Design storm data for Upper Tugela Basin	6.7
6.4 Design storm data for Upper Reaches of	
Tugela Basin	6.10
6.5 Summary	6.12
6.6 Conclusion	6.15
APPENDIX A: Tests and techniques employed to develop	
surface-fitting procedures	
A.1 Steps to minimize effects of ill-conditioning	A.1
A.2 Limitations of computer memory storage	A.2
A.3 Goodness of fit	A.3
A.4 Economy in the use of computer time	A.4

	Page
A.5 Analysis of errors inherent in the data	A.6
A.6 Pilot study	A.8
A.7 Tests on the surface-fitting procedure	A.10
A.8 Discussion	A.16
APPENDIX B: Reduction in computational effort	B.1
B.1 Properties of the matrix	B.1
B.2 Defining the matrix	B.6
B.3 Conclusion	B.7
APPENDIX C: Computer program logic employed in preparation of library of storm data	C.1
C.1 Explanatory notes for Fig. C.3	C.4
C.2 Explanatory notes for Fig. C.4	C.6
C.3 Explanatory notes for Fig. C.5	C.8
C.4 Explanatory notes for Fig. C.6	C.10
C.5 Explanatory notes for Fig. C.7	C.12
C.6 Explanatory notes for Fig. C.8	C.12
C.7 Explanatory notes on programs for frequency analysis	C.16
APPENDIX D: Computer print out of	
D.1 Programs employed in dissertation	D.1
D.2 Data and results of analysis of a storm	D.6
APPENDIX E: Tables indicating errors in coaxial plots	E.1
APPENDIX F: Regional diagrams	F.1

L I S T O F T A B L E S

		Page
Table 4.1	Comparative moisture content values for Pretoria and Cape Town stations	4.13
5.1	Variation of proportional depth for different recurrence intervals at East London station..	5.3
5.2	Lists of percentage depth-area-duration for the cell of a major storm	5.14
6.1	Four-day duration precipitation depths	6.3
6.2	Comparative averaged PMP over Orange River Catchment	6.7
6.3	Point rainfall depths and depths adjusted for area - storms of ten-hour duration	6.11
A.1	Coefficients in the polynomial derived for storms numbers 170 and 8 recognizing differing numbers of significant digits in the computations.....	A.12
A.2	Results of tests on group-weighting with increasing degree of polynomial	A.12
A.3	Effects of inherent errors on precision of surface-fitting - Data for storms numbers 8, 55 and 170	A.12
E.1-28	Tables of errors inherent in coaxial plots for each sub-region	

LIST OF DIAGRAMS

	Page
2.1 Distribution of rainfall stations in South Africa	2.2
2.2 Locations of pilot study storms	2.14
2.3 Isopercental maps of storm number 2	2.17
2.4 Isopercental maps of storm number 55	2.18
2.5 Isohyetal maps - storm number 2	2.20
2.6 Isohyetal maps - storm number 55	2.20
2.7 Mass curves and total storm depth-area curves :	
storms numbers 2 and 55	2.22
2.8 Depth-area-duration curves : storm number 2	2.28
2.9 Depth-area-duration curves : storm number 55	2.28
3.1 Meteorologically similar regions of South Africa	3.4
3.2 Division of South Africa into strips	3.6
3.3 Relationship between strips and sub-regions	3.8
3.4 Depth-area relationship derived by eye and by computer	3.8
3.5 Typifying three extreme distributions	3.8
3.6 Typical plots of depth-recurrence interval taken	
from data	3.17
3.7 Typical plots of depth-recurrence interval taken	
from computer analysis	3.17
3.8 Depth-area curves for selected recurrence interval	3.19
3.9 Development of two quadrant coaxial diagrams	3.21
3.10 Extrapolation of depth-recurrence interval relationship ..	3.23
3.11 Coaxial plot : area-recurrence interval-duration-	
precipitation	3.23

	Page
4.1 Moisture content as a function of pressure and temperature	
when the atmosphere is saturated	4.7
4.2 Maximized 3-day depth-area curves for region 12 (1000+ mm)	4.10
4.3 Maximum depth-area curves for region 12 (1000+ mm)	4.10
5.1 Comparison of proportional depth-area curves for areal	
and point rainfall	5.3
5.2 Location of autographic rainfall stations and delimitation	
of rainfall regions	5.3
5.3 Variation of depth-recurrence interval relationship with	
changing mean annual precipitation	5.6
5.4a Short-duration relationship of depth versus mean annual	
precipitation	5.6
5.4b Long-duration relationship of depth versus mean annual	
precipitation	5.6
5.5 Depth-duration-frequency diagram for point rainfall	5.7
5.6 Non-dimensional mass curves of 8 hours' duration	5.10
5.7 Lower envelopes of mass curves	5.10
5.8 Duration versus percentage duration with percentage depth	
as parameter	5.11
5.9 Smoothed dimensionless mass curves	5.11
5.10 Time distribution for intermediate durations	5.12
5.11 Upper envelope of depth-area relationship	5.15
5.12 Extrapolation of depth-area relationship	5.15
5.13 Precipitation over given area expressed as proportion of	
point rainfall	5.16

	Page
6.1 Catchment area of Upper Orange River catchment and division in sub-regions	6.3
6.2 Probable maximum storm of 4-day duration over Upper Orange River catchment	6.5
6.3 Probable maximum depth-area-duration curves for Upper Orange River catchment	6.5
6.4 Isohyetal map of design storm over catchment area of the Makendeni dam	6.8
6.5 Time distribution for design storm over catchment area of Spioenkop Dam	6.11
A.1 Computer time required for surface-fitting routine (Polynomial of sixth-degree) ,.....	A.5
A.2 Estimated error in F (Rainfall percental)	A.5
A.3 Difference map for storm number 55(4th order).....	A.13
A.4 Difference map for storm number 55(5th order).....	A.13
A.5 Difference map for storm number 55(6th order).....	A.13
C.1 General arrangement of computer program	C.2
C.2 Key to flow charts	C.1
C.3 Logic of program "LATEL".....	C.3
C.4 Logic of program "BLOCK".....	C.7
C.5 Logic of program "BOB".....	C.9
C.6 Logic of program "MING".....	C.11
C.7 Logic of program "STORM".....	C.13
C.8 Logic of program "TRAP".....	C.15
F.1-27 Regional diagrams	

C H A P T E R 1STORM STUDIES IN SOUTH AFRICA1.1 Motivation

In general the word 'storm' implies intense atmospheric activity, such as strong winds, electrical discharges and precipitation in its many forms, and may take place over land or over the oceans. In this study attention is focused on precipitation, in the form of rain in relatively large quantities or at high intensities, over the land areas of South Africa.

When the rate of precipitation exceeds the infiltration capacity of the land surface runoff results. Intense or prolonged storm activity leads to flood. Millions of rands are spent annually on structures designed to withstand or convey flood discharges, e.g. storm water drains, culverts, spillways, training walls and bridges. To satisfy requirements of economy and safety the design of such structures demands knowledge of flood behaviour and ways of determining magnitudes of flood discharges and their frequencies of occurrence. It follows that hydraulic design presupposes a knowledge of the cause of floods and therefore a knowledge of the behaviour of storms - particularly their magnitudes and frequencies of occurrence. Described in this dissertation is the development of methods of analysis of storm data to provide readily usable diagrams for design storm determination anywhere in South Africa.

Damage wrought by the severe floods along the south coast of Natal in 1959 served to focus the attention of engineers on the lack of suitably analysed South African data upon which they could base the use of modern hydro-meteorological techniques for design flood determination. As a result of the interest shown in this important subject by the South African Institution of Civil Engineering, funds were made available by Government, semi-Government and private organizations for the establishment of a Hydrological Research Unit, hereafter referred to as the 'Unit', in the Department of Civil Engineering at the University of the Witwatersrand.

The objectives of the Unit were :

1. To compile Design Storms of various recurrence interval for all parts of South Africa;
2. To prepare synthetic unitgraphs or other tools to permit stream response to storm precipitation to be predicted for all parts of South Africa;
3. To compile infiltration indices for various soil conditions for conversion of design storms to excess rain;
4. To prepare a Manual to assist engineers in the use of modern techniques together with South African data for the hydraulic design of spillways, culverts, bridges and urban and airfield drainage.

It is apparent therefore that storm studies, the subject of this dissertation, form an important part of the broader objectives of the Unit.

1.2 Storm studies in other countries

From frequency analysis of data from autographic rainfall stations the United States Weather Bureau has compiled an atlas¹ of design storms of various durations and frequencies of occurrence throughout the United States. In Canada, most recorded large-area storms have now been fully documented; for each storm a sheet is issued showing the locality, the synoptic situation, the isohyetal pattern, the depth-area-duration curves and contemporaneous dew-point readings. In addition, efforts are being made to provide probable maximum storm data^{2,3} for Canada and to compile an atlas on the lines of that for the United States.

Few countries of the western world have brought storm data analyses to the state reached in the United States and Canada.

Australian hydrologists⁴ and meteorologists seem to have rejected the idea of being able to estimate probable maximum precipitation; they rely on statistical extrapolation and storm transposition to extend the catchment storm experience.

1.3 Subdivision of storm study

From consideration of the hydrological equation, (viz. rate of outflow from a system is equal to the difference between the rate of inflow to and the rate of change of storage within the system), it follows that the larger the catchment, or the larger the storage within the system, the less sensitive will be the outflow to local variations of rate and amount of inflow (i.e. of precipitation).

From examination of meteorological principles it is clear that the rate of precipitation averaged over the duration of a storm and the depth of precipitation averaged over the area of influence of the storm both vary inversely with duration and area of storm.

Several conclusions follow, viz :

- (a) Maximum response from small catchments is likely to result from high-intensity localized storms of relatively short duration. To predict catchment response, accurate knowledge of the time distribution and the quantity of both precipitation and infiltration would be necessary.
- (b) Critical responses of rivers draining relatively large areas, on the other hand, are likely to result from correspondingly more widespread precipitations of longer duration and consequently of lower average intensity than those associated with small areas. For a large drainage area, changes of

catchment response, due to local variations in depth and time of incidence of precipitation, and variations in infiltration capacity would be largely smoothed out by storage components.

Storm studies can thus logically be separated into (i) small-area short-duration storms and (ii) large-area long-duration storms.

Small-area storm studies imply analyses of autographic records of precipitation and of daily observations at densely grouped rainfall gauges. Few such data are available in South Africa. Despite the paucity of data a study of high intensity precipitation was undertaken by van Wyk⁵ and the results of his small-area storms study were reported in a paper by van Wyk and Midgley⁶. Some aspects of this work have been revised and incorporated herein for the sake of completeness, but the major part of the dissertation is concerned with analyses of large-area storms.

1.4 Author's contribution

The supervisor requested that for the sake of completeness aspects handled by other members of the Hydrological Research Unit be incorporated in this dissertation - for instance, selection and preparation of storm data, the concept of weighting by isopercental method and of fitting an equation to the isopercental surface.

When the author became associated with the Unit, the large-area storms study had progressed conceptually to the stage of fitting polynomial surfaces to observed rainfall data of selected large-area storms. Implementation of this concept, however, was successfully accomplished only after lengthy investigations undertaken by the author. All the computer routines outlined and discussed in this work were designed and written by the author. The routine handling of storm data through the various stages of analysis was performed by sub-professional members of the Unit.

1.5 Scope of dissertation

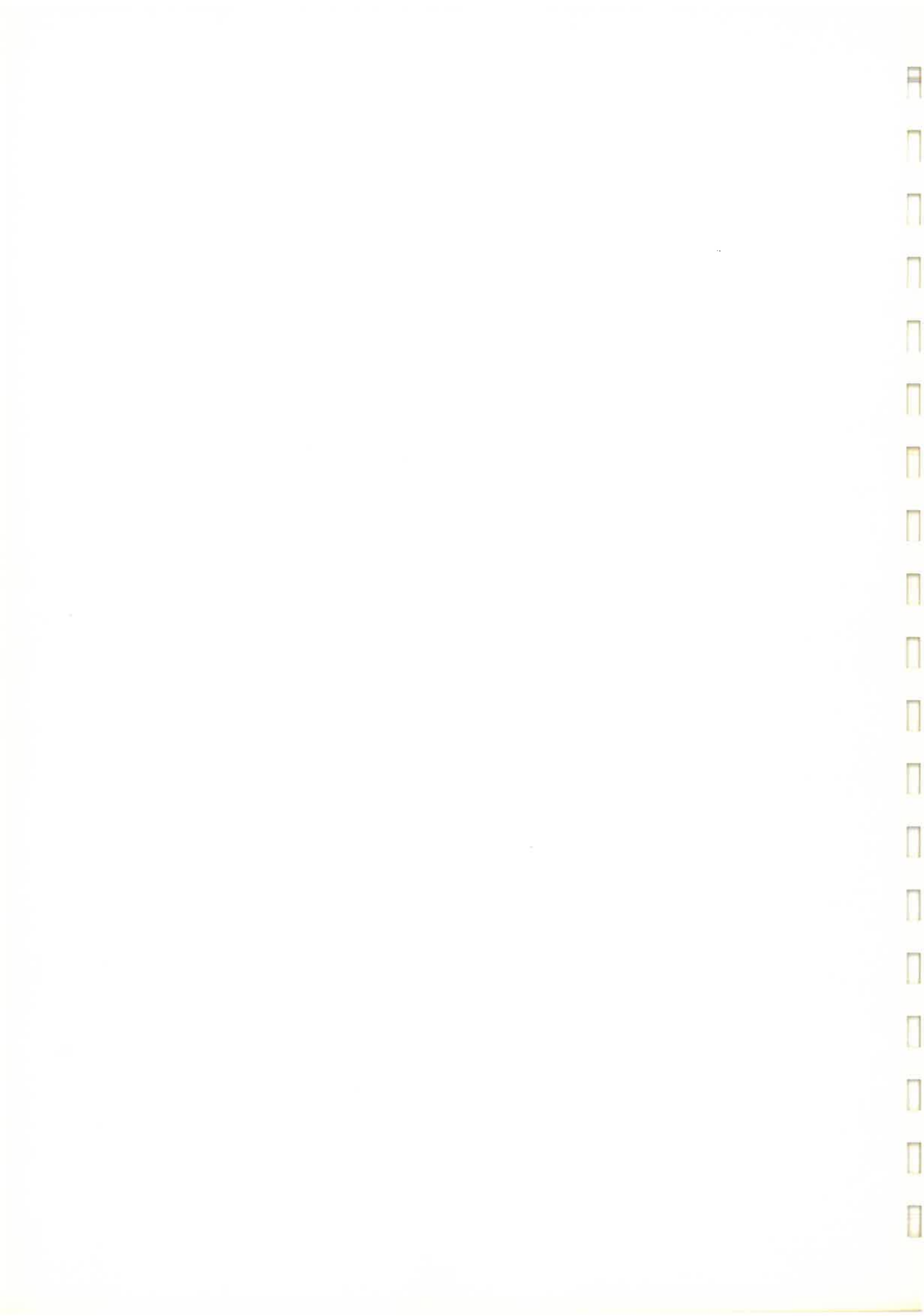
The object of this dissertation was to present the results of analyses in a form suitable for ready application of modern hydro-meteorological techniques to flood determination. Clearly it was necessary to establish for homogeneous regions of the country the inter-relationships of depth, area, duration and recurrence interval, but to enable the designer to synthesize a design storm from the relevant inter-relationships it would be necessary also to provide him with a guide as to the likely orientation and general shape of the isohyetal pattern.

Methods of deriving the depth-area-duration relationships are developed in Chapter 11 and the frequency aspect is introduced in Chapter 111 where also the requirements of statistical independence, homogeneity and stationarity are discussed and an acceptable basis for subdivision of the country into similar regions is established.

For the design of a hydraulic structure, failure of which might entail loss of life or intolerable damage, the engineer usually seeks an estimate of the probable maximum precipitation-area-duration relationship. Details of the theory developed and the techniques employed to derive such relationships are presented in Chapter IV.

Extrapolation of relationships derived for large-area storms downwards to yield relationships for small-area storms is no more permissible than is the reverse procedure because of the inherently different phenomena entailed. Data available for deriving relationships for large-area storms have a time resolution of one day (8 a.m. to 8 a.m.) whereas data for the derivation of relationships for small-area storms (point-precipitation to accurate time resolution by autographic recorder) unfortunately have a coarse spatial resolution - only 22 stations with records of adequate length for analysis. There is thus a serious gap in the data and this affects the development of depth-area-duration-frequency inter-relationships for storm areas essentially in the medium range. In Chapter V methods are developed for the bridging of this gap.

Chapter VI is devoted to detailed demonstration of practical applications embodied in the dissertation of the procedures and diagrams.



C H A P T E R 11

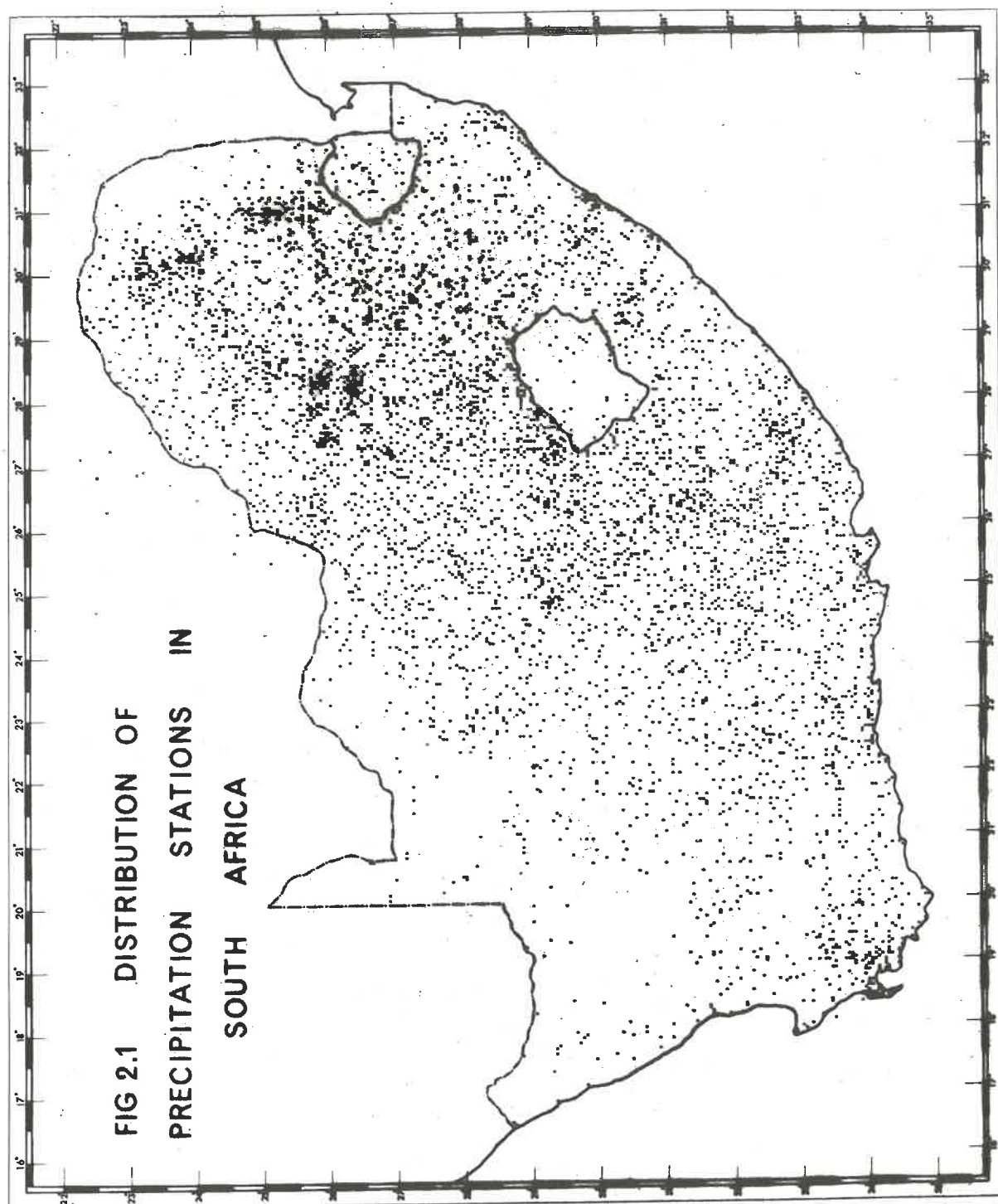
DEPTH - AREA - DURATION ANALYSIS

In this chapter the methods adopted for selecting and preparing South African storm data are described and steps in the development and testing of methods of performing depth-area-duration analyses with the aid of a digital computer are explained. Techniques employed for streamlining the adopted processes, so that the 170 selected storms could be analysed in a reasonable time, are discussed. The idea of establishing a storm data library is introduced.

2.1 Selection of storms for analysis

Average monthly and annual precipitation at daily-observed rain-gauging stations in South Africa are published periodically by the Weather Bureau ⁷. In these publications details of the Bureau's system of station-numbering are described. The numbering is based on a primary sub-division of the country into half-degree square 'section', numbered consecutively from west to east progressing northwards from number 1, viz. that embracing the southern-most tip of the continent at Cape Agulhas.

Stations from which daily-observed records have at one time or another been submitted to the Weather Bureau number about 6,000, of which about half are still operated. The distribution of rain-gauges over the country is depicted on Fig. 2.1



For each observation station there exists at the Weather Bureau a file bearing the station number and containing the original sheets from the observer's calendar book. Assembly of daily precipitation data for analysis entails abstraction of information from these files.

As a preliminary basis for selection of storms for study, the records of one reliable station in each 'section' were examined by members of the Unit. Guidance of the official in charge of rainfall records was relied upon in selecting a suitable sample station in each section. The data of the twelve heaviest falls of rain at each of these stations were abstracted. Records were examined only back to the year 1932 - that being the date subsequent to which most of the records were available in a form reasonably convenient for inspection. When data for one station in each 'section' had been compiled, the information was transferred to maps according to date of event. The maps were then scrutinized and events of relatively insignificant severity or areal extent rejected. In this way the dates and approximate localities of the severest widespread storms experienced since 1932, satisfactorily distributed over the whole country, were defined.

Next came the problem of delineating the storm fringe. With the aid of maps published in daily Weather Bureau reports showing precipitations at selected daily-reporting stations, it was usually possible to demarcate the area of influence of each of the selected

storms. In this way the dates and section numbers appropriate to a total of 170 selected storms were listed and each storm was allotted an identification number in the records of the Unit.

Thereafter, files for all the stations in the country could be brought in small batches from the strongroom to the workroom, the precipitations for the pre-selected dates abstracted from each and the files returned. By adopting this procedure, possibility of misplacement of files could be minimized, and it was generally not necessary to refer to a particular file more than once during the whole study.

2.2 Preparation of data

In preparation for analysis by digital computer in the manner to be described presently, information in the form of station number and precipitation for six days embracing the storm event was punched by hand on IBM Port-o-punch cards. Punching commenced for the stations in Section 1 and proceeded section by section northwards. Thus, data for a particular storm did not become available for final processing until the files in all sections influenced by that storm had been scrutinized.

Abstracting and punching of the data at the Weather Bureau was performed by three part-time assistants of the Unit stationed in Pretoria. On the average, cards were punched for about 20 rainfall sections per month and the task of abstracting data for the 170 storms, some of which covered about 150,000 square miles, was accomplished in

three years. In the records prior to March 1953 precipitations appear in inches and had to be converted to metric units before punching. Data from the hand-punched cards were transferred with the aid of an S.P.S. program to conventional data cards. Before further processing the cards were checked against a subsidiary deck containing a card for each rainfall station to eliminate duplications, observations from unreliable stations, and obvious errors. At the same time the strict serial order of the cards in terms of station code-number was verified.

2.3 Isopercental patterns

The observations at daily-read official rain gauges within the area embraced by a storm represent at best a rather inadequate sample of varying depths of precipitation, at coarse time resolution, and at points sometimes sparsely scattered within the area of influence of the storm. If the area covered by a storm is devoid of significant topographic features areal weighting of sample observations by Thiessen polygon technique is usually acceptable; where topographic and other factors influence the distribution of precipitation isohyetal mapping is to be preferred.

Positioning of the isohyets for a storm event presents the same difficulties as does the drawing of isohyetal maps of mean annual rainfall, conventional techniques for which are explained in standard hydrology texts. A valuable aid to the positioning of storm isohyets - also described in standard texts - is based on the hypothesis that topographic, orographic and other factors affect the areal distribution of precipitation depths during a storm in much the same way as they

affect the mean annual rainfall and that therefore the mean annual isohyetal pattern should form an acceptable basis for lateral extension of sample observations to indicate the probable spatial distribution of rainfall. Usually a relatively smooth pattern of isometric lines can be drawn among sample observations when expressed as percentages of local mean annual rainfalls; these lines are usually referred to as isopercentals. Isohyetal mapping of a storm by isopercental method should in general yield a more accurate representation of the storm than one based on straightforward linear interpolation among sparse observations of rainfall depth. Planimetry of the areas enclosed by isohyetal lines of descending value on each map of a set of maps indicating the areal distribution of rainfall during intervals between observations throughout the storm would be the ideal way of deriving the depth-area-duration graph of the storm.

Faced with the task of constructing depth-area-duration graphs for 170 storms, members of the Unit gave careful consideration to the possibility of performing the analyses by computer.

2.4 Analytical procedures

In developing methods of analysis attention was directed not only to storm analysis per se, but also to the ultimate goal of synthesizing the hydrograph of direct runoff from a catchment subject to a given storm.

A lag-and-route technique for determining river response to a design storm precipitated on a catchment of known physiographic characteristics had been developed for digital computer operation.

By this technique the hyetograph of storm input to each elemental area of the catchment, reduced to rainfall excess by subtraction of basin recharge, is modulated in a mathematical model of the catchment storage and drainage systems to produce the hydrograph of river response. This synthesization technique was based primarily on an areal resolution of one minute of latitude by one minute of longitude. Provision was made, however, for the resolution to be reduced to any degree that might be desired to suit the size of catchment under consideration. Included in the computer program for hydrograph synthesization were adjustments to express in square mile units the areas enclosed by the orthogonally intersecting meridians and parallels (see section 2.9). Testing of the method was reported in a paper by Midgley and Schultz ⁸.

It was considered highly desirable that the techniques to be developed for both storm and flood analyses should be closely integrated so that the method might ultimately be employed also for flood forecasting and flood control purposes.

Interpolation among the percental values of storm precipitation at observation stations can be performed in any of the following three ways:

(a) Thiessen polygons

Percental values assigned to the areas embraced by Thiessen polygons constructed around observation points would present a 'columnar' distribution of the storm in

mean annual rainfall percental units.

(b) Linear interpolation

Linear interpolation from station to station would imply representation of the storm percental distribution as a multi-facet surface. This could be dubbed the 'tin-roof' method.

(c) Smooth surface

By isopercental concept the storm percental configuration could be recognised as a smooth surface. If the pattern were not too severely contorted it might be possible to fit a continuous mathematical function to the percental values at the gauging stations.

The rainfall depth distribution over the area embraced by a storm can be evaluated if the corresponding storm percental distribution (depicted in one or other of the three ways discussed above) were made to operate on the mean annual rainfall distribution represented by values read from isohyetal maps at points located at the intersections of a grid of suitably fine mesh. A computer program can readily be written to perform the operation and to integrate the results to produce the depth-area relationship.

Should records be missing at one or more stations, generalization of the pattern of the 'column-tops' or 'tin-roofs' associated with methods (a) and (b) respectively would offer difficulties. It seemed

that, to conform with the requirements of the flood hydrograph synthesization technique, the best way of representing storm configurations independently of variations in the number and location of sampling points would be by means of a continuous mathematical function of latitude, longitude and storm percental.

Since latitude and longitude constitute a spherical coordinate system a function in spherical harmonics might have been adopted. Individually, the storms to be analysed, however, cover relatively small portions of the global surface and the observational errors in data are relatively large. As application of spherical harmonics would have entailed highly sophisticated mathematical techniques, it was felt that, in the circumstances, these would not be warranted. It was considered that, provided a relatively small part only of the sphere is handled at a time and latitude corrections of area are made, errors introduced by adoption of polynomials in a rectangular coordinate system, instead of spherical functions, would be negligible compared with errors in precipitation observation.

Results of tests carried out by members of the Unit in fitting high-degree polynomials to the percental values of several hypothetical storms were highly encouraging and it was therefore decided to adopt the method. Steps were accordingly taken in the Unit to prepare, for the whole of South Africa, a set of data cards, one for each square minute of arc, addressed according to latitude (measured in minutes southwards from the equator) and longitude (measured in minutes eastwards from the Greenwich meridian). Along with its address each card bore the appropriate mean annual rainfall value in millimetres and other

information referred to in a separate work⁹. Mean annual rainfall values were read from the 1:250,000 work sheets from which the isohyetal map of the Republic was prepared in the Department of Water Affairs by Mr. B.R. Schultze, onetime Deputy Director of the Weather Bureau.

To facilitate access to these data by the computer the information was transferred section by section to a magnetic disc. In effect, then, the rainfall map of South Africa could be stored in a manner readily accessible to the machine. Basic cards forming a supplementary deck were also prepared, one card for each of the 6,000 (approximately) rainfall stations that had at one time or another been operative in the Republic. Each of these cards bore the code number, latitude, longitude and mean annual rainfall at the station.

2.5 Fitting the isopercental surface

The polynomial of high degree

Throughout the area affected by a storm under study point rainfall, expressed as a percentage of local mean annual rainfall, i.e. the percental, for a given duration, can be represented by polynomial in which the dependent variable (percental value) is expressed in terms of latitude and longitude. The terms in the equation are products of a coefficient, a , and the latitude, x , and longitude, y , each raised to a power. The polynomial can be written in the general form :

$$z = a_0 + a_1y + a_2x + a_3y^2 + a_4xy + a_5x^2 + \dots + a_{m-1}yx^{n-1} + a_mx^n \quad (2.1)$$

A set of observations can theoretically be represented mathematically on the basis of an exact fit but, if there are M observations to be exactly fitted, the equation would demand M coefficients and if M is large, the equation would become unmanageable. Bearing in mind that both observed storm rainfall and mean annual rainfall are of relatively low accuracy and the fact that the isopercental concept is not necessarily everywhere a sound weighting procedure, an exact fit is not particularly desirable. What is wanted rather is a representation of the general trend of the isopercental pattern as a basis for weighted interpolation of storm rainfall at places interspersed between observation stations. A surface based on the least squares criterion, i.e. minimization of average deviations of the observations from the computed polynomial surface, would adequately describe the trend of the percental pattern. If the percental surface is now transformed to yield the areal distribution of storm precipitation, which is then numerically integrated and expressed as a depth-area relationship, the result would probably be found to be just as accurate as or possibly more so than that derived from an exact-fit hyetal surface which could not readily be described mathematically.

Surface-fitting based on least square criterion

The coefficients to be determined are those associated with minimum average deviation of N observations from the computed surface. For each observation, i , an observation equation was set up in the form :

$$z_i = a_0 + a_1 y_i + a_2 x_i + a_3 y_i^2 + a_4 x_i y_i + a_5 x_i^2 + \dots - d_i \quad \dots (2.2)$$

in which, z_i is the percental value of the observation i ,

$a_0, a_1, a_2, a_3 \dots$ are coefficients,

x_i and y_i are latitude and longitude respectively, and

d_i is the amount by which the observed percental value,

z_i , differs locally from the computed value.

From equation (2.2), difference equations for each observation were derived :

$$d_i = (a_0 + a_1 y_i + a_2 x_i + a_3 y_i^2 + a_4 x_i y_i + a_5 x_i^2 + \dots) - z_i \quad \dots (2.3)$$

The criterion for best fit of the polynomial requires that

$f = \sum_{i=1}^N (d_i)^2$ be a minimum. Normal equations were written to meet this condition, thus :

$$\frac{\partial f}{\partial a_0} = 2 \sum (a_0 + a_1 y_i + a_2 x_i + a_3 y_i^2 + \dots) - z_i = 0$$

$$\frac{\partial f}{\partial a_1} = 2 \sum (a_0 + a_1 y_i + a_2 x_i + a_3 y_i^2 + \dots) - z_i \cdot y_i = 0$$

$$\frac{\partial f}{\partial a_2} = 2 \sum (a_0 + a_1 y_i + a_2 x_i + a_3 y_i^2 + \dots) - z_i \cdot x_i = 0$$

$$\frac{\partial f}{\partial a_3} = 2 \sum (a_0 + a_1 y_i + a_2 x_i + a_3 y_i^2 + \dots) - z_i \cdot y_i^2 = 0$$

$$\frac{\partial f}{\partial a_4} = 2 \sum (a_0 + a_1 y_i + a_2 x_i + a_3 y_i^2 + \dots) - z_i \cdot x_i y_i = 0 \text{ etc.} \\ \dots\dots\dots(2.4)$$

As many normal equations as there are coefficients in the polynomial were set up and transposed into the form :

$$\begin{aligned} a_0 \sum 1 &+ a_1 \sum y_i &+ a_2 \sum x_i &+ a_3 \sum y_i^2 \\ &&&+ \dots - \sum z_i &= 0 \\ \\ a_0 \sum y_i &+ a_1 \sum y_i^2 &+ a_2 \sum x_i y_i &+ a_3 \sum y_i^3 \\ &&&+ \dots - \sum y_i z_i &= 0 \\ \\ a_0 \sum x_i &+ a_1 \sum x_i y_i &+ a_2 \sum x_i^2 &+ a_3 \sum x_i y_i^2 \\ &&&+ \dots - \sum x_i z_i &= 0 \\ \\ a_0 \sum y_i^2 &+ a_1 \sum y_i^3 &+ a_2 \sum x_i y_i^2 &+ a_3 \sum y_i^4 \\ &&&+ \dots - \sum y_i^2 z_i &= 0 \\ \\ a_0 \sum x_i y_i &+ a_1 \sum x_i y_i^2 &+ a_2 \sum x_i^2 y_i &+ a^3 \sum x_i y_i^3 \\ &&&+ \dots - \sum x_i y_i z_i = 0 \text{ etc.} \\ &&&\dots\dots\dots(2.5) \end{aligned}$$

The computer was programmed to solve by Gaussian elimination¹⁰, the m simultaneous equations (2.5) in which there are m unknowns.

Steps to minimize effects of ill-conditioning that result from application of the least squares method to optimization of the coefficients in high-degree polynomials are discussed in Appendix A, in which also are discussed the limitations of computer memory storage, selection of degree of polynomial, economy of computer time



and analysis of errors inherent in the data.

2.6 Pilot study

A pilot study, described in Appendix A, was undertaken to test, for several storms, the influence on the precision of the surface-fitting routine of repetitive manipulation of each of the following factors : degree of polynomial, number of significant digits recognized, and intensity of group-weighting of observations.

The locations of the storms selected for the pilot study are shown on Fig. 2.2. Storms numbers 2 and 8 were the first for which complete data were received from the team in Pretoria. Unfortunately, because of proximity to the coast-line, these two storms were by no means ideal for test purposes.

Rainfall data for storm number 55 - the Natal storm of May, 1959, which caused widespread damage in Natal and Transkei - had been listed for an earlier study by Kriel¹¹. Likewise, the relevant rainfalls for storm number 170 - the Karoo storm of March 1961, which caused unprecedented floods over wide areas of the Karoo - had been compiled by Triegaardt¹² and Taljaard¹³.

Results of the pilot study indicated that a polynomial of sixth degree, involving 28 terms, could represent with acceptable accuracy the isopercental surface of storms up to approximately 50,000 square miles in area, provided an adequate number of significant digits was recognised in optimizing the coefficients of the polynomial. It was found further that, by group-weighting the observations in blocks

having side dimensions of between 15 and 25 minutes of arc, computer time could be reduced two- to threefold without significant loss of precision.

It was found after some experimentation that for a sixth degree polynomial surface to represent reasonably accurately the percental pattern the storm area handled should not exceed about 50,000 square miles. Accordingly, it was necessary to subdivide all storms that covered areas larger than 50,000 square miles. Sixth order polynomials surfaces were fitted to subdivided storms, a half-degree or one-degree overlap being allowed at the boundaries between subdivisions to maintain continuity of the mathematical fit over the entire storm area.

2.7 Visual comparisons

Isopercental patterns

Visual comparison of some of the isopercental maps resulting from the analysis performed in the pilot study confirmed the conclusions arrived at from scrutiny of the 'difference' maps and statistics which are reproduced in Appendix A. A 'difference' map is one on which are plotted at each station the deviations, positive and negative, of the observed from the calculated values.

In Figs. 2.3 and 2.4 appear isopercental maps drawn from computed values plotted at quarter-degree grid intersections. These correspond to the analyses marked with asterisks in Table A.2 of Appendix A, viz. storms numbered 2 and 55 respectively. Arranged for

FIG 2.3

ISOPERCENTAL MAPS OF STORM
NUMBER 2

- NOTES: a) Group - weighting: numeral denotes number of groups into which the observations were subdivided.
b) Isometric lines indicate total storm as percentage of local mean annual rainfall.

a) ISOPERCENTALS INTERPOLATED BY EYE

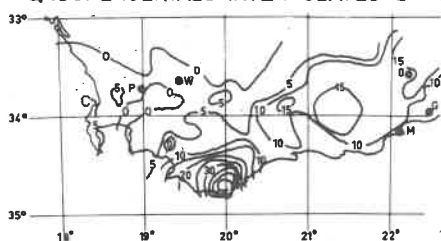
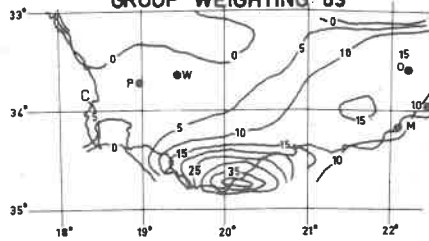
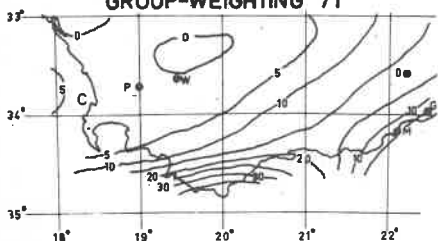
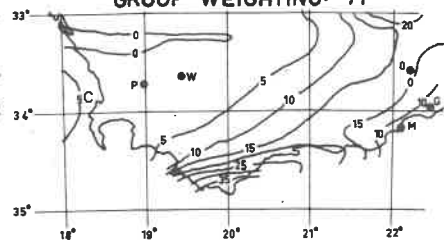
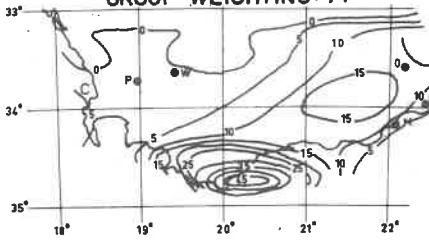
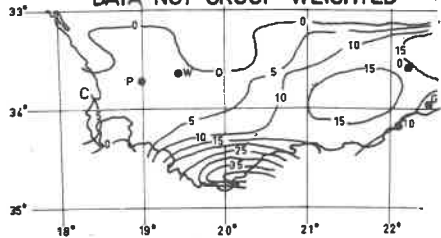
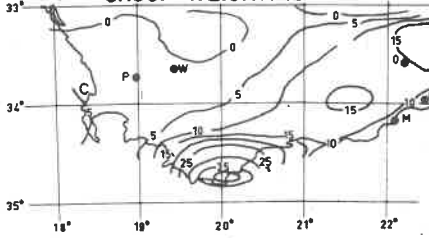
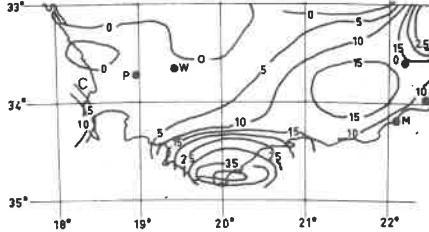
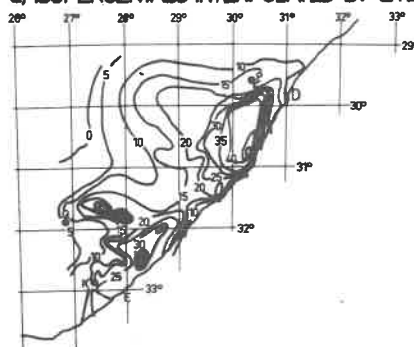
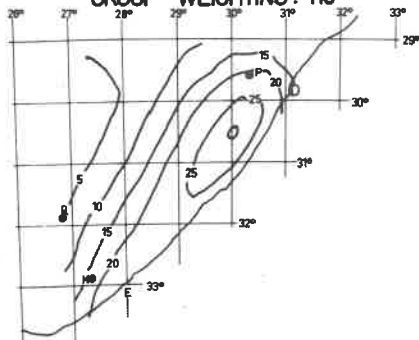
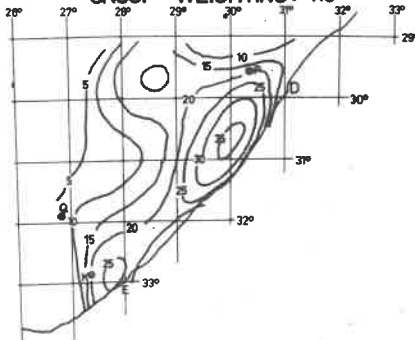
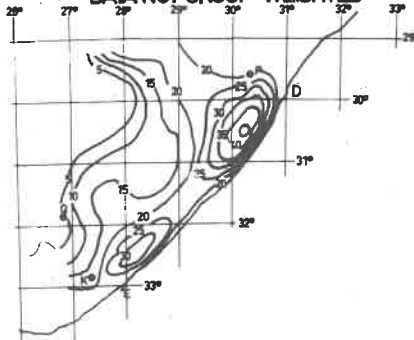
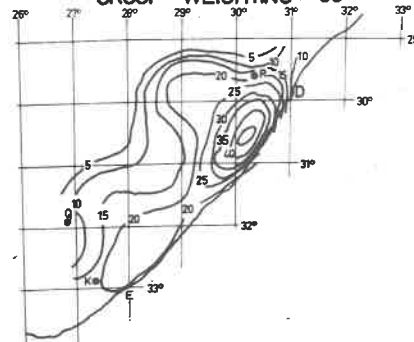
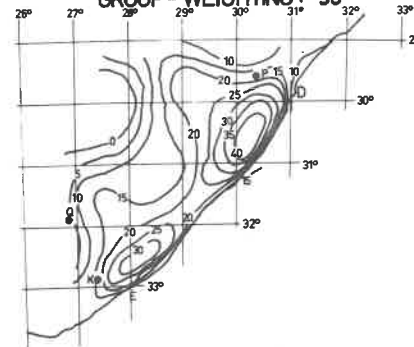
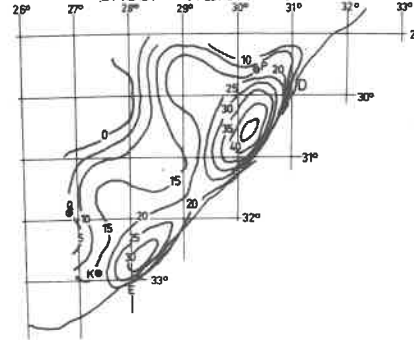
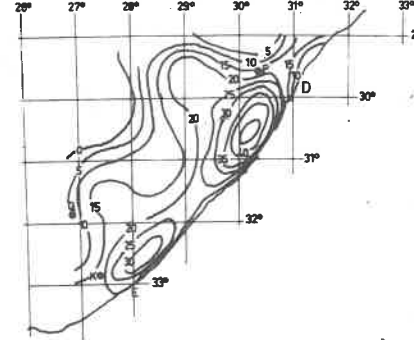
e) FROM POLYNOMIAL OF 6TH DEGREE
GROUP WEIGHTING 63b) FROM POLYNOMIAL OF 4TH DEGREE
GROUP-WEIGHTING 71c) FROM POLYNOMIAL OF 5TH DEGREE
GROUP WEIGHTING: 71f) FROM POLYNOMIAL OF 6TH DEGREE
GROUP-WEIGHTING: 71d) FROM POLYNOMIAL OF 6TH DEGREE
DATA NOT GROUP-WEIGHTEDg) FROM POLYNOMIAL OF 6TH DEGREE
GROUP-WEIGHTING: 79h) FROM POLYNOMIAL OF 6TH DEGREE
GROUP-WEIGHTING: 79

FIG 2.4 ISOPERCENTAL MAPS OF STORM NUMBER 55

- NOTES: a) Group - weighting: numeral denotes number of groups into which the observations were subdivided.
b) Isometric lines indicate total storm as percentage of local mean annual rainfall.

a) ISOPERCENTALS INTERPOLATED BY EYE

b) FROM POLYNOMIAL OF 4TH DEGREE
GROUP - WEIGHTING: 118c) FROM POLYNOMIAL OF 5TH DEGREE
GROUP - WEIGHTING: 118d) FROM POLYNOMIAL OF 6TH DEGREE
DATA NOT GROUP-WEIGHTEDe) FROM POLYNOMIAL OF 6TH DEGREE
GROUP - WEIGHTING: 59f) FROM POLYNOMIAL OF 6TH DEGREE
GROUP - WEIGHTING: 98g) FROM POLYNOMIAL OF 6TH DEGREE
GROUP - WEIGHTING: 118h) FROM POLYNOMIAL OF 6TH DEGREE
GROUP - WEIGHTING: 165

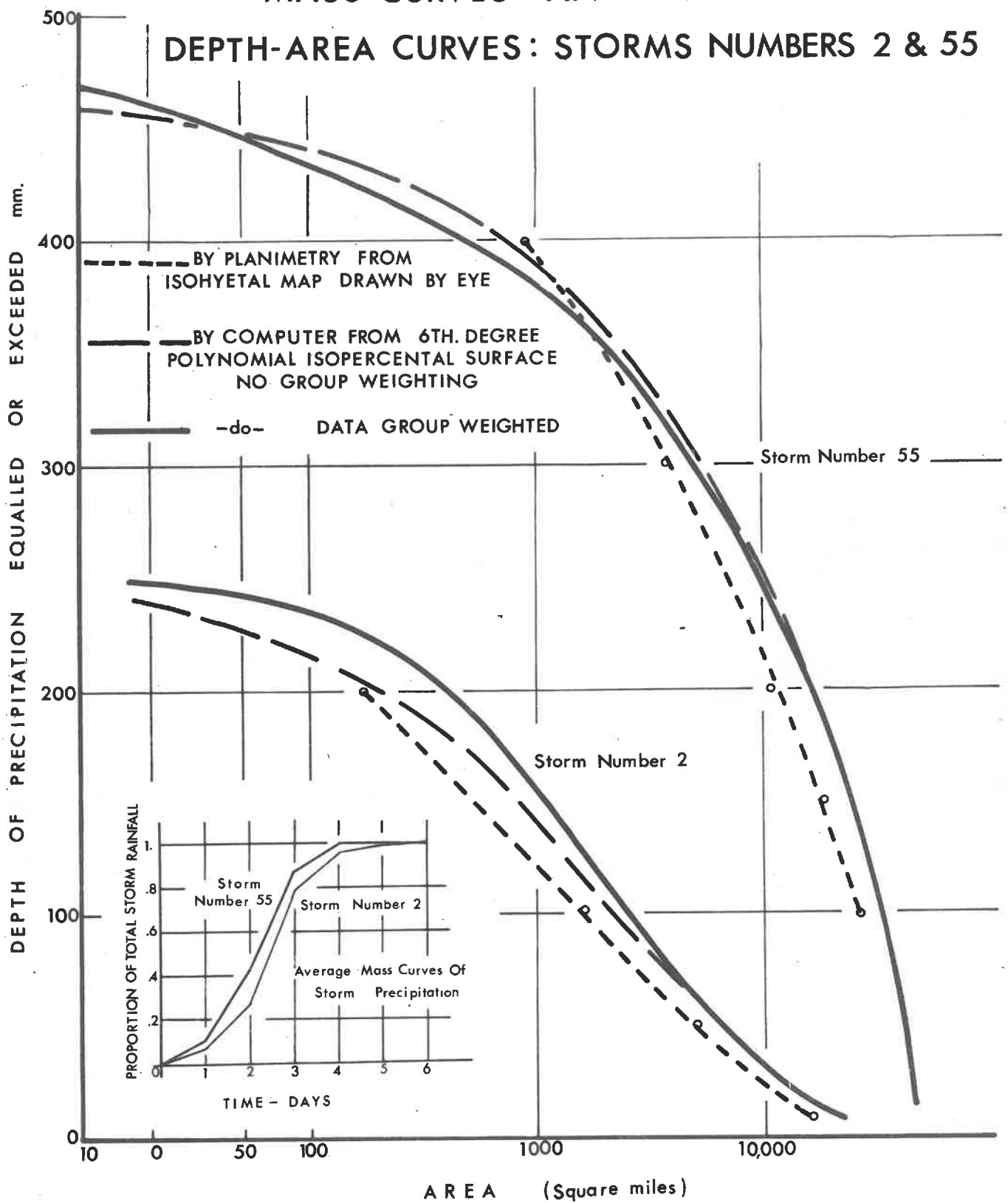
ready comparison in Figs. 2.3 and 2.4 are the corresponding isopercental maps plotted by eye from observed percental values.

Scrutiny of the difference maps and the maps in Figs. 2.3 and 2.4, coupled with examination of the corresponding variations in the root-mean-square deviations, leaves no doubt as to the improvement in definition to be achieved by raising the degree of polynomial, but there is apparently no sharply defined optimum intensity of group-weighting.

Isohyetal patterns

Although visual comparison of graphical representation of the mathematically determined isopercental surface, on the one hand, with that based on interpolation by eye among the observation on the other confirmed that the task could be accomplished by machine, it was felt that it might be comforting to compare also machine-produced with conventionally-drawn isohyetal maps. Such comparisons for storms 2 and 55 can be studied in Figs. 2.5 and 2.6 respectively, the captions of which render them self-explanatory. Figs. 2.5 (c) and 2.6 (c) were drawn by the method commonly accepted when dealing with large-area storms, viz. smoothing by eye of isohyets drawn among the plotted observations. Maps (a), (b) and (c) are not strictly comparable, however, because mere interpolation of isohyets by eye is strongly subject to sampling error, owing to the general lack of high altitude rainfall stations. As mentioned earlier, the weighting process inherent in the isopercental method is such that it should yield the more accurate result. Accordingly, where differences occur

FIG 2.7
MASS CURVES AND TOTAL-STORM
DEPTH-AREA CURVES: STORMS NUMBERS 2 & 55



between the machine-produced and the hand-produced results, it is difficult to distinguish between inaccuracy due to the surface-fitting procedure and that due to sampling error or subjectiveness of the draughtsman. It must, nevertheless, be conceded that the machine-produced representations of the storm maps are strikingly similar to those constructed directly from the observations.

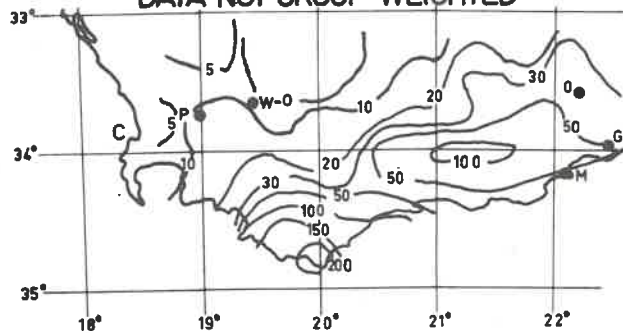
2.8 Alternative representations of depth-area distribution

It is convenient at this stage to distinguish between alternative ways of representing areal distribution of storm precipitation. Conventional methods of deriving depth-area-duration curves are described in considerable detail in Technical Report No. 1 on Cooperative Studies undertaken by the U.S.B.R. and Weather Bureau¹⁴.

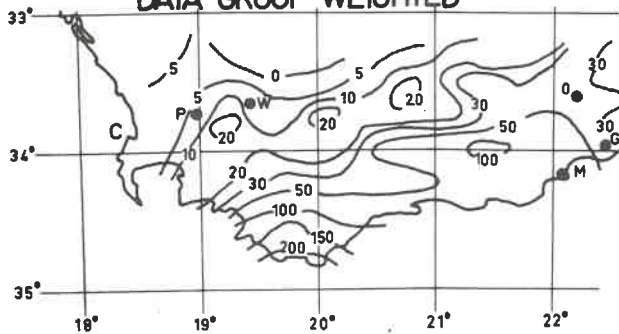
Fundamentally, the method involves determination of the maximum average-depth of precipitation occurring within selected time intervals throughout the total-storm period on areas encompassed by each closed isohyet of the total-storm isohyetal map. Thus, against a selected value on the area scale of the depth-area-duration graph, the value of depth read on a given duration curve represents the maximum volume of rain that occurred within that duration divided by the area value selected. The result represents therefore the maximum value of average-depth precipitation over a given area within a given period during the storm.

An alternative way of representing areal distribution of storm precipitation is to plot, against the precipitation indicated by an isohyet, the area encompassed by that isohyet. Fig.2.7 is compiled

FIG 2.5
ISOHYETAL MAPS-STORM NUMBER 2
a) FROM POLYNOMIAL OF 6TH DEGREE
DATA NOT GROUP WEIGHTED



b) FROM POLYNOMIAL OF 6TH DEGREE
DATA GROUP-WEIGHTED



c) ISOHYETS INTERPOLATED BY EYE

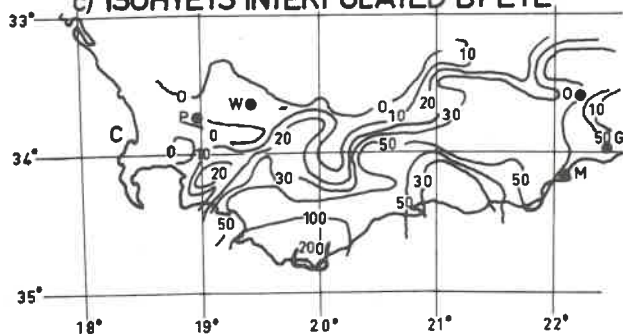
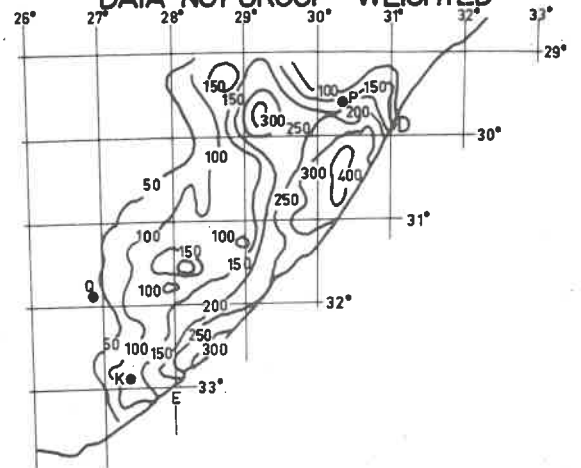
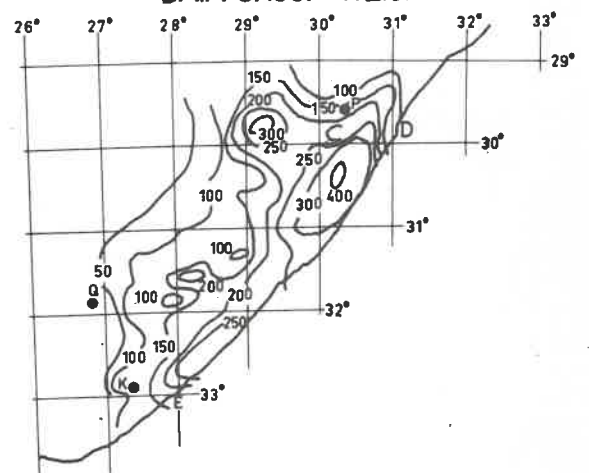


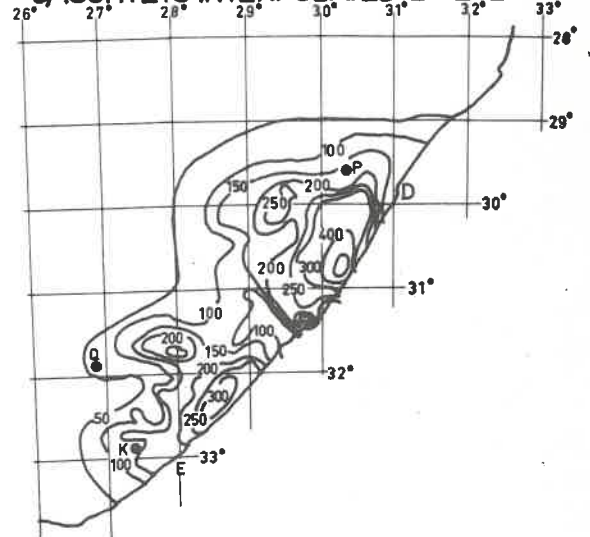
FIG 2.6
ISOHYETAL MAPS-STORM NUMBER 55
a) FROM POLYNOMIAL OF 6TH DEGREE
DATA NOT GROUP-WEIGHTED



b) FROM POLYNOMIAL OF 6TH DEGREE
DATA GROUP-WEIGHTED



c) ISOHYETS INTERPOLATED BY EYE



in this fashion. The resulting graph is analogous to a hypsometric curve or a particle-size distribution curve; it indicates at a given area ordinate the depth of precipitation equalled or exceeded within that area.

It follows that if it were desired to synthesize a plausible isohetal map of a design storm over a problem catchment, it would be permissible to abstract, from depth-area curves derived for the appropriate meteorological region, the depth of precipitation corresponding to the area embraced by the catchment and to place at or near the periphery of the catchment an isohyet of that value. Isohyets of rising value could then be trial-fitted within the catchment, following the appropriate storm pattern, in such a way as to encompass areas stipulated by the depth-area curve. By shifting the storm centre in relation to the catchment outlet, but avoiding violation of meteorological principles, the critical location of the storm can be determined from trial flood hydrograph synthesizations, and the probable critical stream response thus estimated.

It is difficult to envisage how such procedures could readily be followed if the depth-area relationships were to be presented in the conventional manner. The conventional method was evidently developed with an eye to application to unit hydrograph techniques, for which precipitation is assumed to be uniformly distributed over the catchment or over zones into which the catchment has been subdivided.

2.9 Depth-area graphs

Area Adjustments

The area corresponding to each one square minute of arc is dependent on latitude and is calculated as follows :

From Chambers¹⁵

1° of latitude represents $69.06 - 0.35 \cos 2\phi$ miles and

1° of longitude " $69.23 \cos \phi - 0.06 \cos 3\phi$ miles

where ϕ is latitude in degrees.

Area enclosed by 1° latitude by 1° longitude

$= (69.06 - 0.35 \cos 2\phi) (69.23 \cos \phi - 0.06 \cos 3\phi)$ square miles

$= 4781.0238 \cos \phi - 4.1436 (\cos^3 \phi - 3 \cos \phi) - 24.2305 (2 \cos^2 \phi - 1) \cos \phi$

$+ .0210 (8 \cos^5 \phi - 10 \cos^3 \phi + 3 \cos \phi)$

$= 4817.7481 \cos \phi - 65.2454 \cos^3 \phi + .168 \cos^5 \phi$ square miles.

The last term is negligible as decimal digits beyond the fifth are ineffective.

Area enclosed by one square minute of arc

$= \frac{1}{3600} (4817.7481 \cos \phi - 65.2454 \cos^3 \phi)$ square miles

where $\phi = \frac{\psi}{60}$ and ψ the latitude in minutes of arc

$= 1.33826 \cos \phi - .0181237 \cos^3 \phi$ square miles.

Areal changes over a distance of half a degree in latitude are negligible in the region of South Africa. The area represented by one square minute of arc was calculated once for each section from the latitude at the centre of section and this correction was applied to data over the entire section.

Conversion from isopercental surface to depth-area graph

To establish depth-area relationships for the total storm the computer was programmed to convert percental values to hyetal values at a convenient latitude - longitude resolution, at the same time integrating numerically to yield the depth-area relationship.

Where variations of mean annual precipitation from place to place are gradual the hyetal and percental surfaces are similar and as a rule relatively free from contortions. In such cases it was convenient to coarsen the resolution at which integration was to be performed. Depending upon the degree of contortion of the mean annual precipitation pattern, resolutions of 4, 9, 25 or 36 square minutes of arc were prescribed for each section of the country, as shown in Fig.3.2. In this way, the volume of calculations to determine depth-area relationships could be proportionately reduced without significantly affecting accuracy.

Integration was performed in the following way :

A suitable range of storm rainfall depth was allocated to each pigeonhole of a set in the machine memory and adjusted areas corresponding to the grid resolution adopted were accumulated by the machine in the appropriate pigeonholes as it scanned the entire storm area under study. Upon completion of scanning, the accumulated areas in each pigeonhole were summed, starting with the areas corresponding to the highest rainfall interval, and the results were printed out in the form of a depth-area tabulation.

Perhaps the final test of suitability of the method adopted is

the success with which a total-storm depth-area graph can be compiled. Computer-compiled depth-area graphs for storms numbers 2 and 55 are reproduced in Fig. 2.7 in which are plotted also the corresponding graphs derived by planimetry of the areas enclosed by isohyets of decreasing value on Figs. 2.5(c) and 2.6(c) respectively.

Again, there is little to choose between the machine- and the hand-produced graphs. As the mathematical surface tends to cut through the peaks and stretch above the hollows of the actual percental configuration, it is to be expected that the machine-produced depth-area curves might tend to over-estimate the depths of precipitation on the larger areas and to under-estimate towards the small-area end of the graph. The former tendency, although not particularly marked in either of the tests, is on the side of safety while the latter tendency - also not marked in the tests - is unimportant because small-area storms form in any event the subject of a separate study ⁵.

2.10 Time distribution of storm precipitation

So far discussion has been confined to depth-area relationships of total-storm precipitation. It remains to describe the procedures adopted for introducing the time distribution aspect.

Methods of preparing and weighting mass curves of storm rainfall from which suitable time subdivisions of the total duration of a storm can be measured are explained in a Co-operative Studies Technical report¹⁴. Principal reliance is placed on the records of autographic

rain gauges, although attention is drawn to the need to seek as many other clues as possible on the timing of changes in the rates of storm precipitation throughout the area of influence. In South Africa up until 1948 there were fewer than a dozen autographic rain gauges and it is only since about 1960 that a reasonably dense network of such gauges has been established. Moreover, one searches in vain in the records for a satisfactory number of observer's notes of times of start and cessation of heavy rain to facilitate construction of mass curves. Weather Bureau instructions to rainfall observers stipulate that rain gauges must be observed daily at the standard time of 8.00 a.m., but it is clear from the records that precipitation has frequently been allowed to accumulate for more than a day and it is not unusual for observations to be recorded against the incorrect date.

It follows that the duration parameter in the depth-area-duration analysis, at least in respect of the earlier storms on record, will be of low accuracy. It was decided to perform the duration analyses first to a resolution of one day and at a later stage, after examination of the collective results, to review the analysis with the object of improving the time resolution.

Accordingly, the machine program was written to permit the average mass curve of each storm at one-day time resolution to be printed out. When performing the depth-area integration process the machine proportioned the depths of precipitation according to the average mass curve, selecting first the maximum one-day precipitation, then the maximum two-day and so on ultimately to the total-storm precipitation.

FIG 2.8

DEPTH-AREA - DURATION CURVES STORM NUMBER 2

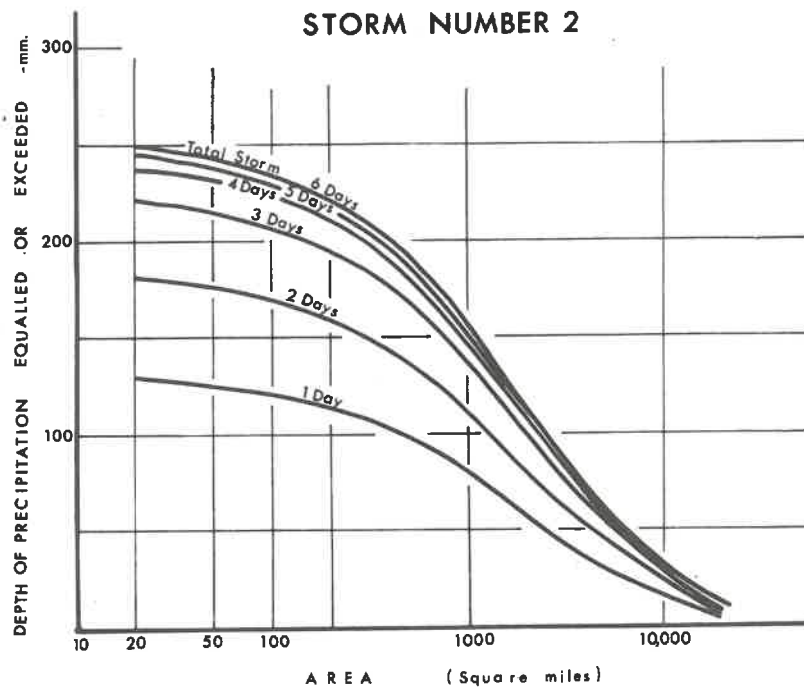
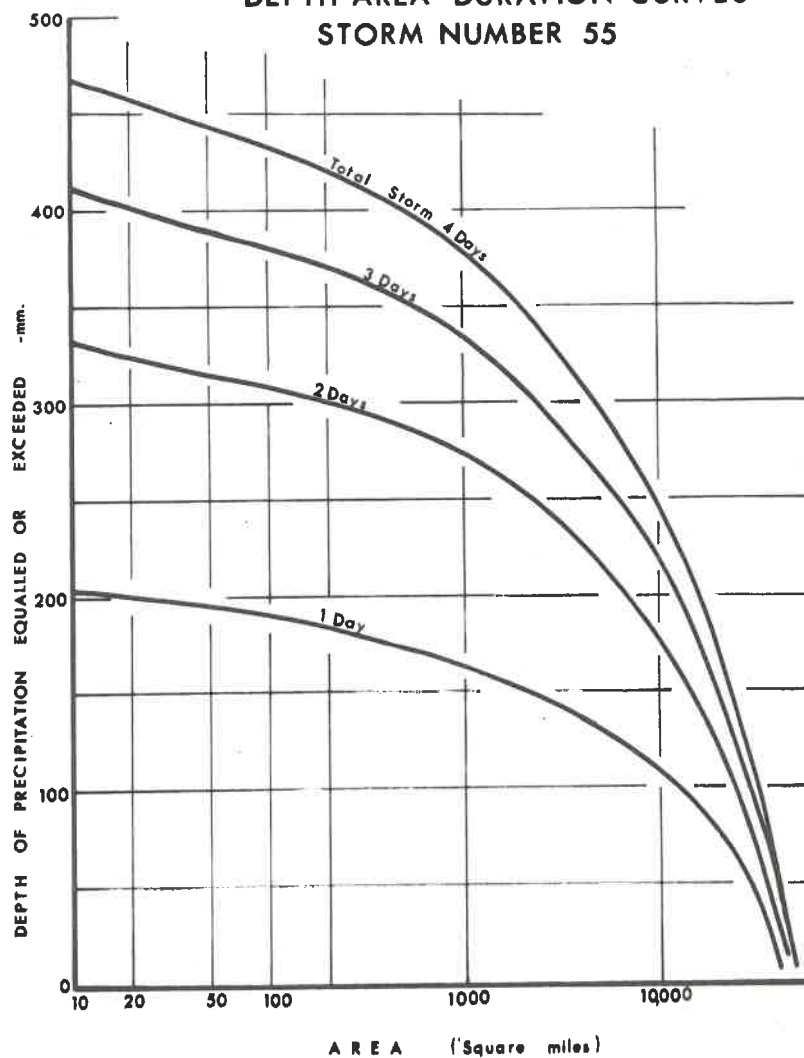


FIG 2.9

DEPTH-AREA - DURATION CURVES STORM NUMBER 55



It should be noted at this stage that the use of an average mass curve as described above implies that duration is independent of areal variations. It is indeed not possible in the absence of adequate well distributed autographic recording stations, to establish accurate duration-area relationships. The short-comings of a depth-area-duration analysis performed by the adopted method are well appreciated. The results will nevertheless be of immediate value in the application of hydro-meteorological techniques to design flood determinations for catchment of response time longer than two days.

Mass curves and depth-area-durations analyses performed according to the foregoing procedure for storms numbers 2 and 55 appear on Figs. 2.8 and 2.9 respectively.

2.11 Routines streamlined

The techniques and routines developed were programmed to run on an IBM 1620 Mod II computer under supervision of a non-professional operator. Computer time requirements were gradually reduced by streamlining successful routines. For instance, when allocated time on the machine had expired, it was possible for the operator, by flicking a switch, to transfer the entire contents of the memory core storage to a relocatable address on a magnetic disc pack. At the start of the next computing session the machine could take up the computations where it left off without loss of more than about 30 seconds of computing time. This facility enabled the storm studies program to be operated during intermittent periods and in this way to exploit otherwise unused computer time.

Group-weighting of data and constant improvements of computer techniques also helped to reduce computer time. Continuous effort to reduce time was essential to ensure that all 170 storms could be analysed within a reasonable period. The most time-consuming procedure was that in which each element of the matrix had to be calculated for each data point.

In Appendix B, a technique¹⁵ is described in which advantage is taken of the fact that only the fundamental elements of the matrix need be evaluated; after these elements had been located in the matrix, corresponding identical elements could be subsequently filled in and conventional procedures then followed to solve for the coefficients.

With the aid of this technique analysis of a typical storm for which there were, say, 800 observations spread over an area of about 50,000 square miles, absorbed approximately $1\frac{3}{4}$ hours of computer time - about one hour being required to fit the percental surface and three-quarters of an hour to compile the isohyetal map and tabulate the depth-area-duration relationship.

To fit a sixth-order percental surface to the observations of the aforementioned storm, without employing group-weighting and properties of the matrix, would require approximately ten hours of computer time.

By employing the group-weighting technique the computer time would be reduced to approximately four hours.

2.12 Large-area storms library

Once the methods adopted for analysis had been streamlined the data for the selected large-area storms were processed and the results placed in files - one for each storm - to comprise a library. Details of the procedures followed and computer programs used in preparing the library of storm documents are outlined in Appendix C. A typical computer print-out of a storm analysis appears in Appendix D.

Presentation of the results of each storm analysis takes the following form :

1. A map showing the adopted boundary of the storm data and the boundaries of the storm subdivisions .
2. In respect of each subdivision :
 - (a) computer print-out of:
 - (i) data to be analysed,
 - (ii) distribution of group-weighting,
 - (iii) coefficients of polynomials representing surface fitted to percentals,
 - (iv) various statistics as described in Appendix A,
 - (v) percental values at quarter-degree grid intersections throughout the area covering the subdivision;
 - (b) isopercental pattern drawn from data in 2(v);

- (c) tabulation of selected sections covering the storm area for which depth-area-duration relationships are to be calculated;
 - (d) computer print-out of :
 - (i) hyetal values on same basis as 2(a)(v);
 - (ii) depth-area-duration tables;
 - (e) isohyetal map drawn from data in 2(d)(i).
3. Isohyetal map of the entire storm, provided such storm was considered to be one of the severest recorded in the region.

The depth-area-duration tables referred to in 2(d)(ii) comprise one tabulation for each relevant strip and its mean annual precipitation subdivision. In Chapter III the conclusion is reached that, since depth-area-duration tabulations for storms covering very large areas would be of little value for design purposes, it would be necessary to divide the country into reasonably homogeneous regions with subdivisions based on mean annual precipitation. The regions are areas confined by convenient meridians and parallels, referred to as strips, and for each region depth-area-durations are housed in separate files in the storms library.

2.13 Summary

Members of the Unit selected one hundred and seventy large-area storms from records at the Weather Bureau. Information for each station within the selected storm boundary in the form of station number and precipitation for six days embracing the storm event was punched on cards ready for analysis by computer.

Because of the complexities associated with generalizing either Thiessen polygon or linear interpolation methods for computer application - particularly to account for stations at which data were missing - a method was to be preferred that comprised computer fitting of a smooth surface describing the percental pattern of the storm.

Sixth-order polynomials having one dependent and two independent variables were successfully fitted by the method of least squares to observed rainfall data expressed as percentals. To preserve accuracy, it was found necessary to subdivide large storms into areas not exceeding 50,000 square miles.

By allowing the isopercental surface function to operate on the mean annual isohyetal map held in storage readily accessible to the machine, an acceptable isohyetal map of the storm could be reproduced and, by integration processes, the average storm mass curve and depth-area-duration curves could be derived therefrom. The depth parameter of the depth-area-duration relationship is the depth of precipitation equalled or exceeded. From this relationship isohyetal

lines can readily be drawn for a design storm.

Expression of depth of precipitation as an average over the catchment, for unitgraph applications, is referred to in Chapter 111.

The results of analyses of the data of 170 major large-area storms constitute a storms library housed by the Hydrological Research Unit.

With minor amendments, the surface-fitting techniques developed can aid not only flood hydrograph determination but also operation of flood warning systems.

C H A P T E R 111

DEPTH - AREA - DURATION - FREQUENCY ANALYSIS

Where the likelihood of hazard to life or intolerable damage to property is remote, either a calculated risk may be accepted that extreme conditions will not occur during the design life of a structure or the hydraulic capacity may be set such as to minimize total annual costs of construction and of repair or replacement of the structure, including costs of recompense for damages resulting from hydraulic inadequacy or failure. These criteria imply a statistical approach - a determination of the frequency distribution of flood discharges¹⁶ and hence of storm rainfall in order that risks may be calculated or annual costs of damages estimated. The summed costs of repair, replacement or recompense can be estimated by multiplying the costs of such eventualities by the average annual frequency and the results incorporated in a hydro-economic analysis.

Statistical methods may be employed provided the data are stationary, statistically independent and homogeneous. In this Chapter, the degrees to which these prerequisites were satisfied are discussed and development of a technique for introducing the frequency parameter into the analysis is outlined. The resulting depth-area-duration-frequency relationships are presented in a form suitable for design purposes.

3.1 Stationarity

Kokot¹⁷ examined Southern African climatic data covering the period from early historical times up to 1946 and concluded that the

violent fluctuations of rainfall that had been experienced were characteristic of the climate. In some localities there had been a decreasing rainfall while in others rainfall had increased but, taken as a whole, there was no general trend of changing rainfall pattern during the period studied. The variations that have occurred have been largely oscillatory in character and do not indicate any medium term change of trend. It can accordingly be assumed for the purposes of an engineering study of this type that rainfall data are reasonably stationary and will remain so in the future.

3.2 Homogeneity

Storm data derived from different parts of the country are obviously not homogeneous and must be grouped for statistical analysis under regions within which homogeneity might reasonably be expected to hold. The need to subdivide the country into homogeneous storm regions exists not only from the point of view of statistical analysis but also from the point of view of defining the extent to which storms may be transposed in design flood determinations. Subdivision of the country to satisfy the homogeneity conditions can therefore best be discussed under the heading of storm transposition. The question of statistical independence is dealt with much later in this Chapter in discussion of extreme value analysis of depth-area-duration relationships.

3.3 Storm transposition

Two problems arise in storm transposition; they are, first, the definition of meteorologically similar regions within which storms can legitimately be transposed and, secondly, determination of the degree to which the orientation of a storm pattern may be changed to create critical runoff rates and volumes¹⁸. Major orographic barriers would represent obvious limits to transposition, as would be strikingly illustrated by a plot of mean annual precipitation against elevation in South Africa. One might also be guided by consideration of the causes of major storms, e.g. whether frontal or cyclonic. Another clue would be the fact that areas of low mean annual precipitation are less likely to experience the same number or type of storms than areas of high mean annual precipitation. As a large percentage of the mean annual precipitation in most parts of South Africa is generally made up of a relatively small number of severe storms, it may be concluded that an area of low mean annual precipitation experiences either lower frequency of occurrence of severe storm events or lower precipitation per storm event than an area of high mean annual precipitation, or both. It would seem that there could be little justification for transposition of storms between localities which differ markedly in mean annual precipitation.

Clearly the limits within which storm transposition would be permissible provide the basis for determination of boundaries of homogeneous regions and these would be defined not only by orographic factors but by ranges of mean annual precipitation. From examination

of the isohyetal map in relation to the orographic boundaries of the country it was decided to recognise four categories of mean annual precipitation, viz. 0-250, 250-500, 500-1000 and 1000+ mm.

3.4 Regional subdivision

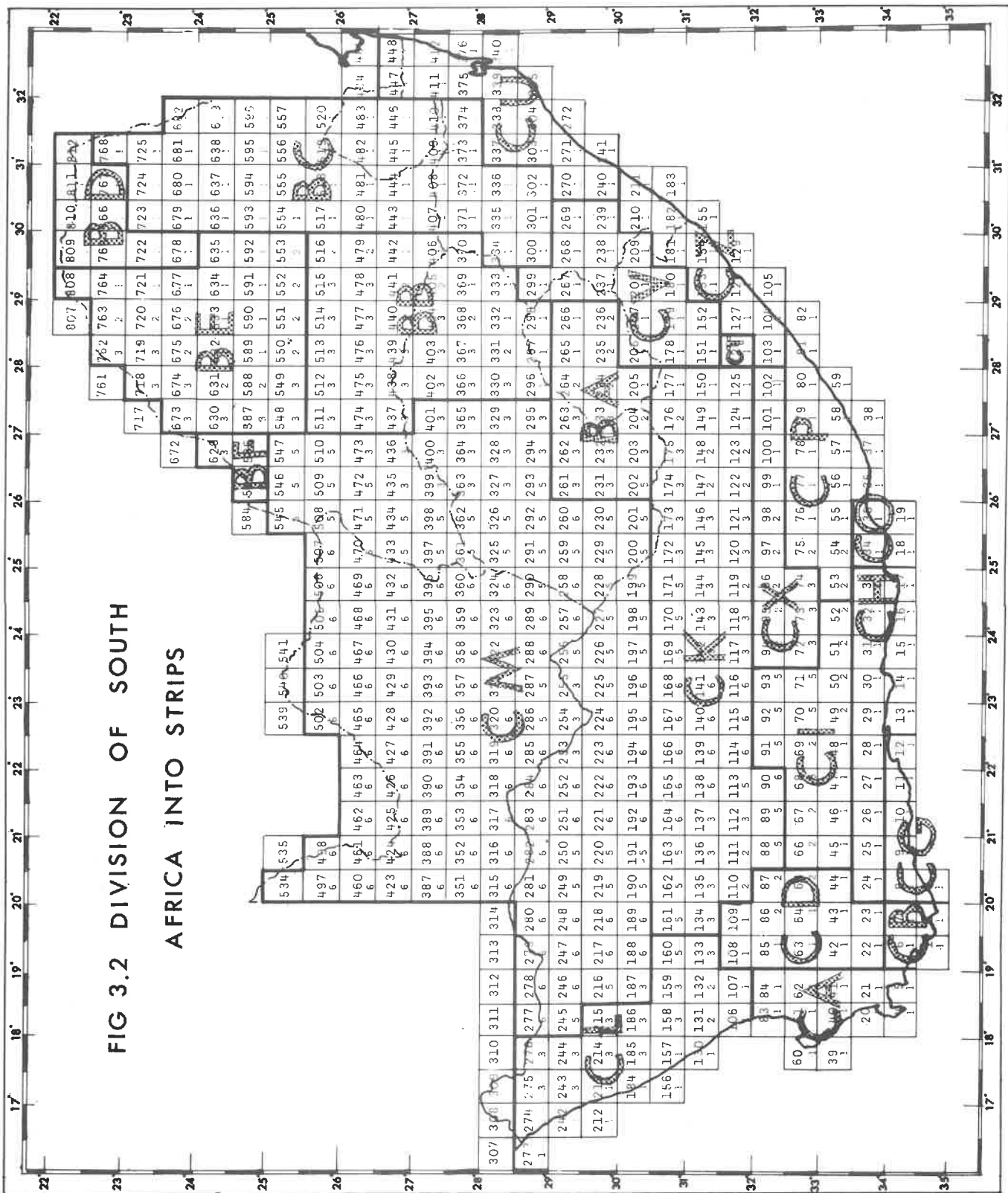
In general, the orographic boundaries coincide with the main mountain ranges and escarpments and these in turn are defined by one or other of the four mean annual precipitation ranges selected.

It would have been possible to delineate the regions and sub-regions on a map and either add the appropriate storm region code to all cards of the basic decks or assign catchment code numbers to the regions. The first process was considered impracticable because of the possibility of later redefinition of regional boundaries (which was in fact found desirable during the initial stages of the depth-area-duration analyses) and because of subjectiveness in the selection of storm regions. A prerequisite for the alternative procedure was that the catchment codes were to have been punched on the cards of the basic deck before this analysis got under way. In the event, however, this did not happen and, at time of writing, the punching of the cards had still not been completed.

The manner of storing the data in the computer is such that the machine can readily recognise the boundaries of a "section" and of a range of mean annual precipitation and so the country was broken down, as shown in Fig. 3.1 into 15 regions each of which was further subdivided according to the boundaries of the selected ranges of mean

FIG 3.2 DIVISION OF SOUTH

AFRICA INTO STRIPS



annual precipitation, viz. 0-250, 250-500, 500-1000, 1000+ mm, to form 29 regions and sub-regions in all.

As shown in Fig. 3.2, sections were grouped in strips chosen in such a way that the data could be readily categorized in regions. The computer was programmed to calculate depth-area-duration tabulations for each mean annual precipitation category within the relevant strip. Compilation of depth-area-duration tables from different strips but from the same mean annual precipitation category, see Fig. 3.3, resulted in a depth-area-duration tabulation for each regional subdivision.

In some sub-regions, mainly in the South Western Cape, where the isohyetal gradient is very steep, subdivision according to the selected range of mean annual precipitation gave rise to several diminutive sub-regions, and to avoid this the range was increased from 250 mm to 500 mm steps in this part of the country.

Depth-area-duration relationships, as described in Chapter 11, were derived for each sub-region and the results were incorporated in a set of regional storm files.

3.5 Regional analysis

It is assumed that each depth-area-duration graph for a given sub-region is applicable to any part of the sub-region, provided account is taken of characterisation and orientation of storms within the region. For instance, it is argued that a major storm

FIG 3.3
RELATIONSHIP BETWEEN STRIPS AND
SUB-REGIONS

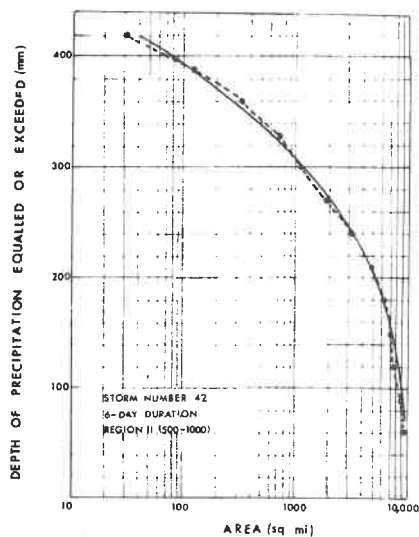
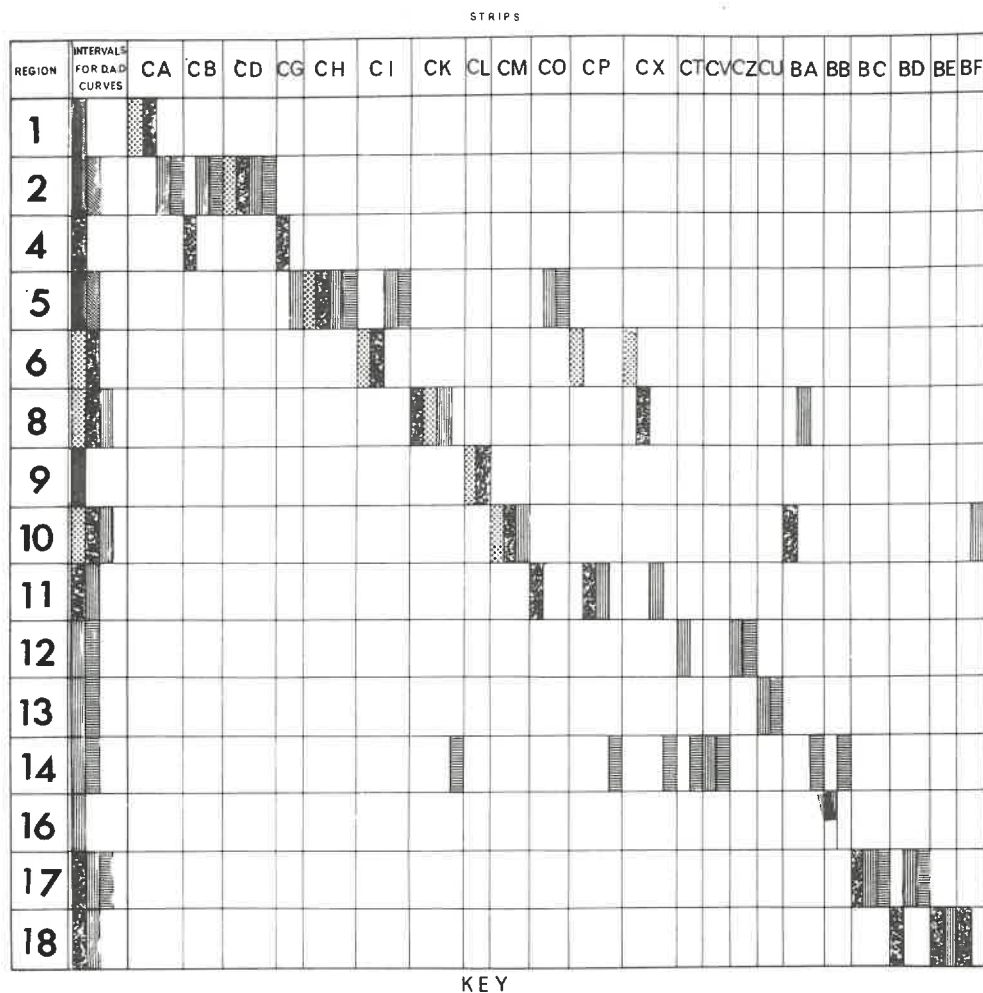


FIG 3.4 DEPTH-AREA RELATIONSHIP
DERIVED BY EYE AND BY COMPUTER

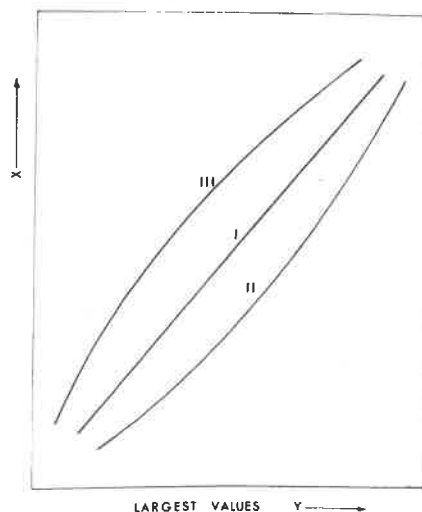


FIG 3.5 TYPIFYING THREE EXTREME DISTRIBUTIONS

observed in one part of a sub-region could just as well have occurred anywhere within that sub-region but possibly with a different shape or orientation.

For design purposes, given area and duration for a subdivision, it is desirable to assign a frequency of occurrence to a depth of precipitation. Within most sub-regions depth-area-duration graphs for as many as twenty storms could be constructed - in general, sufficient to form the basis of frequency analyses.

It can readily be appreciated that there is a tremendous amount of routine work involved in ranking precipitation values for appropriate areas and durations within each sub-region. Resort was therefore had to the computer, which was programmed to fit by least squares to each depth-area tabulation a parabola of the form

$$z' = a x^2 + b x + c \quad \dots\dots\dots 3.1$$

where z' stands for $\log z$ and

where a , b and c are the coefficients, x the depth of precipitation and z the area. Depths of precipitation were calculated from the parabolic equations and ranked by the computer in descending order of magnitude, independently for each selected area, duration and regional subdivision. Details of the program are presented in Appendix C. In Fig. 3.4 a typical depth-area relationship interpolated by eye is compared with the computed parabola derived from the same tabulation. Differences can be seen to be negligible in the light of the underlying assumptions and inherent observational errors.

3.6 Extreme value analysis

Extreme value analysis entails essentially the assignment of a probability of occurrence to each ranked event and the fitting of a probability distribution to the ranked events. Probability papers form a valuable tool for statistical analysis. The aim in the construction of probability papers is the transformation of probability distribution to a linear function of the variate. Choice of a specific probability paper implies acceptance of the distribution for which the paper was constructed.

Various ways of assigning probability values or plotting-positions have been suggested but, for extreme value analyses of rainfall data, use of the Gumbel theories seems to offer an acceptable approach.

The following discussion on extreme value theory is presented with the object of clarifying some questions that may arise from its application to storm studies and is an abbreviated form of a discussion of extreme value theory presented, with emphasis on droughts, in a dissertation by Pearce¹⁹. Early development of the theory started from the assumption that the initial distribution of the observations was 'normal'. Extreme value theories for initial distributions other than 'normal' and ones that are unknown were developed after much research had been carried out by von Mises²⁰, Pearson²¹, Gumbel²², Fisher²³, Frechet²⁴, Gredenko²⁵. It was noted that the largest values taken from different initial distributions sharing a common property may have a common asymptotic distribution.

If the initial distribution of, say, daily depths of precipitation were known, a knowledge of the statistical theory of extreme values would lead to a formulation of the exact distribution of storm rainfall. However, the initial distribution is not known and is unlikely to be easily defined because of such difficulties as the interdependence of consecutive events, but mathematical theories can nevertheless be used for the construction of extreme value probability functions in situations where the underlying distribution is unknown.

In the study of high extremes, the upper tail of the initial distribution is of major concern; behaviour at this end may be of three kinds²⁶:

Type 1 The probability function may be unlimited to the right (for the largest value), but may approach unity for increasing values of the variable in the same way as an exponential function 1^{-x} approaches zero. Such functions are said to be of the exponential type; they possess all moments.

Type 2 The initial distribution may be unlimited to the right but may have such a long tail that high moments diverge. Such distributions are of the Pareto type or, if symmetrical, of the Cauchy type.

Type 3 The initial distribution may be limited to the right, i.e. the probability function approaches unity at a specific value of the variable x .

Probability paper was initially constructed to suit the first probability function but suitable transformation of the independent variable x can render the use of such paper valid for all three distributions. Probability is expressed in terms of a reduced variate, y , which is then plotted linearly on the abscissa, and the criterion for acceptance of a type 1 function is a fit of observed extremes to the straight line:

$$x = u + y/\alpha$$

where in all cases $x = u$ corresponds to a probability of $\frac{1}{e} = 0.36788$ and $\alpha > 0$. The resulting equation, which expresses Gumbel's reduced variate in terms of recurrence interval, T , is

$$y = \ln (- \ln (1 - 1/T (x))).$$

Transformations of x provide the second and third types of distributions.

In general, the criterion for choice of distribution is based on the nature of the transformation and for large values can be specified as follows :

If the largest observed values when plotted on extremal paper scatter about a straight line, the first type of distribution might be presumed to apply. If the points fit

a curve concave (upwards) (downwards) the (second) (third) type would be appropriate. Fig. 3.5 illustrates these criteria for choice of distribution.

Storm precipitation depths for various areas, durations, and sub-regions were plotted in the manner illustrated in Fig. 3.6 to ascertain which distribution would be the most appropriate and as may be seen the trends differed from one set of data to another. It was concluded that sampling was not adequate to permit the distribution to be clearly defined; the tendency ranged through all three distributions. Ways of overcoming this difficulty are discussed later in this Chapter.

Plotting positions

Extremal paper has a natural scale for the observed variate x , (in this context, depth of precipitation), and as horizontal axis a non-linear scale in T , the recurrence interval, such that the reduced variate, y , would plot to a linear scale. The reduced variate, y , is a function of probability or recurrence interval and it is therefore necessary to assign to each event a recurrence interval in order to define its plotting position. The return period or recurrence interval, $T(x)$ is the average interval between events of magnitude equal to or greater than x , and is defined from the probability $F(x)$, which is the probability of occurrence of a value equal to or less than x , as follows :

$$T(x) = (1 - F(x))^{-1}$$

Several plotting position formulae are in existence and are discussed by Peirce¹⁹, who concludes that the most practicable and logical is that given by Weibull's formula, viz :

$$T_m = \frac{N+1}{m}$$

where T is the recurrence interval in years,
 m the rank in the descending array, and
 N the number of values in the array, i.e. the
 number of years of record analysed.

The discussion may be summarized thus :

- (a) By means of some acceptable formula, assign probabilities to ranked values ' x ' of the sample. Unless there are special circumstances Weibull's formula is considered the most suitable.
- (b) Gumbel's reduced variate can then be used for scaling.
- (c) Choice of one of three extreme value distributions exists, see Fig. 3.5. Following steps (a) and (b) plot, on correctly scaled paper, reduced variate on horizontal axis and variable x on vertical axes (natural scales). Only high extreme conditions are considered in this test.

- i) If the data are found to be scattered about a straight line, the Type 1 extreme value distribution applies,
- ii) If the data are found to be scattered about a line concave upward, the Type 2 extreme value distribution applies, and
- iii) If the data are found to be scattered about a line concave downward, the Type 3 extreme value distribution applies.

The appropriate transformations for each of the above distributions can be found in Péirce's dissertation¹⁹ and in papers by Gumbel^{26,27}.

3.7 Extreme value analyses applied to depth-area-duration data

The prerequisites of homogeneity and stationarity of data were discussed earlier and were shown to be satisfied but some attention to statistical independence of events to be analysed is needed before proceeding further with the analysis.

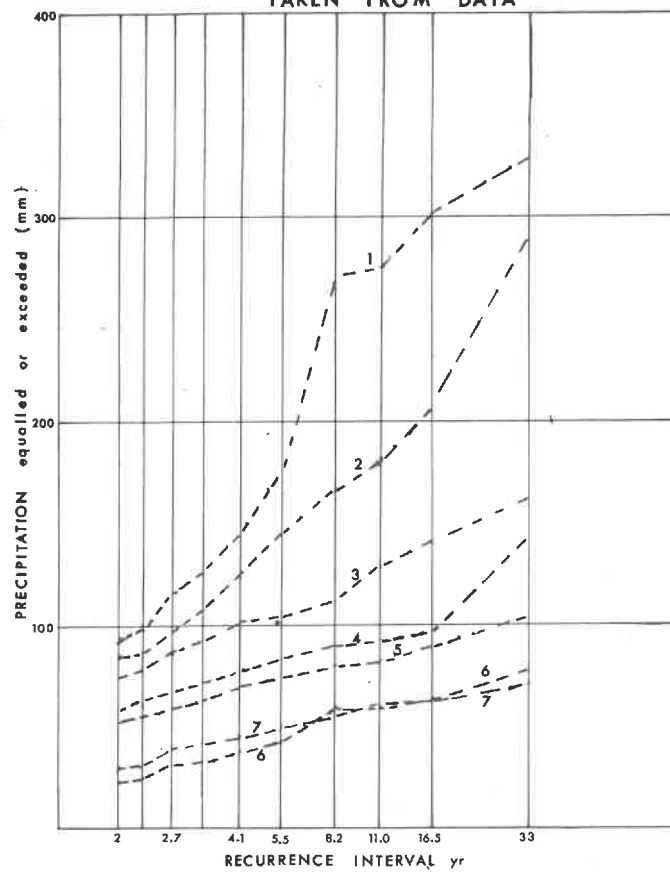
Although the maximum was not abstracted for each year of record in each sub-region, it was presumed that storms selected for analysis contained the maximum events that had occurred during the period and that therefore N could be assigned the value 32 years rather than a value equal only to the number of events analysed.

As discussed in Chapter 11, the storms selected for analysis were major, distinct events. It is a matter for conjecture whether the onset or magnitude of a storm is influenced by the occurrence of a storm say a week beforehand. In selecting for analysis events such as floods and droughts (which are resultant rather than causative events) it is usual to leave a minimum time period between events to ensure mutual independence. In this study the storm events are deemed indeed to be independent events. Thus, for any one sub-region there may appear among the data depth-area-duration curves of storms that occurred during the same year. Selection of all the precipitation values from the available curves associated with a sub-region, for given area and duration, yields a set of statistically independent precipitation events. These can be ranked in descending order of magnitude and extreme value theory could then be applied to this ranked set of precipitation values.

Theoretically, the sets of ranked precipitation values come from the same population and hence should conform to one of the three possible extreme value trends. It was found, however, that they did not. The reason can be attributed to inadequate sampling, accentuated by the fact that a maximum value was not in fact abstracted for each year of the analysis period.

As no specific trend could be established it was clear that extrapolation of the curves about which the data scattered would not be permissible. Means whereby extrapolation might, however, be meaningful are discussed later in this Chapter.

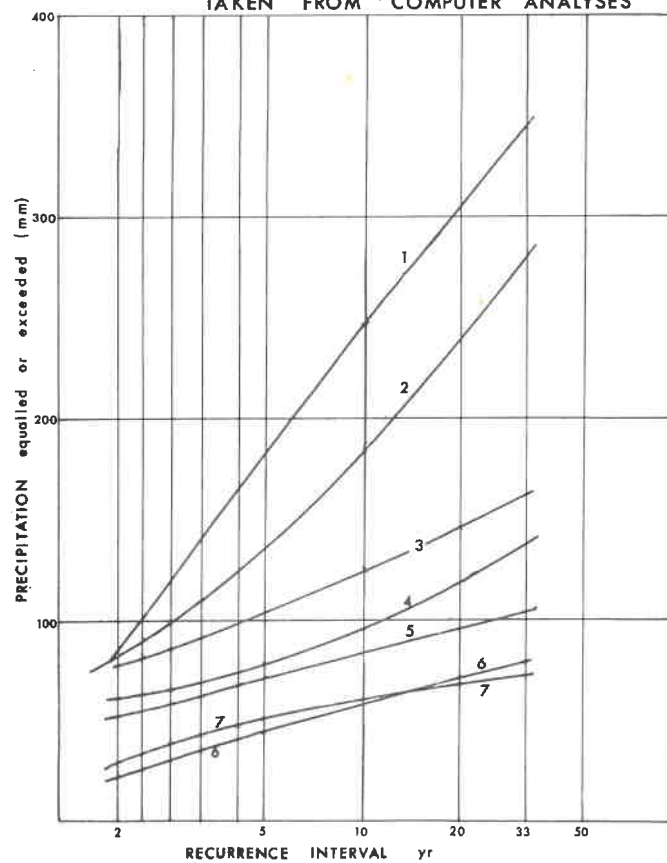
FIG 3.6 TYPICAL PLOTS OF DEPTH - RECURENCE INTERVAL
TAKEN FROM DATA



No.	Region	Duration
1	13 1000+	3 day
2	12 500-1000	3 day
3	10 500-1000	4 day
4	5 500+	1 day
5	8 0-250	5 day
6	18 250-500	1 day
7	10 0-250	2 day

AREA 1000 sq mi

FIG 3.7 TYPICAL PLOTS OF DEPTH - RECURRENCE INTERVAL
TAKEN FROM COMPUTER ANALYSES



Although the samples were poor, it was nevertheless felt that a curve fitted to the data would serve to permit extraction of precipitation values for different durations corresponding to suitably spaced recurrence intervals.

As discussed in Appendix C, the computer was programmed to fit to the data plotted on Gumbel paper parabolas of the form :

$$x = a y^2 + b y + c$$

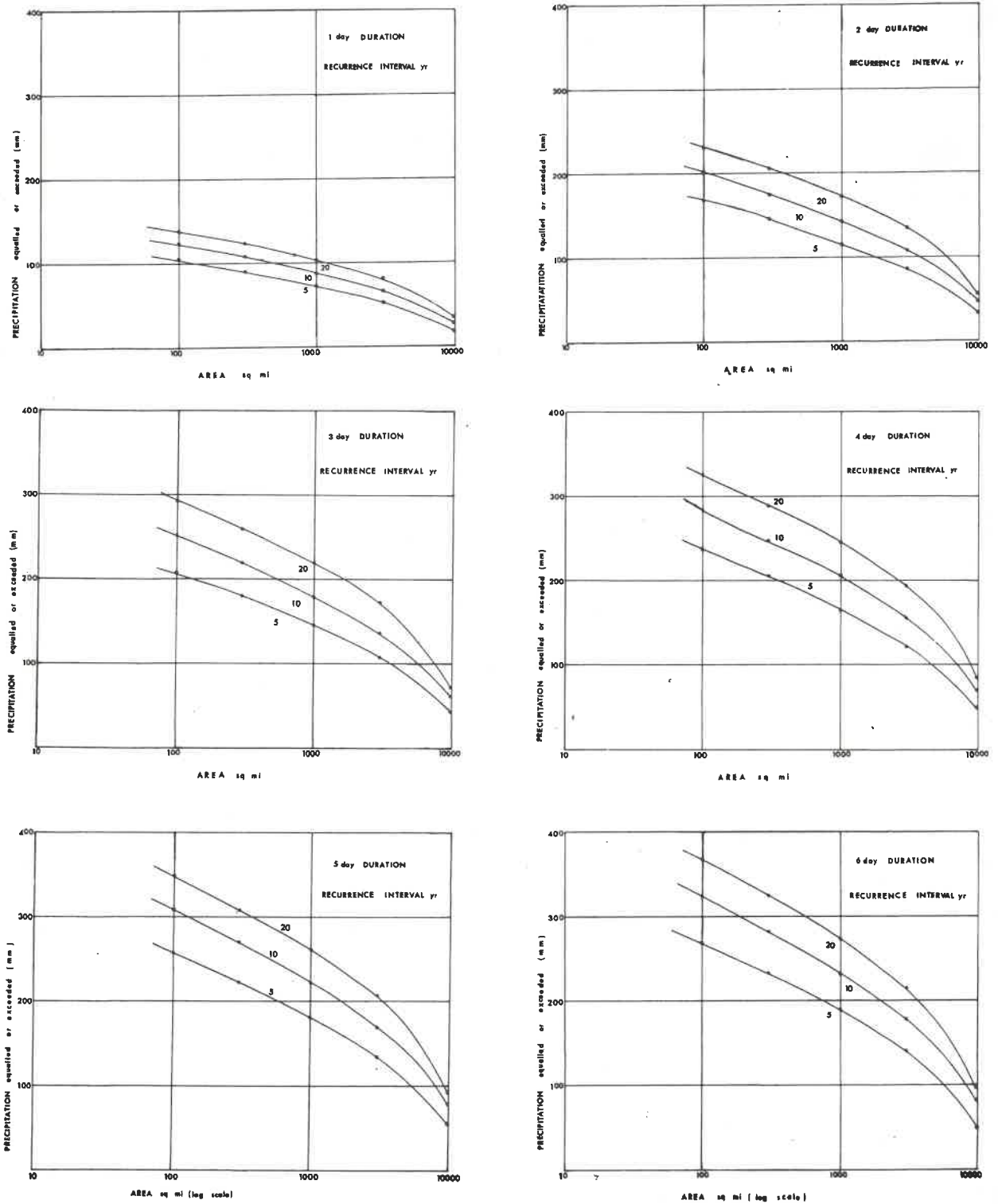
in which a , b and c are constants, the reduced variate, y , is the independent variable and precipitation, x , the dependent variable.

Typical results are shown in Fig. 3.7. The computer was programmed to print out calculated precipitation values at the desired interpolated recurrence intervals.

3.8 Coaxial diagram

For each sub-region precipitation values were computed for recurrence intervals of 5, 10 and 20 years, for each duration (one to six days) and for each selected area (100, 300, 1000 sq. miles up to the total area of the sub-region). From the results a family of depth-area-frequency curves for each duration could be drawn on semi-log paper as in Fig. 3.8, with area (log scale) on the horizontal axis, precipitation on the vertical axis and recurrence interval as parameter. From Fig. 3.8 it may be seen that the curves for the different durations, each curve representing a separate recurrence interval, display similar

FIG 3:8 DEPTH-AREA CURVES FOR SELECTED RECURRENCE INTERVALS (Region 11 (500-1000))



characteristics. To facilitate handling of the results, the data were replotted coaxially as shown in Fig. 3.11. Explanation of the construction of the coaxial diagram follows.

As shown in Fig. 3.9(a) the three-day depth-area-frequency values for a region are first plotted on semi-log paper but the parametric lines denoting recurrence interval are omitted. The vertical axis (precipitation to natural scale) is then rotated in a counter-clockwise direction through 90° . If precipitation is now read on the new horizontal axis a 45° line in the second quadrant will represent the three-day duration parameter. The so-called rotating-an-axis process can be clarified thus :

An equation $y = x$ plotted on graph paper, both axes to the same natural scale, describes a 45° line through the origin. If the independent variable ' x ' represents precipitation depths, the dependent variable ' y ' will then represent the same precipitation depths. Three-day precipitation depths can thus be read off the rotated axis via the 45° line in the second quadrant.

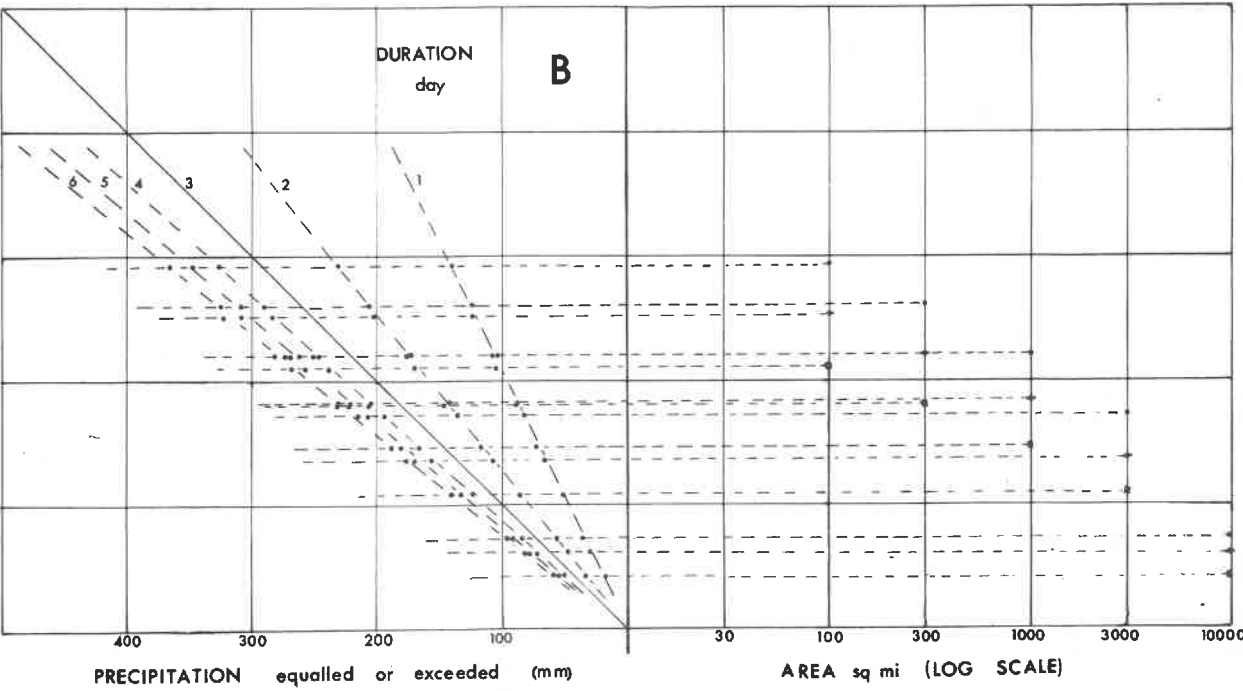
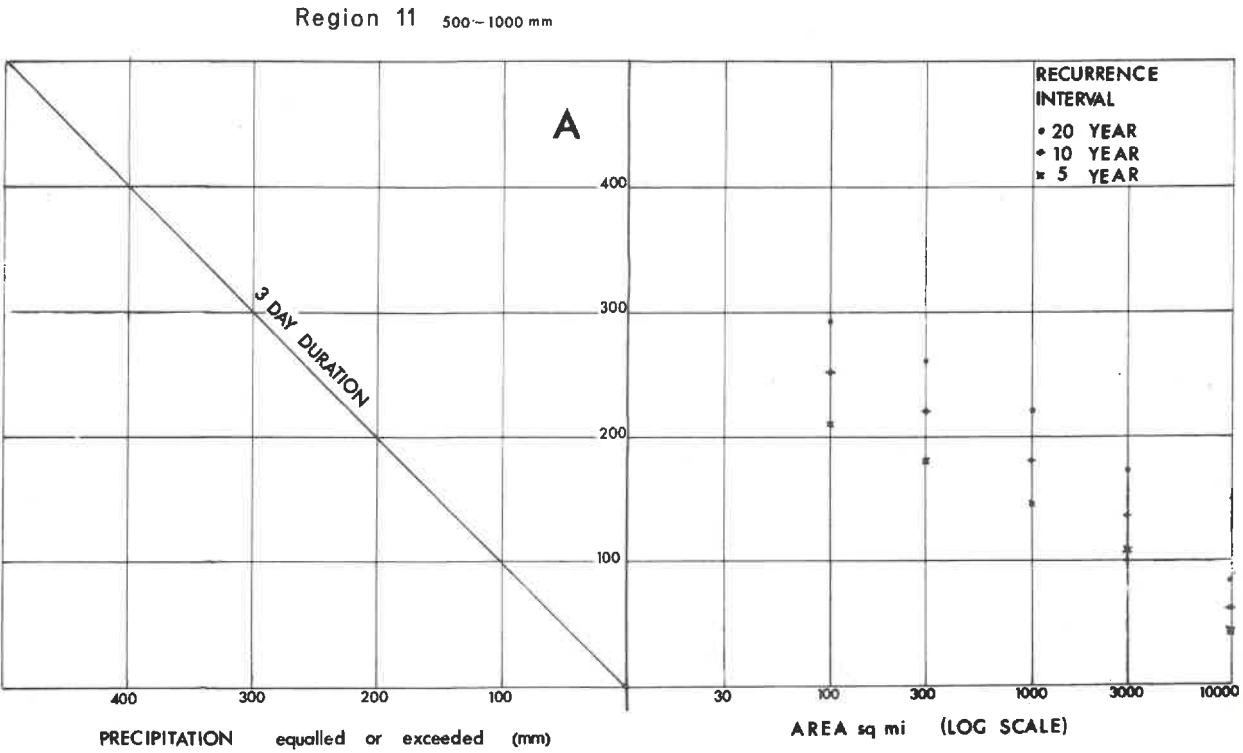
Conversion from three-day depths to depths appropriate to other durations requires establishment of lines of the form

$$y = ax + b$$

in the second quadrant to provide a suitable scaling factor.

The constants a and b depend on the scaling desired; ' x ' represents three-day depths and ' y ' the depths corresponding to other durations.

FIG 3.9 DEVELOPMENT OF TWO QUADRANT COAXIAL DIAGRAM



The rays $y = ax + b$ are established graphically for the various durations in the following manner. Points plotted in the first quadrant for three-day depths would represent the depth-area-frequency relationship for all durations if a suitable scale scaling factor in the second quadrant exists. In order to plot corresponding depths for all durations a horizontal line is drawn through each plotting position in the first quadrant and extended into the second (left-hand) quadrant, see Fig. 3.9(b). The manner in which first estimates of the position of the plotted points on horizontal lines are located in the second quadrant is depicted in Fig. 3.9(b).

Once all plotting positions for all durations have been filled in the second quadrant, straight-line rays are interpolated by eye. The scatter about these lines is generally narrow. Scatter in the second quadrant can usually be reduced by slight adjustment of points in the first quadrant. After the scatter has been minimized the family of recurrence interval lines can be drawn in through the corrected positions in the first quadrant. These adjusted points in the first quadrant are then replotted on Gumbel paper, Fig. 3.10, to permit precipitation values appropriate to 50- and 100- year recurrence intervals to be extrapolated. These extrapolated values are then transferred to the first quadrant and dotted lines of recurrence intervals drawn, Fig. 3.11. It was felt that the inconsistencies in the data in regard to shape of the frequency curves would be ironed out by super-imposing several duration analyses. The resultant plots on Gumbel paper could be extrapolated with

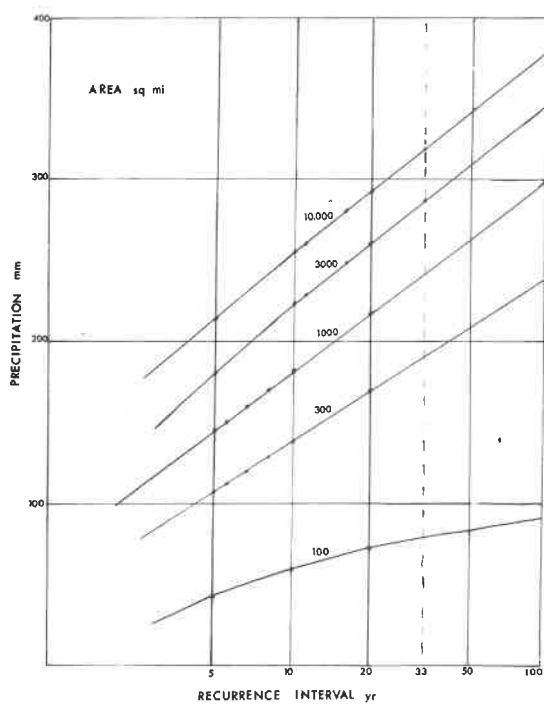
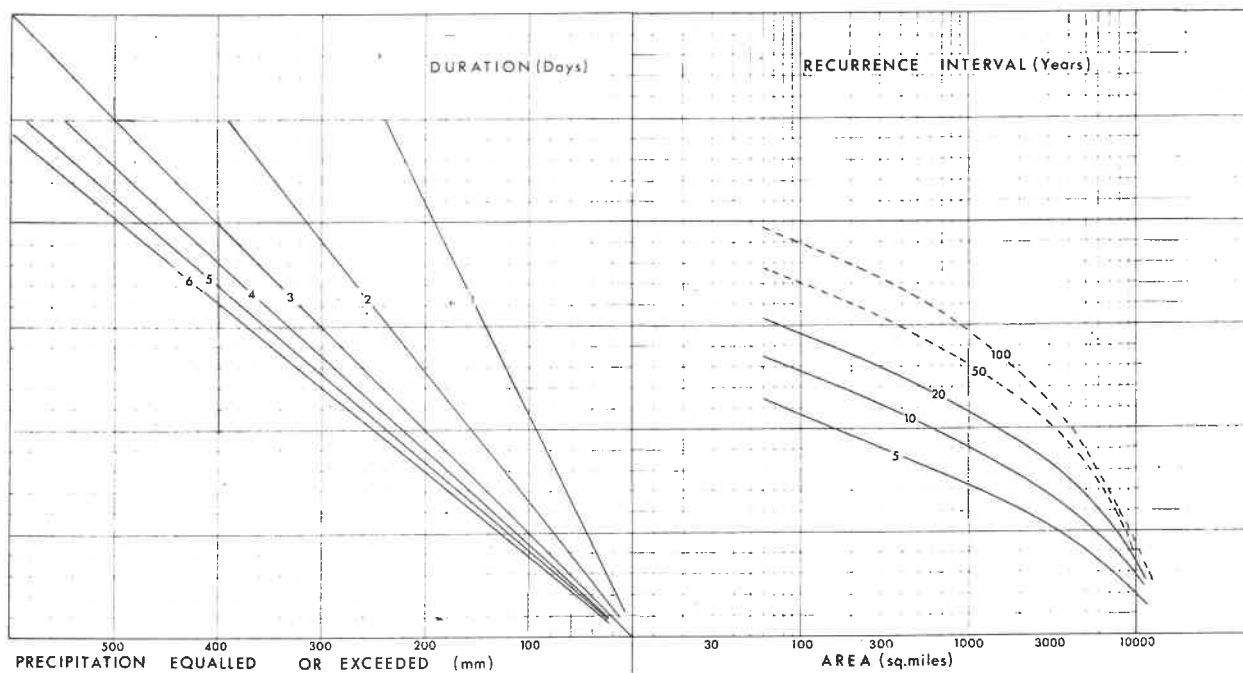


FIG 3.10 EXTRAPOLATION OF DEPTH —

RECURRENCE INTERVAL RELATIONSHIP

Region II 500-1000 mm

FIG 3.11 COAXIAL PLOT : DEPTH-AREA-DURATION-FREQUENCY (Region II 500-1000mm)



reasonable confidence as the points plotted suggested straighter lines than was the case previously when the frequency curves for each duration analysis were considered separately.

3.9 Average depth of precipitation

Up to now the precipitation parameter has been interpreted as a value equalled or exceeded. Diagrams based on this interpretation are appropriate to design storms for use in hydrograph synthesis by routing procedures. On the other hand, where a design storm is to be compiled for use with unit-graph procedures, it is the average depth of precipitation over the catchment that is needed, and the assumption is made that excess rainfall is uniformly distributed in time and space. Values of precipitation equalled or exceeded are not of direct value for such applications and the user would be put to considerable inconvenience in converting the results to the required form, viz. precipitation averaged over area. It was felt wise therefore to provide in the coaxial diagram two further quadrants in which the conversions from value equalled or exceeded to value averaged could be performed. This is presented in Appendix F. Where averaged precipitation values are desired the procedure in reading of the coaxial diagram would then be as follows :

Start in the first quadrant at given area and desired recurrence interval proceed via pivot line in second quadrant to reach third quadrant where correction is made via recurrence interval curves and finally to fourth quadrant where the selected duration parameter is encountered; the resulting average precipitation is read on the horizontal axis.

3.10 Accuracy of coaxial plot

Because of the lack of a precise inter-relationship discrepancies are bound to arise in endeavouring to fit curves to the depth-area and depth-frequency tabulations. To gauge the error introduced in fitting the curves of the coaxial diagrams, depths of precipitation with associated recurrence interval values taken from the depth-area tabulation for each duration were plotted on the coaxial diagram. The error band was sketched in for each duration curve in the second quadrant and the values read off these error bands at convenient recurrence intervals are listed in Appendix E.

Cross-comparisons were made among coaxial plots so that inconsistencies could be ironed out. The diagram for sub-region 8 (500-1000 mm) was the only plot that had to be adjusted to conform with other plots. Too few values were available to warrant a frequency analysis for region 9 and region 17 (250-500 mm).

3.11 Summary

Gumbel's theory of extremes was employed to rank precipitations for selected values of area and duration, thereby permitting precipitation values to be calculated for desired interpolated and extrapolated recurrence intervals. Resulting depth-area-duration-frequency relationships were represented on a coaxial plot for convenient use by engineers in practice.

With unitgraph application in mind, means whereby a conversion from precipitation equalled or exceeded to precipitation averaged over area was incorporated in the coaxial plot.

The resulting coaxial diagrams - one for each sub-region - are presented in Appendix F. As a guide to selection of a suitable orientation of the design storm there appears on each diagram an isohyetal map of the most severe storm observed in the region. Also incorporated in the diagram for each region is a graph of PMP-area-duration, the development of which is discussed in the next Chapter.

C H A P T E R 1V

PROBABLE MAXIMUM PRECIPITATION (PMP)

For the design of important hydraulic structures, such as major dams and bridges, failure of which through the effects of storm might result in loss of life or intolerable damage, one would wish to estimate the probable maximum flood discharge to which the structure might be subjected. In a hydro-meteorological approach such an estimate would be reached through an attempt to predict the physical upper limit of precipitation on the catchment. It is the intention in this Chapter to put forward a technique whereby this physical upper limit, or probable maximum precipitation (PMP), can be estimated for a given area and duration of storm in various localities.

Some workers⁴ have argued that an upper limit of precipitation cannot be defined. They do not imply that, though it cannot be defined, such a limit does not exist. In fact, from consideration of the physics of the precipitation mechanisms, there can be no doubt that an upper limit must exist but, because of limitations of data and proven techniques, its estimation can only be rough.

PMP results from an optimum combination of moisture charge and precipitation efficiency, where the latter involves the rate of ascension and cooling of moist air, normally caused by wind convergence, low pressure and the influence of topography. An attempt to evaluate precipitation efficiency would call for numerous upper air soundings during storms.

In South Africa, however, such measurements have been made only on relatively few occasions and then only during latter years and at few stations, mainly aerodromes. In view of these limitations an approach to PMP based on evaluation of precipitation efficiency had to be shelved. Instead, the problem was approached on the assumption that near-maximum precipitation efficiency would most probably have been attained during at least one of the storms analysed within each region and, if a method could be found of determining and maximizing the moisture content that prevailed during all the storms analysed, PMP might be indicated by the envelope of the resulting maximized depth-area curves.

4.1 Evaluation of moisture content

Calculation of moisture content of the atmosphere from upper air soundings presents no great difficulty but, as mentioned, few measurements are available and so attention was shifted to development of procedures for calculating precipitable water content of a column of air from readings of surface temperature and pressure. There follows a brief resumé of a method by Pullen²⁸ which he based on modifications of conventional procedures.

Pullen made two basic assumptions : first, that the relationship between temperature and pressure in the atmosphere can be represented by the entropy equation for saturated pseudo-adiabatic changes and, secondly, that moist air obeys the ideal gas laws.

The equation from which moisture content is calculated is

$$M = \int_{p_1}^{p_2} \frac{-w}{g} dp \dots\dots\dots 4.1$$

where w is the average mixing ratio of the moist air in the atmosphere between altitudes where the pressures are p_1 and p_2 .

For saturated conditions the mixing ratio can be expressed as :

$$w_s = \frac{0.62197 f_w e_s}{p - f_w e_s} \dots\dots\dots 4.2$$

where e_s is saturated vapour pressure (mb) and f_w is a factor associated with the deviation in behaviour of moisture-laden air from that of an ideal gas, and which may be assumed to be unity since the deviations are small compared with those likely to be associated with the sweeping assumptions on which the method is based.

Pullen employed a simplified equation, suggested by Triegaardt²⁹, for saturated vapour pressure in terms of temperature :

$$e_s = C.10 \frac{At}{T+B} \dots\dots\dots 4.3$$

in which, according to Triegaardt, the constants have the following values :

$$A = 7.54613$$

$$B = 238.98272$$

$$C = 6.10938$$

Temperature values associated with decreasing pressures were calculated from given surface temperature and pressure values by

numerical integration of the equation for saturated pseudo-adiabatic lapse rate.

The equation takes the following form :

$$c_{pa} \ln \left(\frac{T_2}{T_1} \right) - R_a \ln \left(\frac{p_2 - e_{s2}}{p_1 - e_{s1}} \right) + \left(\frac{w_{sL}}{T} \right)_2 - \left(\frac{w_{sL}}{T} \right)_1 + C \bar{w}_s \ln \left(\frac{T_2}{T_1} \right) = 0 \dots 4.4$$

where $\bar{w} = \frac{w_{s1} \cdot w_{s2}}{w_{s1} + w_{s2}}$,

c_{pa} is the specific heat of dry air = 0.995×10^7 ergs per gm per $^{\circ}\text{K}$,

R_a is the gas constant for dry air = 2.8704×10^6 ergs per gm per $^{\circ}\text{K}$,

(temperatures are expressed in $^{\circ}\text{K}$)

and C is the specific heat of liquid water = 4.18×10^7 ergs per gm per $^{\circ}\text{K}$.

From the above equations, provided small pressure increments are recognized, precipitable moisture can be calculated for a column of air of unit cross-sectional area with base at ground level and top at an altitude where moisture content is negligible; this was taken to be at an altitude where the pressure has fallen to 200 mb.

As the atmosphere within the storm centre is seldom fully saturated, the temperature value adopted for the calculation should not be the dry-bulb temperature, but rather the dew-point temperature, i.e. the actual temperature at which saturation would occur.

4.2 Accuracy of moisture content estimates

The method was tested by comparing calculated moisture content values with those observed by upper air sounding. Examination of the moisture content values in Table 4.1 indicates the level of accuracy that can be attained by this method.

For calculation of moisture content from radiosonde data, Solot³⁰ has described a graphical method whereby the mixing ratio can be estimated from dry-bulb temperatures read from Smithsonian Tables³¹ and converted to specific humidity. It should be noted that calculation of moisture content from surface dew-points ignores the effects of possible atmospheric inversions, viz. temperature decreasing with altitude at a lower rate than the normal lapse rate, or temperature increasing with decrease of pressure. Neglect of such factors causes moisture content calculated from surface dew-points generally to be lower than when determined from upper-air soundings. The fact, however, that maximum moisture content values determined from maximum observed dew-point reading will be similarly affected implies that ratios derived by the two processes will be much the same.

Another aspect that required investigation before the method was adopted was whether the order of magnitude of the differences in moisture content determined by the two techniques would differ significantly over different climatic regions. Data for two stations were examined and a statistical procedure, details of which are discussed at the end of this Chapter, was employed to compare the differences. The fact that at sample stations of widely dissimilar

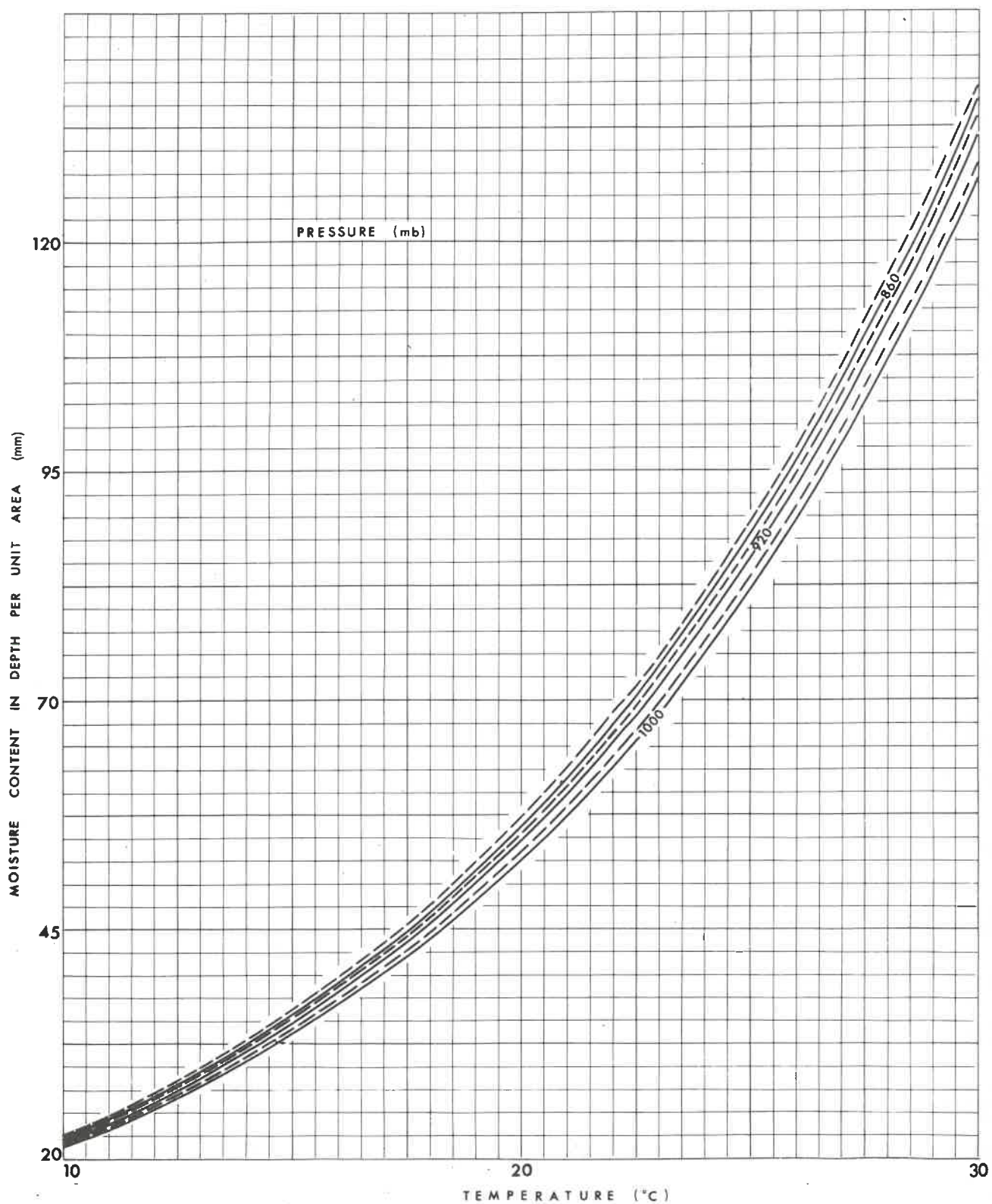
characteristics the differences were not significantly dissimilar allowed one to conclude that the same was true for moisture content data at other stations in South Africa.

4.3 Maximization of depth-area-duration curves

From the techniques described it was possible to calculate atmospheric moisture content for a range of surface temperatures and pressures and to plot the results as shown in Fig. 4.1. Pressures at any one recording station in South Africa seldom vary by more than 60 mb and from Fig. 4.1 it can be seen that in any event the moisture content difference for a 60 mb pressure change is only about 2 per cent. As surface pressure variations do not significantly affect the calculation of moisture content, standard geopotential pressure can generally be adopted for most climatic conditions. Thus, moisture content can be calculated with fair accuracy solely from surface dew-point readings. As wet- and dry-bulb temperatures are recorded at more stations than are atmospheric pressures, distribution of moisture content values based on surface dew-point readings is not as sparse as would have been the case had one to rely only on observations from pressure recording stations.

Within almost every sub-region it was possible to find a temperature recording station that had been in operation with relatively few breaks throughout the period of study. In those sub-regions devoid of suitable stations, records from stations in not too dissimilar neighbouring areas were employed, see Fig. 3.1.

FIG 4.1 MOISTURE CONTENT AS A FUNCTION OF PRESSURE AND TEMPERATURE
WHEN THE ATMOSPHERE IS SATURATED



At some stations there was only one but at others as many as four readings of dew-point per day. The average dew-point value for each day during a number of observed severe storms in each sub-region was calculated and the corresponding average atmospheric moisture content read directly from Fig. 4.1. For each sub-region the maximum dew-point recorded at a representative station for each month of the year was abstracted and the corresponding atmospheric moisture content was read from Fig. 4.1. The records are such that maximum dew-points observed during each month of the year could generally be ascertained throughout South Africa subsequent to the year 1949, but unfortunately only in few areas prior to that date.

The ratio of storm moisture content to maximum moisture content registered in the sub-region at the relevant time of the year was adopted as a basis for maximization. The procedure is detailed in what follows.

Calculated atmospheric moisture contents for each day of storm were examined to reveal the proportional decay of moisture content with time. In other words, the maximum 1-day, 2-day,, 6-day moisture contents were averaged and expressed as proportions of the one-day maximum. A typical moisture content decay pattern for each sub-region was determined by averaging.

The maximum one-day atmospheric moisture content during each major storm in a sub-region was then increased in proportion to the atmospheric moisture content calculated from maximum dew-points recorded during the corresponding month or adjacent month.

The assumptions were now made :

- (a) that a direct relationship exists between depth of precipitation and atmospheric moisture content, i.e. if during a storm the moisture content had been greater (smaller), the depth of precipitation would be proportionally greater (smaller) and
- (b) that proportional changes of moisture content based on point observations would occur throughout the sub-region.

Precipitation depth values in the 1-day depth-area tabulation for each severe storm were thereupon increased according to the aforementioned ratio of atmospheric moisture contents. Depth values in the 2-day, 3-day etc. depth-area tabulations were correspondingly increased according to the equation :

$$X_i = P R_i \frac{M_x}{M_c} T_i \quad \dots\dots\dots 4.5$$

where X is the maximized depth,

P is the 6-day depth,

R is the ratio of the i -th day depth to the total 6-day depth,

M_x is the maximum moisture content for the relevant time of the year,

M_c is the average 1-day maximum moisture content,

T is the ratio of the i -th day to the 1-day moisture content

and subscript i represents 2-day,, 6-day.

**FIG.4.2 MAXIMISED 3-DAY DEPTH AREA CURVES
FOR REGION 12 (1000+mm)**

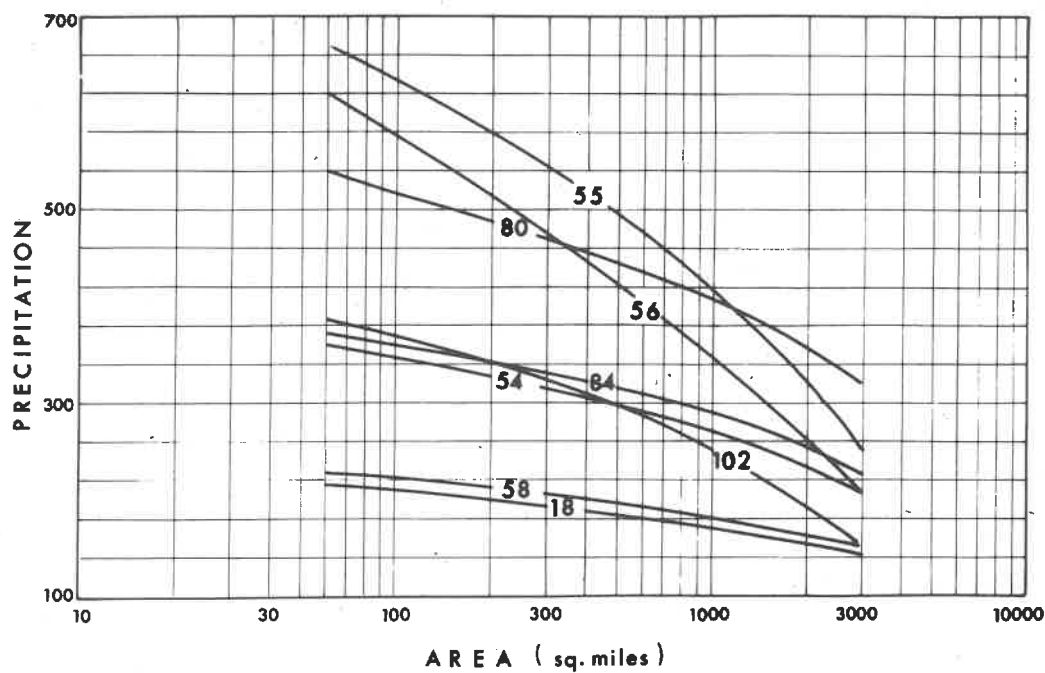
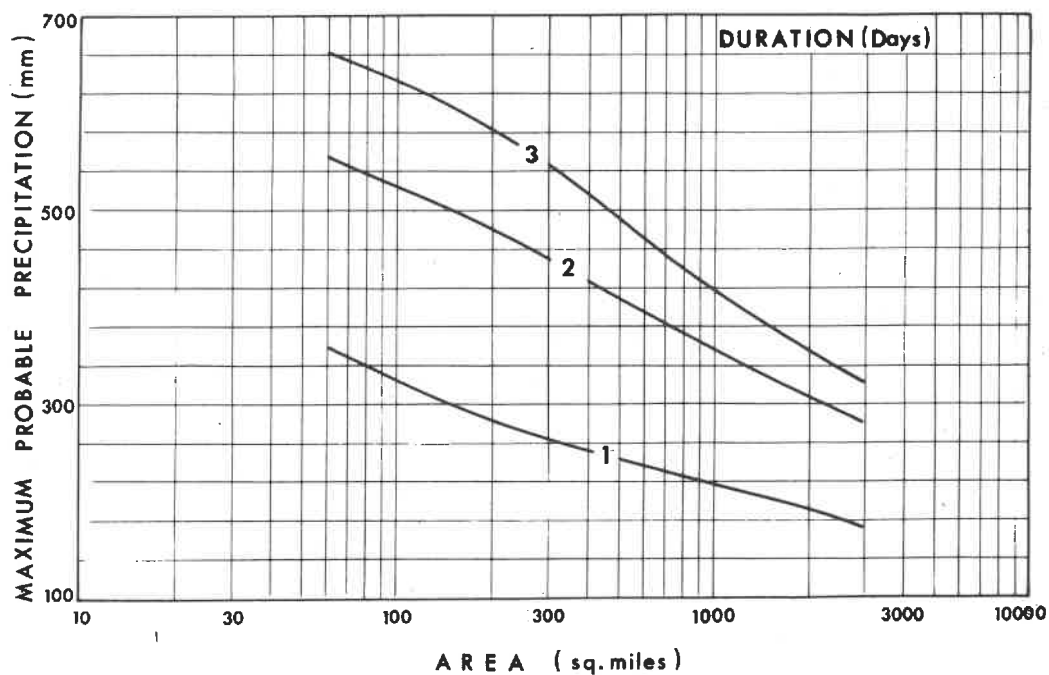


**FIG 4.3 MAXIMUM DEPTH-AREA CURVES
FOR REGION 12 (1000+mm)**



The maximized depth-area tabulations for each storm duration within each sub-region were plotted as in Fig. 4.2 and the upper envelope of depths for each duration was assumed to represent the PMP for the sub-region, as illustrated by Fig. 4.3. The PMP-area-duration curves for each sub-region are to be found in Appendix F.

4.4 Statistical analysis of moisture content differences at two stations

As mentioned earlier in this Chapter, it was necessary to investigate whether differences in moisture content estimated from different techniques would differ significantly at different stations. To ascertain whether atmospheric moisture contents at the Pretoria meteorological station differ significantly from those at Cape Town, a statistical test known as the "run test" was employed³².

The two samples of differences of moisture content were arrayed together and ranked. A run is defined as an unbroken sequence in one sample. The number of runs, d , was counted.

If the distribution of both samples is identical, d has an approximately normal distribution with mean :

$$\xi = \frac{2 N_x N_y}{N_x + N_y} + 1 \quad \dots\dots\dots 4.6$$

and variance :

$$\sigma^2 = \frac{2 N_x N_y (2 N_x N_y - N_x - N_y)}{(N_x + N_y)^2 (N_x + N_y - 1)} \quad \dots\dots\dots 4.7$$

where N_x is the number of values in the sample of x 's;
and N_y is the number of values in the sample of y 's.

If the distributions differ in mean or variance, d will be small and a 'left-tail test' is then applied.

The Pretoria sample, consisting of 11 values, and the Cape Town sample, consisting of 26 values (Table 4.1), yielded $\xi = 16.46$ and $\sigma = 6.21$. The value of d obtained from ranked values was 14, and hence the test statistic or distribution of the standardized normal variable is

$$Z = (d - \xi) / \sigma = (14 - 16.46) / 2.492 = -0.987$$

If a level of significance of 0.1, i.e. 90% confidence that the hypothesis is correct, the critical value of Z would be - 1.28. On the basis of this criterion, the hypothesis that differences in moisture content at the two stations come from the same population is acceptable.

4.5 Error in maximized depth-area-duration curves

The average standard deviation of 11.2 mm extracted from Table 4.1 might be viewed as a probable average error in calculation of moisture content from surface dew-point readings anywhere in South Africa. Error is attributable mainly to inability to take account of possible atmospheric inversion. The calculations which follow indicate that, because of inaccuracies in estimation of moisture content, the PMP-area curves as drawn for each sub-region might be

TABLE 4.1

Pretoria Station

Date	Moisture content (mm)		Date	Moisture content (mm)	
	Dew point	Radiosonde		Dew point	Radiosonde
5.2.59	37.2	44.0	18.12.59	43.9	40.4
6.2.59	39.4	46.4	15.12.59	45.6	51.7
7.2.59	38.7	47.5	24.12.59	35.2	42.5
8.2.59	39.0	47.5	17.3.59	42.7	43.8
9.2.59	38.0	48.1	27.1.59	43.9	49.3
10.2.59	40.5	43.6			

Cape Town Station - D.F. Malan airport

Date	Moisture content (mm)		Date	Moisture content (mm)	
	Dew point	Radiosonde		Dew point	Radiosonde
30.10.56	18.6	30.9	12.7.59	19.3	25.2
31.10.56	20.8	37.4	13.7.59	17.6	24.5
1.11.56	29.9	37.7	14.7.59	20.4	25.7
2.11.56	21.7	39.5	15.7.59	14.3	29.9
3.11.56	17.4	44.7	16.7.59	13.1	33.8
4.11.56	23.2	46.6	1.2.57	46.3	59.8
18.7.57	18.4	30.0	16.3.56	49.2	58.7
11.7.57	24.4	30.0	28.12.57	52.5	65.0
12.7.57	23.4	28.7	25.4.57	28.0	42.4
13.7.57	21.0	22.7	24.2.59	43.0	56.6
14.7.57	14.4	19.5	28.3.59	31.8	47.2
15.7.57	20.1	30.0	22.3.59	26.1	60.0
11.7.59	15.3	30.1	23.3.59	27.6	53.8

subject to errors of the order of 25%.

The multiplying factor involved in maximizing the depth parameter depends on where the error lies. Suppose the moisture content during a storm was equivalent to a depth of 20 mm and the maximum observed moisture content for the relevant time of year was equivalent to 60 mm, then maximization of the depth-area values would involve multiplying by a factor of 3. If, however, storm moisture content had been underestimated by 10 mm, the correct multiplying factor would be 2.33. For another storm the moisture content could well have been overestimated by 10 mm and the correct factor would be 3.5. It can be appreciated that there is an error band associated with each maximized curve. The fact that, as illustrated by Fig. 4.2, there is a spread of the maximized curves themselves can be explained as indicating that some storms were operating at low efficiency. It is reasonable to assume, however, that at least one of the storms would have been operating at or close to maximum efficiency. Accordingly, one might conclude that the upper envelope of the maximized depth-area curves would indeed represent the PMP-area relationship.

Although the analysis was performed for durations up to six days irrespective of storm duration, it is interesting to note from Fig. 4.3 that PMP of 5-day and 6-day durations in Region 12 do not exceed the maximum depths for 4-day durations. This was generally the case throughout the country.

C H A P T E R V

EXTENSION OF SMALL-AREA HIGH-INTENSITY

STORM ANALYSES

On the one hand the results of van Wyk's analyses of short-duration high-intensity precipitation relate to durations of up to one hour and areas of up to 300 square miles. On the other hand, the results presented so far relate to storm durations from one to six days and storm areas generally larger than about 2000 square miles. It follows that design storm diagrams are so far lacking for catchments having critical response times between one hour and one day. There is thus a gap in the time scale between one hour and one day and in the area scale between 300 and about 2000 square miles. The aim in this Chapter is to develop design storm diagrams to fill the gap.

Unfortunately, observational data in the gap are quite inadequate and one must therefore seek a basis for extrapolation of the results of either the small-area or the large-area storm studies.

At first glance it might be imagined that if the depth-area-duration relationship for a particular locality and frequency were to be replotted to bring duration to the abscissa, precipitations for durations shorter than one day could be estimated by extrapolation. As indicated by the time-honoured Talbot equation, the intensity-duration relationships for point rainfall of given frequency can be closely represented by a hyperbolic or decay type function, which plots as a straight line on semi-log

co-ordinates. It follows that the depth-duration relationship should also plot straight on semi-log paper, because depth is merely intensity multiplied by duration. This indeed has been found to be approximately true for a given frequency whether one is considering point rainfall or rainfall averaged over a given area.

In Fig. 5.1 are plotted depth-duration data of low frequency over an area of about 20,000 square miles in the vicinity of East London (curve marked "areal rainfall") and for a recording station within the same area (curve marked "point rainfall"). In Fig. 5.1 the ordinates have been rendered dimensionless (depths divided by the one-day depth). It is clear from Fig. 5.1 that the proportionate depth-duration relationship has a much steeper trend for areal rainfall than for point rainfall. This is explained by the fact that for a particular duration the depth of rainfall averaged over an area decreases rapidly as the area increases, with the result that the denominator for the areal rainfall curve is bound to be far smaller than that for the point rainfall curve. It is therefore evident that one of the relationships cannot be reached by extrapolation of the other and that the filling of the time gap between one hour and twenty-four hours must be tackled from the point rainfall end.

In Fig. 5.2 are plotted the locations of autographic rainfall stations, records of which were analysed by van Wyk (Fig. 5.2 has been reproduced from the paper by van Wyk and Midgley⁶). Small-area high-intensity storm data were dealt with by van Wyk under the following three headings :

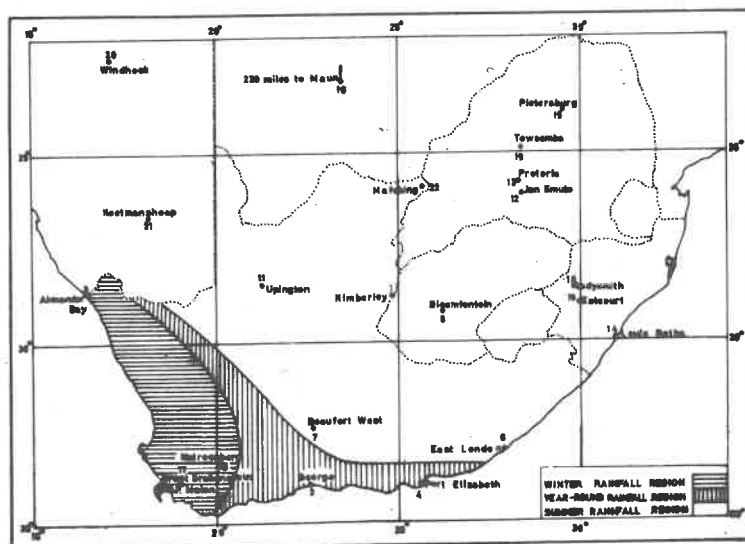


FIG. 5.2 LOCATION OF AUTOGRAPHIC RAINFALL STATIONS AND DELIMITATION OF RAINFALL REGIONS

TABLE 5.1 VARIATION OF PROPORTIONAL DEPTH FOR DIFFERENT RECURRENCE INTERVALS AT EAST LONDON STATION

RECURRENCE INTERVAL YEARS	DEPTH AS PROPORTION OF ONE DAY DEPTH DURATION (MINUTES)			
	15	30	45	60
28.00	0.181	0.343	0.370	0.411
14.00	0.238	0.345	0.418	0.469
9.33	0.261	0.435	0.525	0.551
7.00	0.250	0.317	0.362	0.440
5.60	0.240	0.322	0.344	0.437
4.66	0.198	0.304	0.343	0.405
4.00	0.202	0.263	0.340	0.377
3.50	0.202	0.270	0.354	0.395
3.11	0.181	0.271	0.326	0.386
2.80	0.155	0.245	0.318	0.382
2.54	0.156	0.247	0.316	0.309
2.33	0.142	0.221	0.290	0.280
AVERAGE	0.200	0.298	0.359	0.403

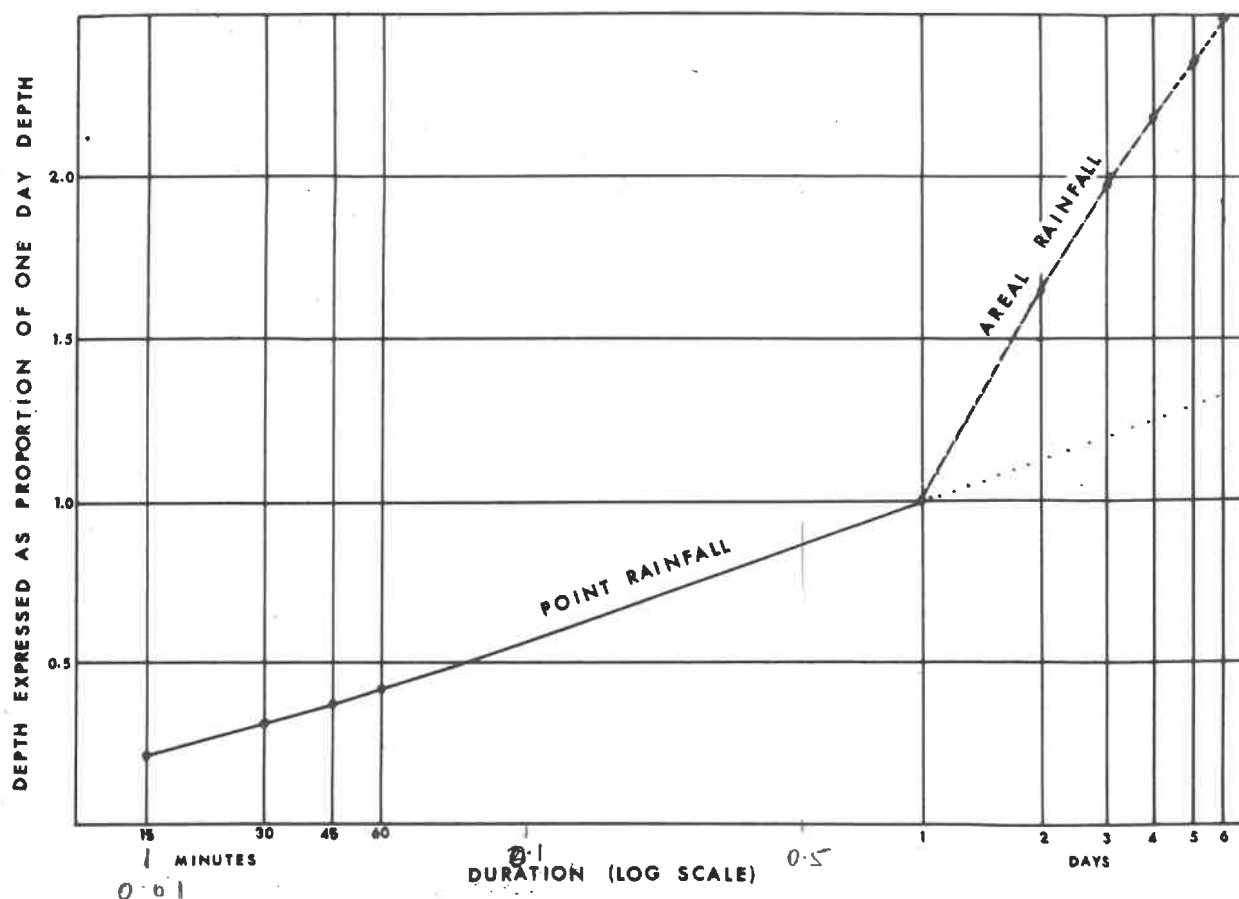


FIG. 5.1 COMPARISON OF PROPORTIONAL DEPTH-AREA CURVES FOR AREAL AND POINT RAINFALL

- (a) Intensity-duration-frequency relationships,
- (b) Time distribution of intense rainfall, and
- (c) Areal distribution of rain within intense storms.

Records at some of the stations were rather short and, as three years of record have accumulated since van Wyk's work was completed, it seemed worthwhile to re-analyse the records to include the additional data. Furthermore, it was considered that to conform to the style of the large-area storm analyses it would be more convenient to develop depth-duration-frequency than intensity-duration-frequency relationships. Apart from this change the small-area high-intensity storm data have been re-analysed under van Wyk's three headings.

5.1 Depth-duration-frequency analysis

From the record for each station, precipitation maxima for durations of 15, 30, 45, 60 and 1440 minutes were abstracted and arranged, by duration, in descending order of magnitude. Recurrence intervals were assigned to the ranked depth values for each duration according to Weibull's expression, viz :

$$T_m = \frac{N+1}{m} \dots\dots\dots 5.1$$

For the East London station the results - depths expressed as proportions of the one-day depth - are listed in Table 5.1, scrutiny of which reveals that there is no discernible trend of change in proportionate depth of precipitation for given duration with changing recurrence interval. It was therefore concluded that the proportionate

depth-duration relationship was reasonably independent of recurrence interval and accordingly the average proportionate depth-duration relationship was transposed to Fig. 5.1.

Long-duration point maxima within the same locality were then abstracted from records employed in the large-area storm study, expressed as proportions of the one-day values, and plotted on Fig. 5.1. For this step, provided extreme values were chosen, a frequency analysis was not called for because recurrence interval had been shown to have little or no influence. The fact that the proportionate depth-duration values for point rainfall could be joined by a reasonably straight line on Fig. 5.1 implied that proportionate depth values lying between 60 minutes and one day could confidently be interpolated.

Interpolation for durations between one hour and one day having been shown to be permissible, the frequency analyses of the autographic rainfall data were continued. Gumbel's first asymptote distribution was adopted and best-fit straight lines were determined by computer. As was found by van Wyk the relationship varies with local mean annual precipitation, as shown by Fig. 5.3, and from the summer to the winter rainfall region.

It was found that there was a discontinuity in the relationship between depth and mean annual precipitation as duration increased beyond one hour. For instance, for short durations (less than one hour) log of mean annual precipitation against storm depth plots as a reasonably straight line (Fig. 5.4(a)) whereas, for longer durations,

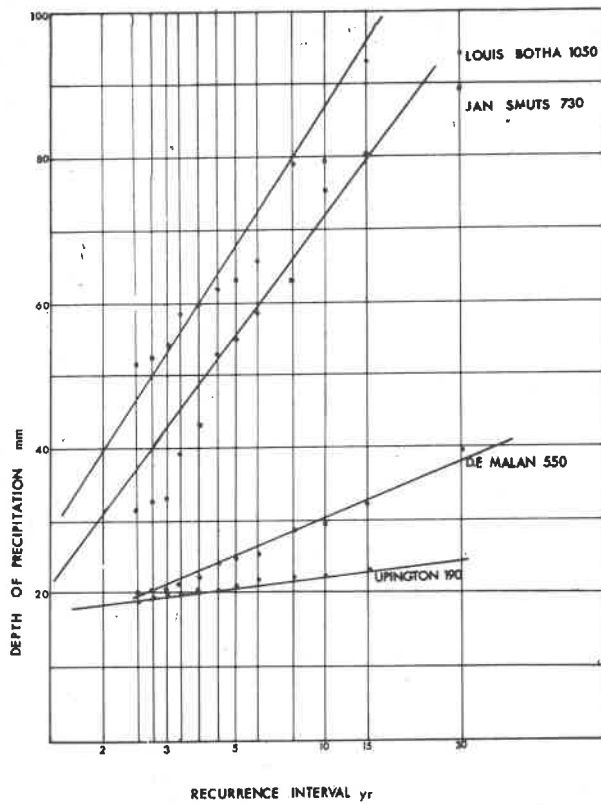


FIG 5.3

VARIATION OF DEPTH—RECURRENCE INTERVAL

RELATIONSHIP WITH CHANGING MEAN

ANNUAL PRECIPITATION

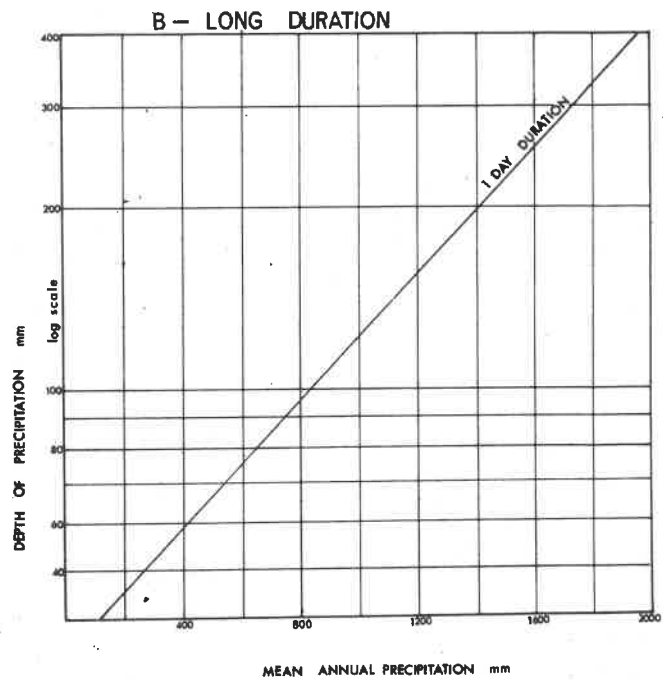
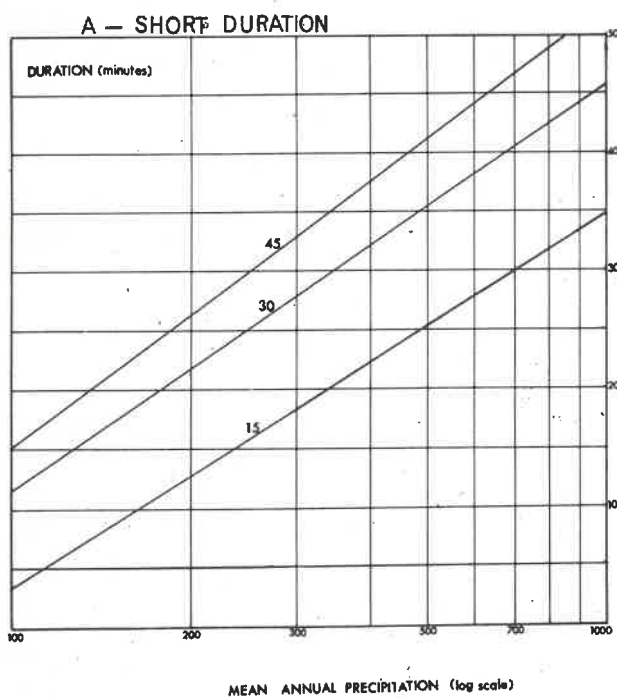
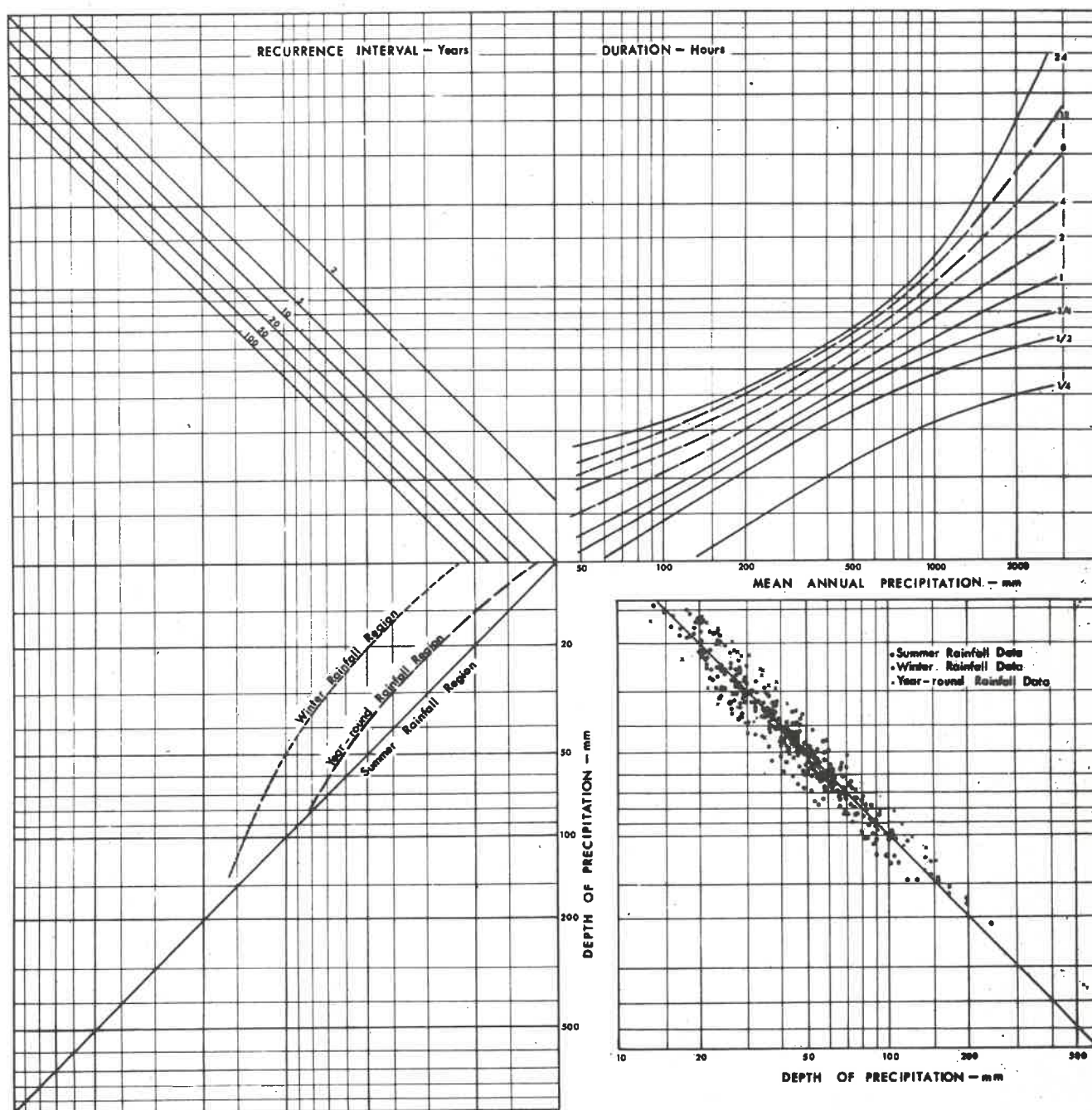


FIG 5.4 RELATIONSHIP OF DEPTH VERSUS MEAN ANNUAL PRECIPITATION

FIG 5.5
DEPTH-DURATION-FREQUENCY DIAGRAM FOR POINT RAINFALL



it is the mean annual precipitation against the log of storm rainfall that plots linearly (Fig. 5.4(b)). Because of this it was advisable to allocate mean annual precipitation and duration to the first quadrant of the coaxial plot.

The results from Fig. 5.3 and 5.4 for all the summer rainfall stations were incorporated in the coaxial plot, Fig. 5.5. After the scatter had been minimized in the fourth quadrant by adjustment of both the duration and the recurrence interval parameters, the limited winter and year-round rainfall data were employed to estimate, in the third quadrant, their relationship to the summer rainfall data.

Several factors contributed to the spread of scatter shown in Fig. 5.5, viz :

- (a) Maxima were abstracted from the records at the Weather Bureau according to clock hours and do not therefore represent true maxima for given durations.
(This aspect is discussed later in the Chapter).
- (b) Observations unfortunately are generally of low accuracy.
- (c) Records are relatively short.
- (d) The assumption that mean annual precipitation and rainfall regions are the main controlling parameters is perhaps rather sweeping.

5.2 Time distribution for intermediate durations

From his design diagram van Wyk was able to reproduce, with reasonable confidence, observed time distributions of high-intensity storms of short duration. It can be appreciated, however, that compilation of a design diagram to show time distribution for longer durations becomes difficult because of fluctuations of storm intensities with increasing duration.

Dimensionless mass curves were plotted for storms of up to 25 hours' duration recorded at the Weather Bureau autographic rainfall station in Pretoria. Mass curves of like durations were superimposed as in Fig. 5.6.

In regard to flood response, for a given duration and total precipitation, the critical time distribution of storm input is likely to be that which exhibits an increasing intensity. Accordingly, the lower envelopes of observed dimensionless mass curves were adopted as representing the critical time distributions; these are depicted in Fig. 5.7.

To smooth out the envelopes, percentage storm duration was plotted against duration on semi-log paper with percentage of storm input as parameter, as in Fig. 5.8. Straight lines were drawn by eye among the plotted points to represent the percentage depth parameter. From these lines Fig. 5.9 was drawn to represent smoothed dimensionless mass curves for selected durations, viz. 2, 4, 8, 12, 18 and 24 hours.

FIG 5.6: NON-DIMENSIONAL MASS CURVES
OF 8 HOURS DURATION

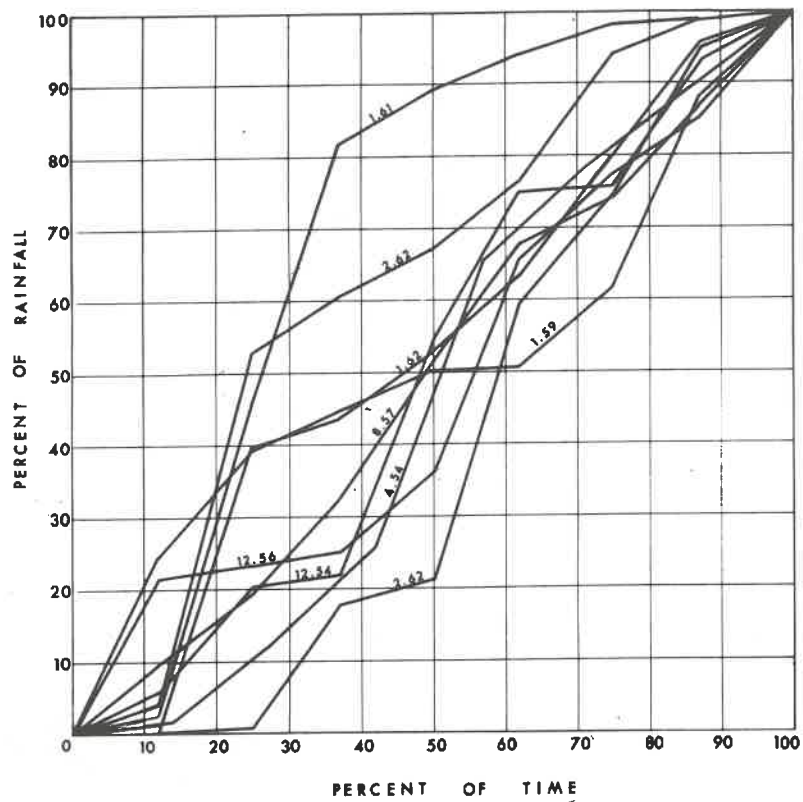


FIG 5.7: LOWER ENVELOPES OF MASS CURVES

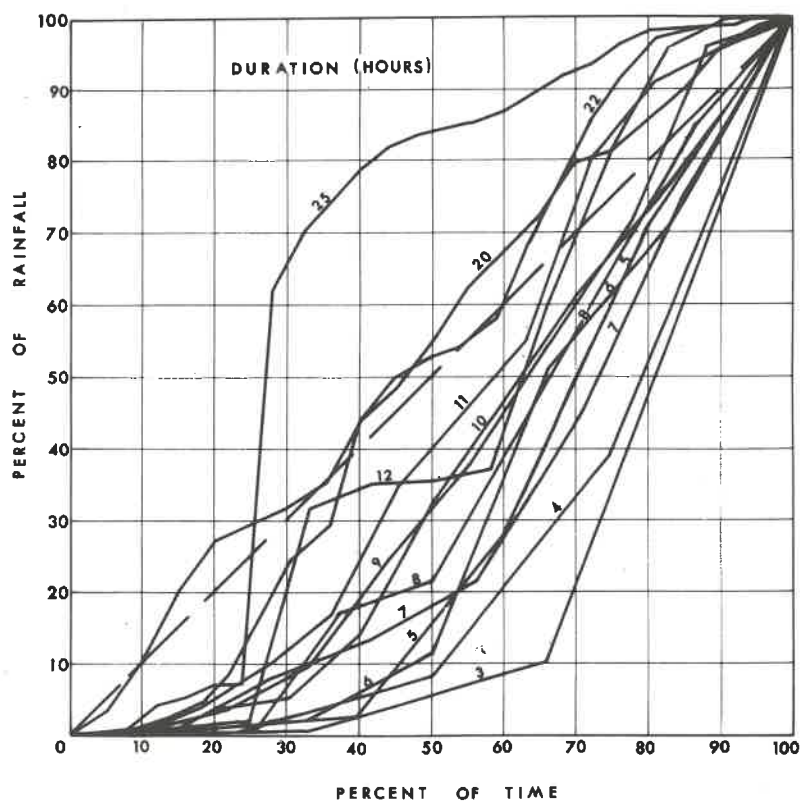
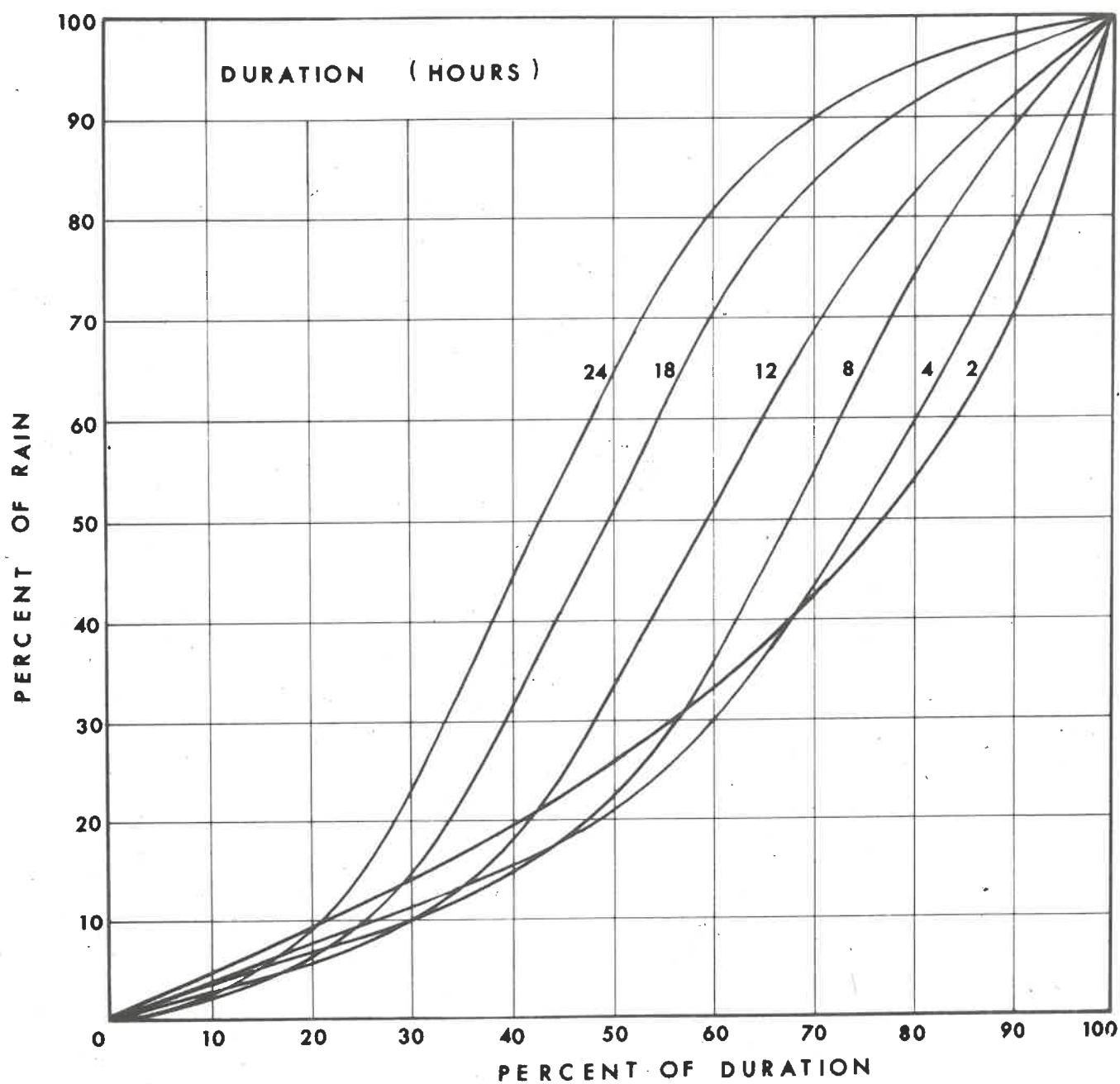


FIG 5.10
TIME DISTRIBUTION FOR INTERMEDIATE DURATIONS



Examination of the distribution, for instance of the two-hour storm in Fig. 5.9, reveals that only 15% of the total depth of that storm occurs during the first hour. This result tends to throw doubt on the accuracy of the lower envelopes for short duration, particularly as the rainfall depths were taken from values recorded according to clock hour and selection of storm duration was almost arbitrary.

Although it is appreciated that maximum rainfall depths selected from values intercepted between the artificially-phased time increments imposed by the clock do not represent true maxima for such time increments, the labour involved in re-analysing all the recorder charts to abstract true maxima was beyond the resources of both the Hydrological Research Unit and the author. It is strongly recommended that the Weather Bureau should revise its procedure for abstracting maxima from rainfall data so that this difficulty can be overcome.

As the lower ends of the envelopes Fig. 5.8 were clearly too low to be plausible they were adjusted upwards using, as guide, values derived from the upper right quadrant of the coaxial diagram (Fig. 5.5). The resulting adjusted diagram appears as Fig. 5.10.

5.3 Areal distribution of small-area storms

The principle employed by van Wyk⁵ to develop his areal distribution diagram was adopted to extend, beyond 300 square miles, the relationship illustrating reduction of average rainfall with increasing area of storm coverage. For durations of one through

six days, average precipitation over increasing areas, from 300 to 10,000 square miles, of the cells of major storms within each sub-region of the country were expressed as percentages of the maximum point rainfall observed within the storm cell. Table 5.2 illustrates a typical listing of percentage depth-area-duration values for the cell of a major storm. The results, plotted in Fig. 5.11, showed relatively small increase of precipitation for durations beyond three days.

Every line on Fig. 5.11 defines the upper envelope of a scatter of points appropriate to the annotated duration. A distinct trend exists with increasing durations up to three days; in other words, the longer the duration, the greater is the proportion of point rainfall for the same areal coverage.

TABLE 5.2

Percentage depth-area-duration data
derived from the cell of Storm Number 12

	<u>Duration</u>					
	1 day	2 day	3 day	4 day	5 day	6 day
Maximum point rainfall (mm)	165.1	231.1	282.7	314.4	342.3	351.7
Area (sq. miles)	<u>Percentage of point rainfall maxima</u>					
992	31	39	44	47	46	46
1990	30	37	43	46	45	46
2980	27	33	38	41	39	40
3980	25	29	34	37	37	37

FIG 5.11 UPPER ENVELOPE OF DEPTH-AREA RELATIONSHIP

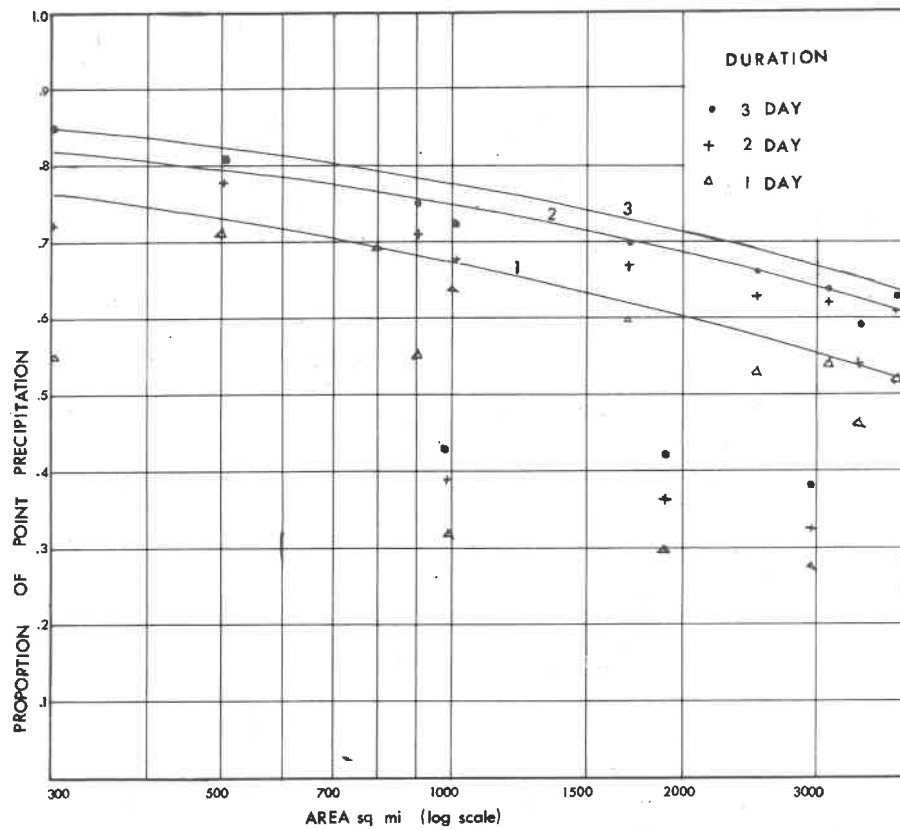
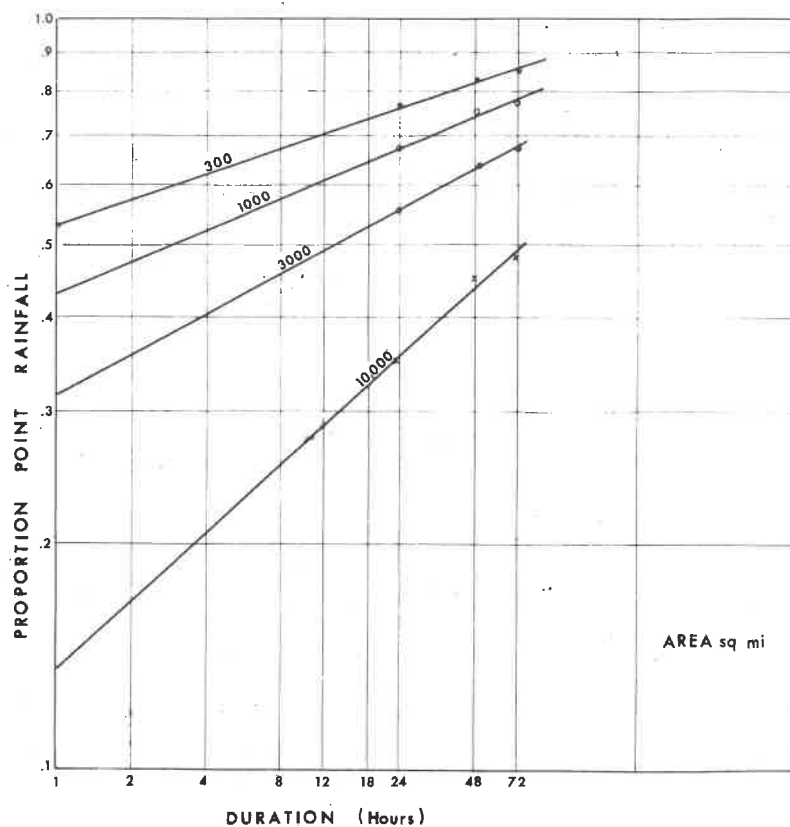
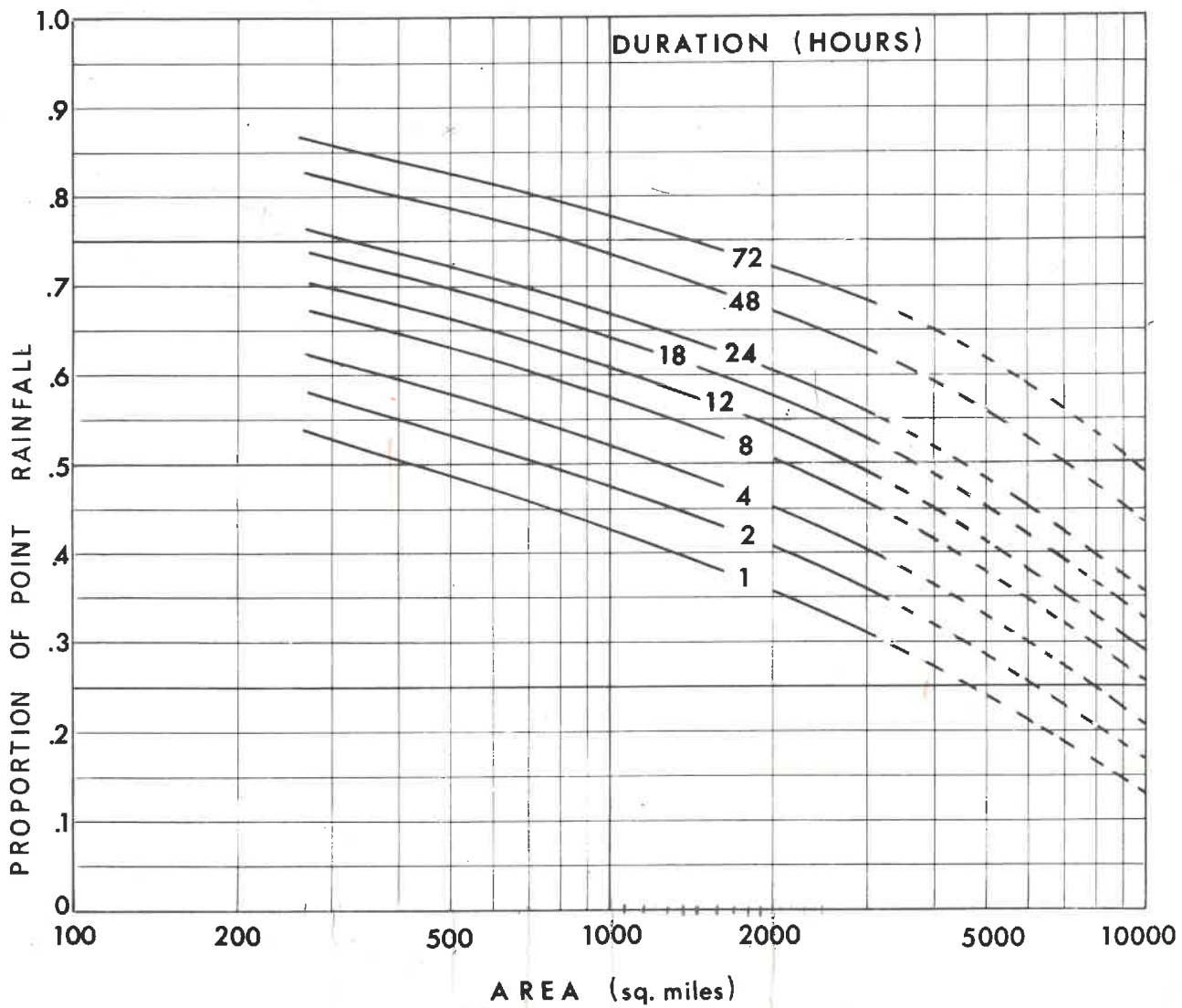


FIG 5.12 EXTRAPOLATION OF DEPTH-AREA RELATIONSHIP



def't average over the area



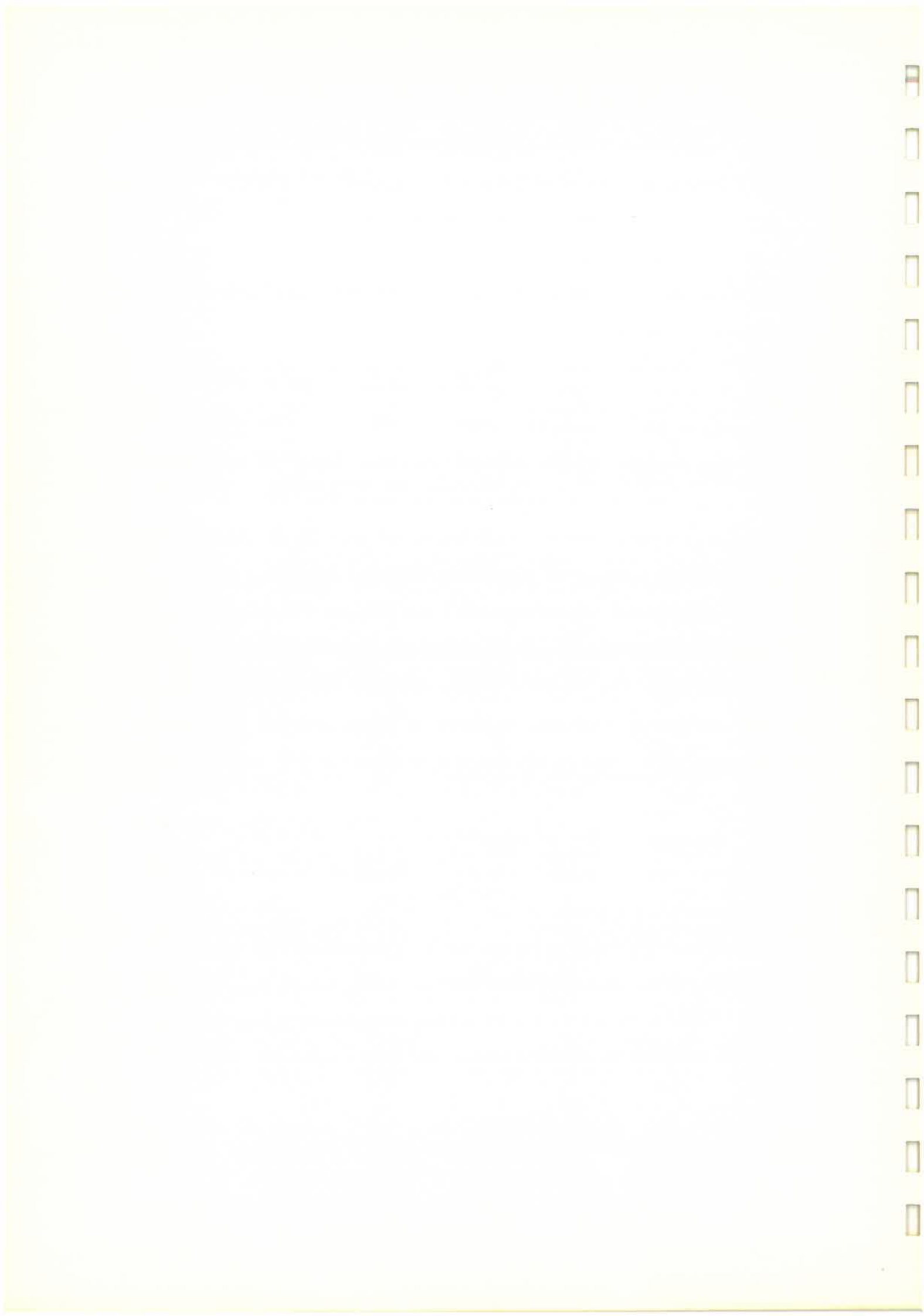
777 1245 1813 2590

**FIG 5.13 PRECIPITATION OVER GIVEN AREA
EXPRESSED AS PROPORTION OF POINT RAINFALL**

To establish similar parametric lines for shorter durations, in less than one day, a suitable abscissa scale was selected, such that values read from Fig. 5.11, and the 60-minute 300-sq. mile value read from van Wyk's areal adjustment diagram, representing depth-duration, would lie on a family of straight lines with area as parameter. The result is shown in Fig. 5.12.

Finally, the relationships have been rearranged in a form convenient for storm design purposes in Fig. 5.13, which provides the link to close the gap mentioned earlier. Fig. 5.13 is a rough universal depth-area-duration relationship in which depth of rainfall, averaged over area, is expressed in terms of the maximum point rainfall for given storm duration from 1 hour to 3 days. It is intended to complement rather than succeed the diagram presented by van Wyk¹⁵. At the same time, the fact that the parameter extends beyond the 1-hour to 24-hour gap, and the area scale beyond the 300-1000 sq. mile gap, it is not to imply that this diagram can be employed in place of the diagrams of Appendix F to design a large-area storm.

Extension of the relationships beyond the required limits resulted from the adopted manner of analysis of the data and helped to establish the trends of the curves. Fig. 5.13 is strictly an aid to the design of what might be called intermediate-size storms covering areas less than about 1000 sq. miles for which, as pointed out, South African data are at present inadequate to permit an analysis to be performed along the lines of the large-area storm studies.



C H A P T E R V I

DESIGN APPLICATIONS

It is important that the design tools presented in this dissertation be correctly interpreted otherwise spurious design storms might result. To facilitate correct application of the diagrams several design storm examples are worked out in detail.

6.1 Probable maximum precipitation over Upper Orange River catchment

Compilation of the hydrograph of the most severe flood likely to occur at the site of the Hendrik Verwoerd Dam in the Orange River near Colesburg would provide the basic information necessary for determination of the spillway capacity. For the compilation of such a hydrograph, e.g. by Pullen's lag-and-route procedures, the spatial and temporal distribution of the design storm would be required.

In this example emphasis is placed on the spatial distribution of the design storm and on the temporal distribution from one day to the critical design duration; temporal distribution for durations less than one day is not attempted.

The catchment area at the site of the Verwoerd Dam is 27,600 square miles. Methods of determining critical storm duration are discussed by Pullen⁹; for the catchment in question the critical duration has been estimated to be four days.

The steps in the compilation of the design storm are as follows :

- (a) From Fig. 3.1 it can be seen that the problem catchment falls into three sub-regions, namely, Region 8 (250-500), Region 8 (500-1000) and Region 14 (1000+). Fig. 6.1 shows in some detail the regional subdivision of the catchment, the areas embraced by each being as follows :

Region 8 (250-500) : 8,000 sq. mi..

Region 8 (500-1000) : 14,000 sq. mi.

Region 14 (1000+) : 5,600 sq. mi.

It is convenient, in the first instance, to base the design storm on only one sub-region; the major sub-region 8 (500-1000) is chosen. The "major" sub-region is selected according to the following principles : (i) strategic position and (ii) relative areal extent over catchment.

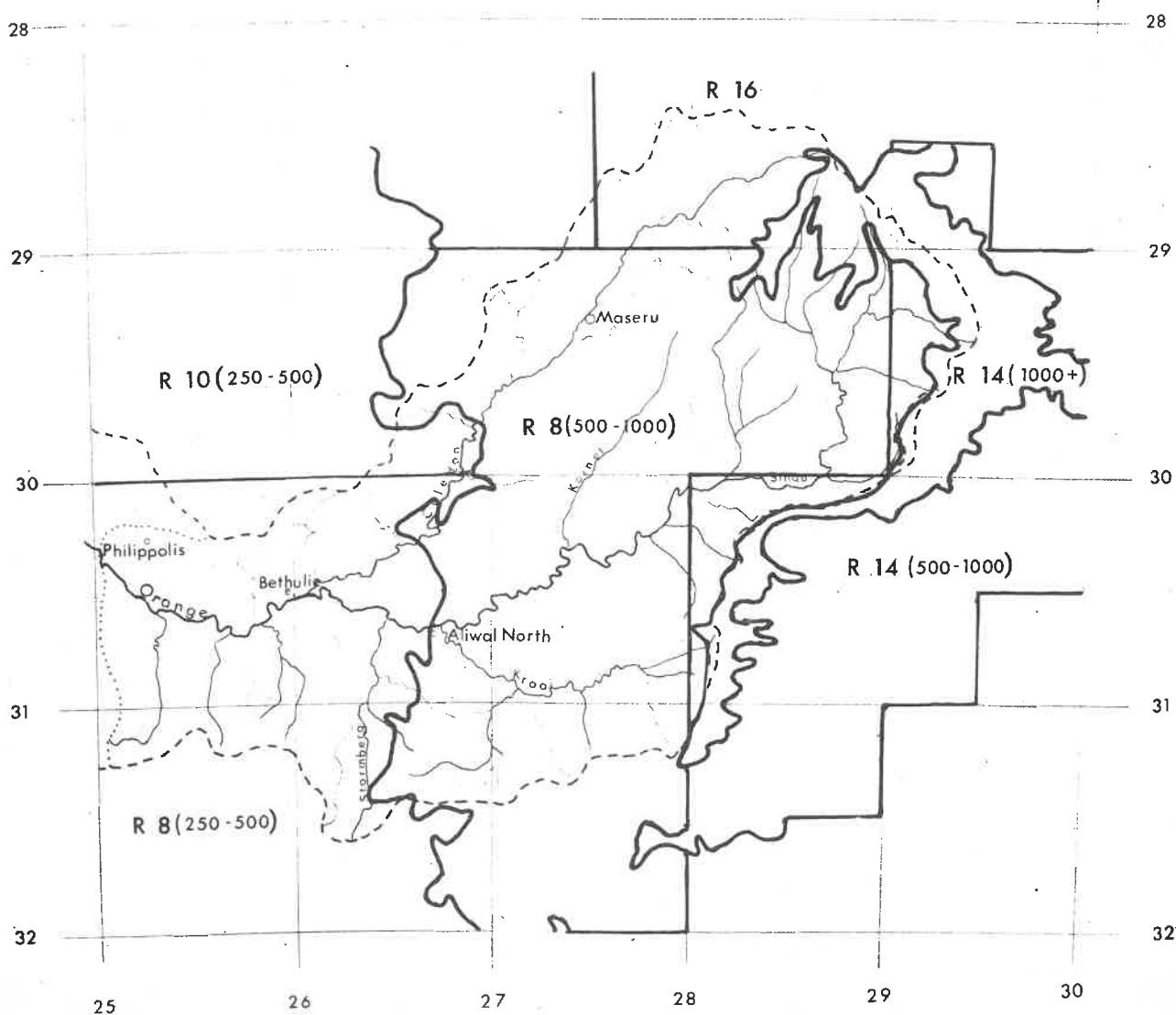
- (b) The isohyetal map of the most severe storm recorded in the major sub-region, i.e. 8 (500-1000), as shown in the storm data diagram of that sub-region, see Appendix F, provides a convenient initial basis for depicting the design storm pattern for the problem catchment. Should such a pattern be clearly not plausible the mean annual isohyetal pattern might be adopted as a guide.

TABLE 6.1

AREA sq. mi.	REGION		
	8(500 - 1000)	8(250 - 500)	14(1000+)
	Probable Maximum Precipitation mm.		
	1 DAY DURATION		
100	205	200	540
300	188	185	405
700	175	172	385
1000	167	163	360
3000	145	140	290
7000	125	115	245
10000	116	105	-
15000	105	-	-
	2 DAY DURATION		
100	327	303	810
300	298	280	740
700	272	255	675
1000	260	246	640
3000	220	210	525
7000	195	175	420
10000	185	158	-
15000	178	-	-

AREA sq. mi.	REGION		
	8(500 - 1000)	8(250 - 500)	14(1000+)
	Probable Maximum Precipitation mm.		
	3 DAY DURATION		
100	345	315	960
300	323	300	870
700	305	278	785
1000	298	268	750
3000	267	234	615
7000	240	205	495
10000	227	193	-
15000	212	-	-
	4 DAY DURATION		
100	360	315	1040
300	338	300	940
700	319	278	855
1000	310	268	820
3000	279	234	675
7000	240	205	540
10000	238	193	-
15000	221	-	-

FIG 6.1 CATCHMENT AREA OF UPPER ORANGE RIVER CATCHMENT AND DIVISION IN SUB-REGIONS



- (c) Four-day duration precipitation depths are extracted from the PMP-area-duration curves for the relevant sub-region and listed in Table 6.1. It is recommended that the spatial distribution for the entire sub-region be estimated as it must be appreciated that the peaks of precipitation as shown by the adopted pattern do not necessarily fall within part of the sub-region covered by the problem catchment. Four-day depth-area values for that sub-region are now assigned to the isohyets of the selected pattern. It is usually necessary to adjust the positions of the isohyets to ensure that the areas intercepted satisfy the adopted depth-area relationship. Adjustments made should be such that the storm isohyets conform generally to the mean annual isohyetal pattern.
- (d) Next, the depth-area relationship for other sub-regions are incorporated in a manner similar to that adopted for the main sub-region, care being taken to preserve continuity from one sub-region into another.
- (e) After the design storm isohyets have been adjusted and depths have been assigned as in Fig. 6.2, the four-day depth-area tabulation for the catchment is compiled; the resulting curve is depicted in Fig. 6.3.
- (f) Steps c, d and e are then repeated for the three-, two- and one-day durations. The resulting depth-area curves are shown in Fig. 6.3. Few changes need be made to the spatial distribution pattern arrived at for the longest duration because the

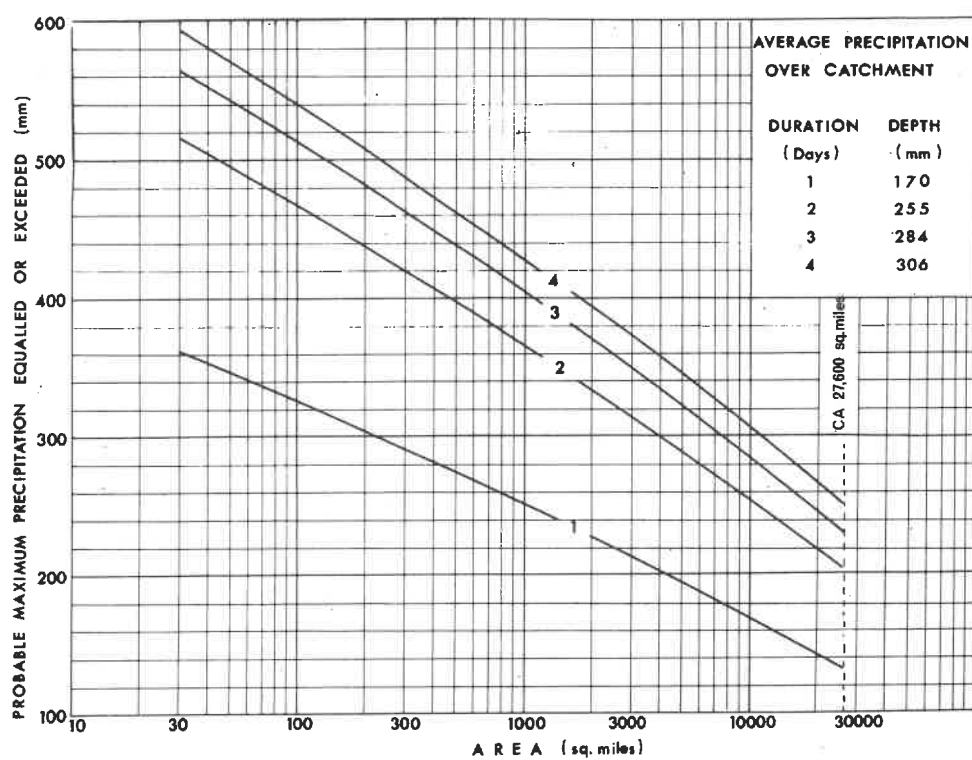
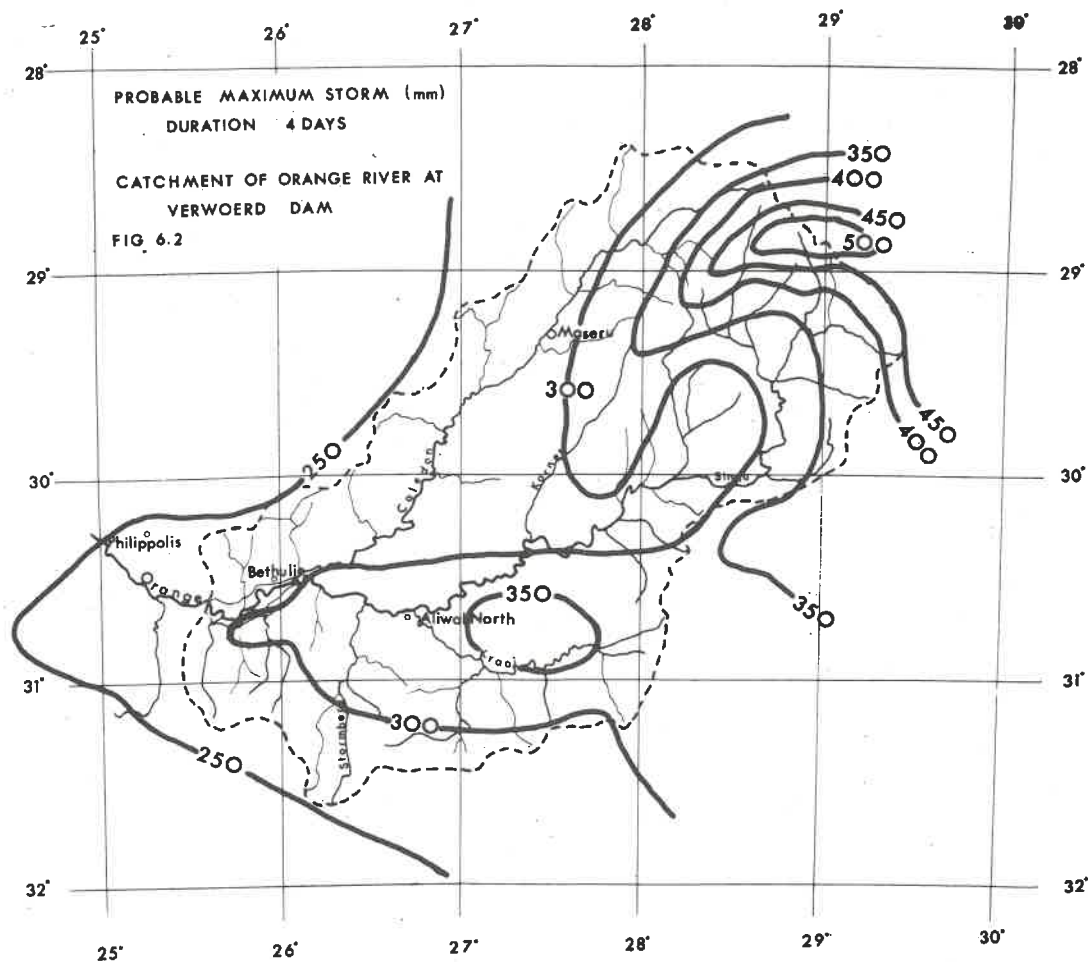


FIG. 6.3 PROBABLE MAXIMUM DEPTH-AREA-DURATION CURVES FOR UPPER ORANGE
RIVER CATCHMENT

design data were developed on the assumption that no spatial variances existed during temporal variations.

- (g) Should it be desired to reduce the time resolution, the data may be replotted with depth on natural scale and duration on log scale. Values appropriate to shorter time intervals may then be interpolated. As explained in Chapter V, extrapolation to durations shorter than one day is not recommended because the semi-log depth-duration plot does not remain linear as area decreases.

6.2 Discussion

The current study was not sufficiently far advanced for a design storm to have been established at the time this was required in connection with determination of the spillway capacity for the Hendrik Verwoerd Dam. The computations were therefore performed elsewhere and results were reported by Jordaan³³.

The results of the two studies are compared in Table 6.2. To permit comparison to be made, it was necessary to convert the depth-area values tabulated in Fig. 6.3 to precipitations averaged over the catchment.

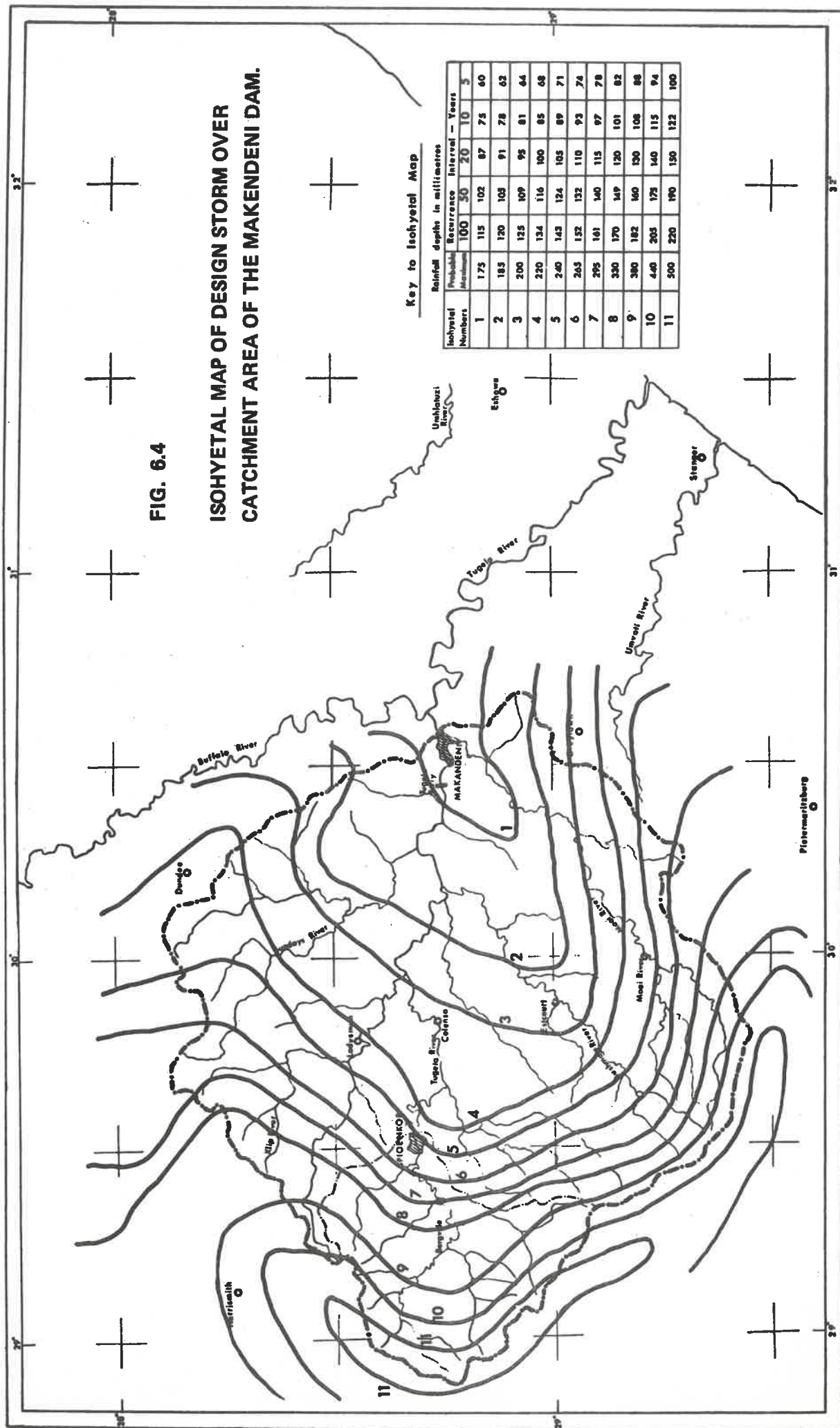
TABLE 6.2

<u>Storm Duration</u>	<u>PMP(mm) averaged over Orange River catchment</u>	
<u>hours</u>	<u>Jordaan</u>	<u>Present Study</u>
24	150	170
48	200	255
72	-	284
96	-	306
120	350	-

As may be seen from Table 6.2 the results of the two studies were in fairly close agreement in the vicinity of the critical duration. However, it should be noted that figures reported by Jordaan reveal a linear increase in depth with respect to duration; this is unrealistic.

6.3 Design storm data for Upper Tugela Basin

Compilation of hydrographs for floods of differing recurrence interval at the Makendeni dam site on the Tugela river would provide the basic hydrological information necessary for coffer dam-, construction bridge- and spillway-design purposes. As mentioned previously, if lag-and-route procedures are to be employed for compilation of such hydrographs, both spatial and temporal distribution of the design storm for each desired recurrence interval will be required.



The emphasis in this example is placed on estimation of storm precipitations of duration less than one day but covering a fairly large area.

The catchment area at the Makendeni site is about 5,000 sq. miles. The critical duration for the catchment has been estimated as 25 hours.

The steps in the compilation of the design storm are as follows :

- (a) For the spatial distribution of storm rainfall of one-day duration the same steps as in the first example are taken, i.e. steps a, b, c, d and e. The pattern for the design storm was initially taken to be similar to that of mean annual rainfall as no characteristic storm pattern for the area emerged from the regional design charts. The results of this step, repeated for various recurrence intervals, are shown in Fig. 6.4.
- (b) It may be appreciated that the temporal distribution cannot be derived from the results of large-area duration study and resort must be had to the design data resulting from extensions of the small-area, short-duration study. The 24-hour parametric line in Fig. 5.10 is assumed, for lack of more accurate design data, to provide an adequate description of the temporal distribution of the design storm. It should be borne in mind that the design data for temporal distribution were established from point rainfall

data and, with extension to larger areas, figures of averaged precipitation are based on a scaling factor.

To facilitate correct application of the design diagrams the catchment area should be subdivided on the basis of depth of rainfall such that average depths over each segment can be calculated without destroying the spatial distribution. The selected temporal distribution curve can be employed to the more significant average depths and it may be considered advisable to apply a shorter-duration temporal distribution curve to the other average depths.

6.4 Design storm data for Upper Reaches of Tugela Basin

The spatial and temporal distribution of design storms of different recurrence intervals over the catchment area of Spioenkop Dam is a prerequisite to the compilation of hydrographs which provide basic information for spillway design purposes. The catchment area at Spioenkop dam site is 929 sq. miles and the critical duration has been estimated to be 10 hours.

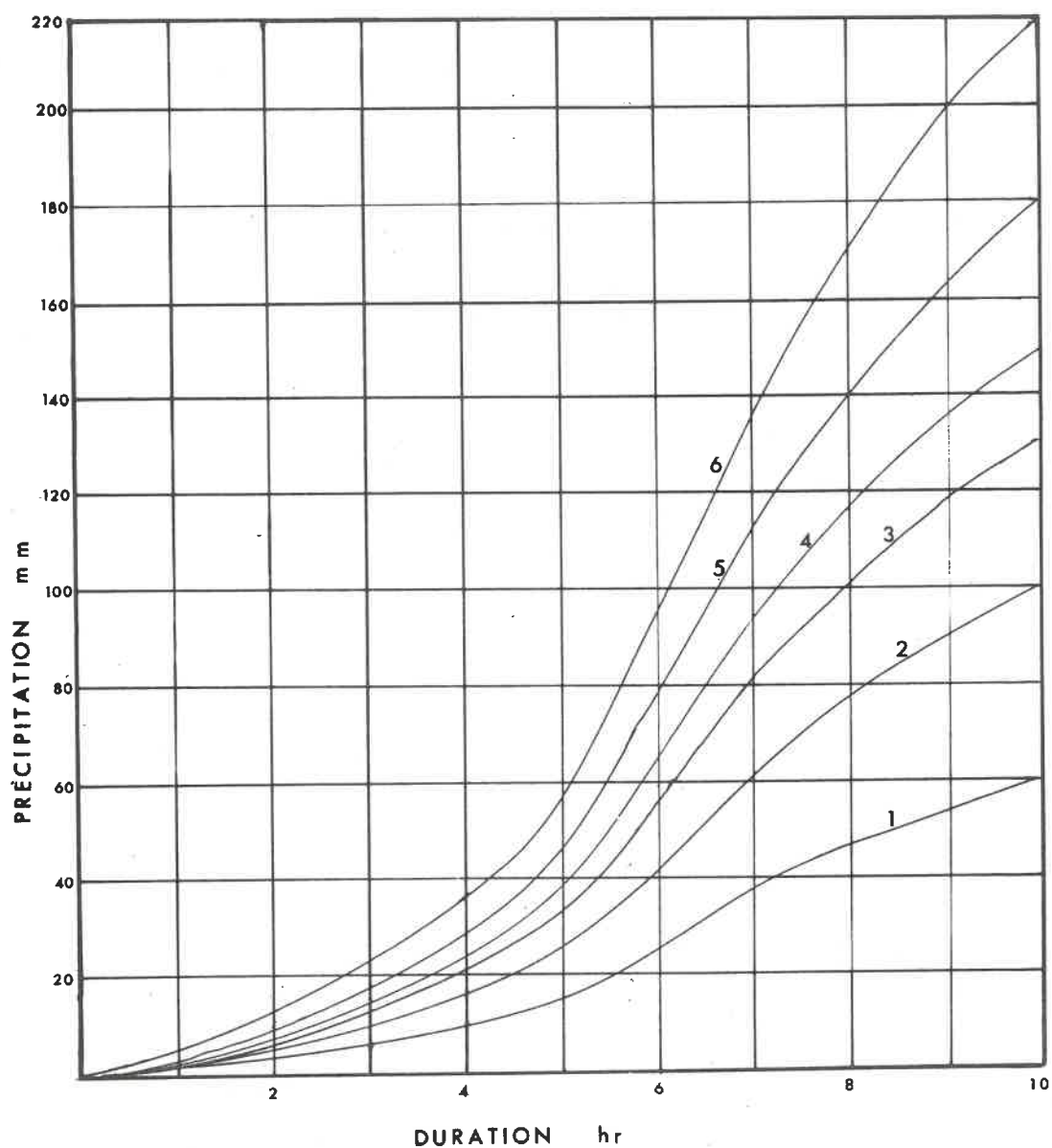
Estimation of a plausible spatial distribution for a design storm over this catchment is not feasible from available design data as the areal extent of the catchment is small compared with that of storms employed in this dissertation to present design spatial distributions.

TABLE 6.3

Point rainfall depths and depths adjusted for area-storms of ten-hour duration

Recurrence Interval yr.	Point rainfall depth mm	Number employed Fig. 6.5	average rainfall mm over 929 sq. mi.
2	60	1	34.8
5	100	2	58.0
10	130	3	75.4
20	150	4	87.0
50	180	5	104.4
100	220	6	127.6

FIG 6.5 TIME DISTRIBUTION FOR DESIGN STORM
OVER CATCHMENT AREA OF SPIOENKOP DAM



Design data resulting from extension of short-duration and small-area storms study, however, provide suitable material for this example. The steps in the compilation of the design storm are as follows :

- (a) Depths of point rainfall, corresponding to the selected duration of 10 hours, for required recurrence intervals assuming a mean annual precipitation of 1100 mm can be interpolated on Fig. 5.5; the results are set out in Table 6.3.
- (b) From Fig. 5.13 a reduction factor of .58 for an area of 929 sq. miles and 10 hours duration can be read off, and the average depths of storm rainfall for the catchment calculated, see Table 6.3.
- (c) The temporal storm distribution (shown in Fig. 6.5) of design storm rainfall, is derived by adopting an appropriate mass curve from Fig. 5.10.

6.5 Summary

South African precipitation data subsequent to 1932 have been analysed on a country-wide basis and the results presented in a form suitable for the application of hydro-meteorological techniques to design flood determination.

The subject was subdivided under the headings small-area high-intensity and large-area long-duration storm precipitation. The two

types of precipitation required separate approaches not only because of inherent differences of storm mechanism but because observational data of satisfactory time resolution for the study of the former (autographically recorded point rainfall) provided poor areally distributed samples whereas data of satisfactory areal distribution for the latter study (daily-read rain gauges) were of inadequate time resolution. A combination of approaches was needed for handling storms of intermediate areal coverage.

Maxima for duration of 15, 30, 45, 60 and 1440 minutes, abstracted from the autographically recorded point rainfall data, were subjected to extreme value analysis and the results grouped under summer-, winter- and year-round rainfall regions (Chapter V). A coaxial diagram, Fig. 5.5 on page 5.7, represents the inter-relationship of depth, duration, frequency and region.

Studies of the spatial and temporal distribution of precipitation within small-area high-intensity storms by a colleague led to empirical diagrams from which the isohyetal pattern and mass curve of a design small-area storm could be synthesized. The scope of these diagrams was extended to embrace storms of intermediate areal coverage in Chapter V. Fig. 5.10 and Fig. 5.13 represent time and areal distributions respectively of storms in the intermediate range.

It was found not possible to maximize point rainfall data to provide information for estimating probable maximum precipitation (PMP).

Data from daily-read raingauges for the dates embracing 170 selected storms distributed over South Africa were expressed in percental form (percentage of mean annual precipitation). Polynomial surfaces were fitted to the percental values by computer which was programmed also to perform the depth-area-duration analyses (Chapter 11).

After examination of the results the country was subdivided into altogether 29 regions and sub-regions within each of which the depth-area-data were subjected to extreme value analysis (Chapter 111). The results were employed to construct for each sub-region a depth-area-duration-frequency relationship which was represented by coaxial diagram (Appendix F). A guide to the accuracy of these plots is presented in tabular form in Appendix E.

A technique was developed for estimating the depth of precipitable water associated with each storm and that associated with maximum representative dewpoint (Chapter 1V). On this basis observed storms were maximized and the upper envelope of the regional group of maximized storm values adopted as the PMP. Thus, on each regional diagram there appears also an approximate PMP-area-duration relationship. The range of possible error is discussed in section 4.5.

As a guide to shape and orientation of a synthesized design storm, the isohyetal map of the most extreme storm recorded within each sub-region is reproduced on the regional diagram.

Practical use of the diagrams is demonstrated in Chapter VI in worked examples of the design of medium-area and large-area storms on appropriate South African catchments in form ready for adoption as input to design flood determination.

6.6 Conclusion

The adequacy of storm analyses is heavily dependent upon the spatial distribution of rainfall stations and on the time resolution of observations and the length and continuity of records. In not one of these respects can it be conceded that the situation in South Africa is satisfactory.

As the average density of daily-observed raingauges is 180 sq. miles per gauge - a figure distorted by the relatively high density in the urban areas - it is not possible to provide a satisfactory analysis of storms of duration shorter than one day or covering less than about 1000 sq. miles and, as there are a mere handful of autographic records longer than two decades, there is a problem of providing satisfactory design data for intense storms of duration shorter than one hour - covering a relatively small area.

Extreme value theory was applied but no distinct trend could be identified either in point rainfall or large-area storm rainfall to indicate what type of distribution should be adopted. Had the records been longer it is possible that a unique distribution might have been revealed.

A serious limitation is that occasioned by the fact that the time scale of events has been arbitrarily subdivided according to the clock hour thus affecting estimation of both storm duration and maximum rainfall for given duration. Unfortunately the effects of errors attributable to arbitrary fixing of the time resolution cannot be gauged.

As the vast majority of catchments for which design storms may be required have response times less than 24 hours, improvements in time resolution and spatial distribution of recording rainfall stations should be brought about without delay.

A P P E N D I X ATESTS AND TECHNIQUES EMPLOYED TO DEVELOPSURFACE-FITTING PROCEDURESA.1 Steps to minimize effects of ill-conditioning

Derivation of coefficients in a polynomial containing m terms requires the simultaneous solution of m linear equations. Hamming³⁴ has shown that, provided the number of observation equations exceeds the number, m , of terms in the polynomial, the determinant of the normal equations is never equal to zero unless all the coefficients are zero. In practice, however, ill-conditioning of the simultaneous normal equations often produces a determinant that is close to zero. If the order of the polynomial is high, use of least squares procedures to optimize the coefficients results in ill-conditioning of the resulting normal equations³⁴. When the matrix is ill-conditioned, and if insufficient significant digits are recognized in the computation, a solution results that is not unique.

Attempts by members of the Unit to minimize the effects of ill-conditioning, by using the maximum pivot in the first column of each set of reduced equations in the Gaussian elimination process, led to insignificant improvements in the results. Pivotal equations were therefore used in the order in which they were derived.

To overcome the effects of ill-conditioning in simultaneous equations involving one independent variable, orthogonal polynomials

could have been generated by employing a three-term recurrence relationship. No satisfactory analogous method could be developed, however, by which to generate orthogonal polynomials for the case of two independent variables and resort had therefore to be had to increasing the number of significant digits recognized in the computation.

Most digital computing units permit the use of single or double word length but relatively few have the facility for intermediate variations of word length. Fortunately the IBM 1620 Mod.II computer available at the University had facilities for increasing the number of significant digits recognized in the computation in steps of one digit from the normal word length of eight digits to word lengths of up to 28 digits. The methods developed would have been difficult to employ on a machine without this variable word length facility.

A.2 Limitations of computer memory storage

Determination of the coefficients in a polynomial with m terms to achieve best fit to a set of data requires solution of a matrix of m by $(m+1)$ terms. Increasing the number of significant digits to be recognized in these terms, with the object of ensuring meaningful results when the degree of the polynomial is high, limits the size of matrix that can be accommodated in the machine memory. A polynomial of sixth degree involving 28 terms expressed to 22 significant digits was the maximum that could be handled in the available computer.

A.3 Goodness of fit

It was hoped that the degree of precision achieved in representing the isopercental surface mathematically could be gauged by examining the effects of adjusting the degree of the polynomial on conventional statistical parameters, such as the root-mean-square deviation of observations from the calculated surface. It soon became clear, however, that not only were the statistical parameters, such as the root-mean-square deviation and correlation coefficient, poor measures of the goodness of fit but also that the problem was largely one of economics in computer time. Furthermore, it was appreciated that the meaningfulness of a comparison between one representation of the storm configuration and another would depend heavily upon the errors inherent in the observational data.

Accordingly, it was decided to perform computer-time and precision analyses as well as an error analysis of the data and thereafter to embark on a pilot study to optimize degree of polynomial, and number of significant digits to be recognized in the computations, as well as other factors affecting economy in computer time.

It was appreciated, too, that increasing the degree of polynomial would enhance the chances that the calculated surface might oscillate between the data points and that tests would have to be introduced to monitor such eventuality.

The criterion upon which the results of the pilot study would be judged was : the optimum surface-fitting routine would be that which

yielded in minimum computing time an acceptable representation of the storm configuration, as disclosed by the statistical parameters and the corresponding difference maps of percentals.

A.4 Economy in the use of computer time

Fig. A.1 illustrates the rate at which computing time needed to perform a sixth-degree polynomial surface-fitting routine rises with increasing numbers of observations. To keep computing time within reasonable bounds a group-weighting technique was resorted to whereby the storm area was subdivided in orthogonal blocks within each of which the weighted mean value of storm precipitation and location thereof were calculated by averaging the values and their coordinates.

Fig. A.1 is based on recorded total computer times required to perform, for ten different storms, both the group-weighting and the surface-fitting procedures. The group-weighting routine takes from three to ten minutes of computer time depending on the extent of the storm. To analyse a storm described by 200 observations without resorting to group-weighting requires approximately 152 minutes (i.e. 160 min., as shown by Fig. A.1, less say 8 min. for group-weighting). Reduction of the number of observations from 200 to between 70 and 100 by group-weighting reduces the machine time for analysis from 152 min. to between 56 and 80 min.

In the pilot study, tests were designed to optimize the intensity of group-weighting. The effects of group-weighting on precision are discussed presently.

FIG A.1: COMPUTER TIME REQUIRED FOR SURFACE-FITTING ROUTINE

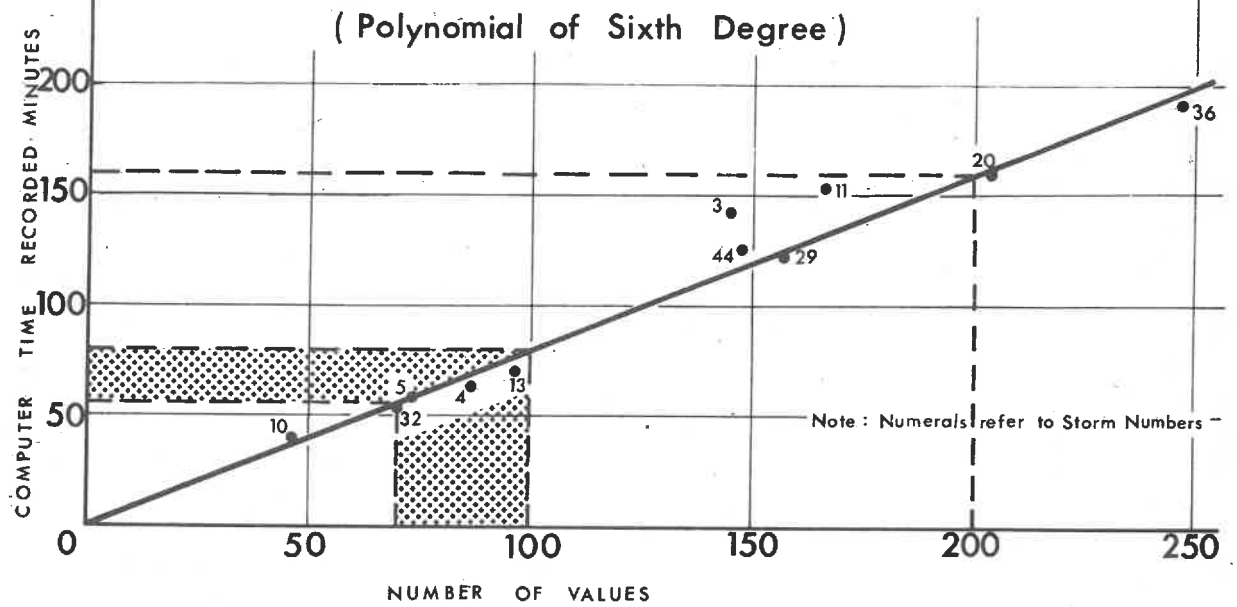
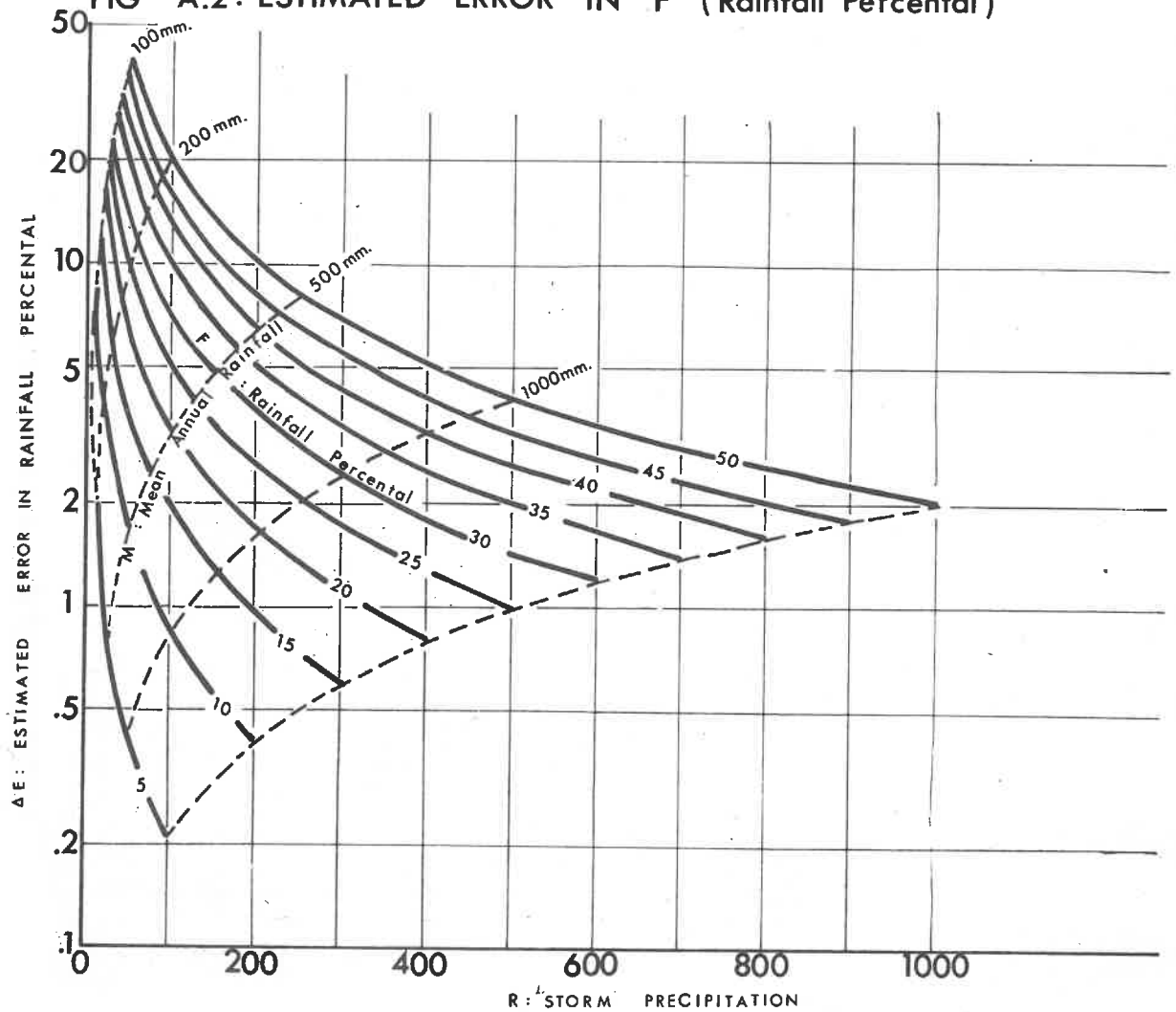


FIG A.2: ESTIMATED ERROR IN F (Rainfall Percental)



A.5 Analysis of errors inherent in the data

The precision with which the mathematical model describes the complexities in the configuration of a storm pattern must be gauged in relation to the range of possible errors both in the storm observations and in the mean annual rainfall distribution employed as the basis for areal weighting. In this context the word error is used in the sense of an indication of the range of accuracy with which the basic measurements could be made and does not include random errors in these measurements. The following are sources and ranges of error in the basic data :

- (a) From discussions with officials of the Weather Bureau it was surmised that field observations of rainfall might be subject to errors of between zero and five millimetres.
- (b) Isometric lines on a 1:250,000 mean annual rainfall map are probably accurate to within about 30 mm (Schultze³⁵).
- (c) In the preparation of the deck of basic cards mean annual rainfall depths were interpolated from the isohyets to the nearest 50 mm.

The percental value F is given by $F = \frac{R}{M} 100$ per cent in which R is the observed storm rainfall and M the mean annual rainfall. Errors in storm rainfall observation and in estimation of mean annual rainfall combine to produce errors in the corresponding percental value, which errors in turn can be evaluated from the

error propagation equation :

$$\Delta F^2 = \left(\frac{\delta F}{\delta R} \Delta R \right)^2 + \left(\frac{\delta F}{\delta M} \Delta M \right)^2$$

whence, $\Delta F = \frac{10^2}{M^2} \sqrt{M^2 \Delta R^2 + R^2 \Delta M^2}$ per cent (A.1)

in which the Δ sign indicates 'error in'.

Within the range of mean annual rainfalls encountered in this study, inaccuracy in the mean annual rainfall, ΔM (a combination of sources of error mentioned in (b) and (c) above) was assumed to be 80 mm.

The error equation A.1 was solved for a range of values of M and R , assuming the error in rainfall observation to be constant at 1 mm. The results are plotted on Fig. A.2. Increasing ΔR to 5 mm was shown to have a significant effect only over the regions of very low mean annual precipitation.

Consider the hypothetical case of a 30 per cent isopercental line passing through a storm area where the storm rainfall varied from 100 mm to 300 mm, i.e. the mean annual rainfall distribution varied from about 333 mm to 1,000 mm. From Fig. A.2 it can be seen that the estimated error in the 30 percental value would range from 2.4 to 7.0 per cent. For any combination of storm rainfall and mean annual rainfall the possible error in the percental value of storm rainfall can be estimated from Fig. A.2.

A.6 Pilot studyComputer routine

The procedure in so far as the pilot study is affected was as follows :

- (a) Cards bearing storm data transferred from Port-o-punch cards were read and the data temporarily stored on the magnetic disc. Mean annual rainfall data together with the corresponding latitude and longitude are read from the supplementary deck for those rainfall stations that experienced the storm under study. For each rainfall station mean annual rainfall, total storm precipitation and latitude and longitude were stored on the magnetic disc.
- (b) Following instructions from the operator the computer either group-weighted the observations according to pre-selected rules or by-passed the group-weighting routine and accepted the unweighted values for analysis.
- (c) A polynomial was then fitted either to the original percental values or to the group-weighted values. On completion of this operation the machine printed out the list of coefficients in the polynomial.
- (d) Observed total storm value and percental value, local mean annual rainfall and calculated percental value at each observation station were used by the machine to

compute the following statistics of the analysis :

- (i) the mean, over all the observations, of the estimated errors in the percental values; obtained by evaluating equation A.1 at each observation point;
- (ii) the statistical root-mean-square deviation of the mathematical surface from the observed percental values;
- (iii) the statistical root-mean-square deviation of the computed surface from the nearest fringe of an error band enclosing the observations and of thickness equivalent to twice the estimated error at each station.

Statistics evaluated in (i), (ii) and (iii) above were expressed in percental units. To facilitate plotting of difference maps and, if necessary, improvement of the analysis, the machine was programmed to list the amount by which the computed surface deviated from the observations.

- (e) If the results of the analysis were acceptable the machine printed out a tabulation of percental values at grid intersections of prescribed spacing (usually quarter-degree points) throughout the storm area. These values were plotted by hand for examination.

- (f) Under instructions from the operator the machine then proceeded with computations of storm rainfall at all addresses within the storm area and the print-out of storm rainfall values at grid intersections of prescribed spacing to form the basis for hand-plotting of the total storm isohyetal map.
- (g) Finally, the machine performed the integration process and printed out the depth-area-duration tabulation.

In routine operation, many of the pauses in the procedure were eliminated, as explained in Appendix C.

A.7 Tests on the surface-fitting procedure

Number of significant digits required in the computation

Comparison of the results of computations based on different numbers of significant digits demonstrates how adversely precision is affected when insufficient digits are recognized. In Table A.1 are listed the coefficients derived in a fifth-degree polynomial for storm number 170, recognizing first 8 then 22 significant digits, and in a sixth-degree polynomial for storm number 8, recognizing first 18 then 22 digits.

Computations on the 1620 M II computer are usually taken to eight significant digits. Theoretically the effects of ill-conditioning of the matrix for 28 simultaneous equations can be

minimized by recognizing about 20 significant digits in the computation. Corresponding coefficients, computed on the basis of recognizing first 8 then 22 significant digits respectively, differ considerably from one another, whereas corresponding coefficients computed on the basis of recognizing first 18 then 22 significant digits agree with one another at least as far as the sixth significant digit; more than half the coefficients check out at the eighth significant digit. It was concluded from this test that increasing the number of digits beyond twenty-two would not bring about any appreciable improvement in precision.

Group-weighting of observations and manipulating of polynomial degree

Tests were carried out on the data for storms numbers 2 and 55 in an attempt to optimize the intensity of group-weighting and the degree of the polynomial. For each analysis computer times required for the surface-fitting routine were recorded. These are listed in Table A.2 together with corresponding root-mean-square deviations resulting from different choices of intensity of group-weighting and degree of polynomial.

Although there is slender mathematical justification for use of the root-mean-square deviation of observed values from the calculated surface as an absolute measure of precision, this statistic nevertheless offers a reasonable basis for comparison of the effects of manipulation of the equations and data for a particular storm.

TABLE A1

Coefficients in the polynomials derived for storms numbers 170 and 8 recognizing differing numbers of significant digits in the computations.

Coefficient number	Storm 170		Storm 8	
	8 digits	22 digits	18 digits	22 digits
	5th degree		6th degree	
1	.13873673 (2)	.29698880(+2)	.83541405(+ 1)	.83541412(+ 1)
2	-.37121326 (1)	-.26223543 (+1)	.11450906(+ 0)	.11450903(+ 0)
3	.78862922 (0)	.22487635 (0)	.20394455(+ 1)	.20394454(+ 1)
4	.37367636 (-1)	.26015976 (-1)	-.37973157(- 1)	-.37973157(- 1)
5	.34239014 (-1)	.28875294 (-1)	.67234355(- 1)	.67234356(- 1)
6	-.10934716 (-1)	-.59618919 (-2)	-.12519898(- 0)	-.12519898(- 0)
7	-.18949903 (-4)	-.12847767 (-4)	.81425331(- 3)	.81425331(- 3)
8	-.34114575 (-3)	-.30406926 (-3)	-.24188436(- 3)	-.24188438(- 3)
9	-.87550604 (-4)	-.61044789 (-4)	-.16227600(- 2)	-.16227600(- 2)
10	.62031179 (-4)	.36844195 (-4)	.25330491(- 2)	.25330491(- 2)
11	-.68932807 (-6)	-.58260913 (-6)	-.99632637(- 5)	-.99632637(- 5)
12	.11816272 (-5)	.73889684 (-6)	.48384846(- 5)	.48384847(- 5)
13	.17030875 (-6)	.48674017 (-6)	.17634476(- 5)	.17634476(- 5)
14	.42081678 (-6)	.23000647 (-6)	.16872368(- 4)	.16872368(- 4)
15	-.23235871 (-6)	-.16969279 (-6)	-.23347506(- 4)	-.23347506(- 4)
16	.43786684 (-9)	.42672822 (-9)	.50797674(- 7)	.50797674(- 7)
17	.33050121 (-8)	.32994370 (-8)	-.34024512(- 8)	-.34024515(- 7)
18	-.66593464 (-8)	-.65488991 (-8)	-.46083860(- 7)	-.46083860(- 7)
19	.39195367 (-8)	-.39062660 (-8)	.42642487(- 8)	.42642485(- 8)
20	-.17544592 (-8)	-.17726004 (-8)	-.80894962(- 7)	-.80894963(- 7)
21	.42888485 (-9)	.43333740 (-9)	.10087871(- 6)	.10087871(- 6)
22			-.90193877(-10)	-.90193878(-10)
23			-.41116045(-10)	-.41116044(-10)
24			.94604715(-10)	.94604715(-10)
25			.72401869(-10)	.72401869(-10)
26			-.25172697(-10)	-.25172696(-10)
27			.14519284(- 9)	.14519284(- 9)
28			-.16594900(- 9)	-.16594900(- 9)

Note: Values listed are to be multiplied by 10 raised to the power shown in brackets.

Degree of polynomials	4		5		6	
Number of groups	R.M.S. dev.	Time: minutes	R.M.S. dev.	Time: minutes	R.M.S. dev.	Time: minutes
Storm number 2						
198+					3.427*	154
91	4.020	26	3.868	41	3.501*	69
84					3.552	64½
79	4.048	25½	3.911	38	3.547*	63
78					3.506	62
77					3.480	59
77					3.484	58
71	4.046*	24½	3.917*	36	3.481*	56½
70					3.524	55
67					3.653	54
63	4.070	23½	3.958	34½	3.554	52
Storm number 55						
243+			7.244	73	5.929*	194
165			7.284	66	6.084	96
143					5.979	85
118	8.446*	-	7.291*	-	6.078*	-
98			7.312	45½	6.037	72
76			7.411	40½	6.358	65
59			7.564	38½	6.635	59
42			7.633	33½		

+ Observations not group-weighted.

* Analyses for which isopercental maps were drawn (see later).

TABLE 2

Results of tests on group weighting with increasing degrees of polynomial

Storm number	8	55	170
(a) R.M.S. deviation of observations from calculated surface-percents	2.971	6.078	11.150
(b) Statistic X	1.809	5.545	5.779
(c) Estimated mean error in percental value of observations	1.497	2.526	10.342

TABLE 3

Effects of inherent errors on precision of surface-fitting - Data for storms numbers 8, 55 and 170

DIFFERENCE MAPS FOR STORM NUMBER 55

To provide a visual appraisal of the surface fit and to disclose any oscillatory tendency, implying incorrect choice of order of the equation, residuals were plotted on appropriate maps Figs.A.3, A.4 and A.5 for storm, No. 55. Scrutiny of these difference maps revealed that a sixth-order polynomial, which was the limiting order that the computer could handle, provided the best fit. The fourth-order polynomial surface was far less contorted than would be an imaginary surface passing through every data point. Fig. A.3 shows that large clusters of data points have residuals of the same sign, indicating poorness of fit. Fig. A.4 illustrates the slight improvement in fit of the fifth-order over the fourth-order polynomial surface but even the fifth-order surface can hardly be considered to portray the trend of the observed percentals. Apart from the fact that the residuals on Fig. A.5 are slightly smaller for a sixth-order polynomial surface, the number of data points in each cluster of the same sign is also smaller than those of the fourth- and fifth-order surface fits. Even a sixth-degree polynomial surface is still not flexible enough to follow the local fluctuations of percentals and, as may be noted, there remain large areas exhibiting uniform sign departures. Computer limitations, time economics and susceptibility to ill-conditioning, however, prohibit further raising of the degree of polynomial. The problem of oscillation of the mathematical surface between data points does not arise because an imaginary exact fitting surface would be far more contorted than that of the sixth-order polynomial.

The effect of liberal group-weighting (i.e. reduction in number

of groups each containing increasing numbers of observations) was less spectacular than raising the degree of polynomial; no clearly defined optimum grouping could be detected. It is evident from the tests, however, that group-weighting can bring about considerable economy in computer time with relatively minor sacrifice of precision.

Effect of observational errors on precision of surface-fitting

To gauge the effect of observational errors on the precision with which a mathematical surface could be fitted, the estimated observational error at each station was subtracted from the difference between the observed and calculated percental value and the root-mean-square of these deviations was computed. This statistic is referred to as ~~Statistic X in Table A.3. The results of these tests for storms numbers~~ 8, 55 and 170 are listed in Table A.3.

Such tests are in the main qualitative because of the broad assumptions made in respect of inaccuracies in observing storm data and in estimating mean annual rainfall. The values of the first and third statistics in Table A.3 indicate the relative degree to which lack of fit is attributable to inadequacy of the mathematics or errors in the observations or both. The values of Statistic X provide a guide as to whether or not an attempt to improve the fit would be rewarding.

It was concluded from Table A.3 that in the cases of storms numbers 8 and 55 the precision of representation was governed mainly by the adequacy of the mathematics, whereas for storm number 170 observational errors detracted as much from the over-all precision as

did the mathematics.

A.8 Discussion

It must be noted that at no stage in this study were the coefficients interpreted to have a physical significance. Two conditions precluded physical interpretation of the coefficients, viz. (a) the matrix was basically ill-conditioned and (b) the degree of polynomial was high.

The majority of storms selected for analysis covered areas greater than those of the storms treated in the pilot study. A sixth-order surface, if the undulations are of the same intensity over storms of different areal extent, would have inadequately reflected the trend of the data and probably a twelfth-order polynomial surface would have been needed to ensure a percental fit to the data of storms covering areas larger than those of the pilot study storms. As discussed previously, it was not possible within the capacity of the computer to increase the order of the polynomial beyond six. To overcome this limitation, it was decided to subdivide the storms and fit sixth-order polynomial surfaces to data covering relatively smaller areas. Storms were subdivided into approximately equal areas, each not exceeding 50,000 square miles, this upper limit having been found by trial. To avoid the inevitable discontinuity at the edges of abutting boundaries, an overlap of from a half degree to one degree was allowed.

A P P E N D I X B

REDUCTION OF COMPUTATIONAL EFFORT

The necessity for a time-saving technique arose during development of the routines for depth-area-duration analyses of numerous large-area storms. Sixth-order polynomial surfaces were to be fitted to the precipitation data of 170 storms each represented by an average of about 1500 observations. It can be appreciated that in view of the tremendous volume of calculation entailed it was essential to devise methods of reducing computer time.

A technique was developed whereby only the fundamental elements of the matrix need be evaluated and whereby these elements could first be located in the matrix and corresponding identical elements subsequently filled in. Thereafter, normal procedures could be followed to solve for the coefficients.

B.1 Properties of the matrix

The general equation of a polynomial surface of n -th order defined by two independent variables x and y and one dependent variable z is :

$$z = a_1 + a_2x + a_3y + a_4x^2 + a_5xy + a_6y^2 + a_7x^3 + a_8x^2y + a_9xy^2 + a_{10}y^3 + \dots + \dots + a_{m-1}xy^{n-1} + a_my^n \quad \dots\dots\dots (B.1)$$

Least squares methods may be adopted to estimate the values of the coefficients ($a_1, a_2, a_3, \dots, a_n$) of the polynomial.

The criterion is that the sum of the squares of differences between observed and calculated values should be a minimum. The sum of the squares of differences between observed z_i and calculated $z(x_i, y_i)$ values is dependent on the values of the coefficients. The equations can be written in the form :

$$\sum_{i=1}^N [z_i - z(x_i, y_i)]^2 = f(a_1, a_2, a_3, a_4, a_5, \dots, a_m) \quad \dots\dots\dots (B.2)$$

in which N is the number of observations to which the surface is to be fitted and m the number of coefficients in the polynomial. It can be shown that

$$m = \sum_{k=0}^n (k+1) \text{ where } n \text{ is the order of the polynomial.}$$

To minimize the deviations, equation (B.2) is differentiated with respect to the unknown a_k and equated to zero, thus :

$$\frac{\partial f}{\partial a_k} = -2 \sum_{i=1}^N [z_i - z(x_i, y_i)] \frac{\partial z(x_i, y_i)}{\partial a_k} = 0 \quad \dots\dots\dots (B.3)$$

for $k = 1, 2, \dots, m$.

One may write $z(x_i, y_i)$ as z , x_i as x and y_i as y and from

$$\frac{\partial z}{\partial a_k} \text{ obtain } \frac{\partial z}{\partial a_1} = 1, \frac{\partial z}{\partial a_2} = x, \frac{\partial z}{\partial a_3} = y, \frac{\partial z}{\partial a_4} = x^2,$$

$$\frac{\partial z}{\partial a_5} = xy \text{ and } \frac{\partial z}{\partial a_6} = y^2 \text{ etc. for particular values of } k.$$

The set of equations (B.3) may now be transformed as follows :

$$\frac{\partial f}{\partial a_k} = -2 \sum_{i=1}^N [z_i - z(x_i, y_i)] x_i^h y_i^j = 0 \quad \dots\dots\dots (B.4)$$

for $k = 1, 2, \dots, m$, where h and j are dependent on k .

These normal equations can be written as follows :

$$\sum_{i=1}^N z(x_i, y_i) x_i^h y_i^j = \sum_{i=1}^N z_i x_i^h y_i^j \quad \dots\dots\dots (B.5)$$

for $k = 1, 2, \dots, m$.

By way of example the set of equations (B.5) for a second order polynomial equation, in which $\sum_{i=1}^N$ is denoted by Σ , are written out in full hereunder :

$$\begin{aligned} \Sigma(a_1 + a_2 x_i + a_3 y_i + a_4 x_i^2 + a_5 x_i y_i + a_6 y_i^2) &= \Sigma z_i \\ \Sigma(a_1 x_i + a_2 x_i^2 + a_3 x_i y_i + a_4 x_i^3 + a_5 x_i^2 y_i + a_6 x_i y_i^2) &= \Sigma z_i x_i \\ \Sigma(a_1 y_i + a_2 x_i y_i + a_3 y_i^2 + a_4 x_i^2 y_i + a_5 x_i y_i^2 + a_6 y_i^3) &= \Sigma z_i y_i \quad \dots (B.6) \\ \Sigma(a_1 x_i^2 + a_2 x_i^3 + a_3 x_i^2 y_i + a_4 x_i^4 + a_5 x_i^3 y_i + a_6 x_i^2 y_i^2) &= \Sigma z_i x_i^2 \\ \Sigma(a_1 x_i y_i + a_2 x_i^2 y_i + a_3 x_i y_i^2 + a_4 x_i^3 y_i + a_5 x_i^2 y_i^2 + a_6 x_i y_i^3) &= \Sigma z_i x_i y_i \\ \Sigma(a_1 y_i^2 + a_2 x_i y_i^2 + a_3 y_i^3 + a_4 x_i^2 y_i^2 + a_5 x_i y_i^3 + a_6 y_i^4) &= \Sigma z_i y_i^2 \end{aligned}$$

In general, equations (B.5) can be written in matrix notation as follows :

$$BA = C$$

in which A and C are column vectors having m elements each, thus :

$$A = \begin{bmatrix} a_1 \\ a_2 \\ a_3 \\ \vdots \\ \vdots \\ \vdots \\ a_{m-1} \\ a_m \end{bmatrix} \quad \text{and } C = \begin{bmatrix} \Sigma z_i \\ \Sigma x_i z_i \\ \Sigma y_i z_i \\ \vdots \\ \vdots \\ \vdots \end{bmatrix}$$

and B is a matrix with m rows and m columns :

$$B = \begin{bmatrix} \Sigma 1 & \Sigma x_i & \Sigma y_i & \Sigma x_i^2 & \Sigma x_i y_i & \Sigma y_i^2 & \dots \\ \Sigma x_i & \Sigma x_i^2 & \Sigma x_i y_i & \Sigma x_i^3 & \Sigma x_i^2 y_i & \Sigma x_i y_i^2 & \dots \\ \Sigma y_i & \Sigma x_i y_i & \Sigma y_i^2 & \Sigma x_i^2 y_i & \Sigma x_i y_i^2 & \Sigma y_i^3 & \dots \\ \Sigma x_i^2 & \Sigma x_i^3 & \Sigma x_i^2 y_i & \Sigma x_i^4 & \Sigma x_i^3 y_i & \Sigma x_i^2 y_i^2 & \dots \\ \Sigma x_i y_i & \Sigma x_i^2 y_i & \Sigma x_i y_i^2 & \Sigma x_i^3 y_i & \Sigma x_i^2 y_i^2 & \Sigma x_i y_i^3 & \dots \\ \Sigma y_i^2 & \Sigma x_i y_i^2 & \Sigma y_i^3 & \Sigma x_i^2 y_i^2 & \Sigma x_i y_i^3 & \Sigma y_i^4 & \dots \\ \vdots & \vdots & \vdots & \vdots & \vdots & \vdots & \vdots \\ \vdots & \vdots & \vdots & \vdots & \vdots & \vdots & \vdots \\ \vdots & \vdots & \vdots & \vdots & \vdots & \vdots & \vdots \\ \vdots & \vdots & \vdots & \vdots & \vdots & \vdots & \vdots \end{bmatrix}$$

By multiplying, in turn, the elements in a row in B by the elements in the vector A, summing the products for each row, and equating this result to the corresponding row element in vector C, one obtains the equations (B.5)

This form of the equation is highly convenient because scrutiny of the configuration of the elements of the matrix discloses the possibility of developing a time-saving technique.

In the first place, since the matrix B is symmetrical about the main diagonal, i.e. $b_{ij} = b_{ji}$, the elements of only the upper triangular matrix need be calculated for each observation. Secondly, examination of the matrix in the upper triangular matrix reveals that several values occur repetitively, e.g. $b_{26} = b_{35}$, suggesting that there exists an array P consisting of the fundamental elements, namely, only those which differ from one another. For instance, for a second order polynomial surface, the array of fundamental elements would comprise the underlined elements in the above matrix B. In general, the number of elements needed to define the array P in full, and hence the matrix B, for a polynomial of order n would be given by :

$$U = \sum_{i=0}^{2n} (i+1).$$

The number of elements that must actually be evaluated is, therefore, reduced from m^2 to U . It follows that the higher the order of polynomial the greater the reduction in computation that can be achieved.

To define the complete equation $BA = C$, only the elements in the column vector C, together with the array P, need be evaluated for each observation to which the surface is to be fitted.

B.2 Defining the matrix

After the array P has been defined, i.e. all the data points have been used in calculating the elements of P, the matrix B can be filled in. To facilitate this procedure, the elements of the basic vector should be serially numbered as they first appear in the matrix B from left to right and row by row in ascending order. For any element in the matrix B, say b_{ij} , there exists an element p_s in P.

To locate the element p_s the procedure is :

Test for the maximum value of k_1 that will

satisfy $i > t_1$, where $t_1 = \sum_{h=0}^{k_1} h$ and similarly

test for the maximum value of k_2 that will

satisfy $j > t_2$, where $t_2 = \sum_{h=0}^{k_2} h$

Now let $k = k_1 + k_2$

and $t = \sum_{h=0}^k h - 1$

Then $s = i + j + t - t_1 - t_2$

For example, suppose one desires to evaluate the element in the 3rd row, 4th column, i.e. $b_{3,4}$. The maximum value of k_1 such that $3 > t_1$ is unity and in this case $t_1 = 1$.

Similarly, for k_2 one has $k_2 = 2$ and $t_2 = 3$.

Hence $k = 3$ and $t = 5$. Thus $s = 3 + 4 + 5 - 1 - 3 = 8$

i.e. the element $b_{3,4}$ corresponds to the 8th element in the array P.

Hence there exists a relationship such that for each element in the matrix B an element in the basic array P can be found to conform with the pattern of the matrix B.

B.3 Conclusion

The technique described proved invaluable in the fitting of high order polynomials to large numbers of arbitrarily spaced data. The resulting time reductions, expressed by the factor U/m^2 , make it feasible to adopt surface-fitting techniques that would not otherwise be justified because of the lengthy machine time entailed.

Although developed for large-area storm studies, the technique has also been successfully applied in the planning of open-pit mines. Procedures for computation of ore and waste volumes by fitting of a polynomial equation to the land topography have been described by O.K.H. Steffen³⁶.



A P P E N D I X C

COMPUTER PROGRAM LOGIC EMPLOYED IN PREPARATION OF LIBRARY OF STORM DATA

Fig. C.1 is a flow chart showing the arrangement of computer programs to bring the analysis of large storms to the stage where the isopercental surface can be plotted on a quarter degree grid. Programs code-named LATEL, BLOCK, BOB, MINC and STORM are used successively and by manipulating sense switches (SW) on the computer, numbered one to four, components of the sequence can be by-passed or re-run. At convenient stages of computation, by executing the sub-program DUMP, the complete memory in core storage can be deposited on two cylinders of a magnetic disc. Computation may thus be interrupted upon expiry of a machine time allocation and continued at a subsequent computing session without the need for recomputing incomplete routines. Because variable word-length is required these programs employ the FORTRAN II-D compiler.

Fig. C.2 : Key to flow charts

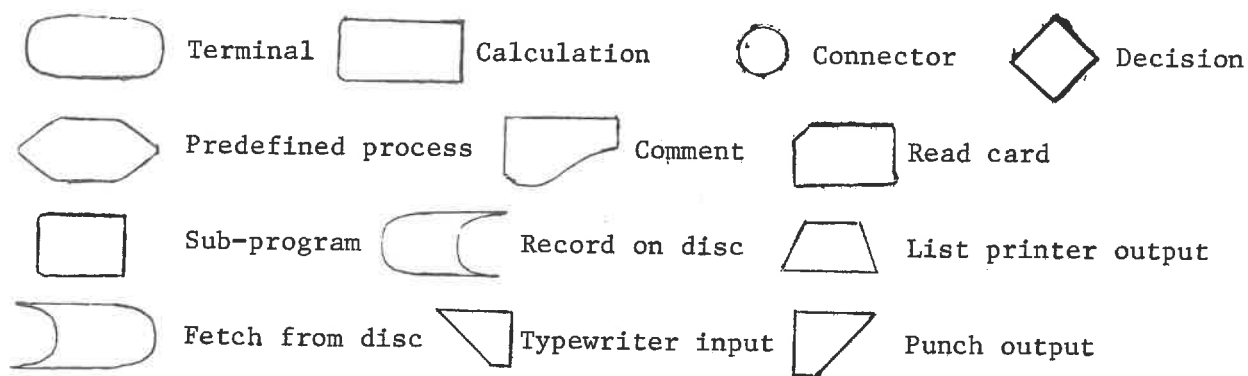


Figure C.1 General arrangement of computer programmes

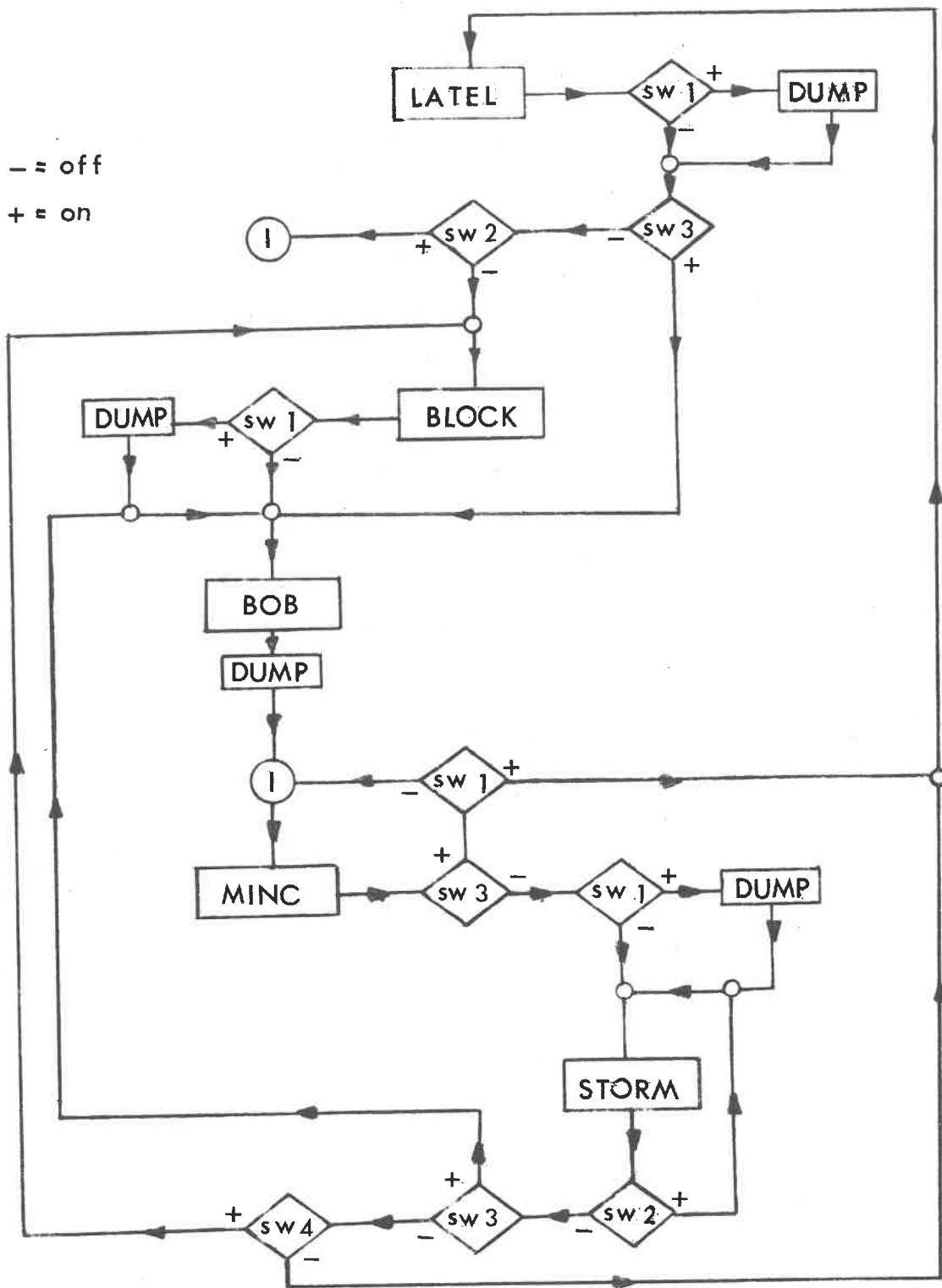
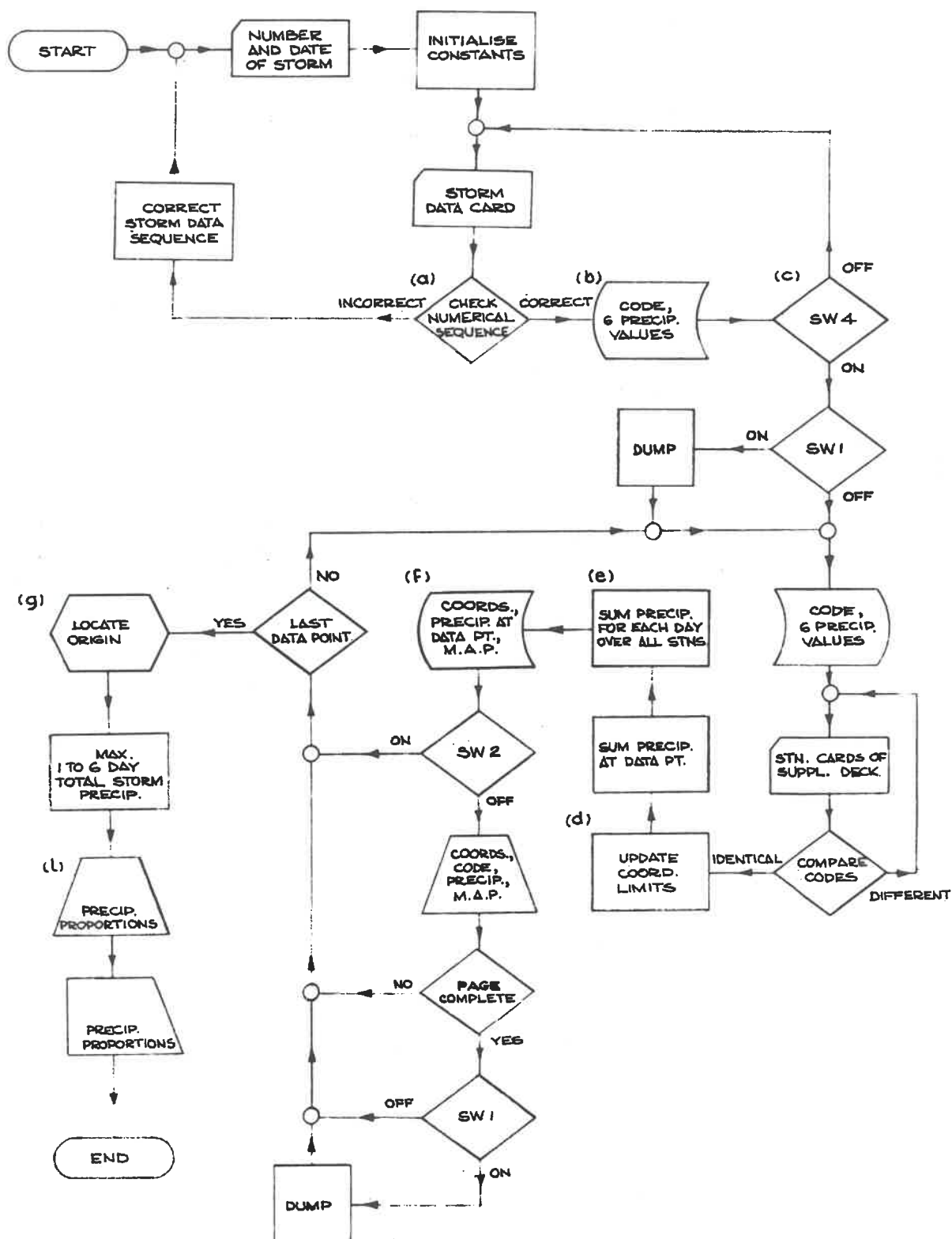


FIG.C.3: LOGIC OF PROGRAM "LATEL"



C.1 Explanatory notes for Fig. C.3

Fig. C.3 is a logic flow chart of the program "LATEL". "LATEL" reorganizes the information on the data cards and station cards in a form suitable for analysis and records this at relocatable sectors on the disc.

- (a) To enable the machine to expedite selection of station cards from the supplementary deck it is necessary that the storm data cards be stacked in strict numerical sequence according to station code number.
- (b) Every number recorded on the magnetic disc occupies 24 storage positions, viz. the 22 significant digits required in the computation and one position each for the decimal point and sign. As there are sufficient storage positions for 100 digits on each sector of the disc, four numbers may be allocated to each sector leaving four positions vacant. Each data card contains 8 numbers (section number, position number and six daily precipitation totals) and therefore occupies two sectors of disc storage.
- (c) After the last two cards have been read in, SW4 is switched to the "on" position to initiate the next phase of the routine. A counter, updated each time SW4 is interrogated, indicates, at the end of the "read" phase, the number of observations handled for the storm under study.

- (d) By comparing updated maximum and minimum latitude and longitude with the latitude and longitude of current data point, the machine determines the outer limits of the storm data. These four numbers are required for positioning the origin, the size of the elementary areas discussed in program "BLOCK" and the extent of the region over which the grid plot of the isopercental surface is to be tabulated.
- (e) Precipitation for each day is summed over all the data points.
- (f) Overwriting the data at that storage space, the machine records the latitude, longitude, total storm precipitation and mean annual precipitation for each data point on a separate sector of the disc. The maximum number of sectors available for storing these data points is 2099, and, as the occupants of these are required in identical form in programs "BLOCK" or "BOB" and "MINC", they are not overwritten until "LATEL" has been executed.
- (g) The origin is established towards the north-west corner at the nearest quarter degree grid intersection outside the storm area.
- (h) On a card are punched maximum precipitation totals for durations of one to six days, expressed as proportions of the total storm depth. These proportions are then printed out.

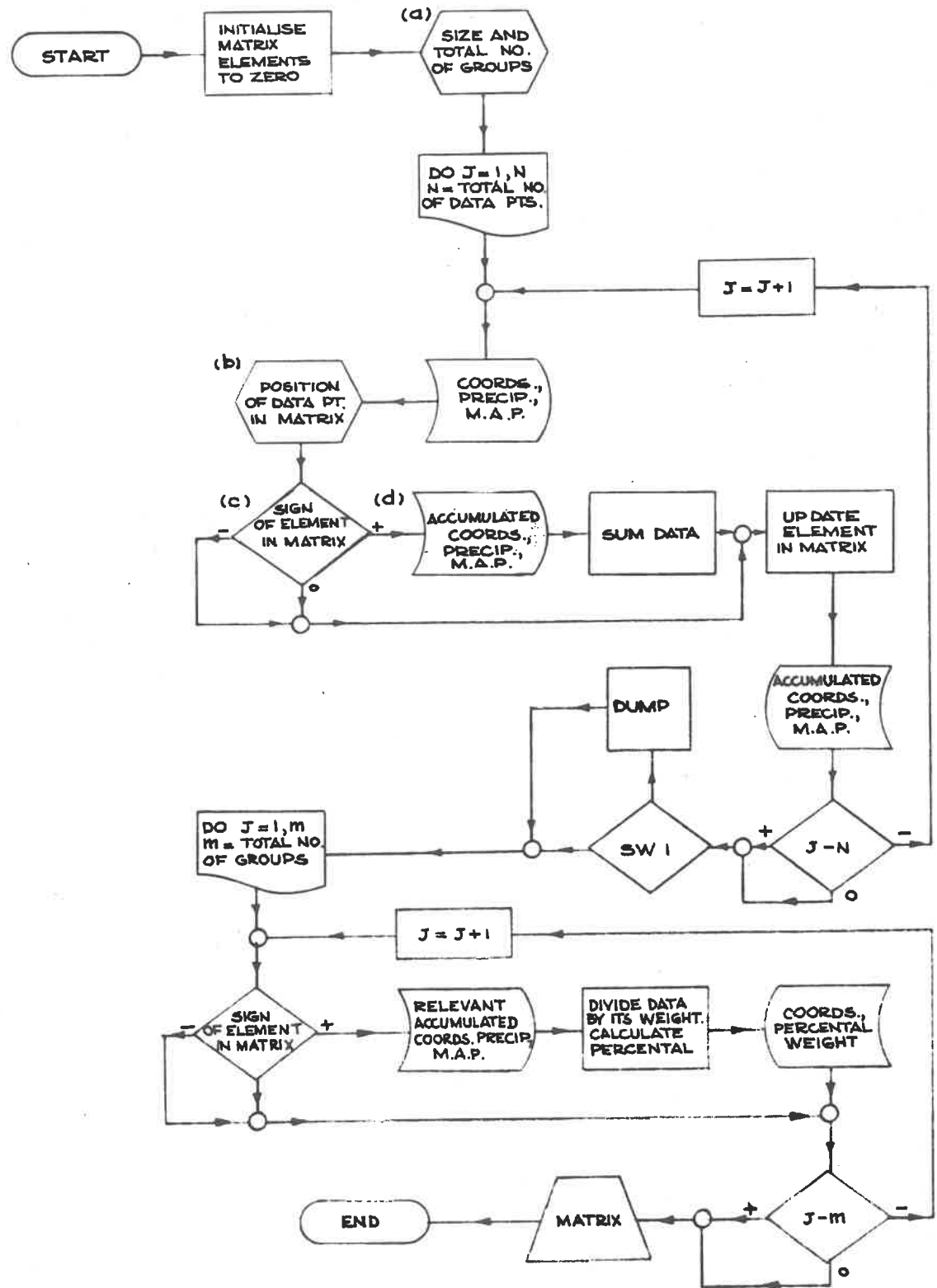
C.2 Explanatory notes for Fig. C.4

Fig. C.4 is the logic flow chart of the program "BLOCK".

"BLOCK" groups and weights the data that have been assembled on the disc by program "LATEL" and records the grouped and weighted data on a different section of the disc.

- (a) Coordinates of the corners of the area for which storm data have been abstracted provide a basis for initial subdivision of the storm area for group-weighting purposes. Nominal side dimensions in east-west and north-south directions are assigned to the subdivisions according to the extent of the total storm in the corresponding direction. For a total storm extending less than 200 minutes of arc along a meridian or parallel, subdivisions are assigned a nominal side dimension of 15 minutes of arc in that direction. Side dimensions of 20 and 25 minutes of arc are assigned to subdivisions of a storm extending between 200 and 400 minutes of arc and over 400 minutes of arc respectively in any direction. The storm area is finally divided into an integral number of subdivisions of which side dimensions approximate to the corresponding nominal dimensions.
- (b) Each data point is assigned to a group according to its position. A matrix is built up of one element for each group of points in their correct relative positions.
- (c) The value of an element of the matrix represents the weight assigned to the average data for the corresponding group. This

FIG.C.4: LOGIC OF PROGRAM "BLOCK"



weight accords with the number of original data points in the group.

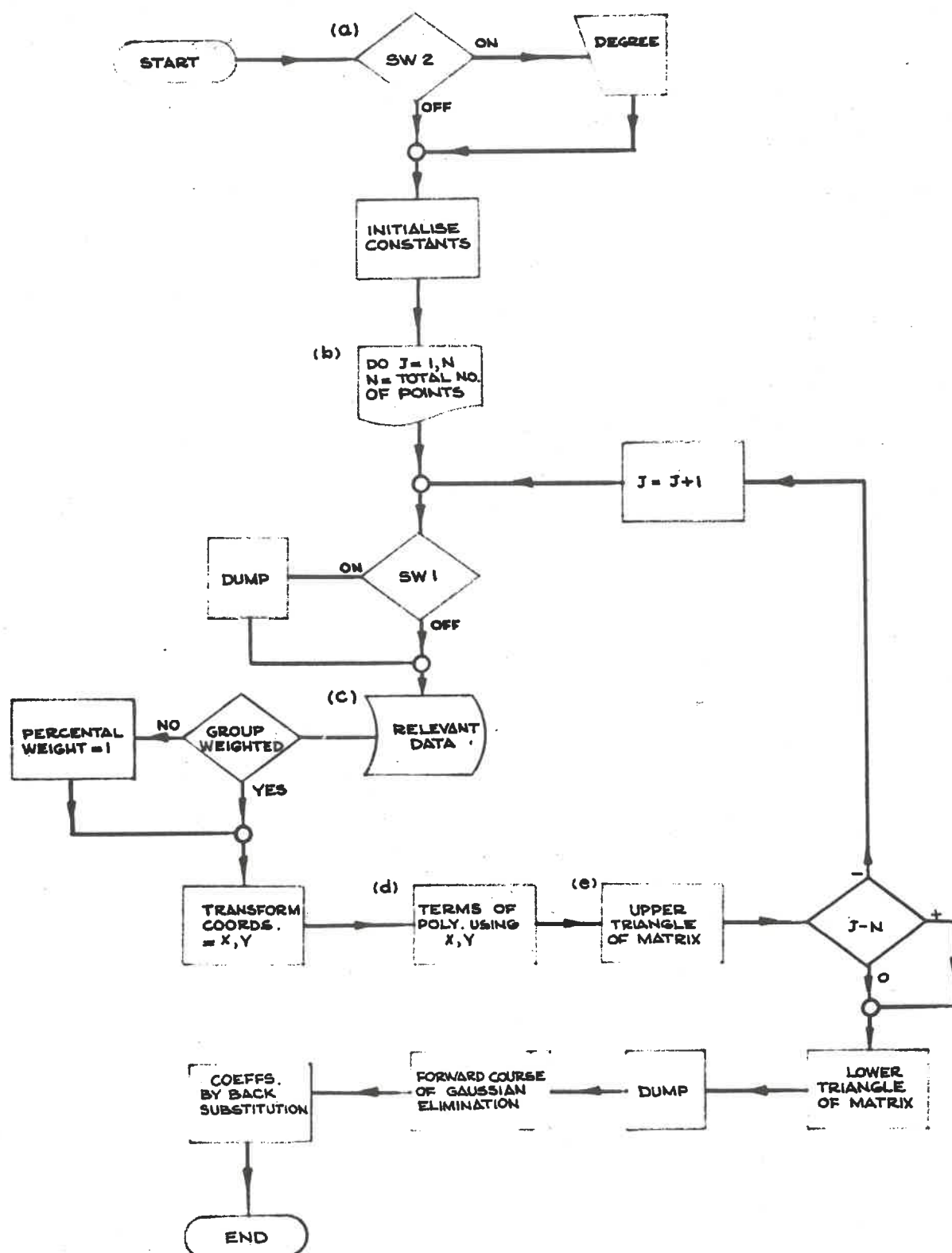
- (d) With a Fortran II-D compiler and one disc drive there are 4349 sectors available for relocatable storage of data. Storage space for data from 2099 observation stations, each station requiring one sector, is reserved at the outset leaving 2250 sectors for the storage of group-weighted data. Provision is made for the circumstance in which there are more elementary subdivisions of area than original observation points. Such a situation could arise where an extremely extensive storm covers an area having sparse, non-uniformly distributed rain gauges, in which case a representative observation may be lacking in some of the subdivided areas.

C.3 Explanatory notes for Fig. C.5

Fig. C.5 is the logic flow chart of the program "BOB". "BOB" fits the mathematical isopercental surface to the data points as prepared by programs "LATEL" and/or "BLOCK".

- (a) In the program, the polynomial is normally set to sixth degree which is the highest that can be handled. If, however, a degree lower than 6 is desired, SW2 must be switched to the "on" position at the start of program "BOB".

FIG.C.5: LOGIC OF PROGRAM "BOB"



- (b) N represents the total number of points to which the isopercental surface is to be fitted and depends on whether the original or the group-weighted data points are to be adopted. If "BOB" follows "LATEL" in the execution order it implies that the original data points are in use whereas if "BOB" follows "BLOCK" group-weighted data points will have been adopted.
- (c) The form in which "LATEL" stored the data on disc is retained if the program follows on from "LATEL". If it succeeds "BLOCK", the form in which "BLOCK" stored the data is retained.
- (d) In this routine the various terms, products of latitude and longitude, required to establish the normal equations are calculated.
- (e) Writing the normal equations in matrix form implies symmetry about the main diagonal, thus only the upper triangular matrix need be established for each point. After all the data points have been used to establish the upper triangular matrix the lower half is defined by transposing the elements of the matrix.

C.4 Explanatory notes for Fig. C.6

Fig. C.6 is the logic flow chart of the program "MINC". "MINC" performs prescribed statistical tests by comparing observed precipitation values with those determined by the mathematical surface or with a surface bounded by the range of evaluated possible error of observation.

FIG.C.6: LOGIC OF PROGRAM "MINC"

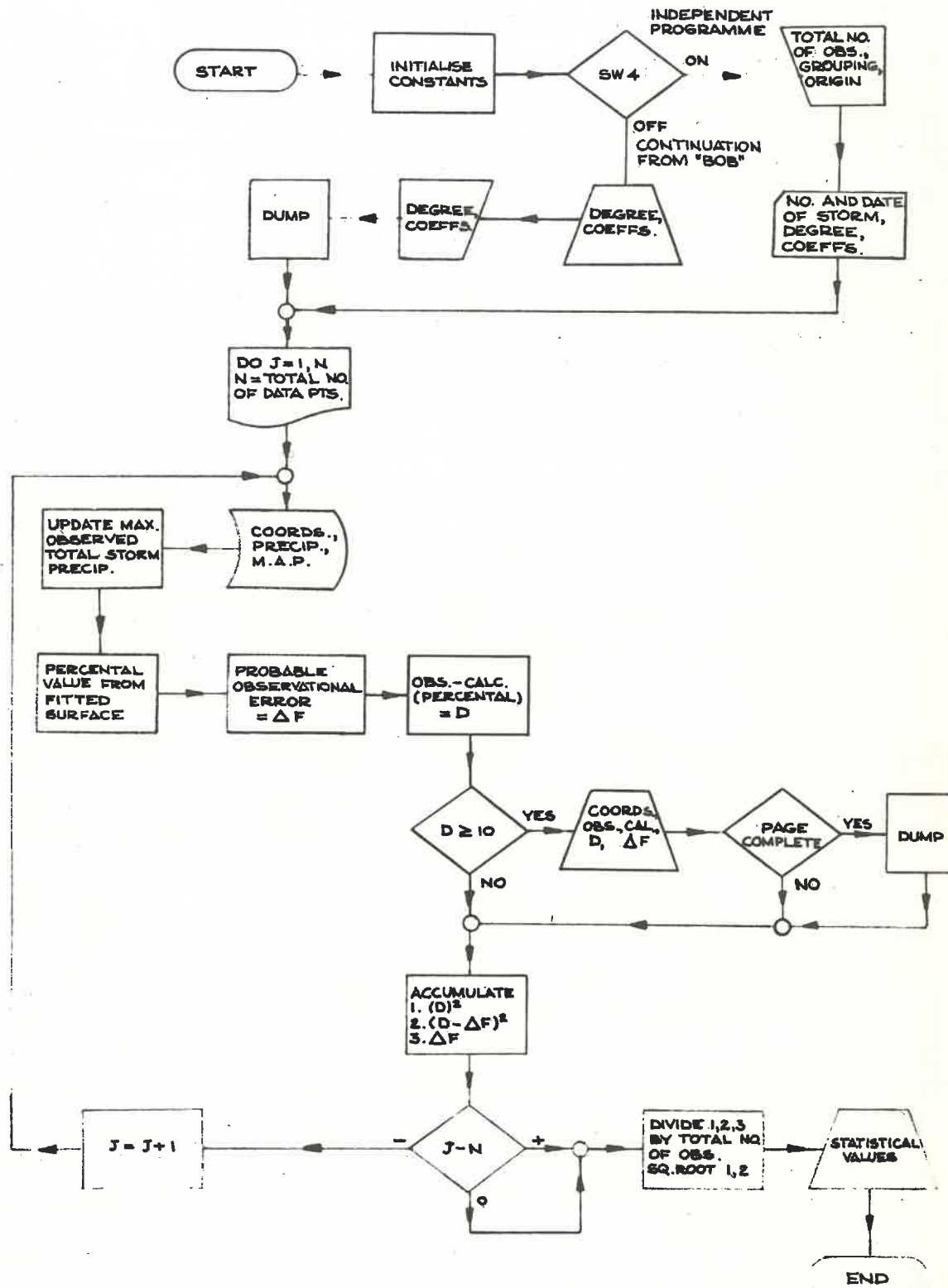


Fig. C.6 is self-explanatory.

C.5 Explanatory notes for Fig. C.7

Fig. C.7 is the logic flow chart of the program "STORM".

"STORM" calculates and prints the value of the mathematical surface at every quarter degree intersection within the area under study.

- (a) The quarter degree intersections fringing the area embracing the data points define the extremities for which the surface is calculated.
- (b) The increment is predefined as a quarter degree at which resolution the surface must be evaluated and printed. If an alternative increment is desired the program must be run with SW2 in the "on" position.

C.6 Explanatory notes for Fig. C.8

Fig. C.8 is the logic flow chart of program "TRAP" which continues the analysis from the isopercental surface to the isohyetal grid plot and the depth-area-duration tabulation. This program uses the "Witrap" compiler which allows 92 cylinders of the disc to be exploited for the storing of data, compared with only 23 when the Fortran II-D compiler was in use.

The basic cards, on which were punched latitude, longitude and mean annual precipitation to a resolution of one minute of arc,

FIG.C.7: LOGIC OF PROGRAM "STORM"

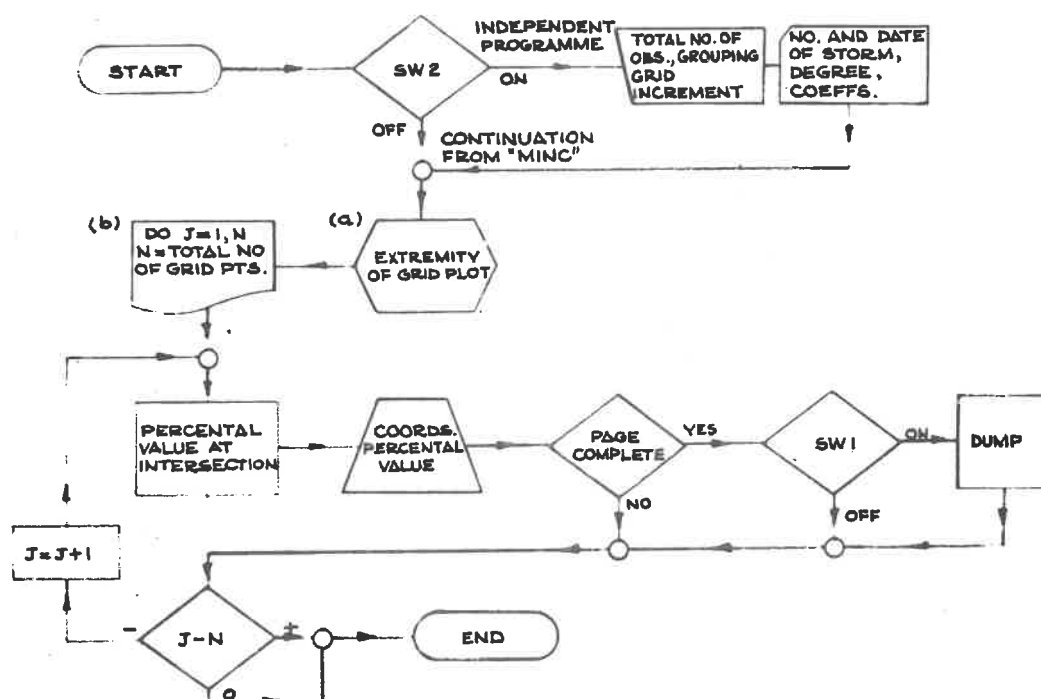
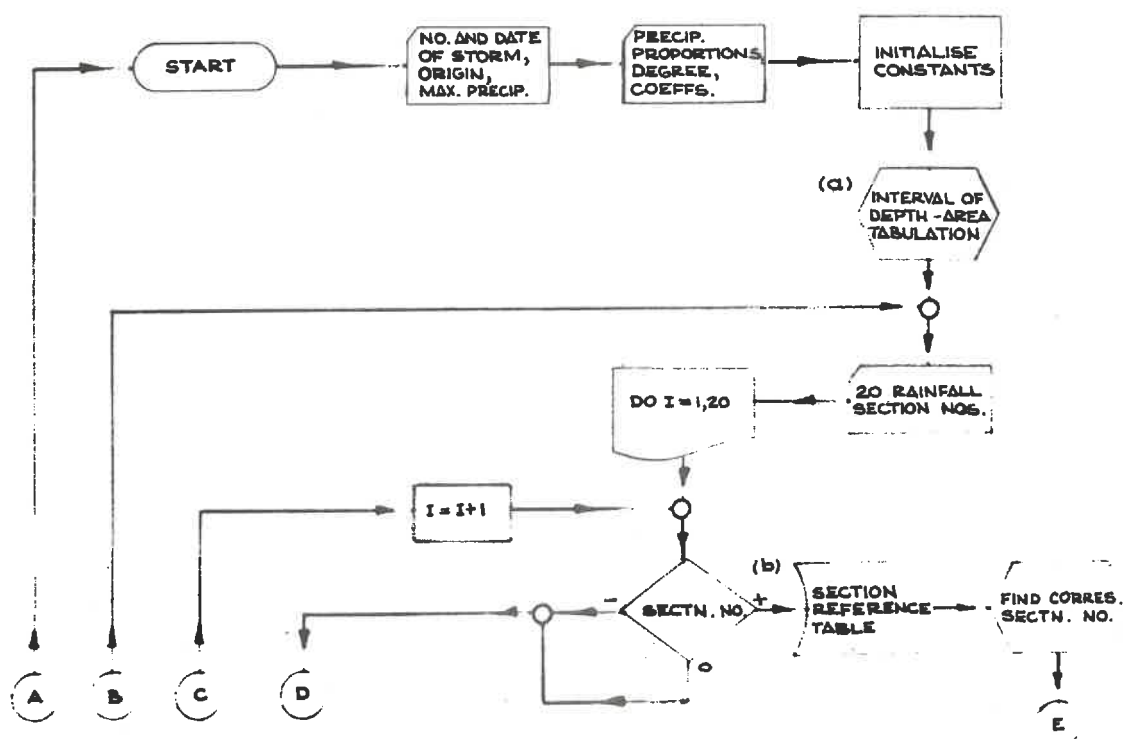


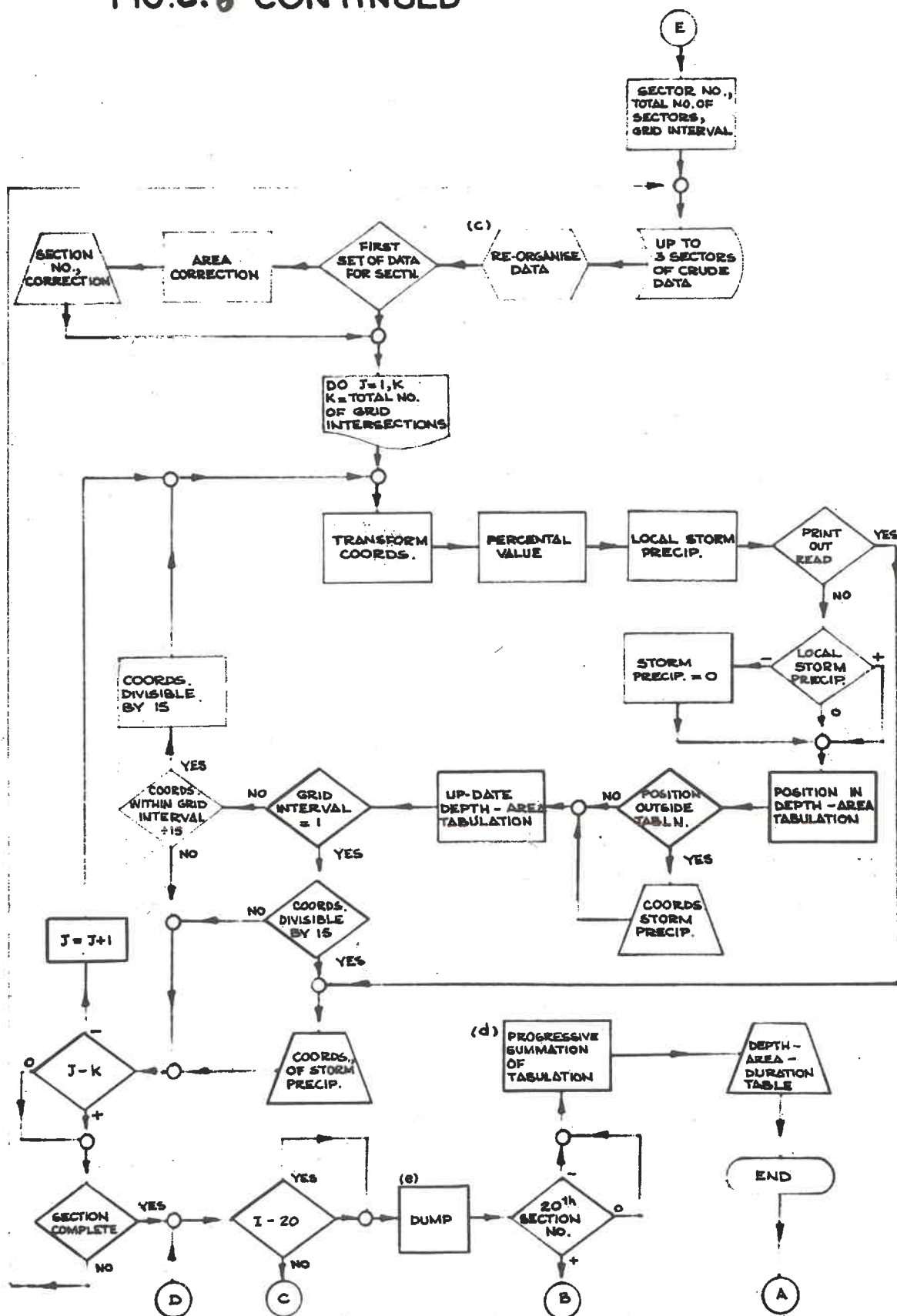
FIG.C.8: LOGIC OF PROGRAM "TRAP"



are now recorded on the remaining cylinders of the disc in suitably compact form so as not to occupy unnecessary space.

- (a) The interval to be selected for the depth-area-duration tabulation depends on the maximum observed precipitation. Convenient intervals would be chosen to cause the maximum precipitation to lie about three-quarters of the way up the tabulation.
- (b) 160 sectors are set aside to accommodate, at five per sector, references to all the sections stored on disc. This permits random access to any section. The reference to a section comprises section number, starting sector (at which the data for the section is stored), number of sectors needed to store that section, and grid interval of stored data.
- (c) Two fixed point numbers of four digits each are floated to eight digits to ensure full utilization of disc storage space. When retrieved from the disc these data must be transformed to original form, viz. coordinates and M.A.P.
- (d) Progressive summation of storm values by area, starting with the area corresponding to maximum precipitation in the tabulation, yields a table of areas over which storm precipitation depths were equalled or exceeded.

FIG.C.8 CONTINUED



- (e) The Witrap compiler interrogates sense switch number one (SW1) after the completion of each "DO" loop; the "DUMP" instruction is automatically executed when SW1 is placed in the "on" position. A "DUMP" instruction is incorporated in the program as a safety device.

The program "TRAP" was modified and called "BUNK" and listed in Appendix D to present depth-area-duration tabulations for each strip as defined in Chapter 111.

C.7 Explanatory notes on programs for frequency analysis

All manually extracted depth-area tabulation of storms for a sub-region from computer print-outs of tabulations for relevant strips are punched onto cards and entered as data from which depths can be ranked for given area and duration. A second order polynomial is fitted by least squares theory to each depth-area tabulation and precipitation values at desired area intervals are extracted and bubble-sorted. The ordered values for each selected area are printed and punched. This procedure is repeated for each duration.

The same procedures are employed when maximizing the depth parameter to obtain the possible maximum precipitation. In this case moisture content values for each storm and maximum observed moisture content values for each month of the year are entered so that each tabulation can be maximized.

To establish precipitation values for desired recurrence intervals the ranked precipitation values extracted from the previous program are interpolated by employing least squares theory to fit a second order polynomial to depth and its associated rank. Again this is repeated for each duration.

These programs are listed in Appendix D.

D.1

CORRELATION AND PREPARATION OF STORM AND STATION DATA

220

224

GROUP AND WEIGHT DATA

UPDATE GROUPS AND WEIGHTS WITH DATA FROM UISC

```

00 14 K=1;N
>ETCH=11R
15 = (K+1)*NKK*1.
16 F=1-K+17+18
15 = N
17 1P = (K+2)-V1*WK*1.
18 1P1P-K*19+16*20
20 1P = K*Y
19 JB = (15-1)*Y+1P
JAJJB1 = JAJJB1+1
1P JAJJB1=154,34,35
00 38 J=1,4
38 WJ = 0.
IT = 209+115-1)*K*1P
00 10 30
35 11 = 209+115-1)*K*1P
FIND1111
IT = 11
FETCH1111B
FIND1111
00 22 J=1,4
22 WJ1 = WJ1+R(J)
14 RECUR1111B
IF 1SENSE SWITCH 1112,2
1 CALL DUMP
PAUSE

```

1040 ALL GROUPS FOR WHICH WEIGHTS ARE NOT ZERO UNTU DISC

```

2 L = 0
3 U1 = 2100
4 DU 23 J=1JC
5 IF (JAL1) J23=23,37
7 I1 = 20994+J
8 FINU(I1)
9 L = L+1
10 FETCH(I1)J1
11 FINU(J1)
12 A = JAL(J1)
13 A = 1/A
14 U1 25 M=14
15 K(I1) = 8+I1*A
16 K(I1) = (R(31)J1/4)+10.0
17 K(I1) = JAL(J1)
18 RECORDU(1)H
23 CONTINUE
24 PRINT 108,NU
30 FORMAT(1X)18X15H STORM STUDIES /28X(2H**
42 125H SURFACE ANALYSIS/23X(312H**//
57 2728X(125H)1/27X(3125H FORM NUMBER 1//28X(92H
62 125H)
70 FORMAT(10X,15H DATE OF STORM 313,64,2UN
80 PRINT 16,1X,J1,J2,J3,J4,J5,J6,J7,J8,J9,J10
90 FORMAT(125H)
105 15H SIZE OF BLOCKS,2F7,2,15H NO OF BLOCK
110 PRINT 29
120 IFENSE SWITCH 3125=27
130 IFENSE DISTRIBUTION OF OBSERVATIONS
140 JC = 3000-(60-K*V1)
150 DU 107 J=JC,3000
160 JAL(J1) = 0
170 DU 109 JB1,KKK
180 IS = (28-J1)*J1
190 IF = 1580+J
200 PRINT 26,1X,J1,J2,J3,J4,J5,J6,J7,J8,J9,J10,J11,KKK,J=JC,3000
210 FORMAT(10(612))
220 PRINT 42,L
230 FORMAT(1739H NO OF UNDEPENDENT BLOCKED OBS
240 IFENSE SWITCH 3125=27
250 L = 2100
260 FINU(I1)
270 PRINT 32
32 FORMAT(13H LATITUDE LONGITUDE ISOPERSENTAL
33 DU 30 I=1,L
34 FETCH(I1)
35 FINU(I1)
36 PRINT 31,IR(J1),J=1,41
37 FORMAT(499,21)
38 IFENSE SWITCH 1133=40
39 CALL OUMP
40 PAUSE
41 IF = 2100
42 CALL LINK(180)

```

D.2

SET UP PRIME TERMS FOR MATRIX FROM DATA

```
*LOISKMB
*PANDK2206
*LIST PRINTER
DEFIN DISK(4,4349)
DIMENSION R(4),A(812)
COMMON NO,ND,NM,NY,NL,LX,LY,IX,JX,IY,JY,II,JI,YI
COMMON KHP,NOT,MNOT,INC,S
Y = LY
X = LX

SELECT DEGREE OF POLYNOMIAL
TYPE 1
1 FORMAT(22H SW2 ON=ENTER DUEK 12)
NOT = 1
IFISENSE SWITCH 219,8
8 KHP = 6
GO TO 10
9 ACCEPT 2,KHP
2 FORMAT(12)
10 DO 3 I=1,KHP
3 NOT = NOT+1
MNOT = NOT+1
N = NOT+MNOT
DO 4 J=1,M
4 A(I,J) = 0
5 J = J+1
N = KHP+1
KS = KHP+KHP
NT = KS-1+MNOT+KS
KS = KS+1

CALCULATE AND SUMMATE PRIME NUMBERS
DO 13 NM=1,L
IFISENSE SWITCH 110,30
6 CALL DUMP
PAUSE
30 FETCH(1)R
IF(11-2100151)52,52
51 V = (K(1)/K(4))*10
L = 1
GO TO 31
52 V = R(3)
E = R(4)
31 JJ = J
G = R(1)-X
F = R(2)-Y
A(MNOT) = A(MNOT)+V*E
MNOT = MNOT+MNOT
NK = MNOT
A(MNOT) = A(MNOT)+V*G*E
MNOT = MNOT+MNOT
A(MNOT) = A(MNOT)+V*F*E
NK = NK+1
A(NK) = G
A(NK+1) = F
MNOT = MNOT+1
A(MNOT) = A(MNOT)+E
A(NK+1) = A(NK+1)+G*E
A(NK+2) = A(NK+2)+F*E
DO 13 K=3,KS
NK = NK+MNOT
NK = NK+1
NT = NK
NK = NK-(MNOT+1)
MNOT = NK
JJ = JJ+1
A(NK) = A(MNOT)
A(NK) = A(MNOT)+A(NK)*E
DO 7 KK=2,K
JJ = JJ+1
NS = NK+1
MNOT = MNOT+1
A(MNOT) = A(MNOT)+F
A(NK) = A(NK)+A(MNOT)*E
7 NT = NT+1
IF(JJ-NOT)5,5,13
5 MNOT = NK
DO 19 KK=1,K
MNOT = MNOT+MNOT
A(MNOT) = A(MNOT)+A(MNOT)*V*E
19 MNOT = MNOT+1
13 CONTINUE
CALL DUMP
CALL LINK(MIND)
END
```

SOLUTION OF MATRIX

```
*LOISKMB
*PANDK2206
*LIST PRINTER
DEFIN DISK(4,4349)
DIMENSION R(4),A(812)
COMMON NO,ND,NM,NY,NL,LX,LY,IX,JX,IY,JY,II,JI,YI
COMMON KHP,NOT,MNOT,INC,S
X = LX
Y = LY

EXPAND PRIME TERMS TO DEFINE UPPER TRIANGULAR PORTION OF MATRIX
KH = KHP+2
KP = KH
MDO = MNOT+KH
NP = KHP+1
DO 14 K2 = 1,NP
MDO = MDO+KH
KH = KH+1
KP = KP+1
M = 0
LM = 0
DO 14 J=1,KH
NR = KHP+J
KN = (2*KP-J)*MNOT+2*KP+1-J
DO 14 K=1,NR
NK = KHP+K
IF(J-I)15,15,16
15 R = NR
16 LM = LM+1
NT = MNOT+(MDO-LM-1)*MDO
DO 14 NM=1,M
NT = NT-1
A(NT) = A(NK)
14 NK = NE-1
A(I) = R

TRANSPOSE TO LOWER PORTION OF MATRIX
DO 17 M=2,NOT
LM = M-1
LL = LM+MNOT
DO 17 J=1,LM
LL = LL+1
K = (J-1)*MNOT+M
17 A(II) = A(K)
NM = NOT-1
CALL DUMP

FORWARD COURSE OF SOLUTION
DO 20 K=1,NM
LM = (K-1)*MNOT
LL = K-1
NT = (K-1)*MNOT+K
Z = 1./A(NT)
DO 20 M=LL,NOT
NS = (M-1)*MNOT
NR = NS+K
K(1) = A(NR)*Z
DO 20 J=1,MNOT
NR = LM+J
NS = NS+J
20 A(NK) = A(NK)-A(NR)*K(1)

BACK SUBSTITUTION TO OBTAIN COEFFICIENTS
NS = (NOT-1)*MNOT+MNOT
NT = NS-1
K = 783+NOT
A(K) = A(NS)/A(NT)
DO 21 M=1,NM
K = NOT-M
LL = K-1
NS = (M-1)*MNOT
NT = NS+K
E = 0
Z = 1./A(NT)
DO 22 J=LL,NOT
LM = 783+J
NR = NS+J
22 E = E+A(NR)*A(LL)
LM = 783+K
NX = MNOT+K
21 A(II) = A(NK)-E*Z
CALL DUMP
```

CALL LINK(MIND)

END

PRINT OR ENTER COEFFICIENTS

```
*LOISKMB
*PANDK2206
*LIST PRINTER
DEFIN DISK(4,4349)
DIMENSION S(29)
COMMON NO,ND,NM,NY,NL,LX,LY,IX,JX,IY,JY,II,JI,YI
COMMON KHP,NOT,MNOT,INC,S
X = LX
Y = LY
INC = 15
TYPE 1
1 FORMAT(20H SW4 ON=ENTER CUEFF)
IFISENSE SWITCH 412,6
2 TYPE 3
3 FORMAT(52H SW2 ON=STAT TEST,UP=GRID PLUT,LOAD PEIGRE,COEFFS,
1/51H LOAD NO OF OBS,BLOCKED OBS,BLOCKING,413,215,DK16,IN)
READ 8,NO,ND,NM,NY,KHP
8 FORMAT(1413/13)
NOT = 1
DO 9 I=1,KHP
9 NOT = NOT+1
MNOT = NOT+1
11 DO 12 I=1,MNOT
12 READ 13,NUM,S(I)
13 FORMAT(131,3K,E14,8)
IF(NUM-114)12,14
14 TYPE 15
15 FORMAT(22H CARDS OUT OF SEQUENCE)
PAUSE
GO TO 11
12 CONTINUE
READ 26,NL,IX,IY,LX,LY
26 FORMAT(413,215)
X = LX
Y = LY
IFISENSE SWITCH 21127,5
5 TYPE 10
10 FORMAT(25H TYPE IN THE INCREMENT 12)
ACCEPT 10,INC
16 FORMAT(12)
CALL LINK(STORM)
6 PRINT 108
108 FORMAT(1H1,28X14H STORM STUDIES/28X9(2H**)/28X9(2H**),
1/23X25H SURFACE FITTING ANALYSIS/23X13(2H**)/)
PRINT 109,NO,ND,NM,NY,NL,LX,LY,KHP
109 FORMAT(9X,2H DERIVATION OF POLYNOMIAL BY METHOD OF LEAST SQUARES,
1/9X13(4H**)/27X14H STORM NUMBER 14/28X9(2H**)/10X DATE OF,
25H STORMS/13,6X13H NO OF OBSERVATIONS/15/21H ORIGIN OF STORM AREA,
32F7,0/14H HIGHEST POWER/13)
IF(IN-140)40,40
40 PRINT 42,XI,YI,L
42 FORMAT(15H SIZE OF BLOCKS/2F,2,3X27H NO OF BLOCKED OBSERVATIONS/15)
41 PRINT 126
126 FORMAT(130H COEFFICIENTS OF ISOPERCENTALS//)
MOIX = (JX+IX)/2
PUNCH 204,2X,Y,MOIX
204 FORMAT(2F6,0,15)
PUNCH 7,KHP
7 FORMAT(13)
DO 300 J=MNOT,29
300 S(I) = 0
DO 124 J=1,NOT
PUNCH 125,J,S(J)
124 PRINT 125,J,S(J)
125 FORMAT(131,3K,E14,8)
CALL DUMP
127 CALL LINK(MIND)
END
```

STATISTICAL TESTS

```
*LOISKMB
*PANDK2206
*LIST PRINTER
DEFIN DISK(4,4349)
DIMENSION R(61),A(4)
COMMON NO,ND,NM,NY,NL,LX,LY,IX,JX,IY,JY,II,JI,YI
COMMON KHP,NOT,MNOT,INC,S,NS,SK,SL,SS,SR,SO,SP,
150,SN,SN,SL,SK,SL,SS,SR,SO,SP,SE,SD,SC,SB,SA
TYPE 1
1 FORMAT(53H SW1 ON=STAKE PRUGHAN,SW2 ON=UBS CAL,SW3 ON=NEW CUEFF)
LB = 0
II = 1
KD = 10
K = 0
US = 0
LM = 0
VAR = 0
DAR = 0
DR = 0
FR = 0
TF = 0
PR = 0
RE = 0
K = LZ
Y = LY
PRINT 108
108 FORMAT(1H1,28X15H STORM STUDIES/28X9(2H**)/28X9(2H**),
1/23X25H SURFACE FITTING ANALYSIS/23X13(2H**)/)
LB = LB+1
PRINT 23,LB,NO,ND,NM,NY,NL,LX,LY,KHP
23 FORMAT(26X17H STATISTICAL TEST/6X PAGE 12/23X13(2H**)/27X,
113H STORM NUMBER,14/25X9(2H**)/10X DATE OF STORM 313,0X,
220H MU OF OBSERVATIONS 15/17X URSCH UP SURFACE/12)
IF(IN-110)16,16
16 PRINT 25,LX,LY,I
25 FORMAT(31H NUMBER OF BLOCKED OBSERVATIONS/15,14H BLOCKING/2F6,2)
16 PRINT 34
34 FORMAT(15H LAT LONG OBS CAL PERCENTAL HAND) (15 CAL MYETAL,
14H N,A,P,/)
DO 17 I=1,N
RE = RE+1
IF(RE-50)2,6,6
6 IFISENSE SWITCH 117,2
7 RE = 0
CALL DUMP
PAUSE
2 FETCH(1)IA
CALCULATE DIFFERENCE OF UNOBSERVED AND CALCULATED VALUES
G = A(1)-E
F = A(2)-Y
GG = A(3)*.1
FF = A(4)
V = F*G
Z = (((((F*SB+SL)+F*SO)+F*SI)+F*SP)+SC)+SA
1/(1/(1/(G*SS+SP)+G*SK)+G*SG)+G*SD)+G*SB+G
M = (1/(F*ST+SI)+F*SN)+F*SL+P+SE
1/(1/(G*SS+SO)+G*SL)+G*SH+G
2/(1/(G*SR+SI)+G*SI)+G*SS)+G*SD)+G*SN)+G*SB+G
Z = Z+M
FI = Z*FF*.01
G = G*E
F = F*Y
T = (GG/FF)*100
M = FI*GG

FIND MAXIMUM AND MINIMUM UNOBSERVED AND CALCULATED PRECIPITATIONS
IF(PH-60)201,200,200
201 PH = GG
IA = G
IB = F
IC = FF
ID = SI
200 DX = UX+VW
IF(ABS(W)-ABS(TT))22,22,20
20 TT = W
IE = G
IF = F
IG = GG
IH = FF
22 IF(FI)19,19,28
28 IF(FI-FF)19,19,30
30 PH = FI
IK = G
IL = F
IM = GG
IN = FF
19 V = FF*FF

CALCULATE POSSIBLE ERROR
V = (100./V)*SQRT(1+64./GG*GG)

SQUARE AND SUM PERCENTAL AND PRECIPITATION VALUES
DAR = DAR+V
M = T-Z
```



```

Q FM = 1
U = 1 - FM/33.
F = -LOG(1 - LOG(D))
M = F + 1.

```

```

FIT DATA TO SECOND ORDER POLYNOMIAL
T(1) = 1.
T(2) = F.
T(3) = F*F.
DO 16 J=1,K
IF(P(J)16,16,17
17 T(4) = P(J)
DO 10 M=1,3
NT = (M-1)*4
DO 10 N=1,4
NN = NT*N
10 A(J,NN) = A(J,NN)+T(M)*T(N)*M
16 CONTINUE
DO 11 J=1,K
DO 7 L=1,2
LL = (L-1)*4
DO 7 I=LL,3
NN = (I-1)*4
NT = NN*L
NS = NN*L
TEMP = A(I,NT)/A(I,NS)
DO 7 N=1,4
NT = NN*N
LJ = NN*N
7 A(I,NT) = A(I,NT)-A(I,LJ)*TEMP
S(J,3) = A(I,12)/A(I,11)
DO 11 I=1,2
L = 3-I
LL = L*1
Y = D.
NT = (L-1)*4
DO 13 N=LL,3
NS = NT*N
13 Y = Y+A(I,NS)*S(J,N)
NS = NT*N
NN = NT*L
11 S(J,L) = (A(I,NS)-Y)/A(I,NN)
I = K+1
DO 20 J=1,7
U(I) = 0.
20 Q(I) = 0.
PRINT RECURRANCE INTERVALS AND PRECIPITATION
-PRINT 12,ME
12 FORMAT(1H2,45X,11H REGION NO,15/45X12H**1/)
PRINT 31,ML,MM,K
31 FORMAT(40X8H M.L.A.P. 15,3H - 15/40X112H**1//45X,15,5H DAY/47X,
1512H**1/)
DO 14 J=1,K
14 P(J) = S(J,1)+S(J,2)*.58+S(J,3)*.58*.58
PRINT 15,P(J),J=1,7)
15 FORMAT(20X15H 300 SQ.MILES 300 SQ.MS. 1000 SQ.MS. 3000 SQ.MS.,
140H 10000 SQ.MS. 30000 SQ.MS. 100000 SQ.MS. //2X12H MEAN ANNUAL,
20H PREC T(F10,3,3X1/5X7H IN MMS/)
PRINT 42
42 FORMAT(3X17H YEARS RECURRANCE)
DO 18 I=1,20
DO 23 J=1,K
FM = I
R = 33./FM
D = 1.-L./R
F = -LOG(1-LOG(D))
Q(J) = S(J,1)+S(J,2)*F+S(J,3)*F*F
23 U(J) = Q(J)/P(J)
18 PRINT 19,R,(DINI,D(N),N=1,7)
19 FORMAT(5X,F0,1,8X,7(F0,1,F3,1,2X))
PRINT PRECIPITATION VALUES FOR DESIRED RECURRANCE INTERVALS
PRINT 21
21 FORMAT(//35X,29H DESIRED RECURRANCE INTERVALS//)
I = 1
R = 5.
36 D = 1.-L./R
F = -LOG(1-LOG(D))
DO 32 J=1,K
Q(J) = S(J,1)+S(J,2)*F+S(J,3)*F*F
32 U(J) = Q(J)/P(J)
PRINT 19,R,(U(J),J=1,7)
GO TO 133,34,35,37,38)1
33 I = 2
R = 10.
GO TO 36
34 I = 3
R = 20.
GO TO 36
35 I = 4
R = 50.
GO TO 36
37 I = 5
R = 100.
GO TO 36
38 PRINT 22
22 FORMAT(//40X13H COEFFICIENTS/)
DO 39 I=1,3
39 PRINT 40,(S(J,I),J=1,7)
40 FORMAT(22X,7(F0,3,4X))
GO TO 1
END

MAXIMIZATION OF DEPTH-AREA-DURATION GRAPHS
DIMENSION A(12),T(1),S(4),B(10,7),IC(10,10,7),P(7),Q(6),R(7),
IP5(6)
ENTER REGIONAL MOISTURE CONTENT RATIOS
1 READ 2,ME,ML,MM,K,PS(1),I=1,6)
2 FORMAT(12,2,14,7F0,6F3,2)
PA = PA/100.
RA = PA
PRINT 30B,ME,ML,MM
106 FORMAT(1H2,30X,9H REGION 14/2130X712H**1//726X,TH M.L.A.P.(14,3H -
114/20X1012H**1//778X,MM,RAK SEAS H CONT 1 DAY 2 DAY 3 DAY 4 DAY 5 DAY,
27H 6 DAY/)
DO 20 I=1,6
DO 20 J=1,10
DO 20 K=1,7
U(I,J,K) = 0.
20 IC(I,J,K) = 0
ENTER DEPTH-AREA-DURATION TABLE FOR A STORM
3 READ 4,ND,(P(1),I=1,7),(P(J),J=1,6)
4 FORMAT(12,7F0,1,7F0,1,3,7)
IF(ND)50,50,5
5 DO 49 J=1,12
49 A(J) = 0.
PRINT 35D,ND,(P(1),I=1,7)
350 FORMAT(14,6X,F10,2,5X,6F6,2)
NT = P(1)/P(12)
6 READ 7,T,T*F
7 FORMAT(13,F5,0)
IP17180,80,8
FIT SECOND ORDER POLYNOMIAL TO PRECIPITATION AND LOG OF AREA
8 F = LOG(F)
T(4) = F.
T(1) = 1.
T(2) = T.
T(3) = T*T.
DO 79 I=1,3
NT = (I-1)*4
DO 79 J=1,4
NN = NT*J
79 A(NN) = A(NN)+T(I)*T(J)
GO TO 6
DO 81 L=1,2
LL = L*1
LN = (L-1)*4
DO 81 I=LL,3
NN = (I-1)*4
NT = NN*L
NS = NN*L
TEMP = A(I,NT)/A(I,NS)
DO 83 J=1,4
NT = NN*N
LJ = NN*N
81 A(I,NT) = A(I,NT)-A(I,LJ)*TEMP
S(3) = A(12)/A(11)
DO 82 I=1,2
L = 3-I
LL = L*1
Y = 0.
NT = (L-1)*4
DO 83 J=LL,3
NS = NT*N
83 Y = Y+A(NS)*S(J)
NS = NT*N
NN = NT*L
82 S(I) = (A(NS)-Y)/A(NN)
I = 0

```


A P P E N D I X E

TABLES OF ERRORS INHERENT IN COAXIAL PLOTS FOR EACH SUB-REGION

Precipitation values mm represent the maximum elevation of observed precipitation from that presented in the coaxial plot.

REGION 1. M.A.P. 0-500 mm

Recurrence Interval yr.	Area sq. mi.	Duration days					
		1	2	3	4	5	6
100	100	7	8	13	33	35	18
5	1000	3	5	6	10	13	6

REGION 2. M.A.P. 0-500 mm

Recurrence Interval yr.	Area sq. mi.	Duration days					
		1	2	3	4	5	6
100	100	8	26	17	20	18	21
5	1000	2	7	4	5	4	6

REGION 2. M.A.P. 500+ mm

Recurrence Interval yr.	Area sq. mi.	Duration days					
		1	2	3	4	5	6
100	100	26	6	19	23	18	26
5	1000	10	12	12	10	12	12

REGION 4. M.A.P. 0-500 mm

Recurrence Interval yr.	Area sq. mi.	Duration days					
		1	2	3	4	5	6
5	1000	6	8	7	5	20	23
100	100	7	33	31	44	30	25

REGION 5. M.A.P. 0-500 mm

Recurrence Interval yr.	Area sq. mi.	Duration days					
		1	2	3	4	5	6
100	100	12	20	14	17	12	17
5	1000	8	12	9	9	8	6

REGION 5. M.A.P. 500+ mm

Recurrence Interval yr.	Area sq. mi.	Duration days					
		1	2	3	4	5	6
100	100	42	66	46	36	40	28
5	1000	8	10	16	6	14	14

REGION 6. M.A.P. 0-250 mm

Recurrence Interval yr.	Area sq. mi.	Duration days					
		1	2	3	4	5	6
5	1000	5	9	8	5	6	6
100	100	11	11	13	8	8	8

REGION 6. M.A.P. 250-500 mm

Recurrence Interval yr.	Area sq. mi.	Duration days					
		1	2	3	4	5	6
5	1000	6	4	3	4	4	3
100	100	7	8	8	5	13	5

REGION 8. M.A.P. 0-250 mm

Recurrence Interval yr.	Area sq. mi.	Duration days					
		1	2	3	4	5	6
5	1000	3	7	4	4	5	9
100	100	8	14	8	9	9	11

REGION 8. M.A.P. 250-500 mm

Recurrence Interval yr.	Area sq. mi.	Duration days					
		1	2	3	4	5	6
5	1000	4	7	4	5	10	5
100	100	5	10	6	7	17	9

REGION 8. M.A.P. 500-1000 mm

As the data resulted in inconsistencies when compared with other plots, no error table is presented.

REGION 10. M.A.P. 0-250 mm

Recurrence Interval yr.	Area sq. mi.	Duration days					
		1	2	3	4	5	6
5	1000	4	3	3	5	6	8
100	100	19	6	12	21	18	32

REGION 10. M.A.P. 250-500 mm

Recurrence Interval yr.	Area sq. mi.	Duration days					
		1	2	3	4	5	6
5	1000	8	9	11	14	11	15
100	100	16	21	23	37	35	40

REGION 10. M.A.P. 500-1000 mm

Recurrence Interval yr.	Area sq. mi.	Duration days					
		1	2	3	4	5	6
5	1000	8	7	6	8	7	7
100	100	13	14	14	9	17	9

REGION 11. M.A.P. 250-500 mm

Recurrence Interval yr.	Area sq. mi.	Duration days					
		1	2	3	4	5	6
5	1000	4	7	6	10	7	10
100	100	10	12	14	9	9	14

REGION 11. M.A.P. 500-1000 mm

Recurrence Interval yr.	Area sq. mi.	Duration days					
		1	2	3	4	5	6
5	1000	6	6	10	16	16	6
100	100	7	21	39	64	50	30

REGION 12. M.A.P. 500-1000 mm

Recurrence Interval yr.	Area sq. mi.	Duration days					
		1	2	3	4	5	6
100	100	17	46	50	90	112	30
5	1000	10	12	12	16	30	26

REGION 12. M.A.P. 1000+ mm

Recurrence Interval yr.	Area sq. mi.	Duration days					
		1	2	3	4	5	6
100	100	14	52	32	30	32	26
5	1000	10	36	24	16	16	14

REGION 13. M.A.P. 500-1000 mm

Recurrence Interval yr.	Area sq. mi.	Duration days					
		1	2	3	4	5	6
5	1000	18	14	14	24	18	8
100	100	32	16	18	48	56	20

REGION 13. M.A.P. 1000+ mm

Recurrence Interval yr.	Area sq. mi.	Duration days					
		1	2	3	4	5	6
5	1000	16	24	24	24	30	20
100	100	22	38	32	54	58	62

REGION 14. M.A.P. 500-1000 mm

Recurrence Interval yr.	Area sq. mi.	Duration days					
		1	2	3	4	5	6
100	100	16	40	40	14	44	48
5	1000	6	15	12	12	10	14

REGION 14. M.A.P. 1000+ mm

Recurrence Interval yr.	Area sq. mi.	Duration days					
		1	2	3	4	5	6
100	100	22	36	54	34	28	66
5	1000	8	14	10	8	8	14

REGION 16. M.A.P. 500-1000 mm

Recurrence Interval yr.	Area sq. mi.	Duration days					
		1	2	3	4	5	6
5	1000	4	7	7	9	8	16
100	100	6	10	21	22	30	40

REGION 17. M.A.P. 500-1000 mm

Recurrence Interval yr.	Area sq. mi.	Duration days					
		1	2	3	4	5	6
5	1000	6	14	26	26	32	26
100	100	14	14	54	72	58	64

REGION 17. M.A.P. 1000+ mm

Recurrence Interval yr.	Area sq. mi.	Duration days					
		1	2	3	4	5	6
5	1000	10	28	30	50	50	60
100	100	10	32	60	70	58	70

REGION 18. M.A.P. 250-500 mm

Recurrence Interval yr.	Area sq. mi.	Duration days					
		1	2	3	4	5	6
5	1000	8	16	17	11	15	14
100	100	9	35	18	26	15	17

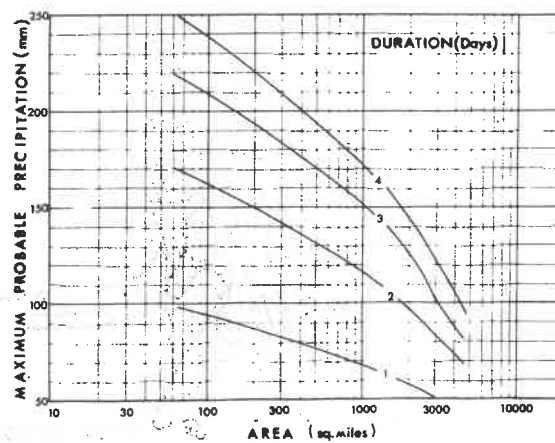
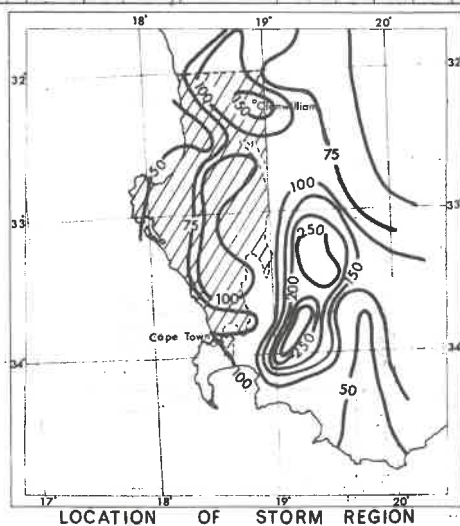
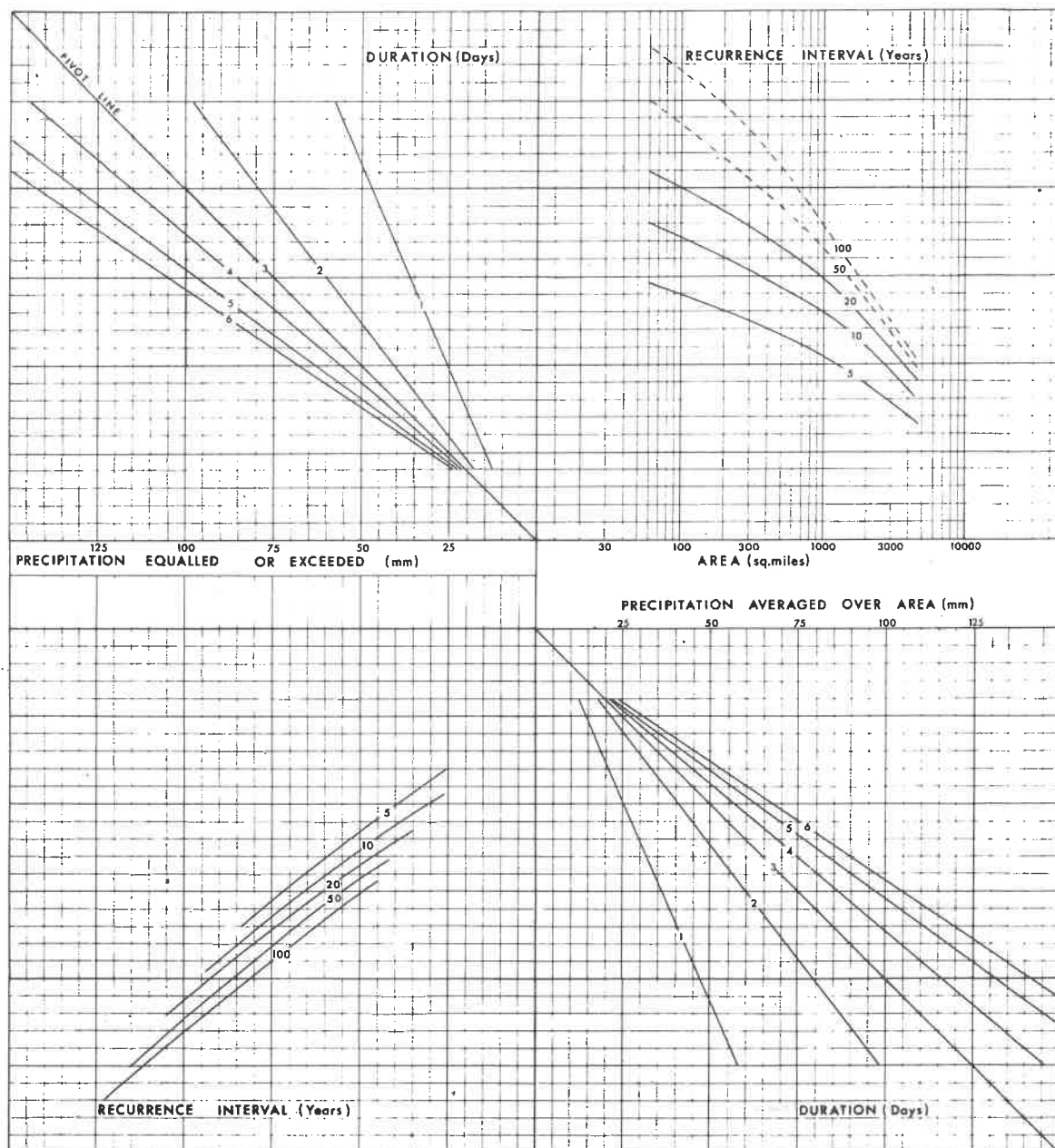
REGION 18. M.A.P. 500-1000 mm

Recurrence Interval yr.	Area sq. mi.	Duration days					
		1	2	3	4	5	6
5	1000	5	8	23	20	23	21
100	100	6	12	26	22	25	23

STORM REGION 1

M.A.P. 0 - 500 mm

DEPTH-AREA-DURATION-FREQUENCY

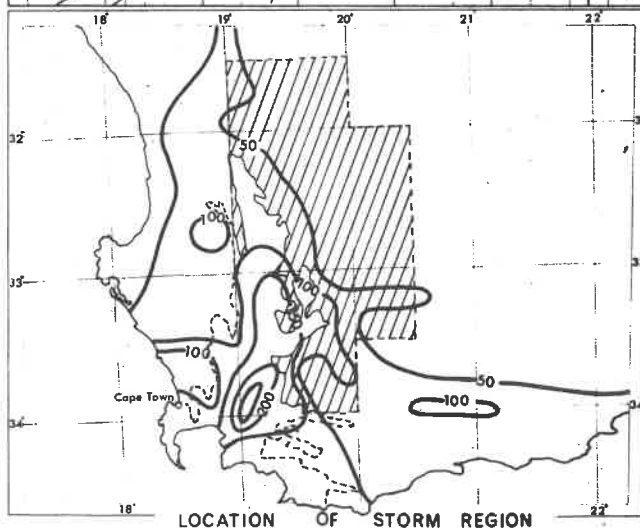
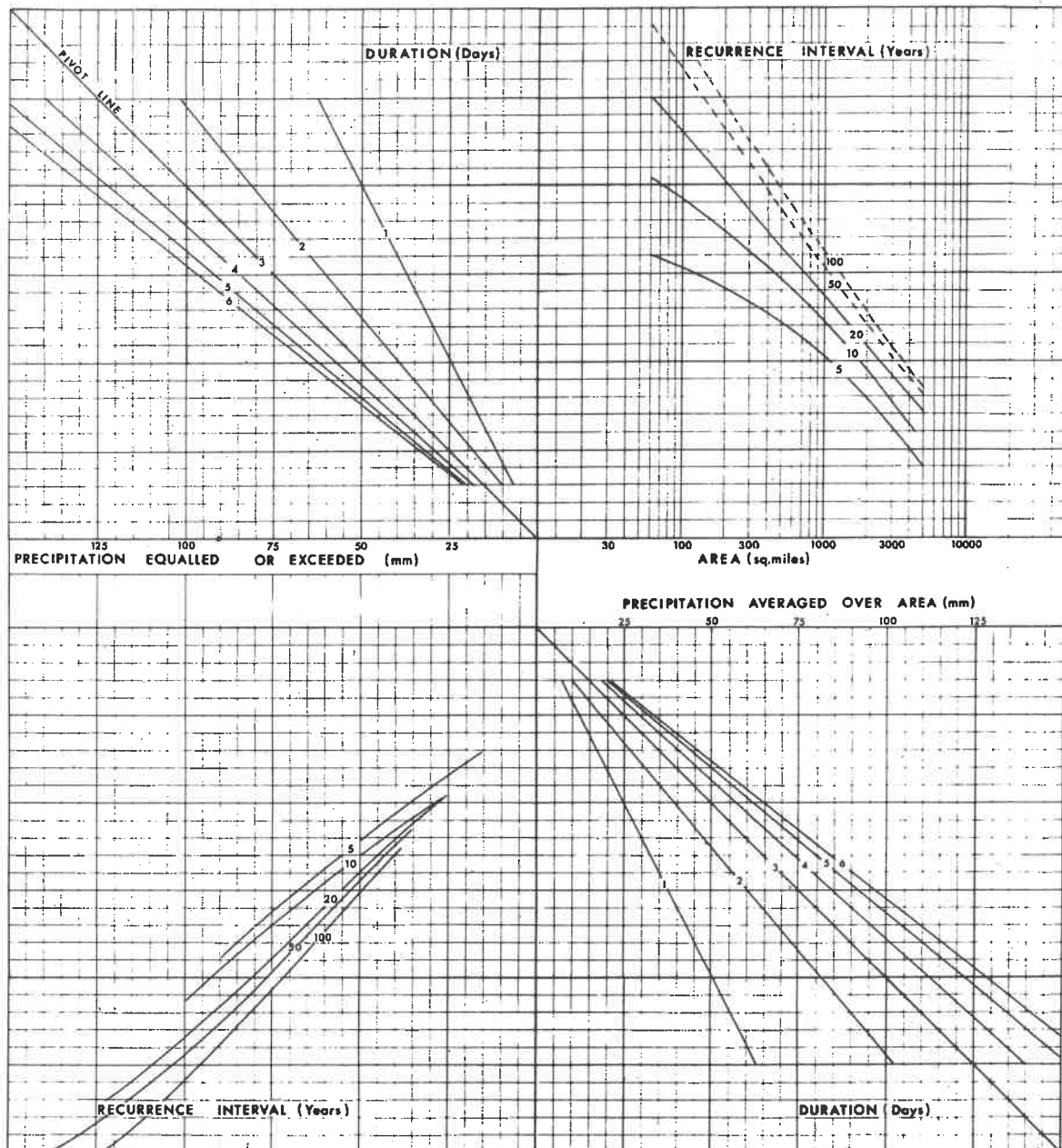


MAXIMUM DEPTH-AREA-DURATION

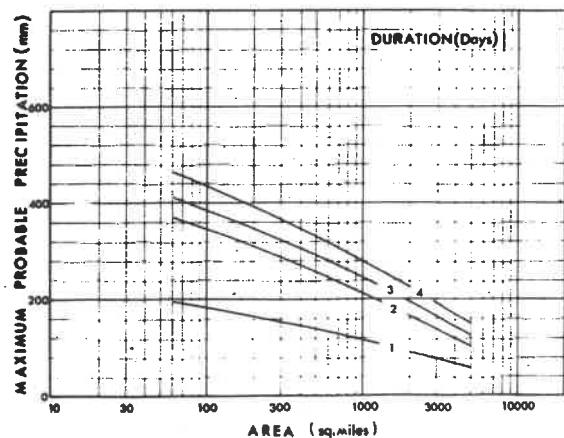
STORM REGION 2

M.A.P. 0 - 500 mm

DEPTH-AREA-DURATION-FREQUENCY



SHOWING MAXIMUM OBSERVED STORM (mm)

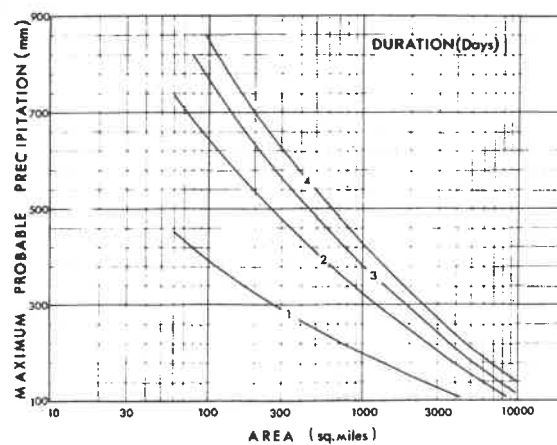
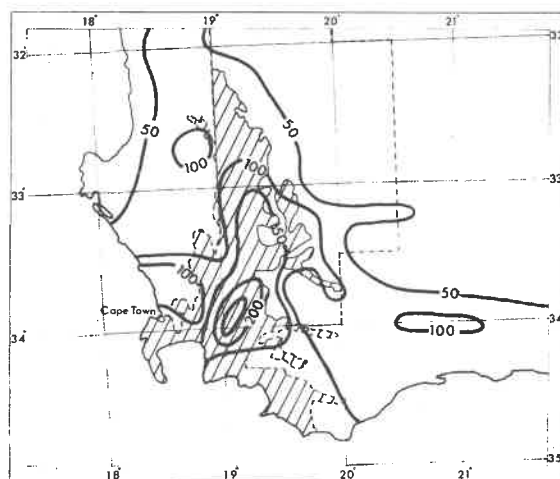
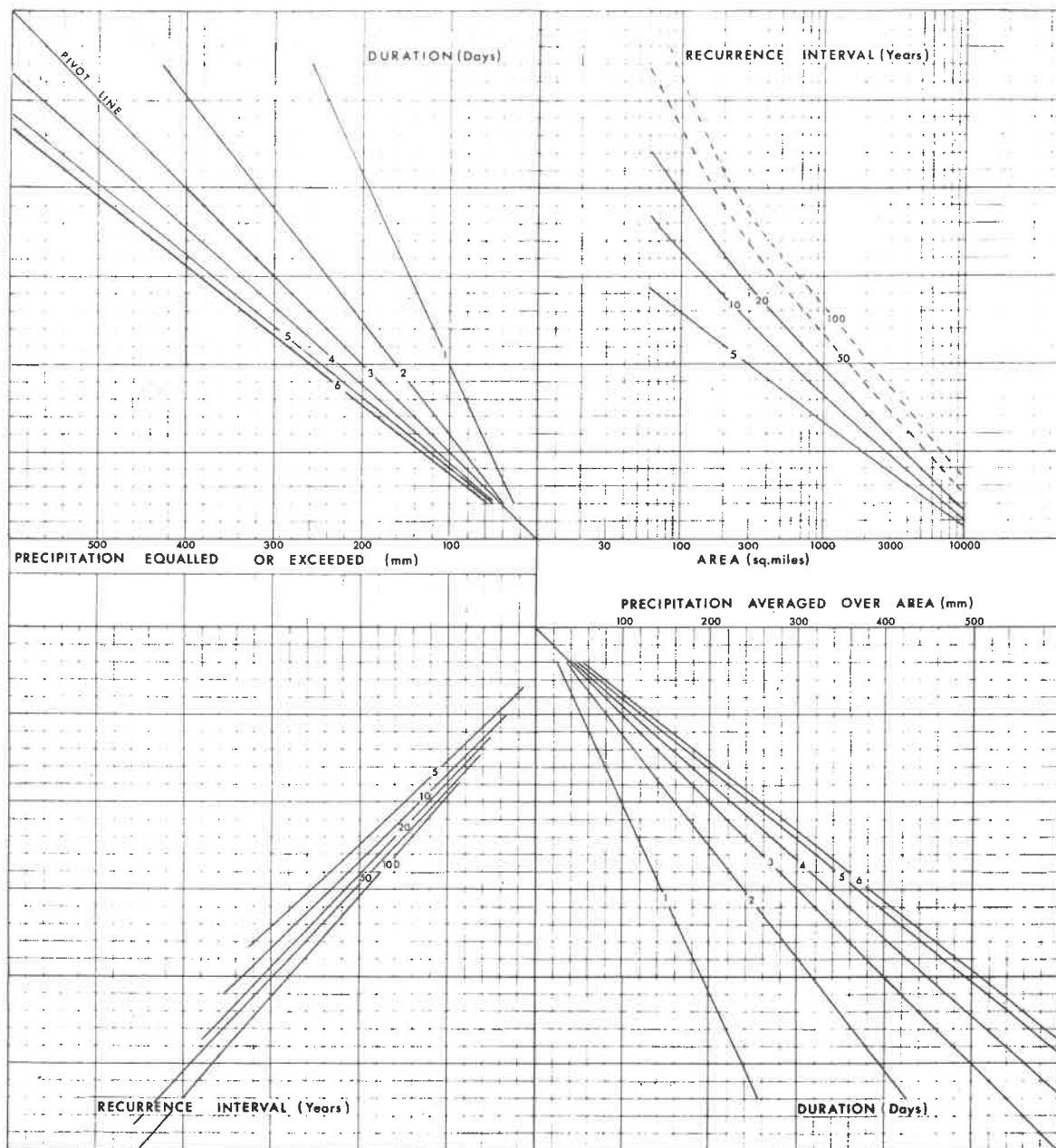


MAXIMUM DEPTH-AREA-DURATION

STORM REGION 2

M.A.P. 500 + mm

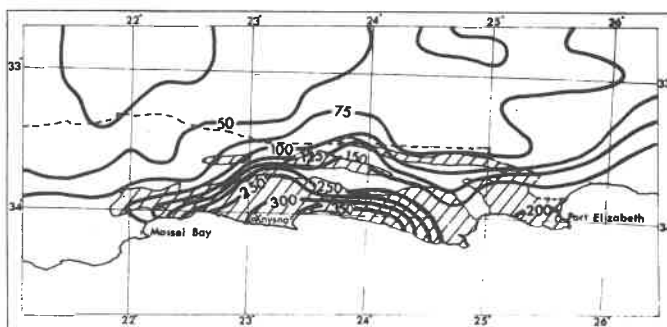
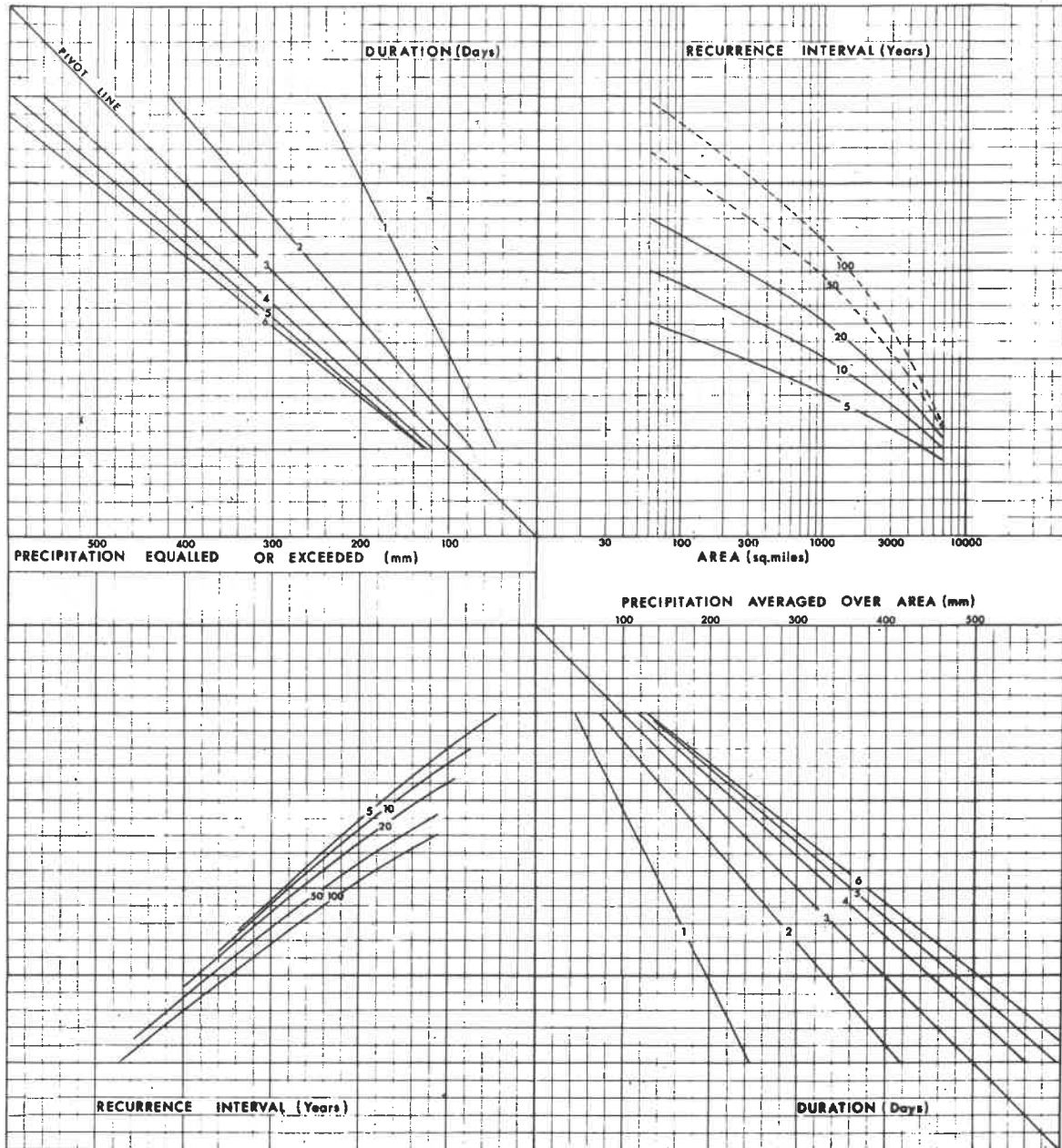
DEPTH-AREA-DURATION-FREQUENCY



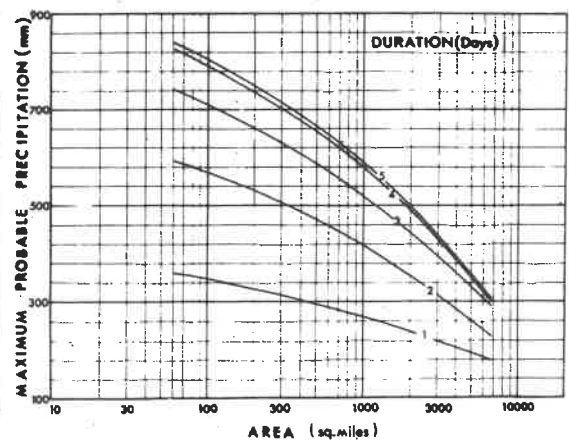
MAXIMUM DEPTH-AREA-DURATION

STORM REGION 5
M.A.P. 500 + mm

DEPTH-AREA-DURATION-FREQUENCY



LOCATION OF STORM REGION
SHOWING MAXIMUM OBSERVED STORM (mm)

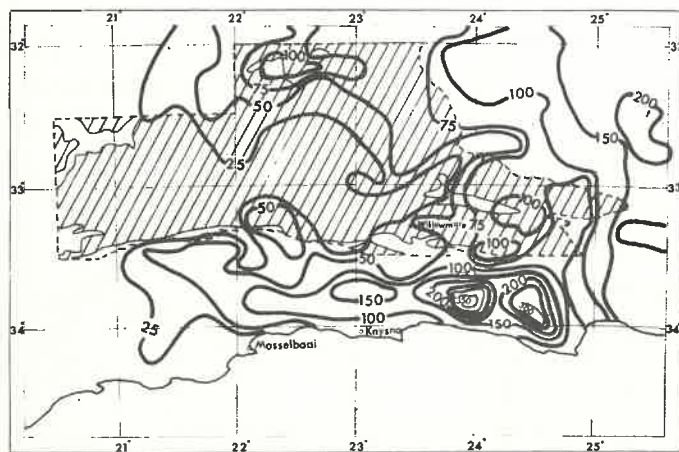
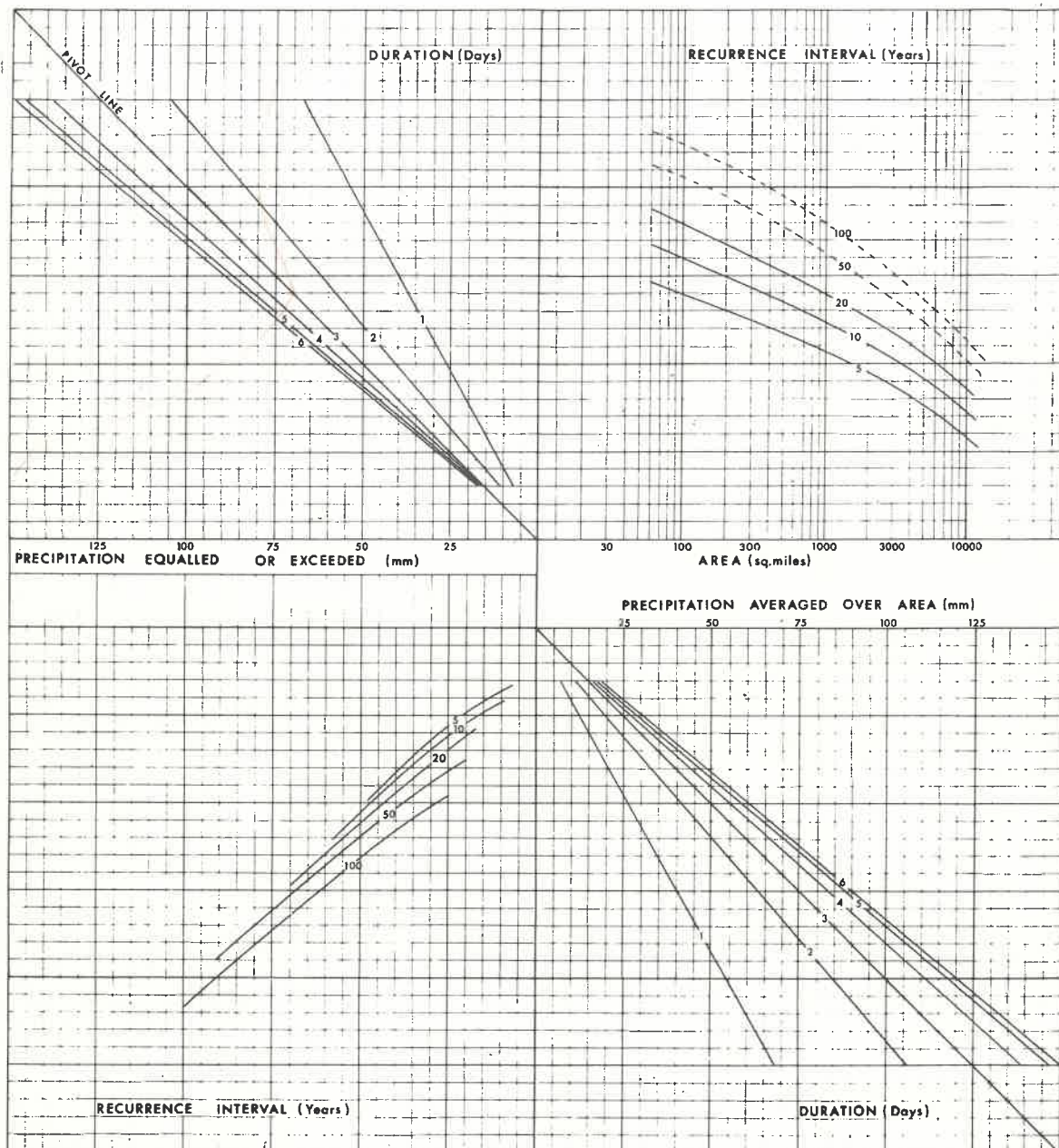


MAXIMUM DEPTH-AREA-DURATION

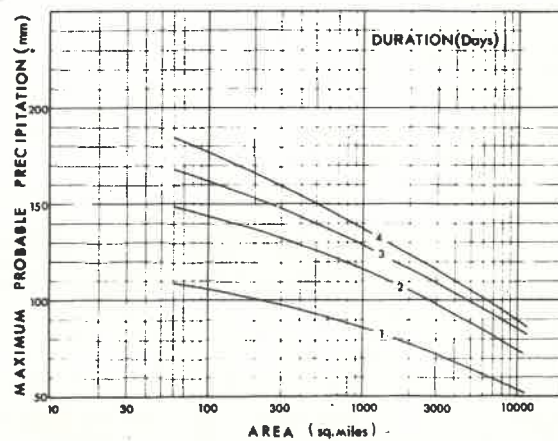
STORM REGION 6

M.A.P. 0 - 250 mm

DEPTH-AREA-DURATION-FREQUENCY



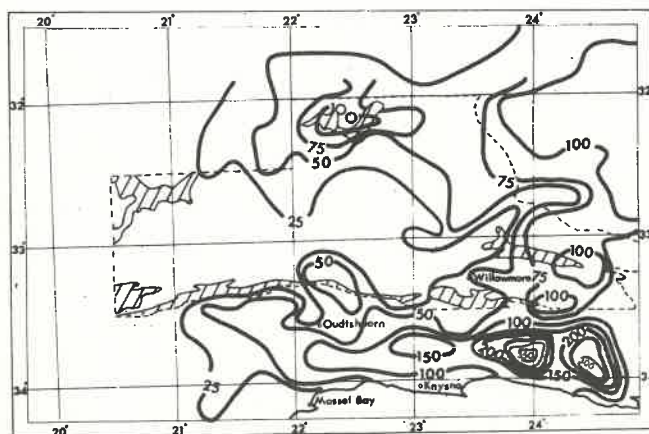
LOCATION OF STORM REGION
SHOWING MAXIMUM OBSERVED STORM (mm)



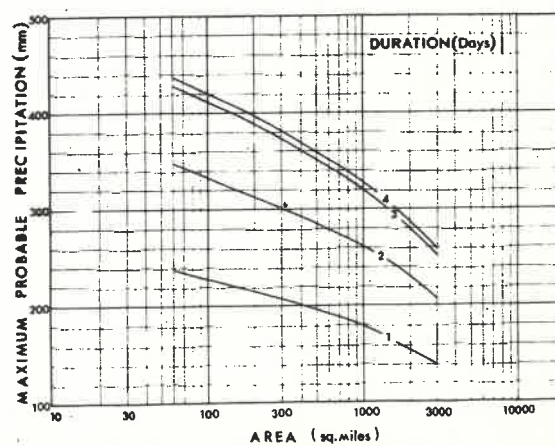
MAXIMUM DEPTH-AREA-DURATION

The figure consists of four panels, each showing a different nomogram for determining flood discharge (CFS) based on various factors. The panels are arranged in a 2x2 grid.

- Top Left Panel:** A nomogram relating **DURATION (Days)** (horizontal axis, 50 to 150) and **PRECIPITATION EQUALLED OR EXCEEDED (mm)** (vertical axis, 50 to 150). It features a series of parallel lines labeled 1 through 6, representing different recurrence intervals. A diagonal line labeled "PIVOT LINE" is also shown.
- Top Right Panel:** A nomogram relating **RECURRENT INTERVAL (Years)** (horizontal axis, 5 to 100) and **AREA (sq.miles)** (vertical axis, 30 to 10,000). It features a series of curves labeled 1 through 6, representing different recurrence intervals.
- Bottom Left Panel:** A nomogram relating **PRECIPITATION AVERAGED OVER AREA (mm)** (horizontal axis, 50 to 150) and **RECURRENT INTERVAL (Years)** (vertical axis, 5 to 100). It features a series of parallel lines labeled 1 through 6, representing different recurrence intervals.
- Bottom Right Panel:** A nomogram relating **PRECIPITATION AVERAGED OVER AREA (mm)** (horizontal axis, 50 to 150) and **DURATION (Days)** (vertical axis, 50 to 150). It features a series of parallel lines labeled 1 through 6, representing different recurrence intervals.



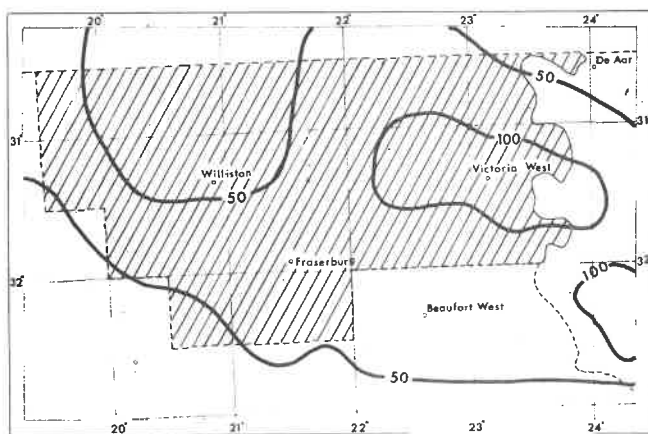
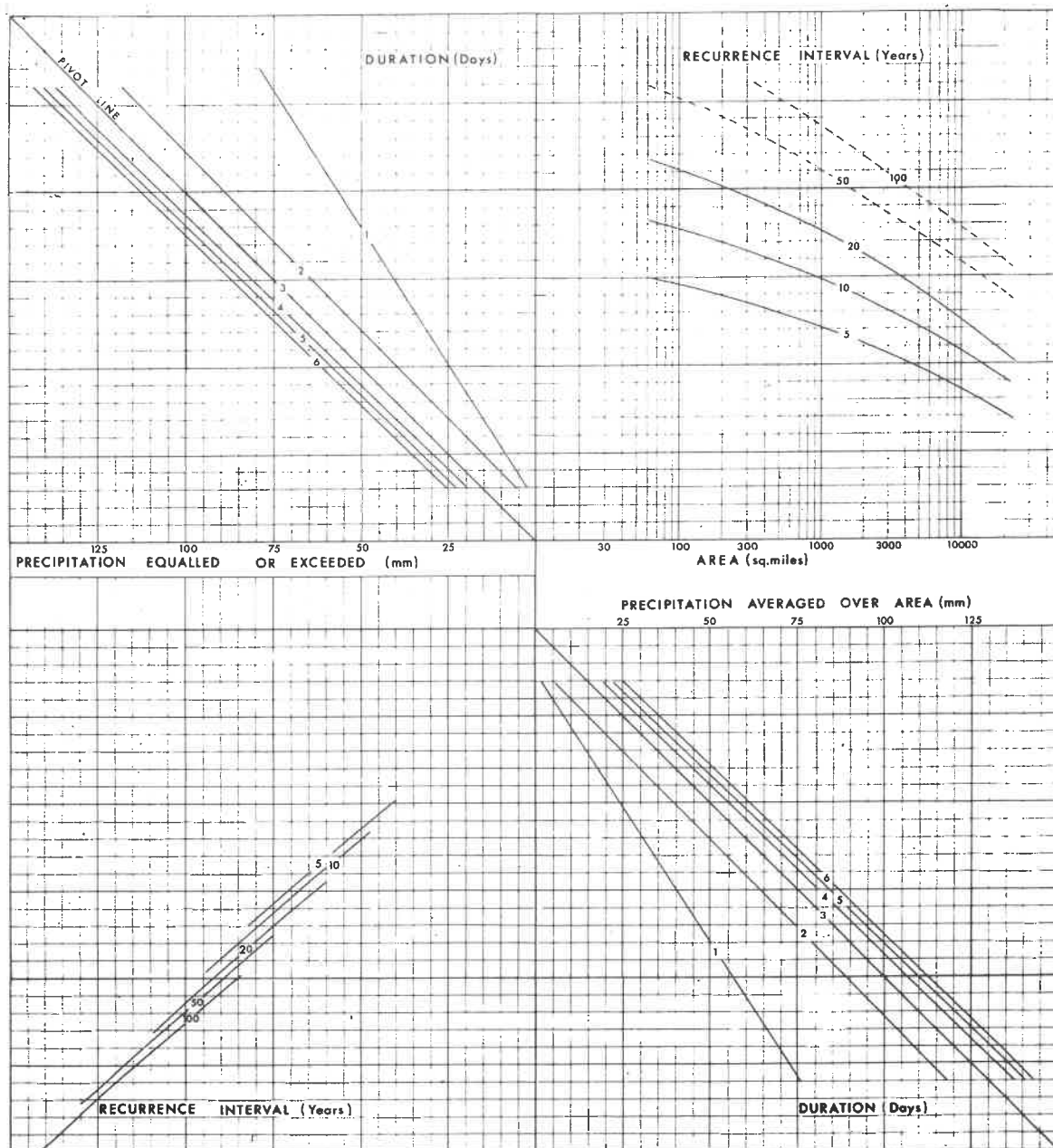
LOCATION	OF	STORM	REGION
SHOWING	MAXIMUM	OBSERVED	STORM (mm)



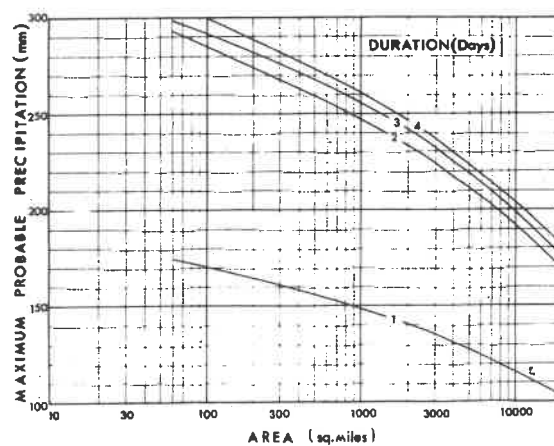
MAXIMUM DEPTH-AREA:DURATION

STORM REGION 8
M.A.P. 0 - 250 mm

DEPTH-AREA-DURATION-FREQUENCY



LOCATION OF STORM REGION
SHOWING MAXIMUM OBSERVED STORM (mm)

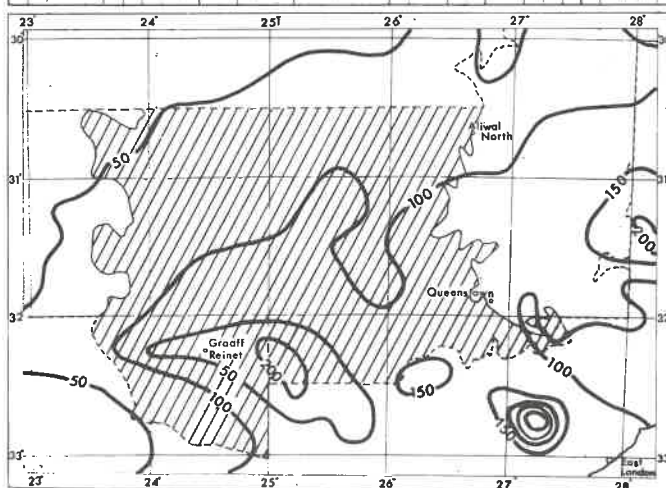
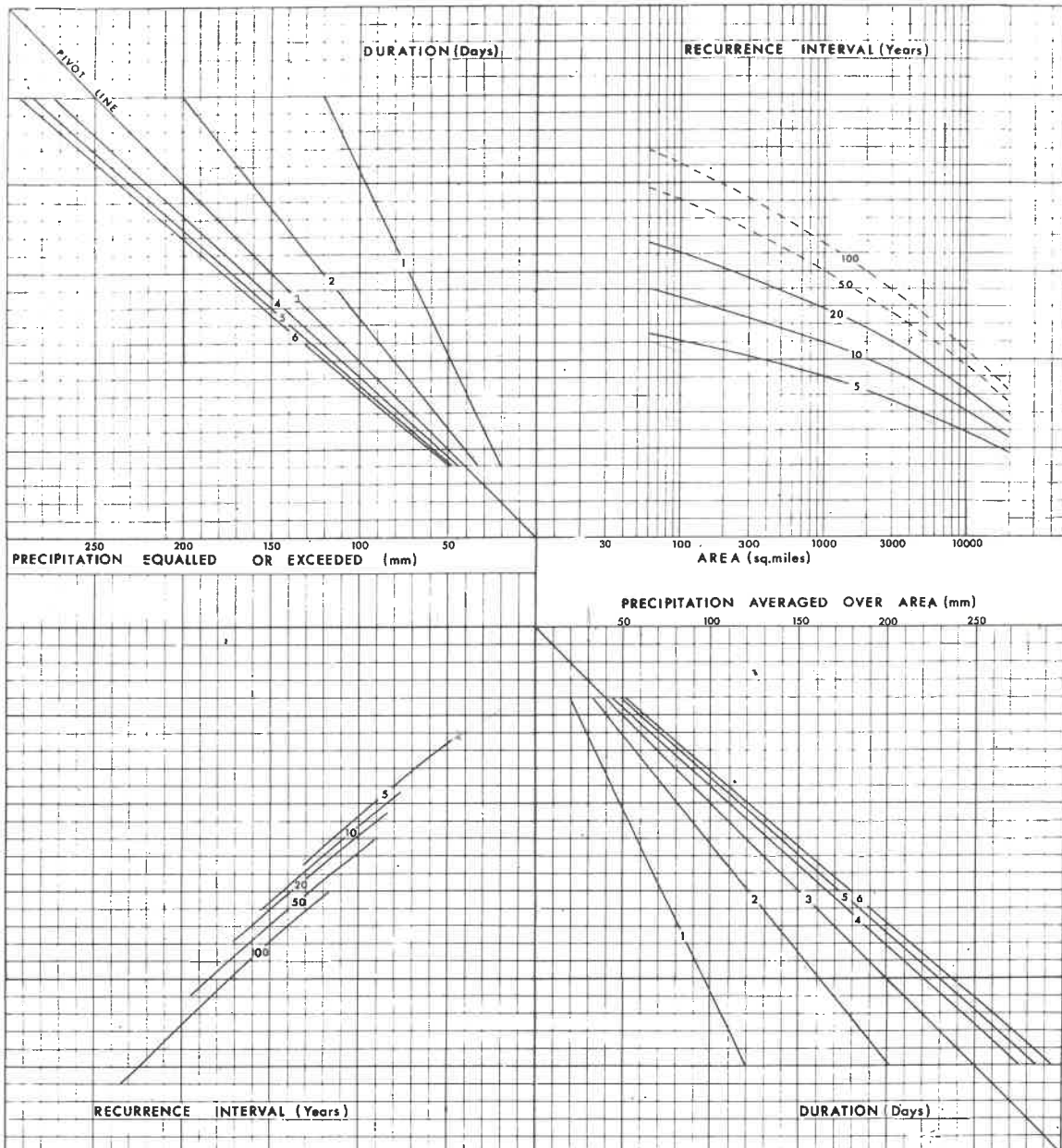


MAXIMUM DEPTH-AREA-DURATION

STORM REGION 8

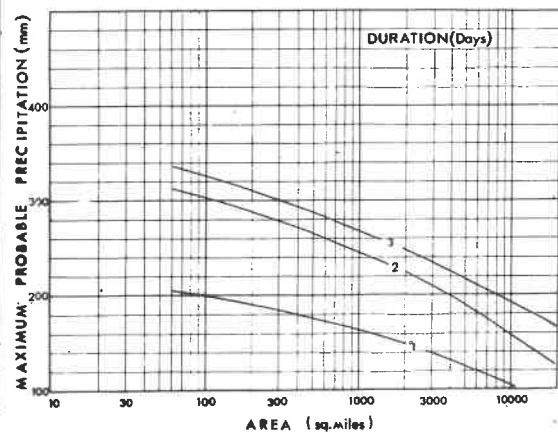
M.A.P. 250 - 500 mm

DEPTH-AREA-DURATION-FREQUENCY



LOCATION OF STORM REGION

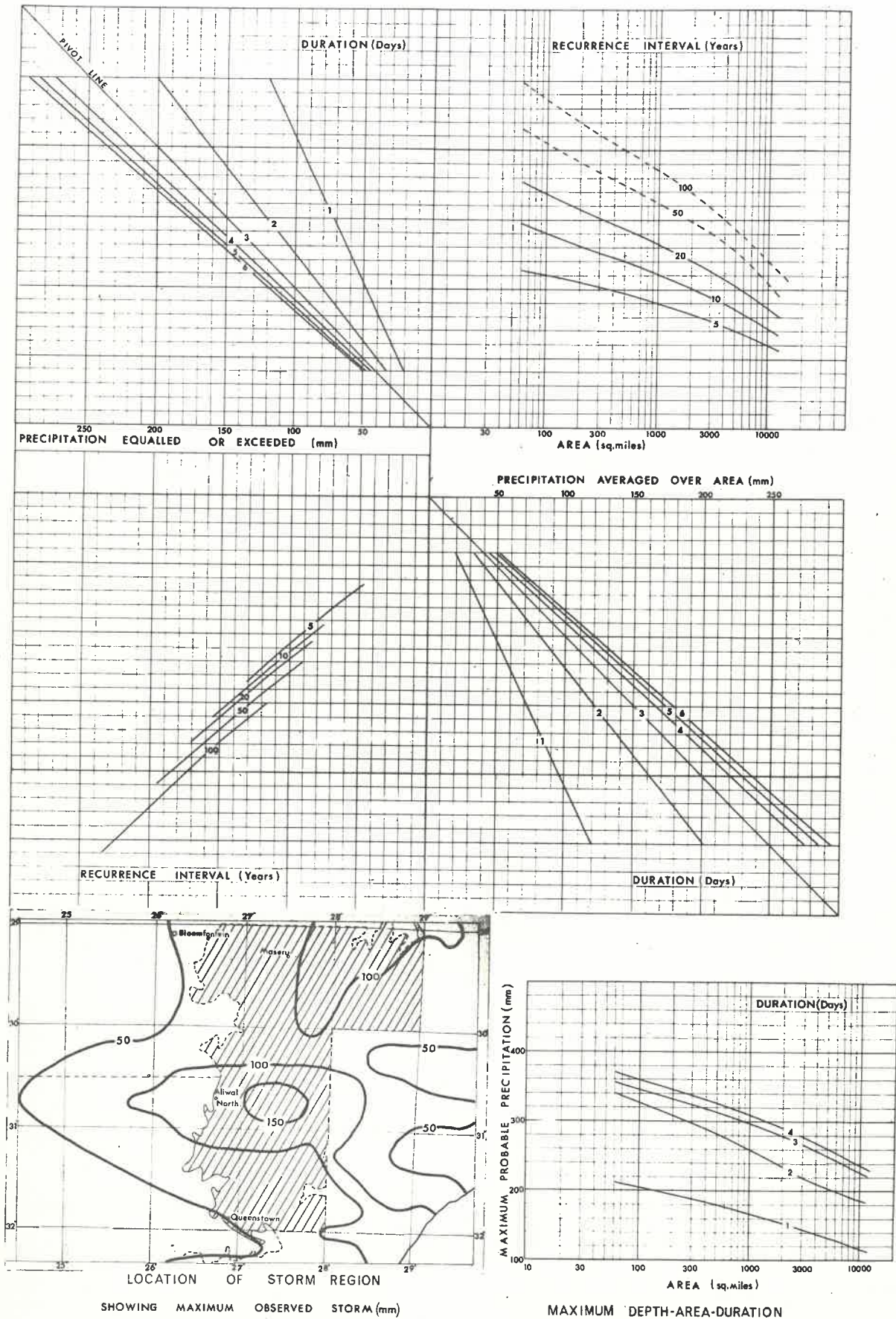
SHOWING MAXIMUM OBSERVED STORM (mm)



MAXIMUM DEPTH-AREA-DURATION

STORM REGION 8 M.A.P. 500-1000 mm

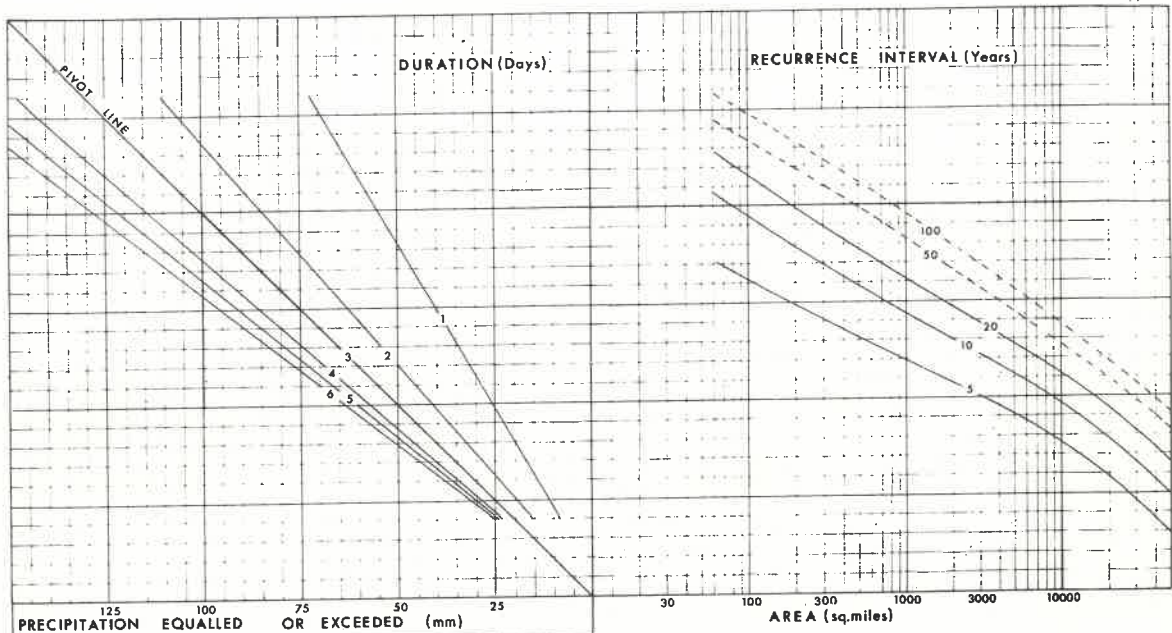
DEPTH-AREA-DURATION-FREQUENCY



STORM REGION 10

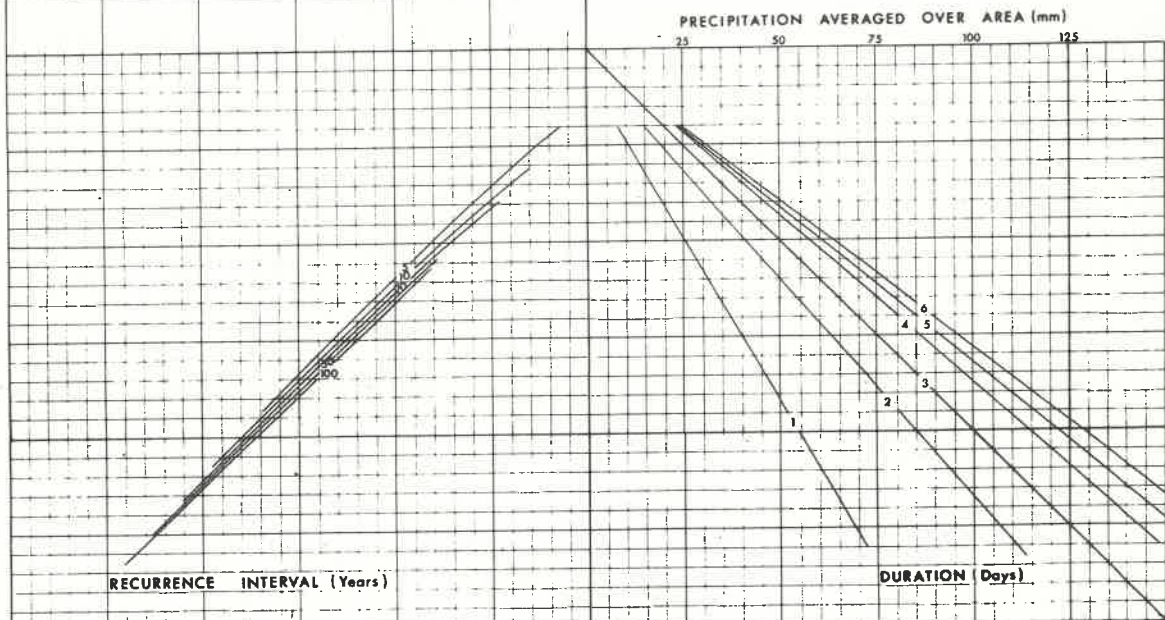
M.A.P. 0-250 mm

DEPTH-AREA-DURATION-FREQUENCY



PRECIPITATION EQUALLED OR EXCEEDED (mm)

AREA (sq.miles)



PRECIPITATION AVERAGED OVER AREA (mm)

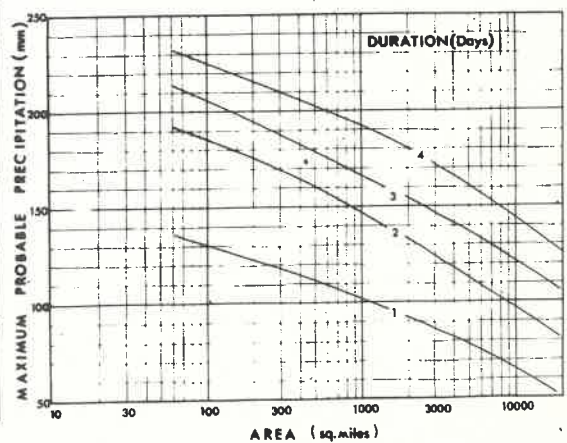
RECURRENCE INTERVAL (Years)

DURATION (Days)



LOCATION OF STORM REGION

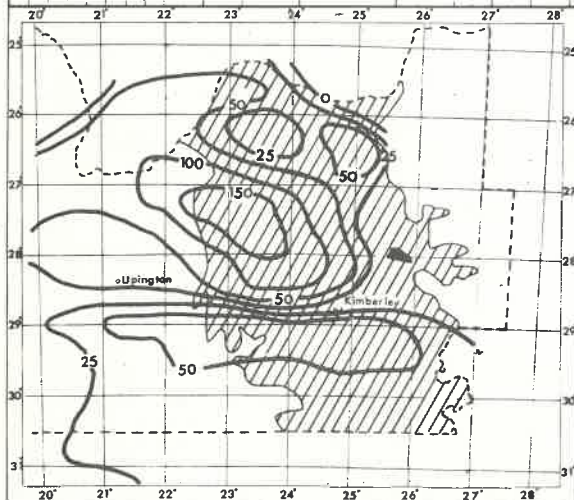
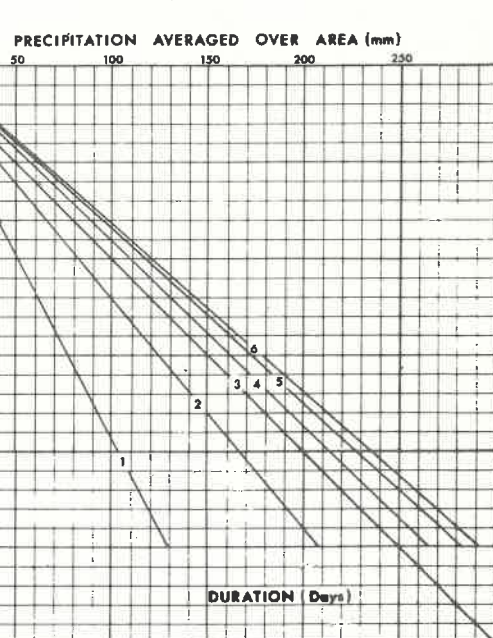
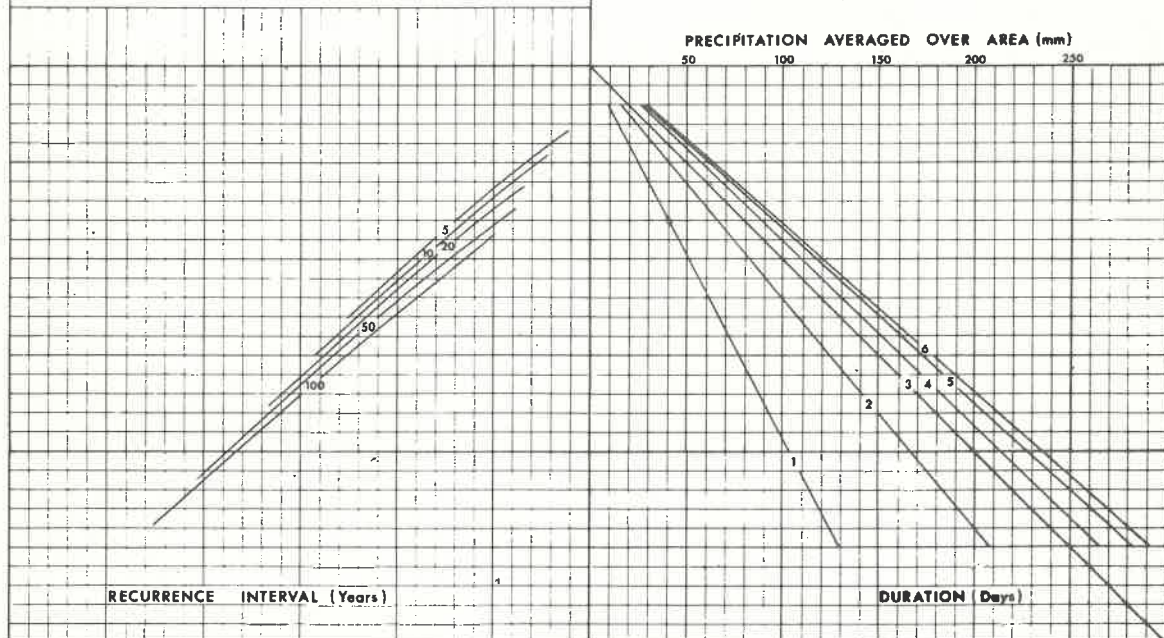
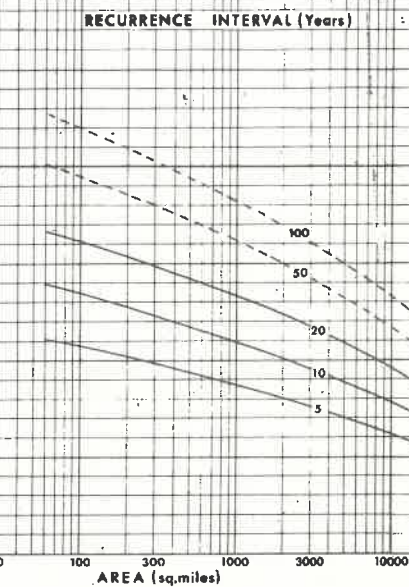
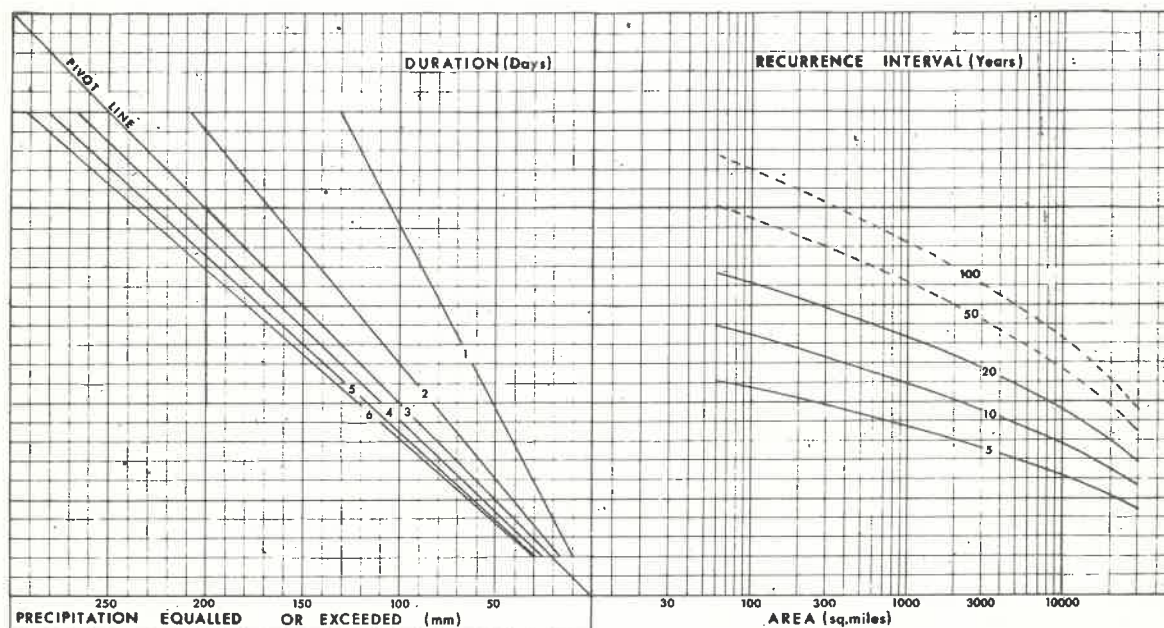
SHOWING MAXIMUM OBSERVED STORM (mm)



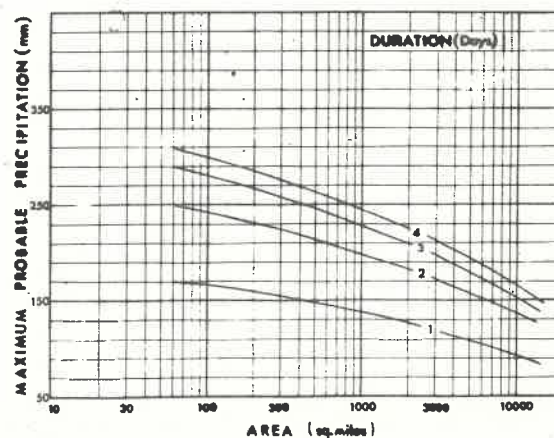
MAXIMUM DEPTH-AREA-DURATION

STORM REGION 10
M.A.P. 250 - 500 mm

DEPTH-AREA-DURATION-FREQUENCY



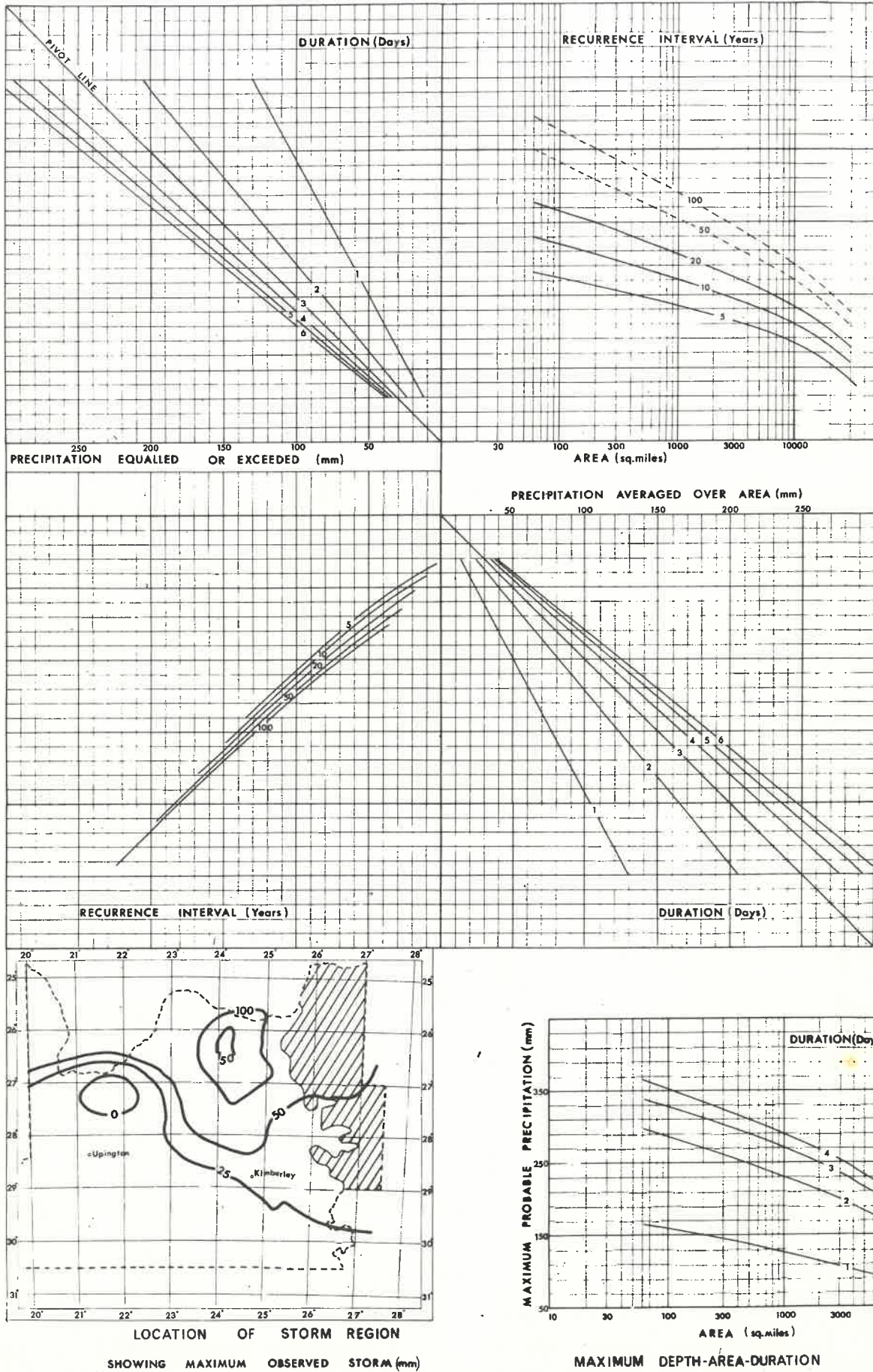
LOCATION OF STORM REGION
SHOWING MAXIMUM OBSERVED STORM (mm)



MAXIMUM DEPTH-AREA-DURATION

STORM REGION 10
M.A.P. 500 - 1000 mm

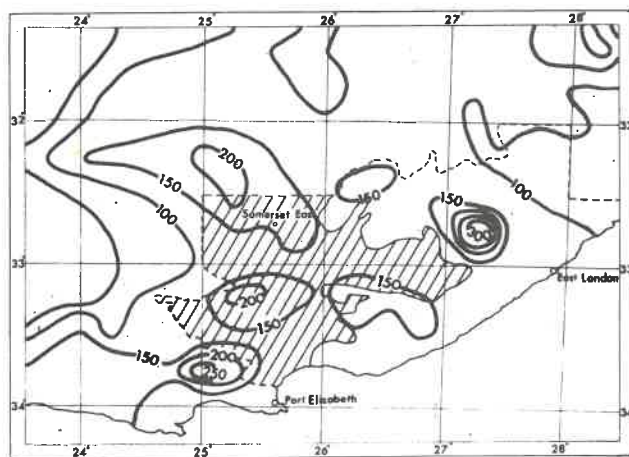
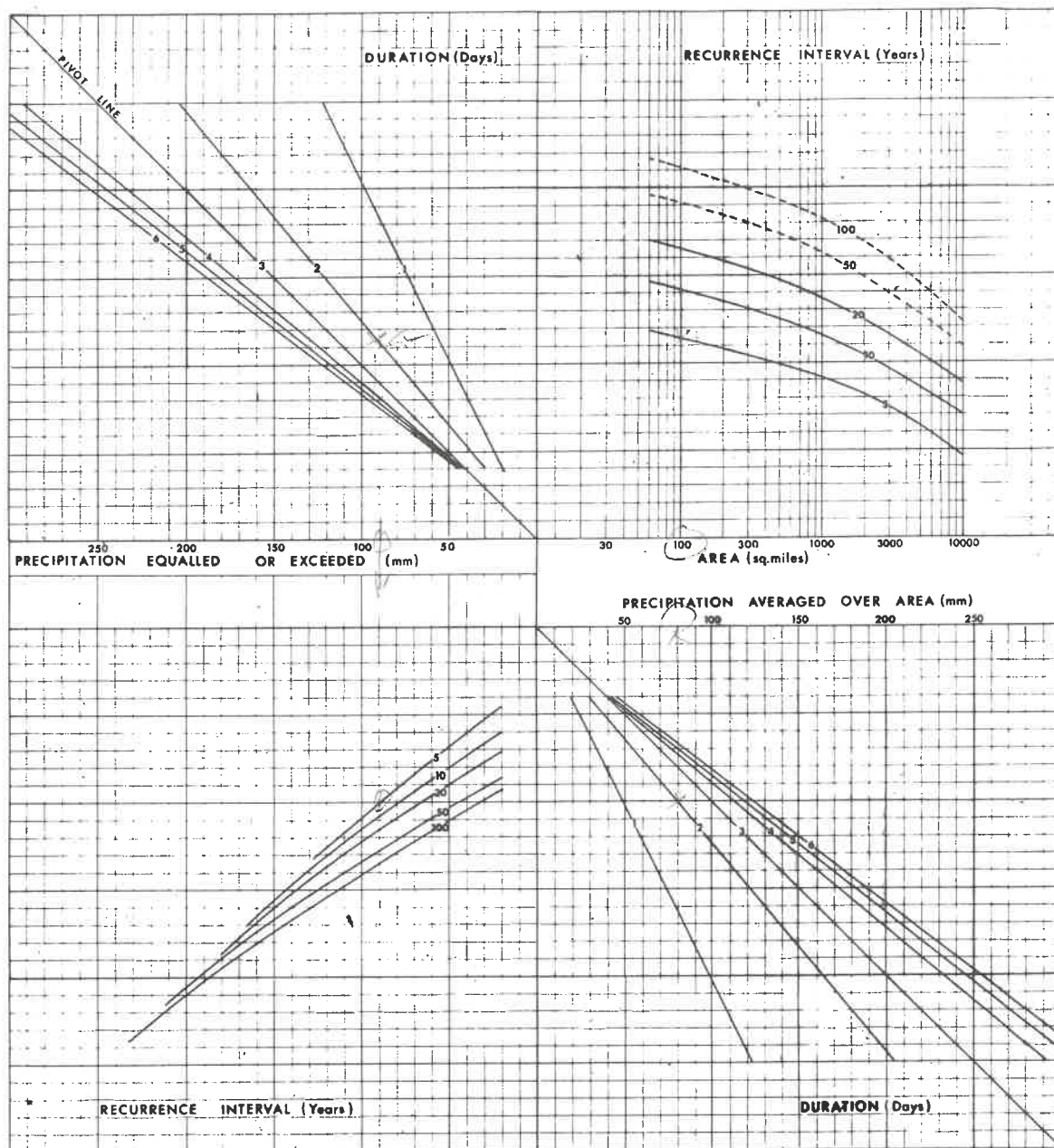
DEPTH-AREA-DURATION-FREQUENCY



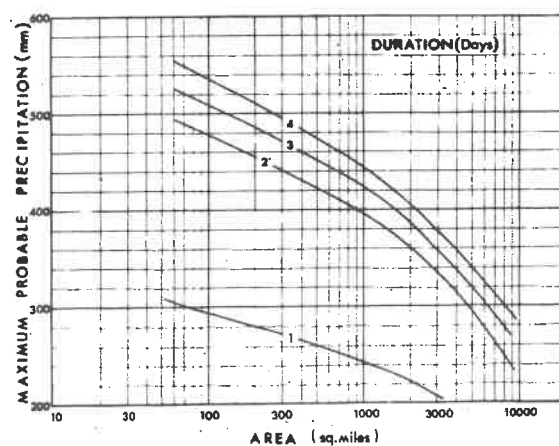
STORM REGION 11

M.A.P. 250-500 mm

DEPTH-AREA-DURATION-FREQUENCY



LOCATION OF STORM REGION
SHOWING MAXIMUM OBSERVED STORM (mm)

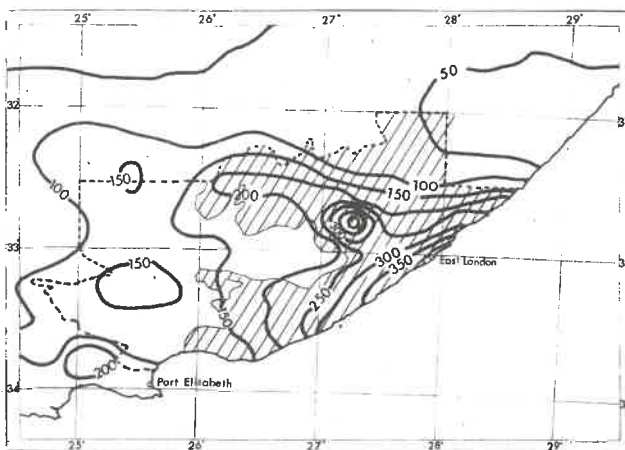
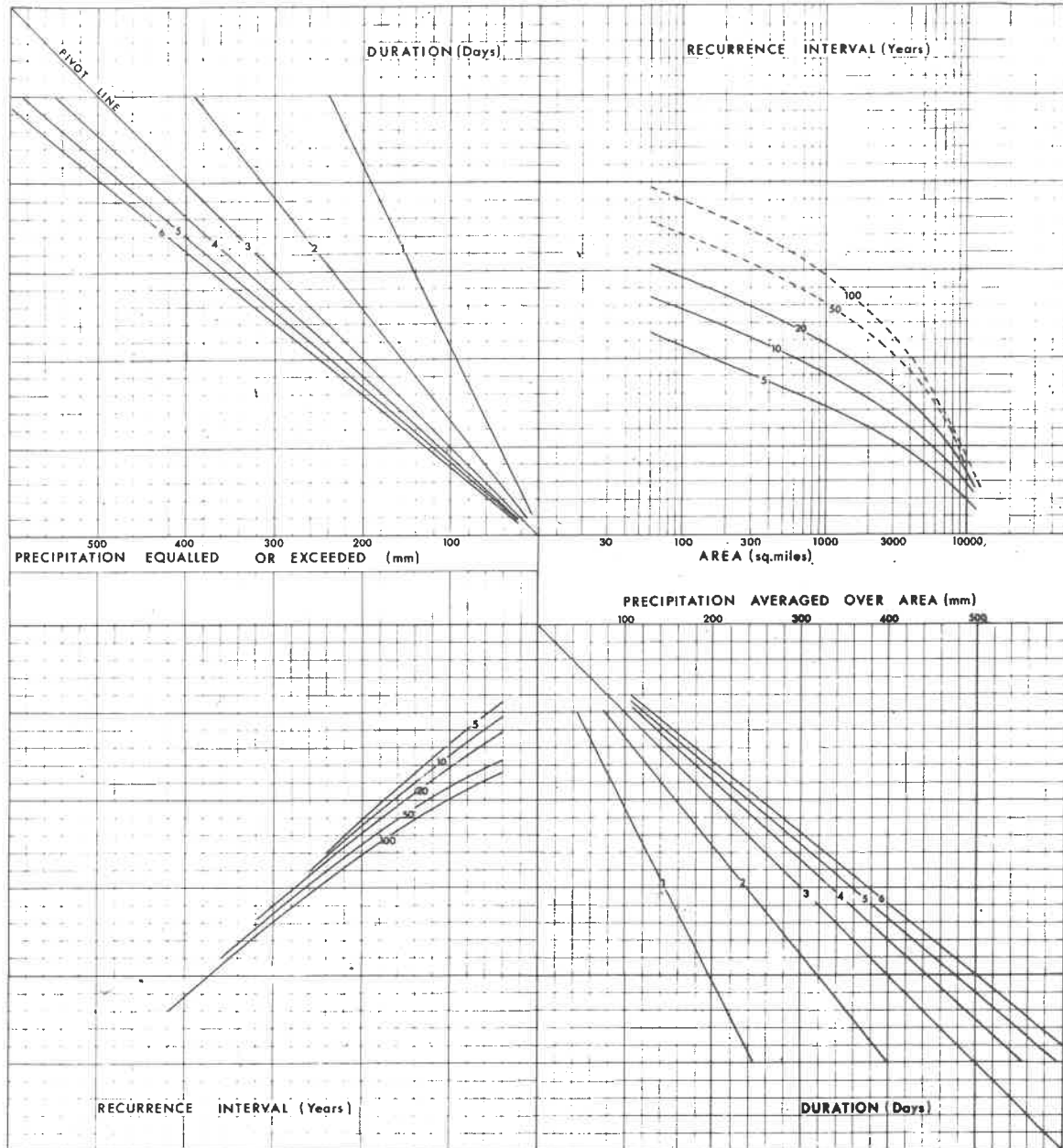


MAXIMUM DEPTH-AREA-DURATION

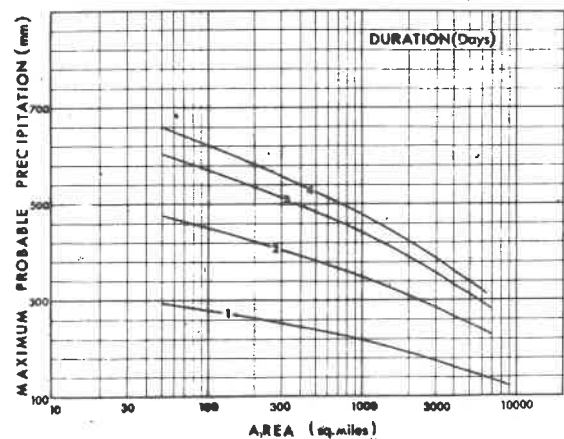
STORM REGION 11

M.A.P. 500-1000mm

DEPTH-AREA-DURATION-FREQUENCY



LOCATION OF STORM REGION
SHOWING MAXIMUM OBSERVED STORM (mm)

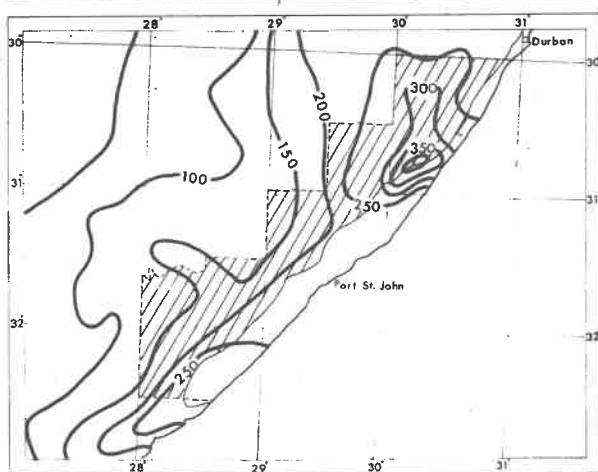
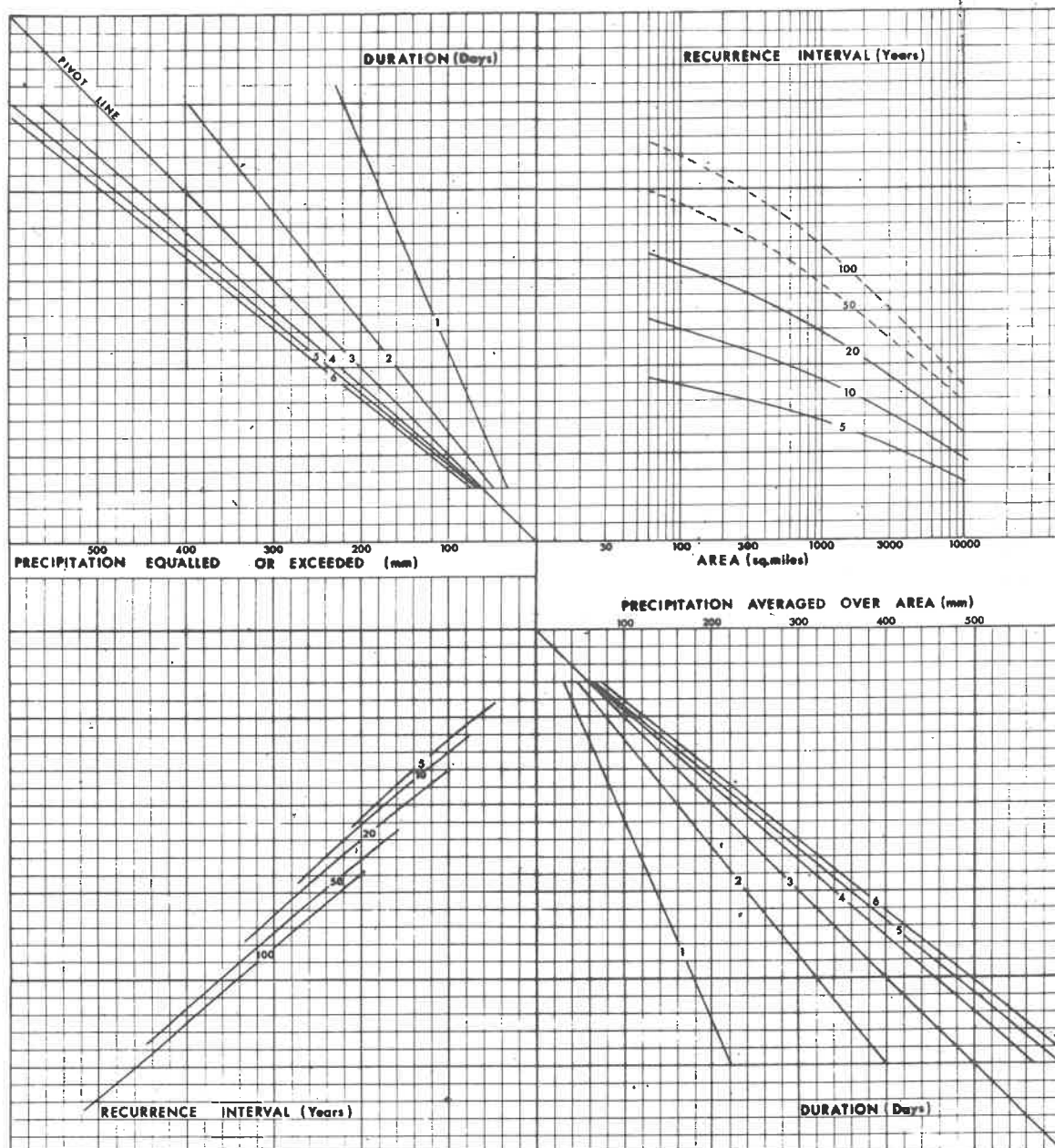


MAXIMUM DEPTH-AREA-DURATION

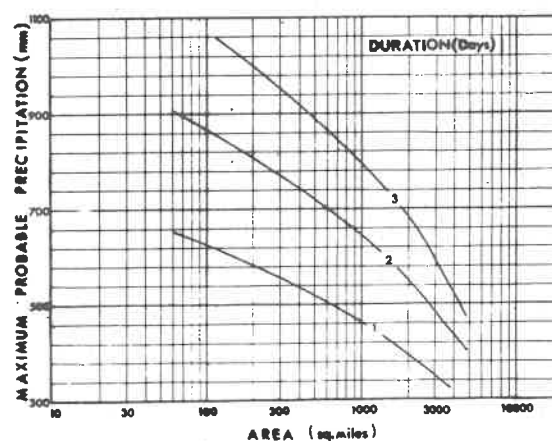
STORM REGION 12

M.A.P. 500 - 1000 mm

DEPTH-AREA-DURATION-FREQUENCY



LOCATION OF STORM REGION
SHOWING MAXIMUM OBSERVED STORM (mm)

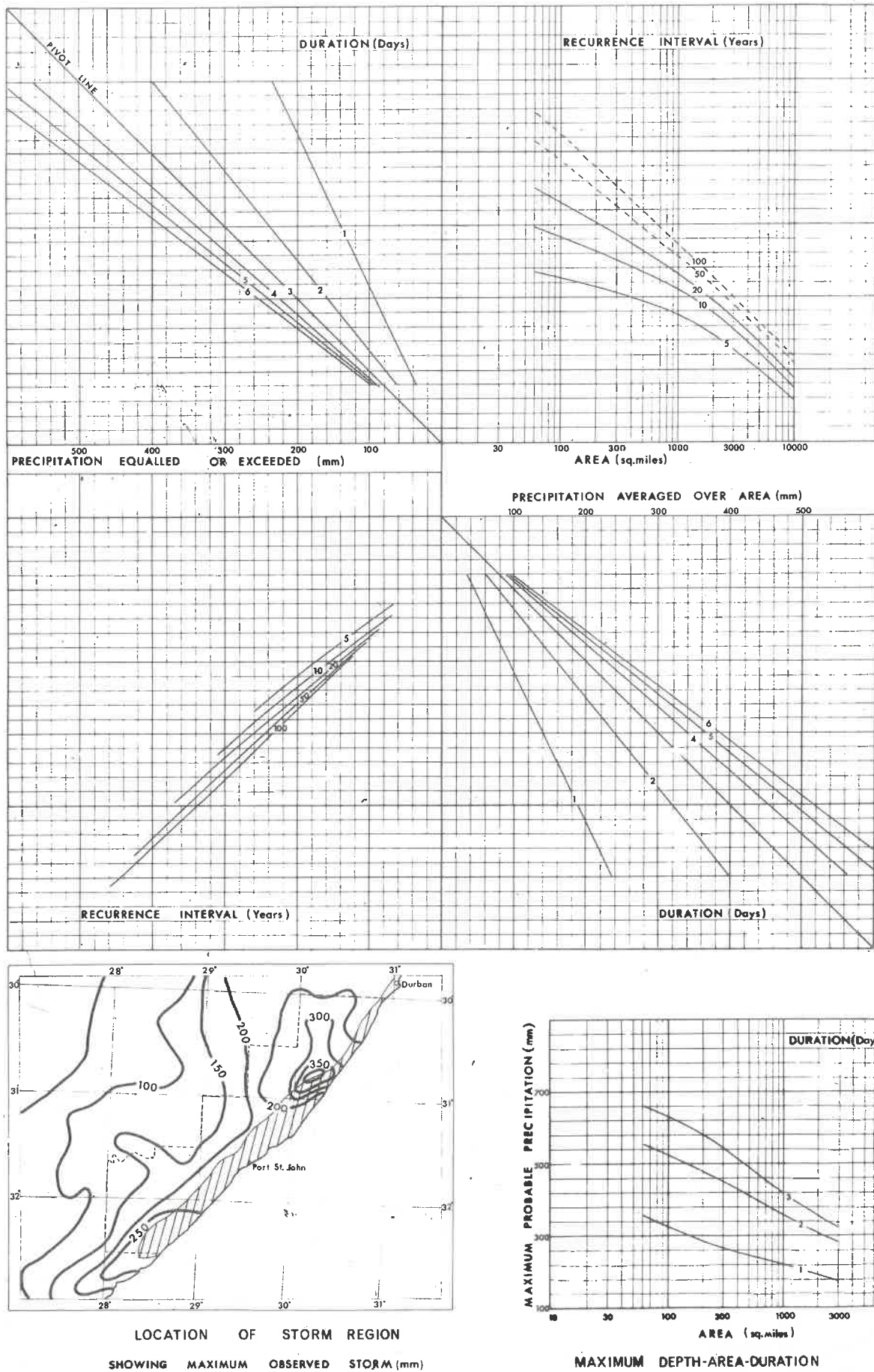


MAXIMUM DEPTH-AREA-DURATION

STORM REGION 12

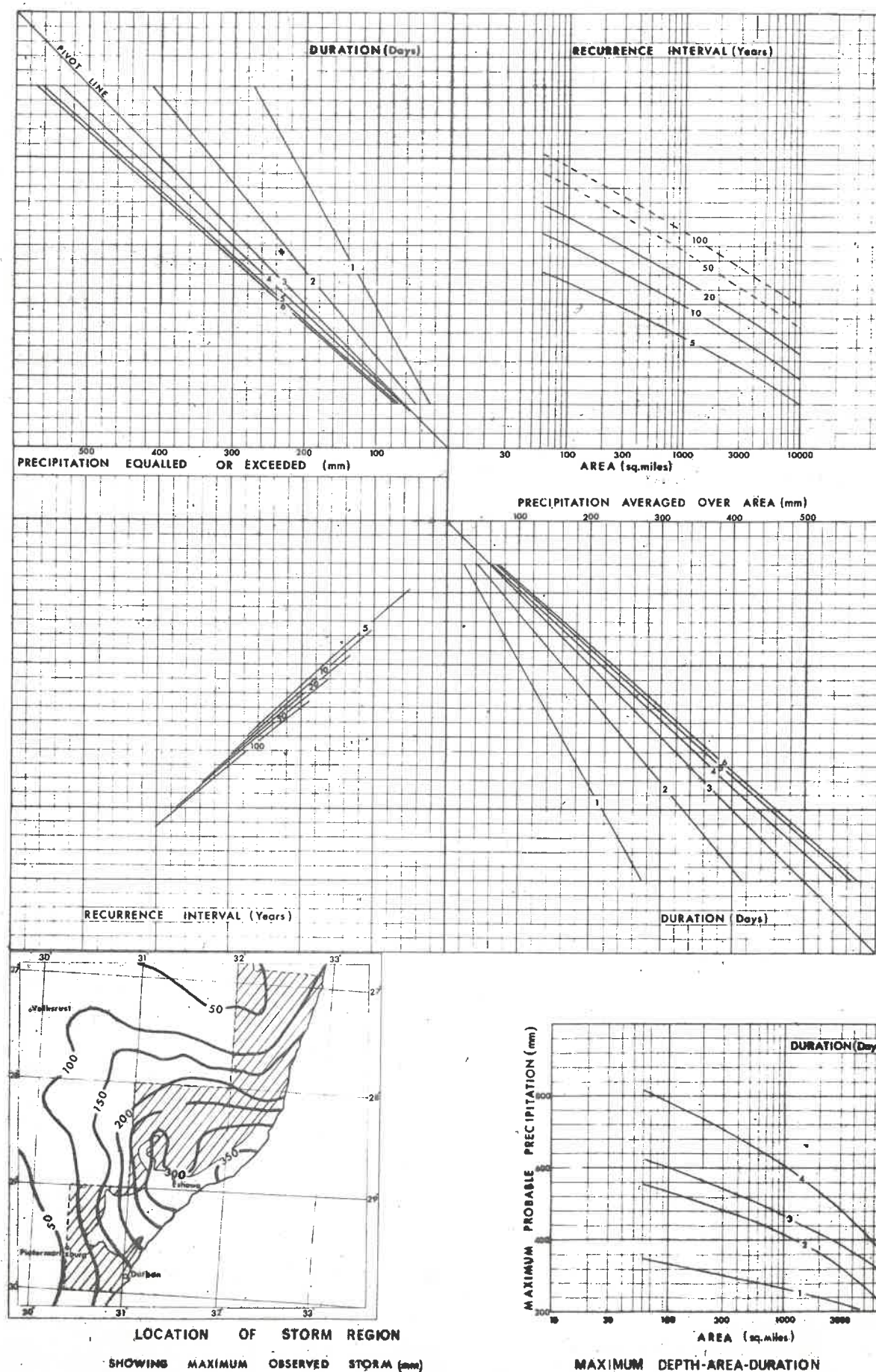
M.A.P. 1000 + mm

DEPTH-AREA-DURATION-FREQUENCY



STORM REGION 13
M.A.P. 500-1000 mm

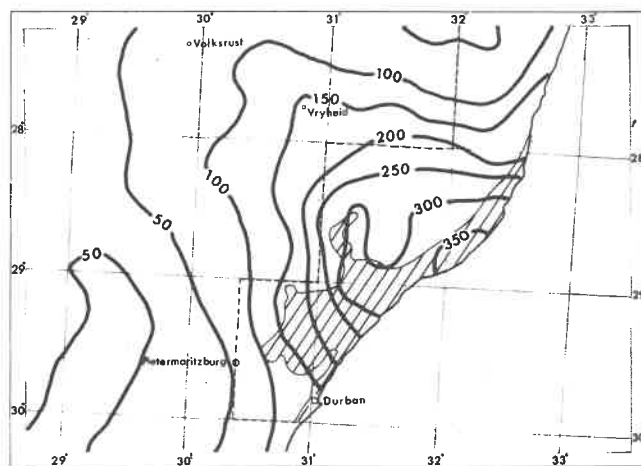
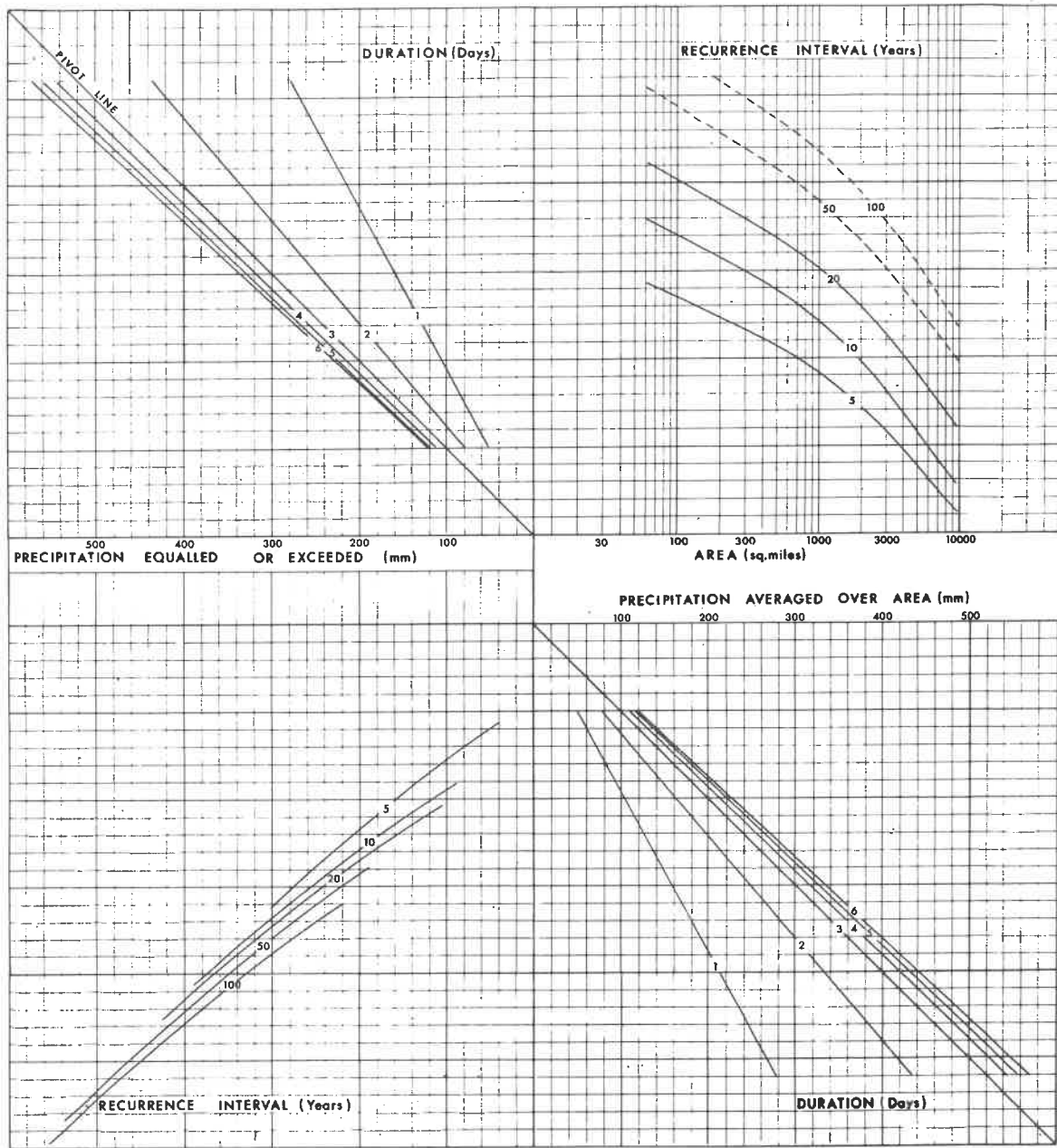
DEPTH-AREA-DURATION-FREQUENCY



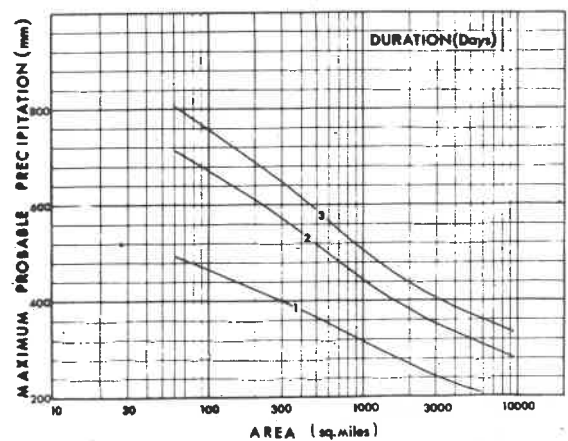
STORM REGION 13

M.A.P. 1000 + mm

DEPTH-AREA-DURATION-FREQUENCY



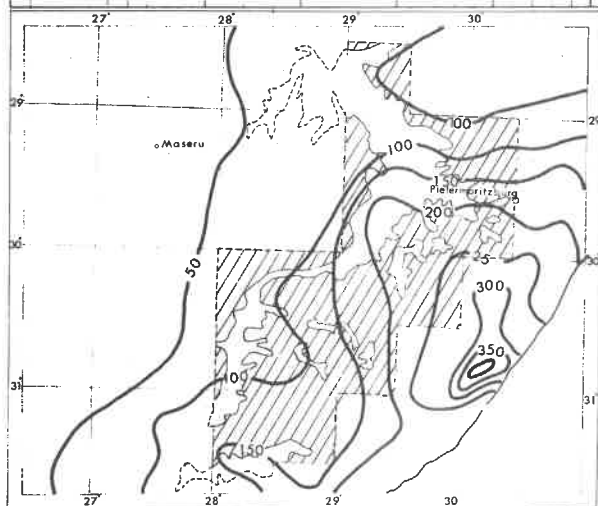
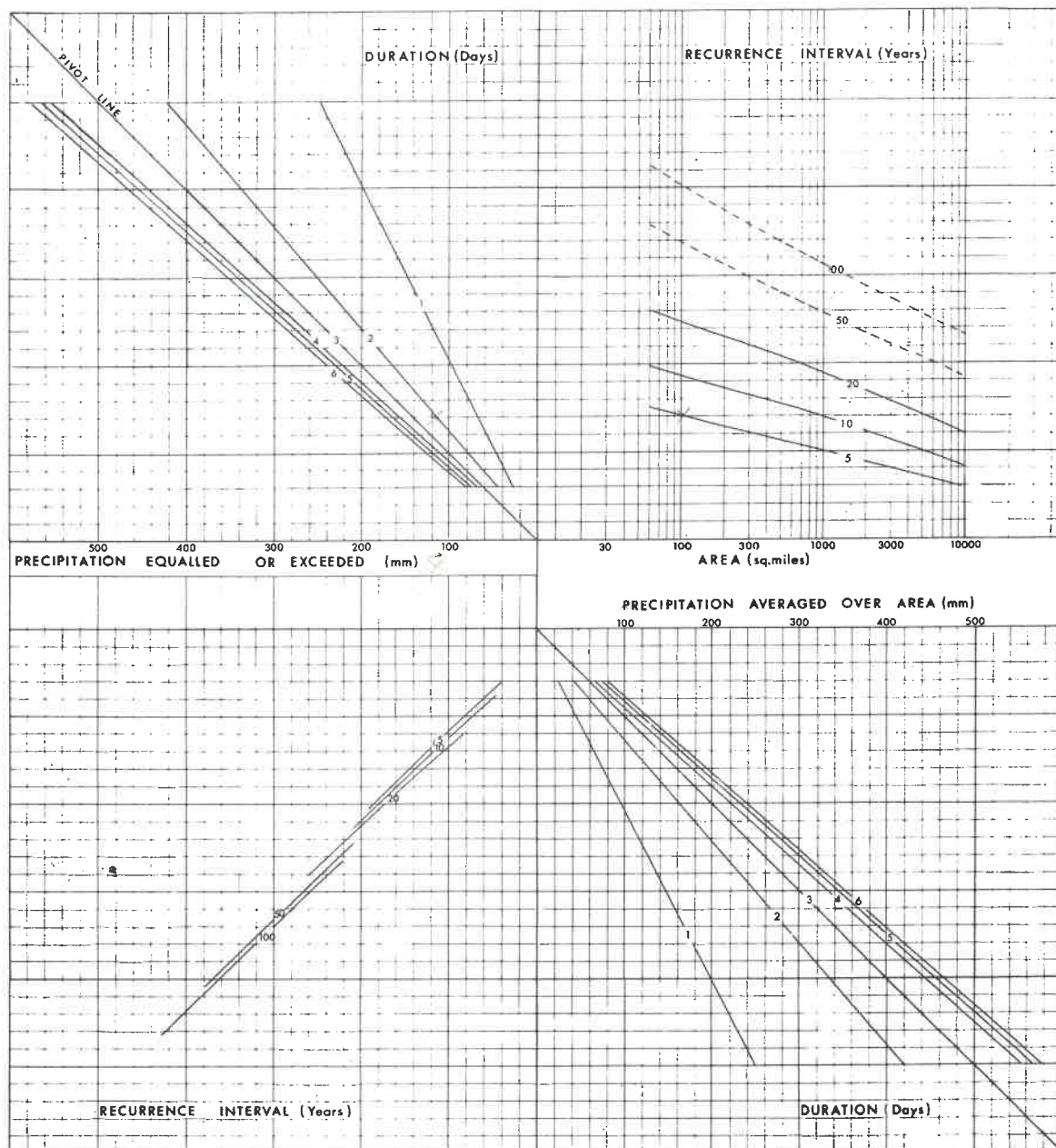
LOCATION OF STORM REGION
SHOWING MAXIMUM OBSERVED STORM (mm)



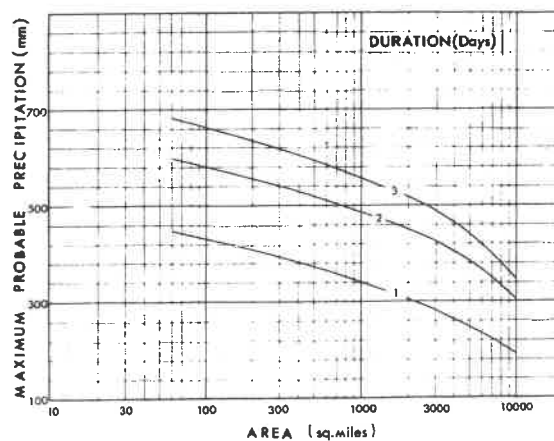
MAXIMUM DEPTH-AREA-DURATION

STORM REGION 14 M.A.P. 500 - 1000 mm

DEPTH-AREA-DURATION-FREQUENCY



SHOWING MAXIMUM OBSERVED STORM (mm)

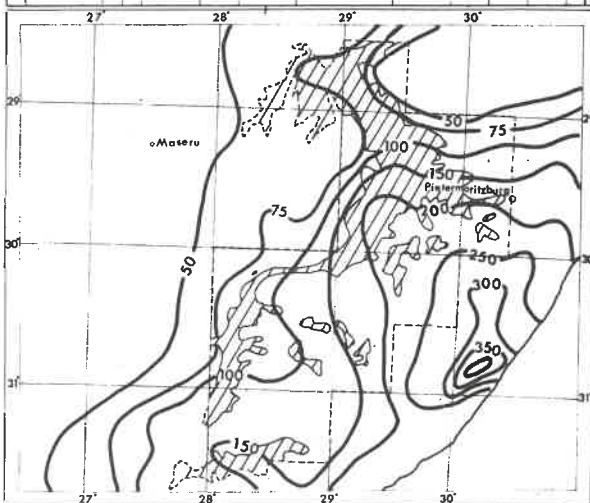
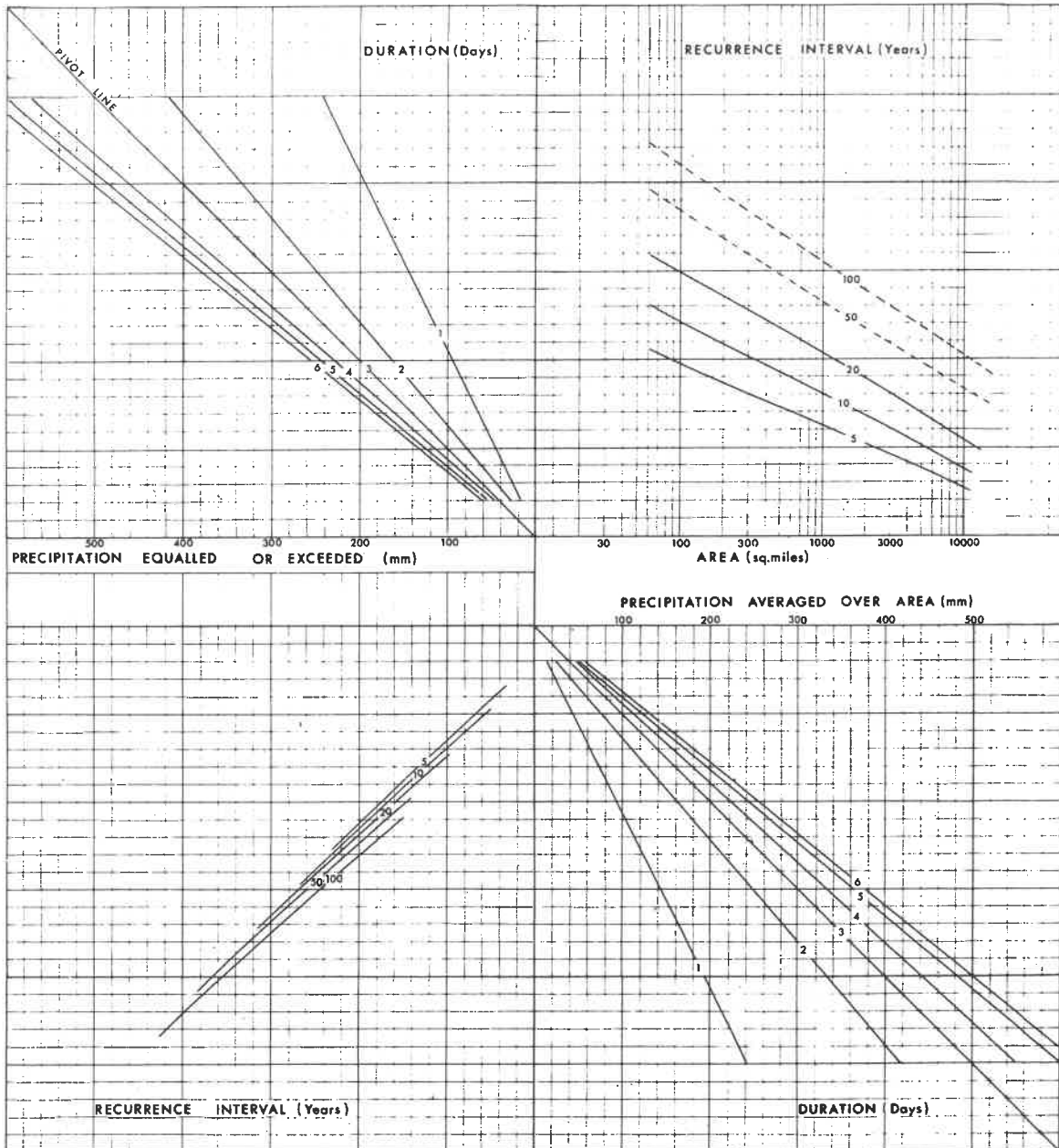


MAXIMUM DEPTH-AREA-DURATION

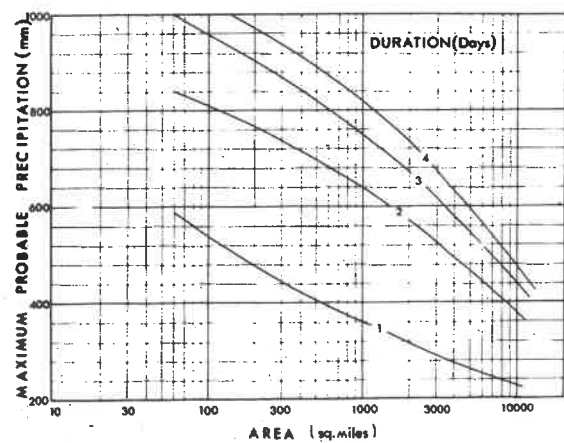
STORM REGION 14

M.A.P. 1000 + mm

DEPTH-AREA-DURATION-FREQUENCY



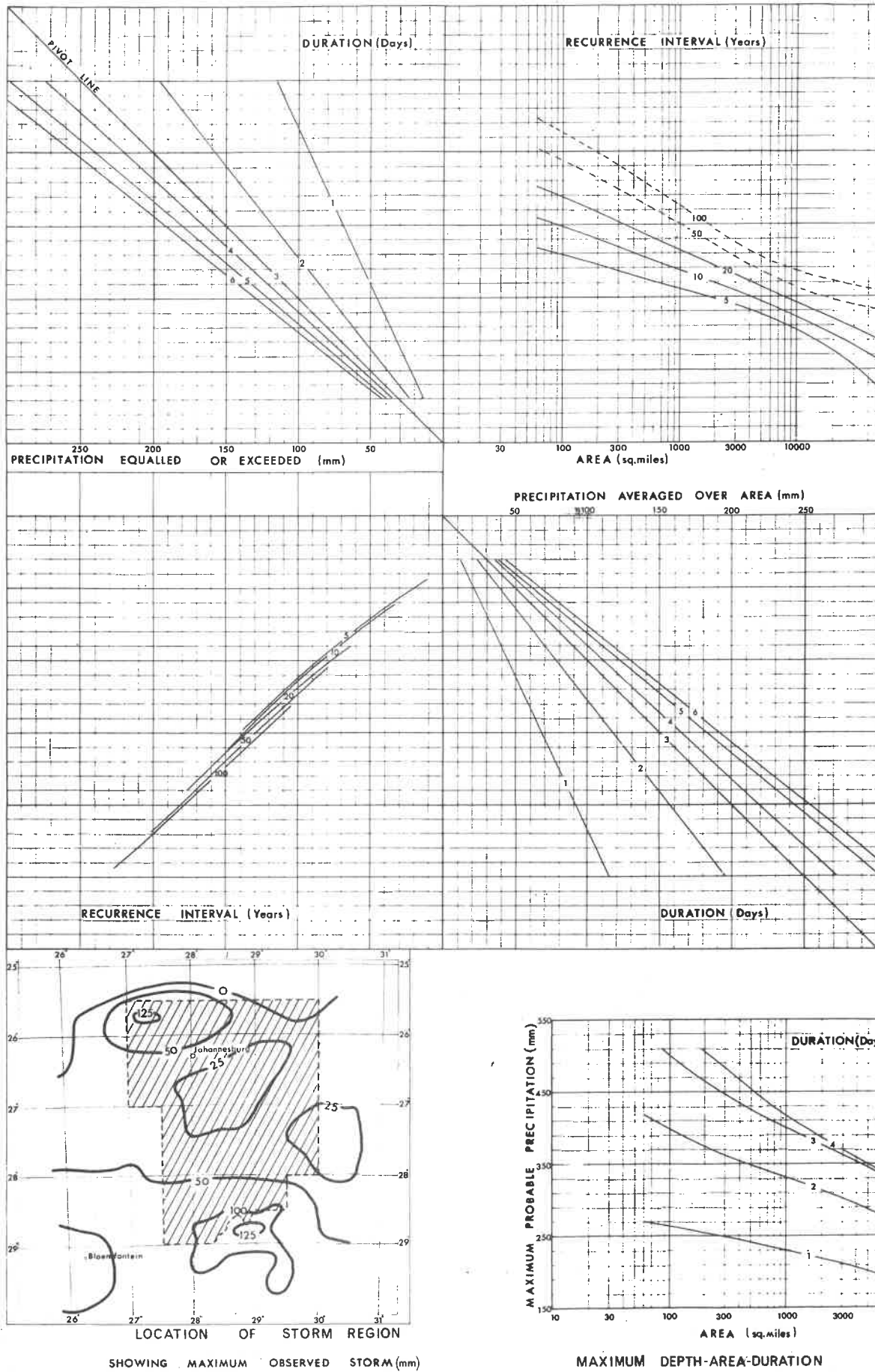
LOCATION OF STORM REGION
SHOWING MAXIMUM OBSERVED STORM (mm)



MAXIMUM DEPTH-AREA-DURATION

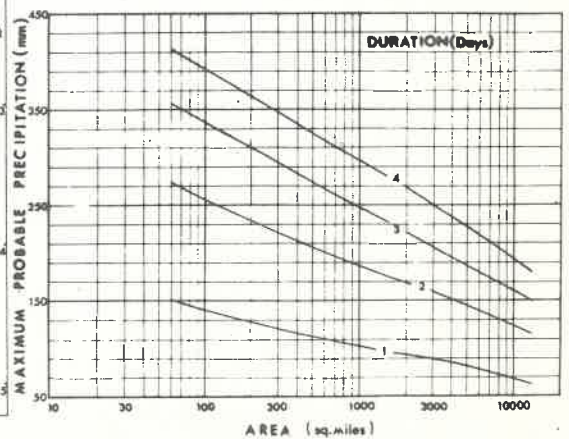
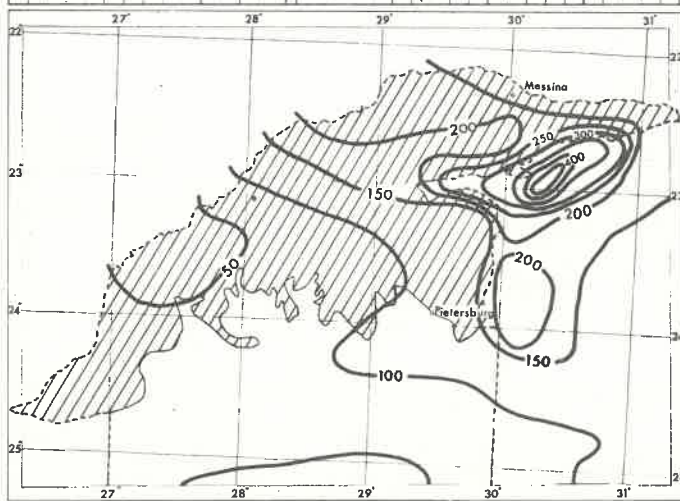
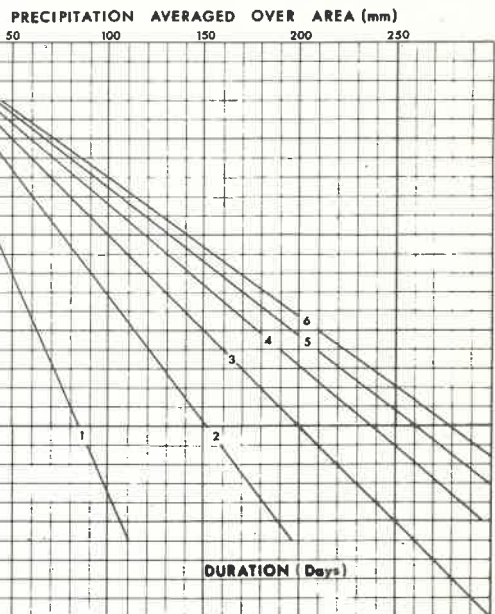
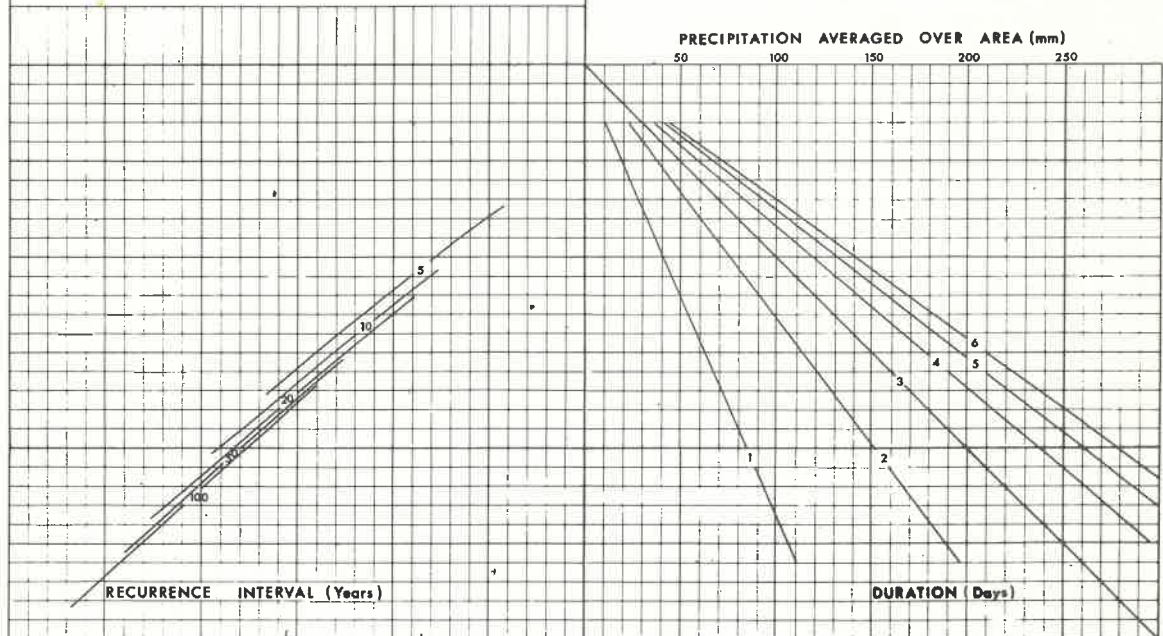
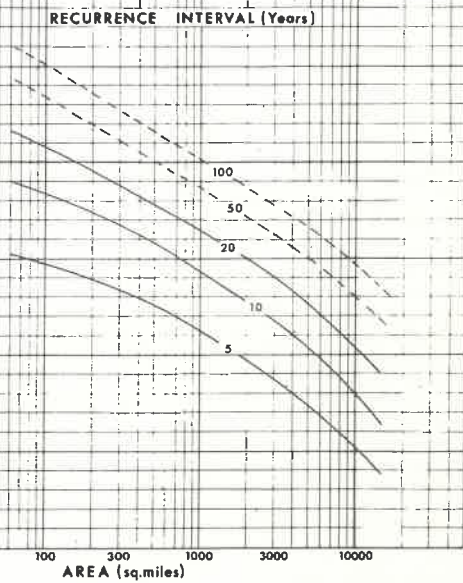
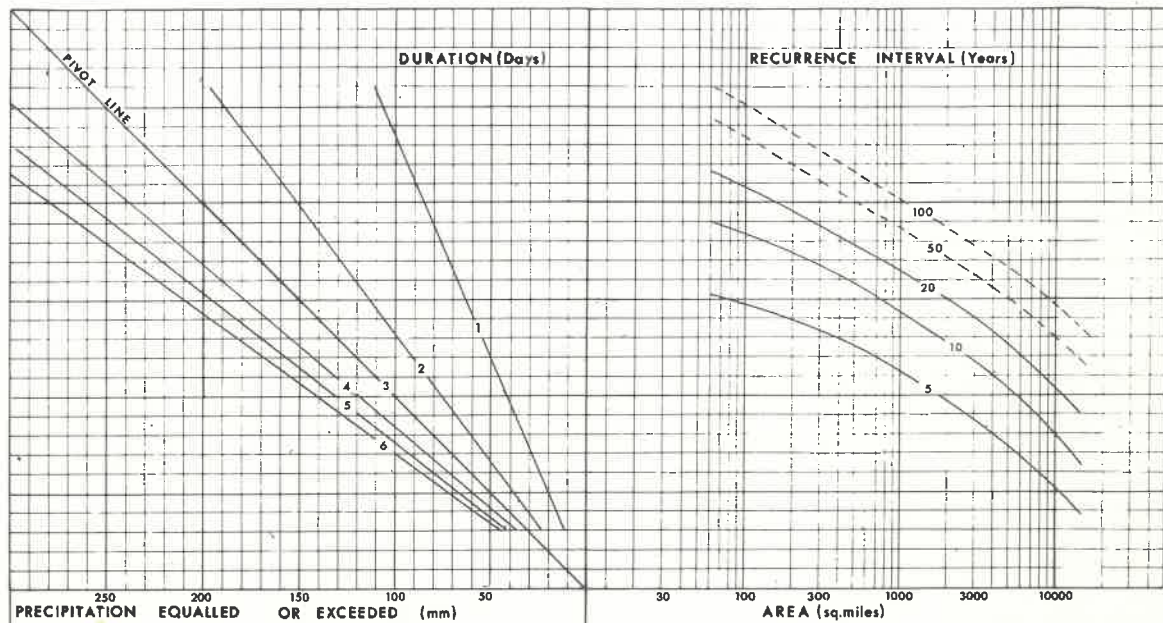
STORM REGION 16
M.A.P. 500-1000 mm

DEPTH-AREA-DURATION-FREQUENCY



STORM REGION 18
M.A.P. 250 - 500 mm

DEPTH-AREA-DURATION-FREQUENCY

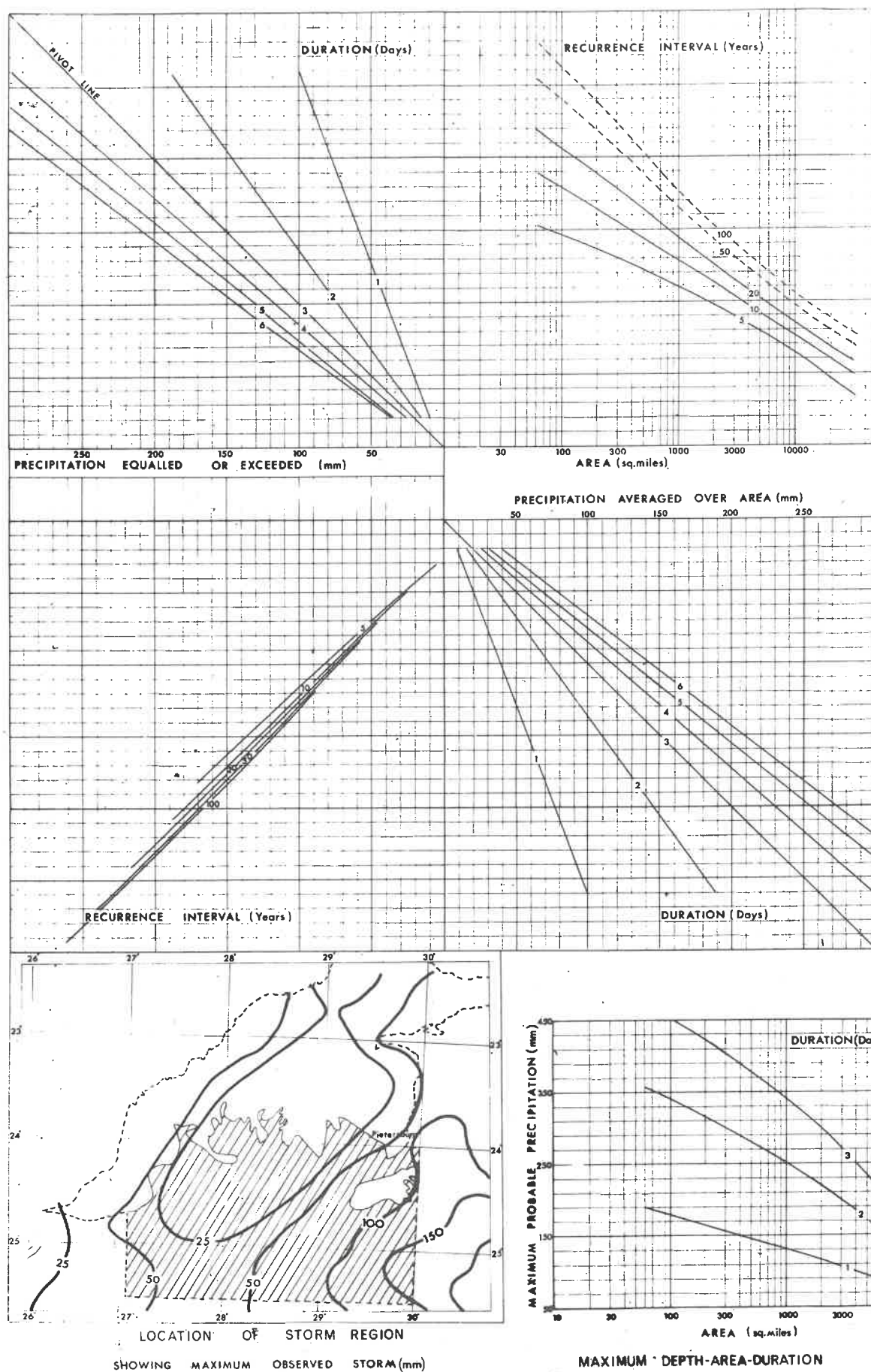


LOCATION OF STORM REGION
SHOWING MAXIMUM OBSERVED STORM (mm)

MAXIMUM DEPTH-AREA-DURATION

STORM REGION 18
M.A.P. 500 - 1000 mm

DEPTH-AREA-DURATION-FREQUENCY



R E F E R E N C E S

1. U.S. DEPARTMENT OF COMMERCE, WEATHER BUREAU : Rainfall frequency atlas of the United States. Washington D.C. May 1961.
2. BRUCE J.P. and SPORNS U. : Critical Meteorological conditions for maximum floods in the St. John River Basin. Canadian Meteorological Memoirs No.14. Department of Transport, Toronto, Ontario. 1963.
3. BRUCE J.P., RICHARDS T.L. and SPORNS U. : Critical Meteorological conditions for maximum inflow, wind set-up and waves, Portage Mountain reservoir, Peace River, B.C. Climatological Studies No.2. Department of Transport, Toronto. 1965.
4. ALEXANDER, G.N. : Discussion on paper 3915 by Snyder, F.F. J. of Hyd. Div. Amer. Soc. Civ. Engrs. Vol. 91, HY1, Jan 1965.
5. VAN WYK W. : Aids to the prediction of extreme floods from small watersheds. M.Sc. dissertation, University of the Witwatersrand. Sept 1965.
6. VAN WYK W. and MIDGLEY D.C. : Storm Studies in South Africa - small-area high-intensity rainfall. Trans. S. Afr. Instn. of Civ. Engrs. Vol. 8. June 1966.
7. WEATHER BUREAU CLIMATE OF SOUTH AFRICA : Rainfall statistics W.B. 20. 1954; Part 3 Maximum 24-hour Rainfall W.B. 21. 1956; Part 4 Rainfall Maps, W.B. 22. 1957; Part 5 District Rainfall. W.B. 23.

1960; Part 9 Average monthly rainfall up to end of 1960.

W.B. 29. 1965.

8. MIDGLEY D.C. and SCHULTZ G.A. : Progress in flood hydrograph synthesization. Trans. S. Afr. Instn. Civ. Engrs. Vol. 7 No. 2. Feb 1965.
9. HYDROLOGICAL RESEARCH UNIT : Hydrograph synthesization by digital computer. Paper in preparation.
10. RAINSFORD H.F. : Survey adjustments and least squares. Constable. 1957.
11. ✓ KRIEL J.P. : Floods in Natal and the Transkei during May 1959. Tech. Report No. 20, Hydrological Research, Dept. of Water Affairs. 1960.
12. ✓ TRIEGAARDT, D.O. : Flood rains in the Karoo, South Africa. Weather Bureau Notes, Vol. 10, No. 1/4, p. 113. 1961.
13. ✓ TALJAARD, J.J. : Maart se reënval en die oorstromings in die Karoo. Weather Bureau, Dept. of Transport, Newsletter, No. 144. 1961.
14. COOPERATIVE STUDY, TECH. PAPER NO. 1. U.S. WEATHER BUREAU AND U.S. BUREAU OF RECLAMATION. Manual for depth-area-duration analyses of storm precipitation. Division of Climatological and Hydrological Service. Weather Bureau, Washington D.C. Sept 1946.
15. WIEDERHOLD J.F.A. : Reduction of computational effort in least squares fitting of polynomial surfaces. Trans. S. Afr. Instn. Civ. Engrs.

Vol. 9, No. 11. Nov 1967.

16. PITMAN, W.V. and MIDGLEY, D.C. : Flood studies in South Africa :
Frequency analysis of peak discharges. Trans. S. Afr. Instn.
Civ. Engrs., Vol. 9. August 1967.
17. KOKOT D.F. : An investigation into the evidence bearing on recent
climate changes over Southern Africa. Irrigation Department
Memoir, Published by Government Printer, Pretoria. 1948.
18. BRUCE J.P. and CLARKE R.H. : Introduction to Hydrometeorology. Pergamon
Press 1966.
19. PEIRCE R.W. : A study of water resources analysis procedures,
with specific reference to the South Western Cape Province
of South Africa. M.Sc. dissertation. University of the Wit-
watersrand. Oct 1967.
20. MISES R. VON : La distribution de la plus grande de n valeurs.
Revue math. de l'Union Interbalkanique (Athens). Vol. 1,
p. 1, 1936.
21. PEARSON E.S. and CHANDRA SEKOR C. : The efficiency of statistical
tools and a criterion for the rejection of outlying observations.
Biometrika 28 : 308, 1936.
22. GUMBEL E.J. : "Statistics of Extremes", Columbia University Press,
New York, 1958.
23. FISHER R.A. and TIPPET L.H.C. : Limiting forms of the frequency
distribution of the largest and smallest number of a sample.

Proc. Cambridge Philosophical Society. Vol. 28, p. 180.

24. FRECHET M. : Sur la loi de la probabilité de l' écart maximum.
Annals de la Société Polonaise de Mathématique (Cracow),
Vol. 6, p. 93.
25. GNEDENKO B.V. : Sur la distribution limité du terme maximum d'une
séni aléatoire. Annals of Mathematics, Princeton, N.J., U.S.A.
Vol. 44, p. 423.
26. GUMBEL E.J. : Statistical theory of floods and droughts. J. Instn.
Wat. Engrs. Vol. 12, No. 3, May 1958.
27. GUMBEL E.J. : Statistical theory of extreme values and some
practical applications. U.S. National Bureau of Standards.
Applied Maths. Series 33. Washington D.C., U.S.A. 1954.
28. PULLEN R.A. : Computation of the moisture content of the atmosphere
using surface level climatological data. J. of Hydrol. Vol. 6,
1968, p. 99-113.
29. TRIEGAARDT D.O. : Computer evaluation of upper air soundings made with
the Väisälä radiosonde. Weather Bureau, Notos 13 (1964)
30. SOLOT S.B. : Computation of depth of precipitable water in a column
of air. Mon. Weath. Rev. Washington D.C. April 1939.
31. SMITHSONIAN METEOROLOGICAL TABLES, (1951) : Sixth revised edition,
Washington D.C.
32. MOOD A. and GRAYBILL F. : Introduction to the theory of statistics.
McGraw Hill 1963.

33. JORDAAN J.M. : Some aspects of the hydrological design considerations of the Orange River Development Project.
34. HAMMING R.W. : Numerical methods for scientists and engineers.
McGraw Hill 1962.
35. SCHULTZE B.R. : Private communications with members of the Unit. 1965.
36. STEFFEN O.K.H. : Private communications. 1967.

